The Pennsylvania State University

The Graduate School

Department of Energy and Geo-Environmental Engineering

EMISSION CHARACTERISTICS OF A NAVISTAR 7.3L TURBODIESEL OPERATED WITH BLENDS OF DIMETHYL ETHER (DME) AND DIESEL FUEL

A Thesis in

Fuel Science

by

Elana M. Chapman

Submitted in Partial Fulfillment
of the Requirements
for the Degree of

Master of Science

August 2002

We approve the thesis of Elana M. Chapman.

Date of Signature

André L. Boehman
Associate Professor of Fuel Science
Thesis Advisor

Alan Scaroni
Professor of Energy and Geo-Environmental Engineering
Department Head of Energy and Geo-Environmental Engineering

Semih Eser
Associate Professor of Energy & Geo-Environmental Engineering
Associate Head of Department of Energy & Geo-Environmental Engineering

Thomas Litzinger
Professor of Mechanical Engineering

ABSTRACT

Several oxygenates have been proposed and tested for use with diesel fuel as a means of reducing exhaust emissions. This paper examines dimethyl ether (DME), which is a potential ultra clean fuel, in blends with diesel fuel. Modest additions of DME into diesel fuel (2 wt.% oxygen) showed reductions in particulate matter emissions, but the previously reported data by the author from a multicylinder Navistar 7.3L Turbodiesel engine were scattered. In this study, experiments were performed on a multi-cylinder Navistar 7.3L Turbodiesel engine to repeatably confirm and extend the observations from the earlier studies. This is an important step in not only showing that the fuel does perform well in an engine with minor modifications to the fuel system, but also in showing that DME can give consistent, significant results in lowering emissions. The Dimethyl ether and diesel fuel were blended to achieve a net addition of 5 and 10 wt. % oxygen in the blended fuel. The data confirms that the addition of DME can reduce the particulate emissions from a compression ignition engine. However, the NO_x emissions were not favorable for all conditions. It is believed that through further modification of injection timing, NO_x emissions can be effectively reduced. Additionally, pressure trace analyses showed that the fuel affects the ignition delay of the combustion process, and that optimization of the engine controls would be needed to further improve performance and reduce exhaust emissions.

TABLE OF CONTENTS

LIST OF FIGURES

LIST OF TABLES

ACKNOWLEDGMENTS

I would like to express my grateful appreciation to my thesis advisor, Dr. André Boehman, for his support, guidance and patience. I am also thankful to my committee members, Dr. Alan Scaroni, Dr. Thomas Litzinger, and Dr. Semih Eser for their help with my research at Penn State during the preparation of this thesis.

I would like to thank all former and current members of our research group for their help, friendship and support during my graduate studies at Penn State: Howard Hess, Chris Frye, Melissa Roan, Shirish Bhide, William Swain, Jim Szybist, Patrick Flynn, Juhuan Song, and Dr. Louis Boehman (University of Dayton).

I would like to acknowledge the support of Air Products and Chemicals, Inc., the Pennsylvania Department of Environmental Protection and the National Energy Technology Laboratory of the U.S. Department of Energy. In particular, I would like to acknowledge the support and encouragement of John Winslow, Mike Nowak, Mike McMillan and Jenny Tennant of NETL, and Barry Halper, Jo Ann Franks, and James Hansel of Air Products. I would also like to acknowledge Glen Chatfield of Optimum Power for providing the PtrAn software, and Navistar for their continued technical support of this project.

This thesis was written with support of the U.S. Department of Energy under Contract No. DE-FG29-99FT40161. Also, this thesis was prepared with the support of the Pennsylvania Department of Environmental Protection.

Finally, I would like to thank my parents, James and Martha Chapman, for setting an example of the kinds of accomplishments which hard work and dedication can manifest. From them, I derived a sense of curiosity and the perseverance to succeed. Additionally, I would like to acknowledge my extended family for their support and encouragement.

Chapter 1

Introduction

1.1 Background

In 1892, it was the intention of Rudolf Diesel to provide a new type of internal combustion engine operating with higher efficiency than conventional steam and Otto cycle engines, and that could be operated on many types of fuels [1]. The engine cycle developed by Diesel involves injection of fuel into a volume of air heated by compression. Over the course of history, the durable and efficient diesel engine has replaced other less efficient modes of power production, including steam engines in the railroad industry.

As our world and our environment have changed, concern about the exhaust emissions from internal combustion engines has driven improvements in both types of widely used engines, spark ignition and compression ignition. These improvements include many types of aftertreatment technologies to combat the specific emissions from each type of engine. For the spark ignition engine, aftertreatment technologies include three-way catalysts, utilizing electronics for fuel and air control, and exhaust gas recirculation. Conversely, the emissions from diesel engines have been managed, up until now, primarily by subtle improvements in the fuel injection timing, turbocharging and

intercooling, and higher fuel injection pressure, without the need for significant exhaust aftertreatment [2]. The challenges which the automotive industry now faces are the more stringent emissions standards promulgated by governing bodies worldwide, and increasing costs of petroleum products. Specifically within the diesel engine sector, improvements in emissions are necessary for future sales, and improvements in efficiency have been made necessary by the rising cost of diesel fuel.

In the U.S., future regulations that take effect in 2004 and 2007 will require diesel engine and vehicle manufacturers to review all aspects of the vehicle system design [3, 4]. Demand for cleaner burning diesel fuels is growing worldwide, as governmental regulations make emissions reductions necessary. To achieve substantial reductions in emissions, it is thought that reformulated diesel fuels will play an important role [5]. The reformulation of diesel fuels could include lowering the sulfur content, lowering the aromatic content, or potentially adding the oxygen to the fuel [6].

One solution for reducing emissions from future and current diesel vehicles is to modify the fuel, without modifying the engine hardware. It has been shown that many oxygenates are effective at reducing particulate emissions from diesel engines [7-27]. Therefore, much research has focused on the screening of oxygenated fuel additives, including alcohols, esters, and ethers [6, 28]. Of particular interest are the glycol ethers, which have been shown to be very effective as blends and as neat fuel. This study focuses on the use of a short chain ether, dimethyl ether (DME).

1.2 Statement of Purpose

The present study involves the use of a light-medium duty diesel engine, for use in class 2 through 8 trucks and buses as suggested by Hower and co-workers, to study the ability of using blends of diesel and dimethyl ether with minimal adjustments to the engine hardware [29]. Various studies with neat dimethyl ether have shown that significant emissions reductions are possible [30]. However, when neat DME was used by Sorenson and co-workers, the durability of the fuel system was significantly reduced. Therefore, this suggests the need for a lubricity improver in the fuel. In this study, it is hypothesized that diesel fuel can provide the lubricating qualities needed, while using DME blended with diesel in a quantity that provides an emissions reduction.

Very little information and data exists regarding the use of dimethyl ether and diesel fuel blended together. Since dimethyl ether has been shown to significantly reduce the durability of fuel system hardware [31], blending DME with diesel fuel will improve the lubricating quality of the fluid. The purpose of this study is to perform initial assessments of emissions reductions with the use of the fuel blends.

1.3 Research Questions and Hypothesis

The motivation for this work is the potential of using DME blended with diesel fuel to reduce emissions, specifically particulate emissions. Since it has been shown that

neat DME eliminates particulate emissions, mixtures of DME and diesel are expected to yield a decrease in particulate emissions. However, what is not known is if this decrease will follow the same trend as observed with other oxygenates mixed with diesel with similar oxygen content.

It is hypothesized that a diesel engine can be operated with modest blends of DME-diesel fuel, with minimal modification to the engine and that diesel fuel can provide the lubricating qualities needed, while DME provides an emissions reduction. The hypothesis is being tested by a three step approach: develop an engine test facility, modify a fuel system to operate with DME-diesel fuel blends, and collect data with regard to total particulate mass emissions. Additional emissions and engine data will be collected to complement and explain the particulate emissions reductions. Some researchers have demonstrated that there is a relationship between oxygen addition to diesel fuel, particulate emission reductions, and carbon monoxide increases [28]. Also, because of the physical properties of DME, which is a liquified gas with high vapor pressure, it is important to observe the temperature and pressure of the fuel as it passes through the engine. Observations of basic engine operation will be discussed in the results. Pressure history traces of the combustion process will be used to understand the changes occurring in the ignition delay, start of combustion and rate of heat release between the diesel and DME-diesel fuel blends.

1.4 Limitations and Assumptions

The following limitations were recognized and assumptions were formulated about the experiment in order to proceed with the research. The purpose of acknowledging these limitations is to establish factors which could be influencing the results and support conclusions from the data. These limitations and assumptions will be discussed later as to how they relate to the results.

- The fuel is a homogenous mixture going into the engine.

- If the DME in the fuel rail is below 50°C, DME will be in the liquid state because the pressure will overcome the vapor pressure of DME.

- The engine will be able to operate with the fuel blend, while reducing the durability of the engine in an unknown way and amount.

- The engine operates per the factory calibration of the electronic controls for the engine. No changes have been made to engine control algorithms or parameters.

- Limitations in the comparisons that can be made and the conclusions that can be drawn are the result of the variability of engine operation as the engine responds to the differences in the physical properties of the fuel.

Chapter 2

Literature Review

2.1 Background

As with any new fuel being developed for use in the transportation industry, a comprehensive study of various aspects and impacts of the fuel are important to review and analyze before moving ahead with implementation. The most important aspect, which is the focus of this research, involves the benefits associated with using the fuel in a compression ignition engine. After confirming its potential use, inquiry shifts to other important aspects such as production cost of the fuel, health concerns, and long term use of the fuel.

The motivation for researching new fuels stems from several factors. Primarily, governments worldwide, including the United States, are setting new standards for emissions from new engines and vehicles. This is being done for the benefit of human health and the environment, via the reduction of particulate matter and smog-causing NO_x [32]. The final ruling in December 2000 from the U.S. EPA sets the new 2007 standards for heavy duty diesel engines to the following:

- Particulate Matter (PM) emissions to 0.01 grams per brake-horsepower-hour (g/bhp-hr) to take full effect in 2007, and

- NO_x and non-methane hydrocarbons (NMHC) to 0.20 g/bhp-hr and 0.14 g/bhp-hr, respectively. These standards will be phased in after 2007 [33].

This is shown in *Figure 2–1*, tracing the history of the tightening emission standards.

Emissions Type	**Current Regulation**	**2004 (gm/bhp-hr)**	**2007(gm/bhp-hr)**
NO_x	4		.2
HC	1.3		.14 (NMHC)
NO_x and HC		2.4	
PM	.1		.01

*Required on-board diagnostics (OBD) systems for vehicles between 8500 and 14000 lbs to be phased-in, beginning in 2005

NO_x- Nitrogen Oxides ; HC- Hydrocarbons; PM- Particulate Matter

Figure 2–1: U.S. Heavy-Duty Diesel Engine Emission Standards [32, 33]

Additionally, a new fuel type that can be made from several fossil fuel sources would benefit the energy security of the U.S. [34]. Finally, it is necessary to confirm the ability of an engine to operate on a fuel in a manner similar to the operation on the fuel for which it was designed to operate. This means that development projects are necessary to experimentally prove concepts and long term operation.

DME is a compound that has been targeted for future use as a fuel, in several countries around the world [35-37]. Motivation to use DME exists for several reasons.

There has been confirmation that the fuel yields low particulate emissions and possibly lower NO_x emissions [30, 38, 39]. In addition, DME can be made from a variety of feedstocks, which can support the use of alternative energy resources [40, 41].

The following review of the literature will cover a summary of the testing completed to examine the potential use of DME as a fuel. Many technical challenges have been discovered through this testing, giving light to new approaches to using DME as a fuel. Researchers have begun to study the fundamental nature of the combustion process, and to understand the mechanisms of DME combustion [42, 43]. Production processes, costs and health concerns will also be covered.

2.2 Emissions from Diesel Engines

Diesel engines have been traditionally high emitters of NO_x and particulate matter. Other pollutants include carbon monoxide (CO) and unburned hydrocarbons (HC), which are typically very low for a diesel engine since the air –fuel mixture is lean of stoichiometric [44, 45]. The following sections will focus on the two major pollutants from a diesel engine NO_x and PM..

2.2.1 NOx Formation

Diesel engines produce significant amounts of NO_x, depending on the load conditions of the engine. Of the 100 to 2000 ppm which is produced, the majority of this is nitric oxide (NO). There are several mechanisms for the formation of NO_x, however,

in the case of the diesel engine, the most significant mechanism is the extended Zeldovich mechanism, also known as the thermal mechanism. The extended Zeldovich mechanism is shown in equations 2.1, 2.2 and 2.3:

$$O + N_2 = NO + N \quad (2.1)$$

$$N + O_2 = NO + O \quad (2.2)$$

$$N + OH = NO + H \quad (2.3)$$

NO_x formation is strongly dependent on temperature [44]. It is typically formed during the first 20 degrees of crank angle rotation, after the start of combustion. Therefore, emission reduction strategies target this time period, and aim to reduce combustion temperatures [1].

2.2.2 Particulate Formation

Particulate matter can be defined as the combination of soot, condensed hydrocarbons, sulfates, oil, and water that attach to agglomerated soot particles in the exhaust stream [46]. Detailed modeling and experiments have been conducted to try to understand the soot formation process in different types of flame structures and in flames of various fuels [47]. It has been established that several classes of higher hydrocarbons,

namely polycyclic aromatic hydrocarbons (PAH) and acetylene (C_2H_2), are important precursors to soot formation and are created in fuel-rich conditions [48]. From the initial formation of a benzene ring, the soot particle increases in size through the addition of acetylene [48].

2.3 Emission Control Techniques

Emission control strategies can be divided into three categories: pre-combustion, in-cylinder, and post-combustion [2, 49]. A list of these approaches can be found below in *Figure 2–2* [50]. For many years, diesel engines have escaped the necessity of post-combustion controls because modifications which could be made to fuel or to the engine combustion and performance to meet new emissions regulations. Also, an important requirement for implementation of many post-combustion technologies is the reduction of the sulfur content of the fuel. Since diesel fuel properties will be discussed later in this section, the following discussion will focus on the in-cylinder and post–combustion strategies of controlling particulate and NO_x emissions.

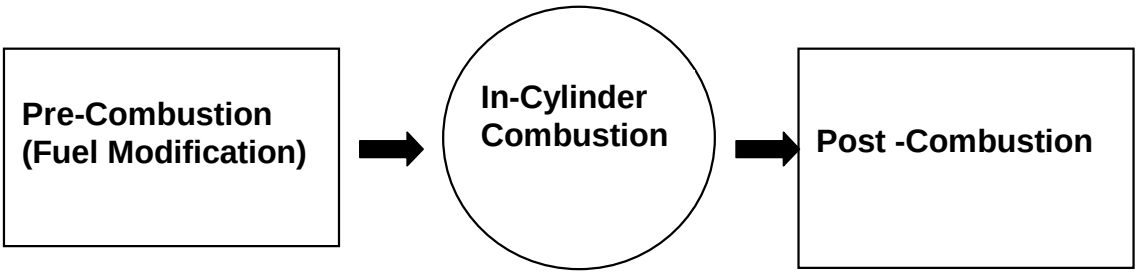

Particulates
Decrease Sulfur
Increase O_2 Content
Decrease Aromatics

NO_x
Increase Cetane No.
Add Water

Particulates
Fuel Atomization
Common Rail Injection
Injection Timing
Rate Shaping
Split Injection

NO_x
EGR (Exhaust Gas Recirculation)
Water Injection
Injection Timing
Rate Shaping
Split Injection

Particulates
Particulate Trap
Particulate
Oxidizer

NO_x
SCR
SNCR (Thermal &
Non-Thermal)
SNR

SCR- Selective Catalytic Reduction
SNCR- Selective Non-Catalytic Reduction

Figure 2–2: Emission control strategies for diesel engines [50]

2.3.1 Particulate Emissions Control

The following sections cover the in-cylinder and post-combustion methods of controlling particulate emissions.

2.3.1.1 In-Cylinder Combustion

In general, the methods used to control or modify the particulates generated during combustion modify the fuel atomization, injection pressure, injection timing, and fuel injection rate. The goal of providing better atomization and controlling the heat release rate is to allow soot particles to be oxidized through improved air entrainment and utilization [51]. However, this must be carefully determined through design and testing. In changing the heat release rate, overall bulk peak temperatures in the cylinder could be reduced, reducing the rate of reactions and increasing time for soot oxidation [44, 52].

2.3.1.2 Post-Combustion

Two general methods exist to control particulate emissions in post combustion. First, a particulate filter can be used. This is typically a ceramic wall flow filter with alternative plugged channels, as seen in *Figure 2–3*. As accumulation increases, heat is supplied to incinerate the carbon. Second, an oxidation catalyst can be used. In this method, flow is not obstructed. It is made from a monolithic substrate (cordierite; $Mg_2AL_4Si_5O_{18}$) with a precious metal washcoat. However, this method only oxidizes the

soluble organic fraction (SOF) of the particulate, but does not address the soot portion (insoluble) [2, 53].

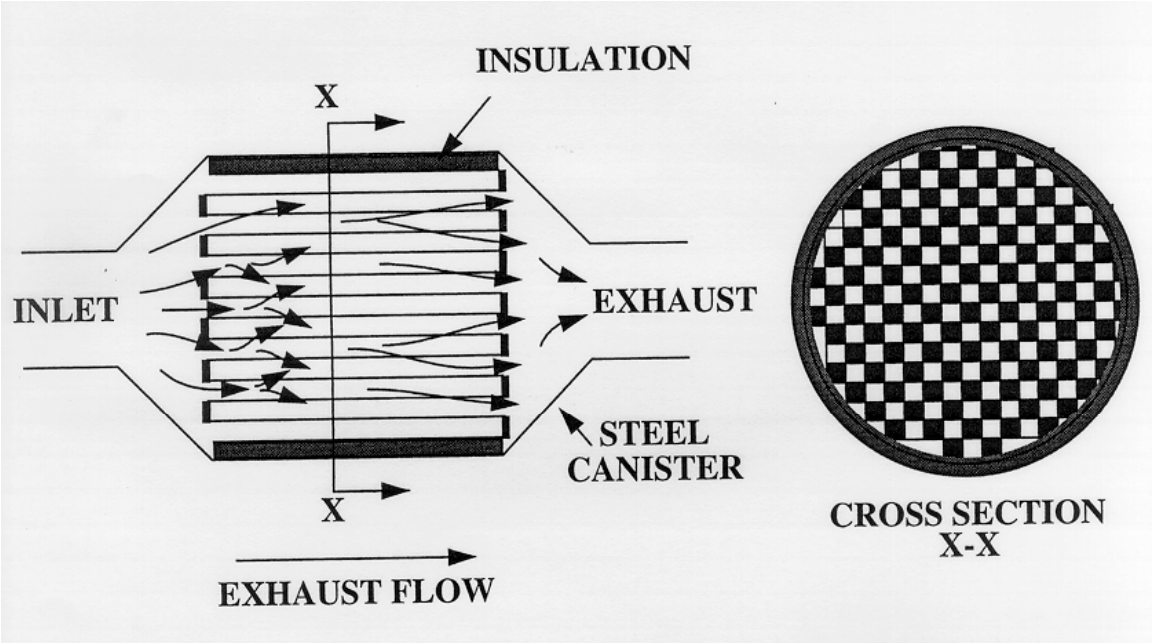

Figure 2–3: Diesel Particulate Filter [53]

2.3.2 NO_x Emission Reduction

The following sections cover the in-cylinder and post-combustion methods of controlling NO_x emissions.

2.3.2.1 In-Cylinder Combustion

There are several techniques which can aid in reducing NO_x emissions. These include exhaust gas recirculation (EGR), injection timing control, and fuel injection rate shaping. The goal of these three techniques is to reduce the peak flame temperature which leads to thermal NO_x formation. However, these techniques also have drawbacks. In altering the fuel injection timing to the cylinder, power decreases and fuel consumption increases. Also, reducing the peak flame temperature causes an increase in the level of soot emissions, due to the reduced rate of reactions, increasing soot formation [44, 52].

2.3.2.2 Post Combustion

The general post-combustion method which exists for controlling NO_x involves some type of catalytic or chemical reaction. As seen in *Figure 4–4*, there is Selective Catalytic Reduction (SCR), and Selective Non-Catalytic Reduction (SNCR), both thermal and non-thermal [2]. The method that is most widely talked about for use is the SCR method, also most commonly known as $DeNO_x$ Catalysis. An example of this is shown in *Figure 4–4.* In this method, a zeolite catalyst is used to adsorb NO_x molecules. A hydrocarbon reagent is injected into the exhaust stream to chemically reduce the NO_x. The typical reagent used is the fuel itself, which reduces the efficiency of the vehicle. It should be noted that this process works in a small temperature band (200-250 °C for

precious metal zeolites and 400-450 °C for base metal zeolites), and for vehicles the NO_x reduction is low and selectivity is poor [53]. Another method of selective catalytic reduction uses ammonia or urea as the reductant [54]. Testing has been completed using SCR, EGR, and intensive engine mapping which resulted in dramatic reduction of NO_x emissions [55].

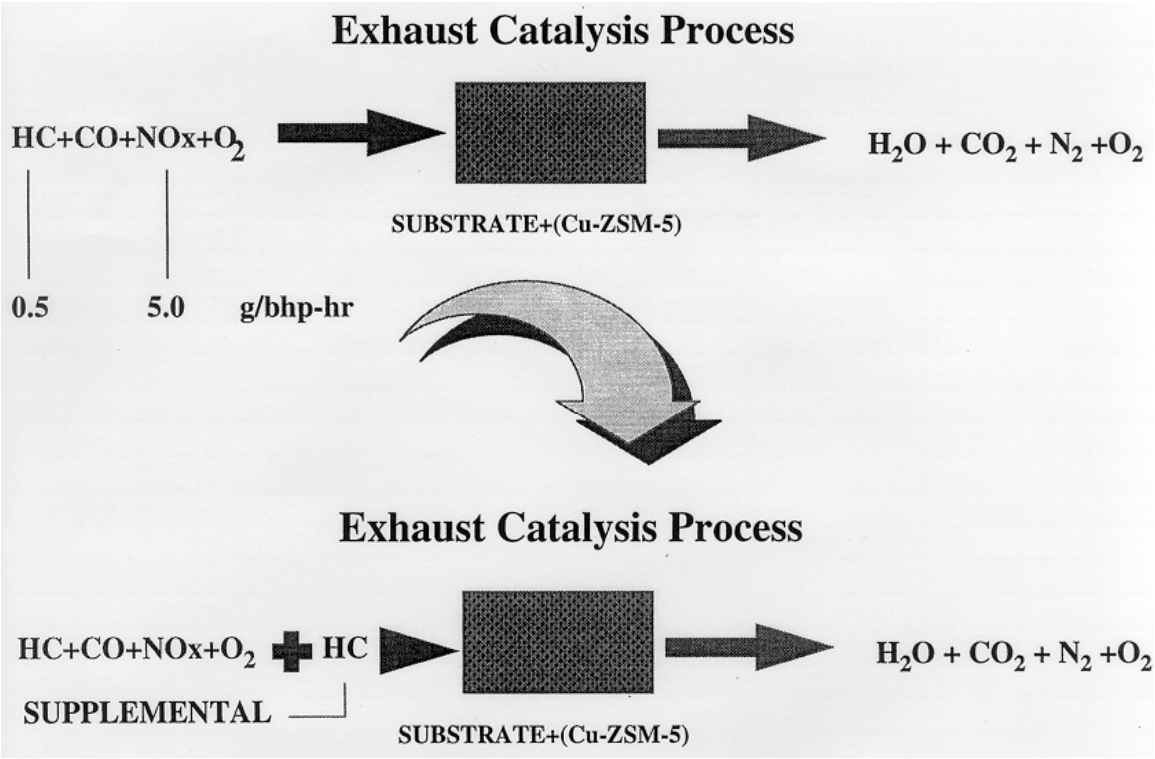

Figure 2–4: DeNO$_x$ Catalyst [53]

2.4 Compression Ignition Engines

The phrase "compression ignition" refers to the engine classification based on method of fuel ignition. The compression ignition (CI) process is used in conventional diesel engines and in gas engines by pilot injection of fuel oil. In this type of engine, air is inducted into the cylinder, and compressed. Just before the combustion process is to start, the fuel is injected into the engine. For a given engine speed, the air flow is essentially constant, and engine load can be adjusted by increasing the amount of fuel injected for each cycle. There are several variations on the type of CI engine including the working cycle (2 or 4 stroke), method of air preparation (naturally aspirated or turbocharged), and method of fueling (indirect or direct injection) [44].

For a typical 4-stroke CI engine, the compression ratio is between 12 and 24, and depends on whether the intake air is naturally aspirated or turbocharged. On the intake stroke, air is inducted into the cylinder as the piston is moving down. Then, as the piston moves up, the air is compressed. A few degrees before the piston reaches the top of its travel, fuel is injected into the cylinder. As the fuel is injected, the combustion process begins, pushing down on the piston. This is the point at which work is performed in the system through diffusion combustion and release of the energy stored in the fuel. The final stroke of the process is for the exhaust valve to open as the piston moves to the top of the cylinder a second time, pushing the products from the combustion process out of the cylinder [53]. A representation of this process is shown in *Figure 2–5* below.

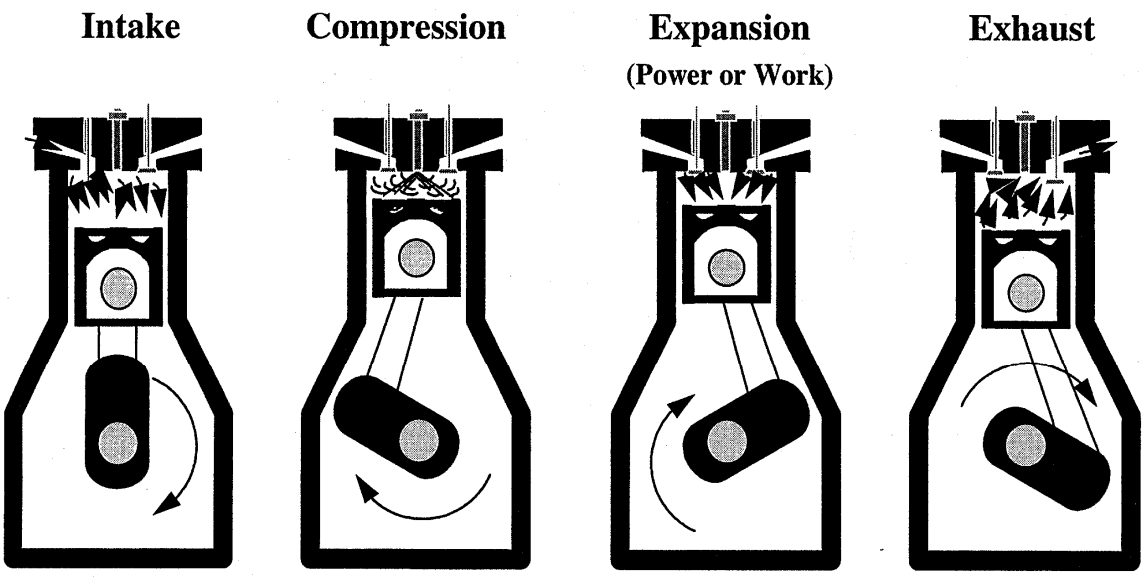

Figure 2–5: Four-Stroke Diesel Engine Operation[53]

Air is inducted into the cylinder at atmospheric pressure and compressed to about 4 MPa (600 lb/in^2) at a temperature of 800 K (1000 °F). A few degrees before Top Dead Center (TDC) of the piston, the fuel is injected into the cylinder. The fuel is atomized as it passes through the injector nozzle ports, and entrains air into the spray plume. As the liquid fuel evaporates, it mixes with the air into proportions which are combustible. Since the air temperature and pressure are above the ignition point of the fuel, there is a short delay period, and then spontaneous ignition of parts of the mixture occurs. This spontaneous ignition can be observed as an increase of pressure in the cylinder [44]. Because the compression ignition engine depends upon spontaneous ignition of the fuel,

a high cetane number fuel is required. The cetane number ensures that the fuel will autoignite when required by the location in the engine cycle.

Combustion in a diesel engine is defined as rapid oxidation generating heat and light. The combustion occurs in a flame mode, encompassing two types of flames: pre-mixed and diffusion flames. In a pre-mixed flame, the fuel and oxidizer are mixed before any rapid chemical reaction occurs. In a diffusion flame, the fuel and oxidizer are separated, and then reaction occurs at the interface between them, as mixing and reaction take place. Diffusion implies that the molecules are diffusing together towards the flame, the fuel and oxidizer moving in from opposite sides. While this molecular diffusioin is occurring on a microscopic level to finish the combustion process, turbulent convection in the cylinder mixes the fuel together on a macroscopic basis [56].

Other methods to describe the 4-stroke cycle include using a pressure vs. volume diagram, and a pressure vs. crank angle diagram. The pressure vs. volume diagram shows the relationship inside the combustion chamber during the cycle. This can be seen in *Figure 2–6*

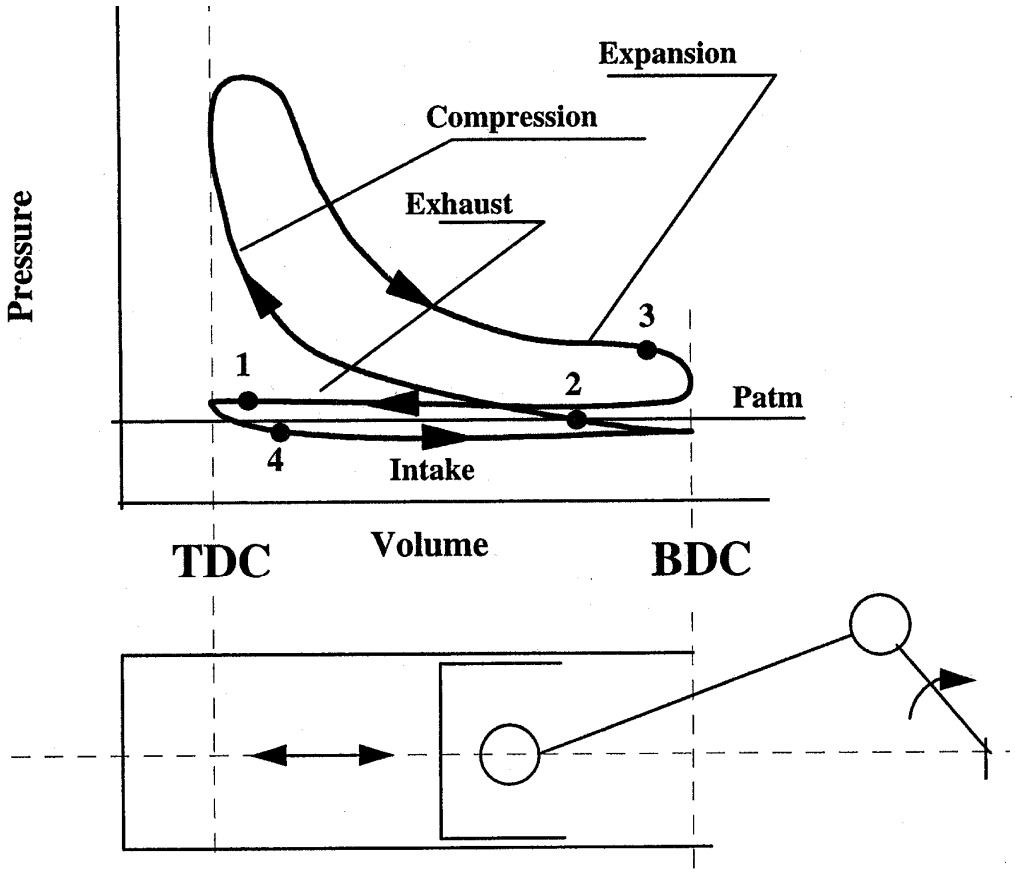

Figure 2–6: Pressure vs. Volume Diagram for a Four Stroke Engine [53]

The pressure vs. crank angle diagram shows the same process cycle, as a function of the degree location on the crank. From this, the peak pressure location can be determined. This can be seen in *Figure 2–7*

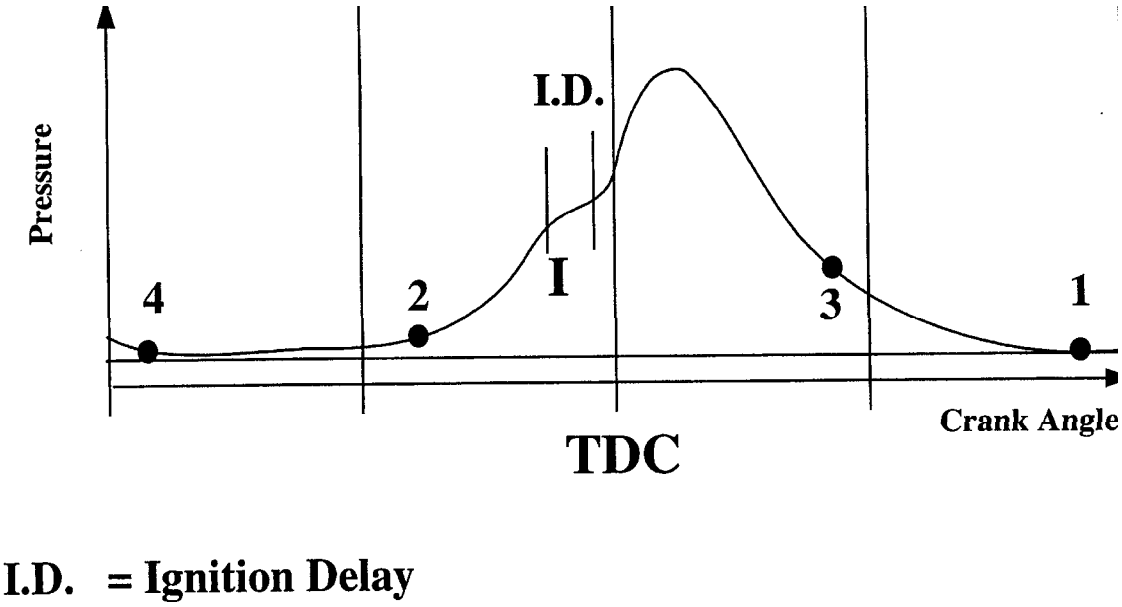

Figure 2–7: Pressure vs. Crank Angle Diagram [53]

2.5 Diesel Fuel Components and Properties: Emission Effect

In 1990, Morris and Wallace of Ethyl Petroleum Additives Limited presented a diagram illustrating the effect of diesel fuel properties on emissions and overall fuel system and vehicle performance, as indicated from their entire research experience [57]. This diagram is found in *Figure 2–8*. Six of the ten properties directly contribute to emissions: sulfur, aromatics, density, distillation, cetane number, and viscosity. The following discussion will place emphasis on these properties.

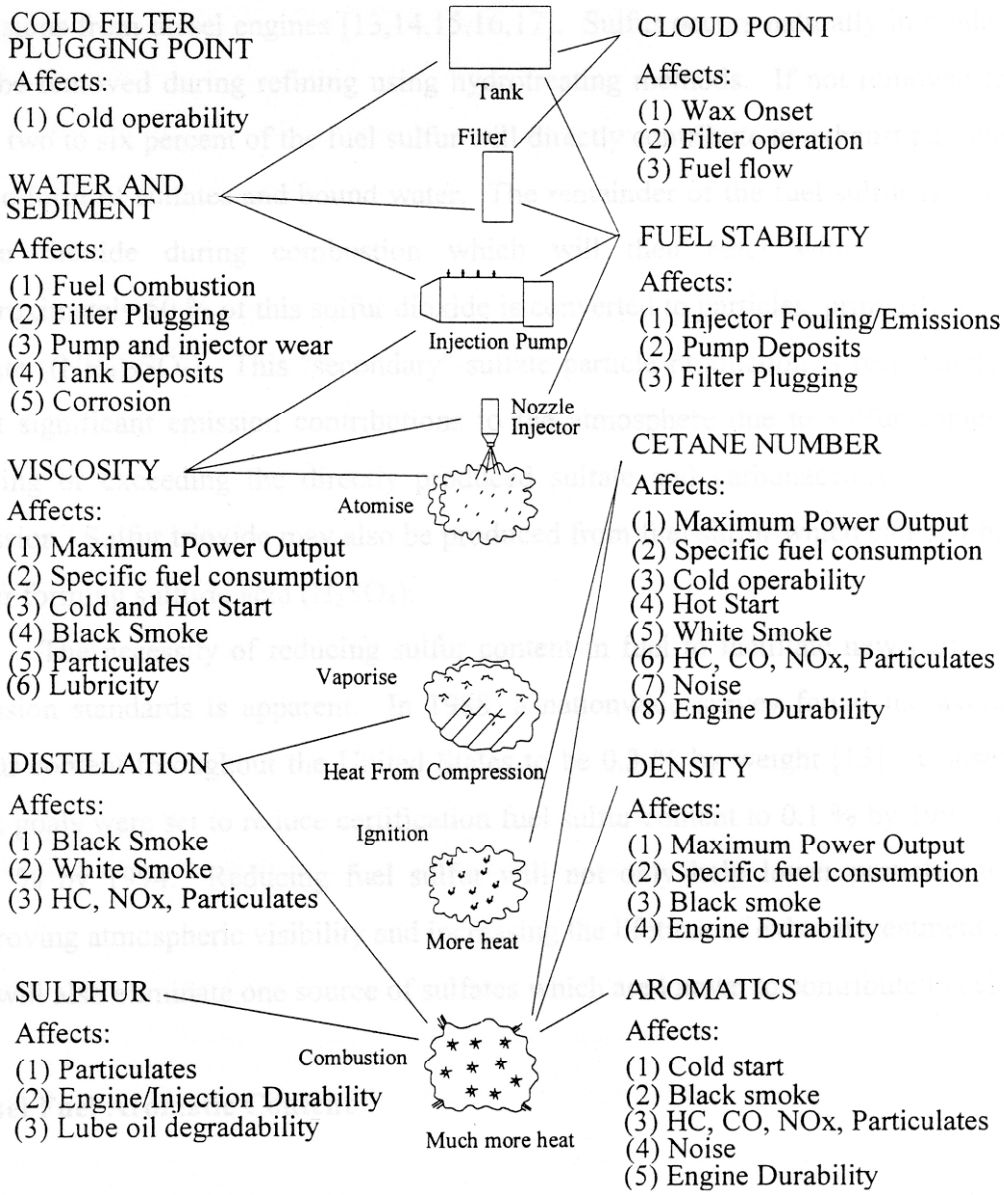

Figure 2–8: Diesel Fuel Properties and their significance [57]

2.5.1 Diesel Fuel Sulfur Content

It has been widely established in the literature that fuel sulfur is the most important contributing factor to brake specific particulate emissions [58-60]. Diesel particulates are composed of four different constituents: the insoluble organic fraction, the soluble organic fraction, lubricants oils, and sulfates with bound water [61]. Specifically, the sulfur has been shown to contribute to the soluble portion of the particulate [58]. When there has been an increase in the sulfur content of the fuel, the engine out particulate emissions have increased, regardless of engine type, emissions levels, and combustion systems [58]. Therefore, lowering fuel sulfur will lower engine out emissions [60].

However, reducing fuel sulfur may have additional positive and negative benefits. The primary motivation for reducing fuel sulfur currently is for manufacturers to be able to implement aggressive exhaust aftertreatment technologies [60]. A potentially negative impact of the reduction of sulfur is the reduction of the lubricating quality of the fuel, known as lubricity [62, 63]. The impact of this lower lubricity may be observed in the fuel injection components and system, but it is not clear how significant this impact is [64-66].

2.5.2 Diesel Fuel Aromatic Content

The effects of aromatics, both as total aromatics (as a combination of mono-, di-, tri-, and polyaromatics) and polyaromatics, is unclear. Schmidt and coworkers showed in

their review of literature that some researchers have found no clear outcomes of the influence of aromatics on particulates and NO_x, where others have found only small reductions in these emissions [60]. Lee and coworkers concluded from their series of experiments across a large platform of engines, that there is a NO_x reduction benefit with lower aromatics [59]. They hypothesized that this is true via the reduction in flame temperature affecting the kinetics of the reaction by lowering the concentration of oxygen radicals. Ryan and coworkers found in their experiments on a Caterpillar 3176 engine that there was some correlation between NO_x and HC emissions, and aromatic content of the fuel [67].

2.5.3 Diesel Fuel Density

Density is commonly used to describe the energy content of the fuel [49]. Typical diesel engine equipment meters fuel on a volume basis. Therefore, if there is a change in density, there is also a change in power output from the engine for a given throttle position [49]. Ryan and coworkers found in their set of experiments, with a Caterpillar 3176B engine, no obvious relationship between density and emissions [67]. However, Lee and coworkers have found that there is a relationship between density and emissions [59]. They hypothesize that the influence arises because of physical interactions within the fuel injection system, specifically changes in the dynamic timing and mass flow rate. The change in density is said to affect the injection spray dispersion angle and penetration, also referred to as liquid length [68, 69]. Lee and coworkers also describe that the effect of density on emissions seemed to change as the engine emissions

equipment changed to meet reduced emissions standards. The modern engines were utilizing higher injection pressures and sophisticated electronic control of injection timing. This could explain why Ryan and coworkers did not find a correlation, as the Caterpillar 3176B has these features.

2.5.4 Diesel Fuel Volatility

Volatility is the measure of the boiling point of a fuel. It characterizes the ability of a fuel to combust, and influences many other properties of the fuel, including density, autoignition temperature, flash point, viscosity, and cetane number [49]. Lee and coworkers determined that the T90/T95 portion had little effect on emissions. However, Schmidt and coworkers found from the literature that reductions in T90 did reduce the particualte matter and HC emissions [60]. Canaan, Dec, and coworkers showed that T50 affects emissions because there is a change in the spray length penetration into the cylinder, and that the chemical processes dominate the physical ones with respect to autoignition [70]. They also declared that the liquid-length penetration is also affected by other fuel properties, such as viscosity and density (specific gravity), which are influential to the atomization and jet break-up process. However, they also suggest that the liquid length penetration is primarily dependent on the evaporation process and the fuel properties which characterize this, such as vapor pressure and boiling point.

The relationship of volatility, or the boiling point, to density, is established in several ASTM standards, D 86, D976, and D4737 [71-73]. These standards present a correlation chart of T50 volatility and density to an index number for cetane [71-73].

Based on these charts, it seems that T50 has a stronger correlation to density then the other boiling points.

2.5.5 Diesel Fuel Cetane Number

In general cetane number refers to the quality of the fuel based in comparison to a standard that has the same ignition delay as the fuel under test, in terms of degrees of rotation of the crankshaft. Simply, it is a measure of ignitability of the fuel. A more specific definition of cetane can be found in ASTM D4737, and is a function of the boiling point (volatility) at T10, T50, and T90, and the density of the fuel at 15 °C [49].

For a compression ignition engine, it has been traditionally thought that the higher the cetane number, the more complete the combustion and the cleaner the exhaust [49]. This has been confirmed through several studies. Ryan and coworkers found no obvious trend between particulate emissions and cetane number [67]. They hypothesized this was due to the reduced pre-mixed burn phase of combustion. However, Lee and coworkers found that changes in particulate emissions are very engine specific. Also, they determined that higher cetane had a beneficial effect on HC emissions, but this was also engine emission level dependent [59]. Since cetane number affects the autoignition quality of the fuel, the shortened ignition delay of the fuel is reducing the time and size of the pre-mixed burn of the fuel. Schmidt and coworkers also confirmed Lee and coworkers findings that higher cetane also lowers NO_x [59., 60].

2.5.6 Diesel Fuel Viscosity

A fluid is defined as a substance that continuously deforms under the action of a shear stress. If there is no shear stress, then there is no deformation. A term used to classify fluids is the viscosity, which is described as the resistance to deformation due to a shearing force. A Newtonian fluid is one in which the shear stress is directly proportional to the rate of deformation. A non-Newtonian fluid is a fluid in which the shear stress is not directly proportional to the rate of deformation [74]. The ratio of the absolute viscosity, μ, and density, ρ, of a fluid is commonly referred to as kinematic viscosity, ν ($\nu = \mu / \rho$).

From a physical effects standpoint, the viscosity of the fluid affects the mass flow rate, injector spray cone angle, fuel distribution and penetration, droplet size of the fuel, and optimum timing of injection. Lower viscosity is characterized as providing better atomization. However, if the viscosity is too low, this could result in leakage through injection equipment clearances. If the viscosity is too high, excessive heat generation in injection equipment could result, because of viscous shear in the clearances between injection plungers and cylinders [49].

2.6 Properties of Dimethyl Ether

Compounds in which two hydrocarbon groups are bonded to one oxygen, represented as R-O-R', are called ethers. The organic groups bounded to the ether may be alkyl, aryl, or vinylic, and the oxygen can either be an open chain or ring configuration

[75]. Ethers commonly observed in long chain structures are referred to as linear ethers. As compared to alkanes of similar structure, for example if the CH_2 group replaced the O atom , the boiling points of ethers are higher [75]. This class of oxygenated compounds have high cetane numbers and excellent cold flow properties [76].

Simply stated, dimethyl ether is an ether with two methyl groups on each side of an oxygen atom. Today, it is predominantly used as an aerosol propellant due to it not being harmful to the ozone layer in contrast to other aerosols used previously [41]. Also, it is virtually non-toxic and is easily degraded in the upper atmosphere. It can be represented by the symbol: CH_3-O-CH_3. The physical properties of DME are shown in *Table 2–1* along with some comparison fuels [30, 38, 77, 78]:

Table 2–1: Properties of Dimethyl Ether [30, 38, 77, 78]

Property	**DME**	**Diesel**	**Propane**
Chemical Formula	C_2H_6O	$C_{10.8}H_{18.7}$	C_3H_8
Mole Weight	46.07	148.6	44.11
Critical Temperature- °C	127	-	95.6
Boiling Point- °C	-24.9	71-193	-42.1
Vapor Pressure at 20 °C-kg/m^2	5.1	<0.01	8.4
Critical Pressure-bar	53.7	-	43
Liquid Viscosity- cP	.15	2-4	.10
Liquid Density at 20 °C-kg/m^3	668	800-840	501
Bulk Modulus (N/m^2)	6.37E+08	1.49E+09	
Specific Density,gas	1.59	-	1.52
Solubility in H2O at 20 °C g/l	70	Negligible	.12
Lower Heating Value- kJ/kg	28430	42500	46360
Heat of vaporization- kJ/kg 20°C	410	233	426
Explosion limit in air- vol%	3.4-17	1.0-6.0	2.1-9.4
Ignition temperature at 1 atm- °C	235	250	470
Cetane Number	55-60	40-55	-

The properties that are significant to the use of DME as fuel for combustion are cetane number, boiling point, and ignition temperature. However, the properties of concern are viscosity, heating value, and vapor pressure.

To gain an appreciation for the advantages and disadvantages of dimethyl ether, one must understand the properties required for diesel fuels in compression ignition engines. *Table 2–2* below provides some insight [49]:

Table 2–2: Fuel Property Description [49]

Property	**Rationale**
Volatility	High volatility aids cold starting and in-complete combustion.
Flash Point	Higher flash point provides safety in handling and storage.
Cetane Number	Measure of ignitability. The higher the cetane number, the more complete the combustion.
Viscosity	Low viscosity leads to good atomization.
Sulfur	Low sulfur content means low wear in the fuel system and lower total particulate content in the exhaust
Density	The higher the density, the greater is the energy content of the fuel.
Waxing Tendency	Wax precipitation can render cold starting difficult and subsequently stop the engine.

The cetane number describes the ignition quality of the fuel. The shorter the ignition delay the better the ignition quality of the fuel, and thus, the higher the cetane number. Since DME has a higher cetane number than conventional diesel fuel, it will ignite readily and burn more completely.

The viscosity of DME is much lower than that of diesel fuels. This offers an advantage in that the fuel will be easier to deliver into the engine cylinder than diesel fuel during cold weather conditions. However, some studies have shown that the fuel leaks from the injectors [79, 80]. In addition, using neat DME within an engine creates some lubricating problems because of the low viscosity. What researchers are now understanding about the fuels used in automotive fuel injection systems, is that inherent lubricating traits of the fuel are also a very significant factor, especially when additives and alternative fuels are being considered [62, 63, 81, 82].

The boiling point of DME is another important advantage for its use as a fuel. Again, it proves to have better characteristics for cold starting conditions, which is a key factor in engine development. The vapor pressure of DME is a concern. Since the fuel is a gas at atmospheric pressure, and since we need to mix the fuel and inject the fuel as a liquid, the fuel and entire fuel system needs to be pressurized. This leads to other complications with fuel delivery, although the technology to do this is similar in nature to LPG (Liquid Propane Gas) because it is also moderately pressurized to keep the fuel in a liquid state [83].

Another important aspect of combustion emissions from a diesel engine fueled on diesel fuel versus DME, is the reduction and elimination of particulate emissions.

Particulate emissions are also commonly known as “soot” or black smoke. The oxygen content of a fuel blend with DME (at roughly 40 to 100 wt.%), allows for the emissions to be smokeless, as shown in the literature [23, 30, 38, 78, 84-86]. Nabi and coworkers evidence shows “smokeless” engine operation from a diesel fuel with an oxygen content at around 38 wt. % [23]. However, the work by Chen and coworkers confirms that even with 80 wt.% DME addition to diesel fuel, some smoke will be produced at high engine loads, even though it is a small amount [84].

The heating value of DME is a concern, because the heating value of diesel is roughly 1.7 times that of DME. This results in the need for more volume of fuel to produce the same output from combustion. By altering injection amounts to the cylinders, the amount can be compensated to counteract the decreased heating value and prevent “de-rating” of engine output.

Other issues will need to be addressed in future work regarding the understanding of DME fuel properties, including, for example, the lubricity of the fuel. Because of the need for the fuel to be tested while in the liquid phase under pressure, further analysis outside of combustion studies may be impractical or require development of highly specialized instrumentation.

2.6.1 Supercritical behavior of DME

A supercritical fluid is defined as the state of a substance at the point above the critical pressure and temperature of a substance [87]. This is a point at which there is a loss in the distinction between the liquid phase and gas phase. Another way to define the

fluid would be through the use of isotherms from a pressure-volume diagram, when temperature is the critical temperature, T, the following relationship is given in equation 2.4 is given:

$$\left(\frac{\partial^2 p}{\partial V^2}\right)_T = \left(\frac{\partial p}{\partial V}\right)_T = 0 \quad \text{at the critical point} \qquad (2.4)$$

This suggests isothermal compressibility, κ_T, defined in equation 2.5, tends to infinity at the critical point. The symbol κ_T defines the rate of change in volume with pressure at constant temperature.

$$\mathrm{K}_T = -\left(\frac{1}{V}\right) \times \left(\frac{\partial V}{\partial p}\right)_T \qquad (2.5)$$

Therefore, in the critical region, the compressibility is high [87].

Supercritical fluids exhibit characteristics such as compressibility, homogeneity, and continuous changing between gas-like and liquid-like properties, as κ_T tends to infinity at the critical point. [87]. The compressibility of the substance is described by the compression factor, Z, and is defined by equation 2.6 as:

$$Z = \left(\frac{pV}{RT} \right)$$ where R is the universal gas constant

(2.6)

and at the critical point $Z_c = \left(\frac{p_c V_c}{RT_c} \right)$

The critical properties for DME are [88]:

Critical Temperature	T_c =	400 K (126.85 °C)
Critical Pressure	P_c =	5370 kPa (53 atm)
Critical Compression Factor	Z_c =	0.273

A graphical representation of a supercritical fluid is shown in *Figure 2–9.*

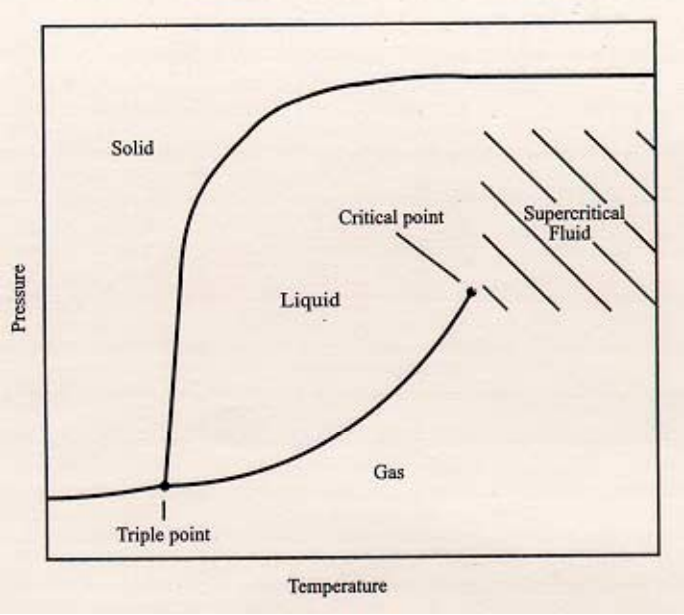

Figure 2–9: The phase diagram of a single substance [87]

In this study, the DME may experience changes in fluid properties as it is drawn into the fuel injector and injected into the engine. The DME and diesel fuel are combined into one miscible fluid at 20° C and 100 psi. Therefore, because the fuel is a mixture, it is assumed that the properties of the two individual fluids combine to yield intermediate property values for the mixture. Since fuel injectors are designed to perform optimally with liquid properties similar to diesel fuel, maintaining the fluid close to the ASTM D 975 specification for No. 2 diesel standard is important. Since temperatures and pressures change throughout the injection process, knowing the temperature and pressure dependencies of the properties of the fluid can give some insight into how the properties of the fuel being injected are changing through the injection process.

2.7 Production of DME

From the production standpoint, if DME does become a replacement fuel in the future, larger production facilites will be necessary. The processes available today to produce DME deliver very small scale quantities. Via the dehydration of methanol, DME is made through a fixed bed catalyst process. Thus, the cost to make DME is more than the cost to make methanol [41]. For DME to become advantageous as a fuel, it must be made cheap enough to compete with diesel fuel costs.

The proposed process for larger scale production would combine methanol and DME synthesis via a single process step for the direct conversion of synthesis gas to DME. This can happen by allowing the methanol synthesis, water gas shift reaction and DME reactions to occur simultaneously. The synthesis involves a series of reactions, which follow via:

$$CO_2 + 3\,H_2 \rightarrow CH_3OH + H_2O \qquad \text{[Reaction 1]} \qquad (2.7)$$

$$H_2O + CO \rightarrow H_2 + CO_2 \qquad \text{[Reaction 2]} \qquad (2.8)$$

$$2\,CH_3OH \rightarrow CH_3OCH_3 + H_2O \qquad \text{[Reaction 3]} \qquad (2.9)$$

The introduction of the DME reaction, equation 2.9 [Reaction 3], serves to help relieve the thermodynamic constraints on the methanol synthesis. Also, the water formed in equation 2.9 [Reaction 3] aids in providing for the equation 2.8 [Reaction 2] , which in

turn provides for the equation 2.7 [Reaction 1]. Therefore, the process is synergistic with high conversion levels [41].

In an effort to determine the short term and long term options for producing DME in mass quantity, scientists at Haldor Topsøe have proposed several methods to utilize existing facilities, as well as new facilities. For small scale production, some recommeded facilities include:

- Direct dehydration of methanol via an adiabatic reactor and catalyst. The reactor would be operated at temperatures between 290 –400 ºC, with the feed rate at 10 bar g. The conversion rate was determined to be 80% for the first pass. Then, DME would be separated via a distillation column.
- Revamp existing methanol plants to make DME as a secondary product by co-producing DME in the methanol synthesis loop.
- Revamp exisiting methanol plants to make DME as the primary product by using a new type of catalyst and a new distillation section.

For medium sized plants, there are several methods to use, and it is recommended to let capacity determine technology. For very large plants, the autothermal reforming of natural gas to systhesis gas is preferred. *Figure 2–10* below shows how this process works [41]:

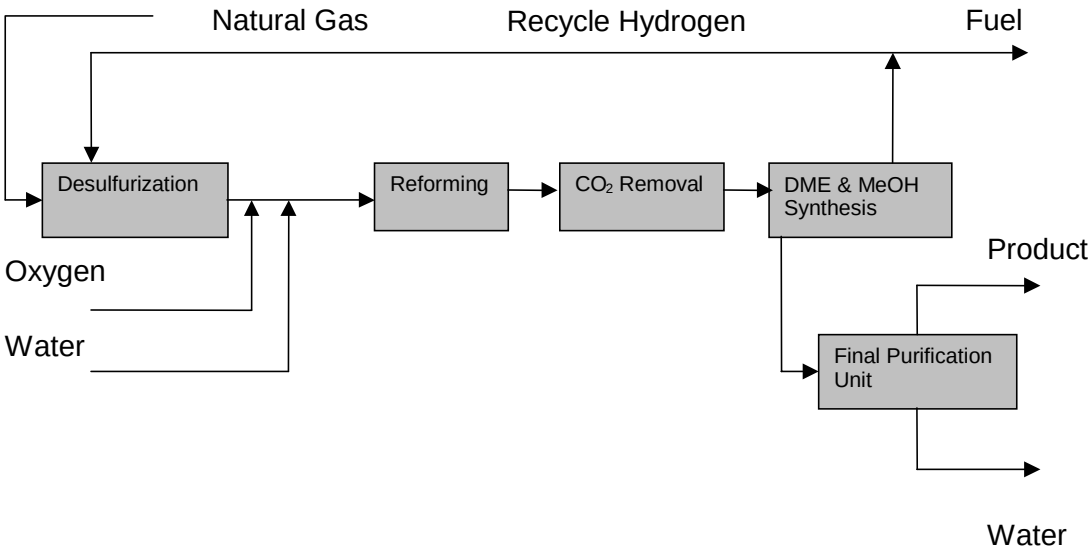

Figure 2–10: Diagram of DME plant based on autothermal reforming [41]

Feasibility studies of the financial cost of DME production in comparison to LNG production confirm the viability of DME as a potential fuel [89]. For a similarly sized plant of LNG compared to DME, operating and capital costs are similar, with transportation costs being an issue for DME for greater than 6000 miles. However, the end fuel costs are very similar to each other, which would then force the application issue to the quality of the fuel for the particular application use.

Another avenue of focus regarding DME is the use of LPDME™ (Liquid Phase DME) , a new fuel process technology created by Air Products & Chemicals Inc. In this process, systhesis gas is converted to LPDME™ in a single slurry-phase reaction using a

physical mixture of a commercial methanol systhesis catalyst and a APCI proprietary catalyst, slurried in mineral oil [40]. LPDME™, through the use of the Liquid Phase™ technology creates a fuel in a liquid phase process rather than a gaseous process. The advantage of this involves controlling the process through heat removal in the liquid, and allows for higher throughput from the reactor. The fuel from the process, which includes DME and, from an additional spearate oxidative coupling process, longer chain linear ethers. These fuels can be used in neat form or as an addative, and are being considered as a cetane improver, and now goes by the name CETANER™. A schematic of this process is shown below in *Figure 2–11*.

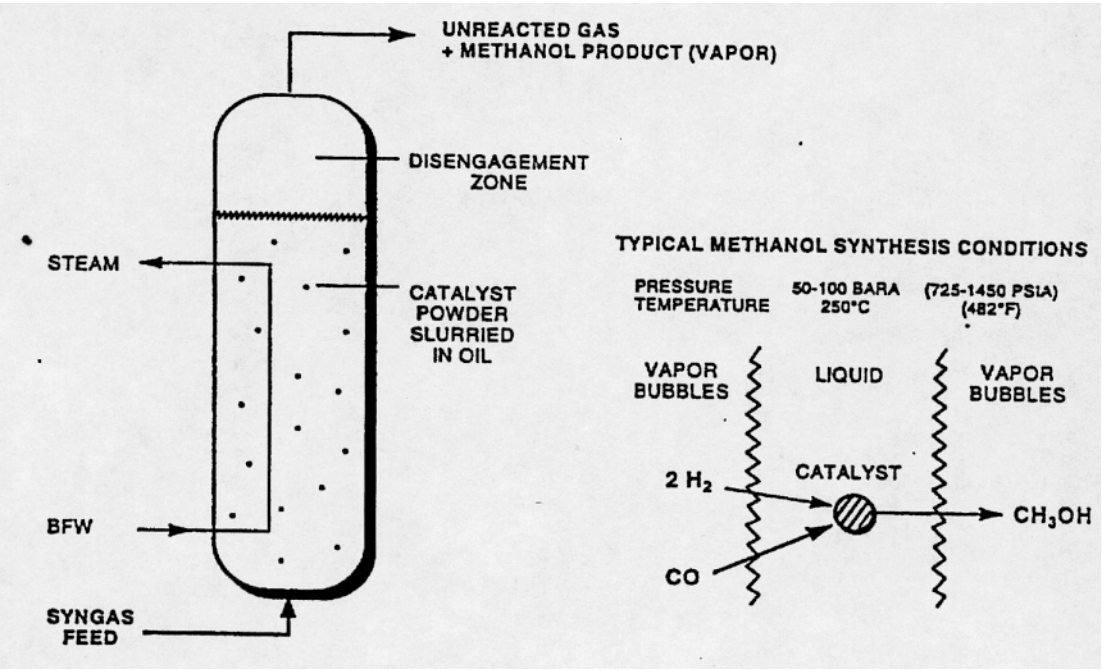

Figure 2–11: Liquid Phase™ Reactor and Reaction Schematic [40]

An important aspect of this process is that it can be incorporated into an Integrated Gasification Combined Cycle (IGCC) facility to fully utilize the capacity of the gasifiers[90]. The Liquid Phase™ technology has been applied for other fuel processing, including methanol, called the LPMEOH™ process[90]. A schematic showing a Once-through LPMEOH™ process design option is shown in *Figure 3–12*.

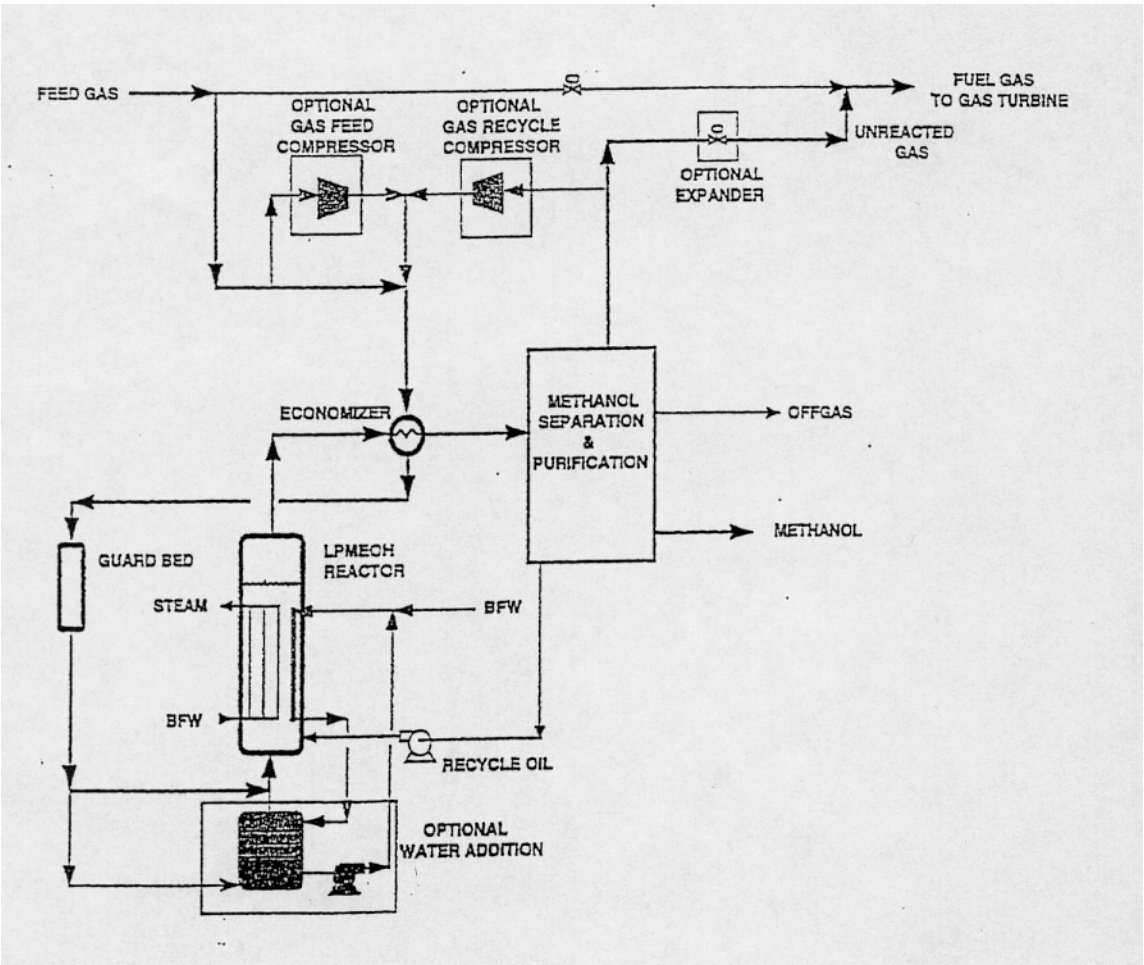

Figure 2–12: Once-through LPMEOH™ Process Design Options [90]

Improving DME processing involves work in several areas. First, understanding how DME is formed leads to improved catalysts, and thus, higher conversion rates. Second, the capital costs for investing in a new facility are significant, and mean that a market needs to be created to demand such an establishment. Finally, creating a market

and addressing distribution issues, even though not addressed in most research, is inherent with any new fuel.

2.8 Research with DME in engine applications

Dimethyl ether is a common chemical used as a propellant for spray cans [26]. The properties of DME are given in *Table 2–1*, and are compared to the diesel fuel used for the baseline testing for this experiment. DME is a liquid when contained under moderate pressure, with a vapor pressure of 5.1 bar at 20°C, and is relatively easy to handle. Over the past ten years, researchers have begun to consider the use of DME as a fuel. Because the cetane number and ignition temperature are close to that of diesel fuel, DME was thought to be an excellent substitute for use in compression ignition engines. However, there were some drawbacks to using the fuel, including the reduced viscosity and lubricity of the fuel in neat form, as well as fuel compressiblity effects [41].

To potentially overcome the fuel property effects of DME, as well as, reduce emissions, the experiments for this study focus on mixing dimethyl ether with diesel fuel. The initial goal is to determine the effect of the oxygen concentration on the emissions, with minimal engine modifications. In this part of the work, no changes have been made to the fuel injection timing, fuel injectors, or engine programming. Changes to the fuel system have been made to allow the fuel to be delivered to the common rail as a liquid by maintaining the DME-diesel blend at over 100 psi.

Over the last ten years, many researches have begun to evaluate the performance and emissions effects of neat dimethyl ether. Sorenson and Mikkelsen [30] found that for a fixed speed and across various loads, the particulate and NO_x emissions from a .273 Liter direct injection single cylinder engine fueled with neat dimethyl ether could be significantly reduced as compared to emissions with diesel fuel. In the same study, the HC and CO emissions showed little or no change. Later, Sorenson and Mikkelsen [91] further studied the HC emissions from this same engine, and found that there was an increase in the HC emissions when using neat DME, with more methane found than in a typical diesel engine, and less light hydrocarbons. With another engine, Christensen and Sorenson [92] looked at various effects on the suite of emissions when using neat DME. Of particular interest, the NO_x emissions were significantly reduced when the injection timing was retarded towards Top Dead Center (TDC). However, there was an increase in the CO emissions, and little effect on the HC emissions. Other tests determined that lower injector opening pressure reduces NO_x, and nozzle types did not seem to influence NO_x emissions. Experiments by Kajitani and coworkers [85] also showed the effects of injection timing on reducing NO_x, which had little effect on HC emissions, from a single cylinder Yanmar engine fueled with neat DME.

However, in the work completed by Hupperich and coworkers [93] with a 1.75 liter single cylinder engine for the ECE R49 13-mode test, the cumulative emissions show some differing results. With the use of neat DME, HC emissions are reduced. The trends with the other emissions are similar to what had been determined with previous studies. One difference to note is the change in injection nozzle size, which may have

affected the emission results in allowing for more complete combustion of all fuels tested in an effort to maintain consistent test conditions.

Recently, experiments completed by Ikeda and coworkers [86] with a single cylinder engine using a binary fuel injection method, showed similar NO_x emissions between diesel fuel and 40 volume % DME mixed with diesel fuel, as injection timing was retarded. Also, HC emissions increased and smoke emissions were reduced as injection timing was retarded. In addition, comparisons were made as a function of BMEP. NO_x was reduced, HC remained constant and smoke increased with increasing Brake Mean Effective Pressure (BMEP). The experiments also included % DME fractions mixed with diesel fuel up to 60 volume % addition, with comparisons made to the baseline diesel fuel. The smoke level, indicating presence of soot in the exhaust stream, showed a slight increase between 0 and 20 % DME addition, and then returned to zero for DME addition over 20%. NO emissions decreased slightly, then increased slightly to the original point for diesel fuel. HC emissions increased slightly up to 45% DME addition, and increased sharply above this point [86].

Many researchers have been evaluating the performance of other oxygenates including blends of glycol ethers with diesel fuel, and have observed decreases in particulate matter emissions with increasing oxygenate concentration. Most recently, Hallgren and Heywood [6] prepared a review of the collection of work which showed that as the oxygen content of the fuel increases, the particulate matter is reduced, suggesting that this occurs regardless of chemical structure or molecular weight. However, their actual testing showed that the oxygenate structure did impact particulate

emissions. Studies completed by Hess and coworkers [15] as well as by Litzinger and coworkers [16, 17] have shown that higher molecular weight glycol ethers are also effective in reducing particulate matter emissions, although to a lesser extent than monoglyme or diglyme.

Although it has been shown that glycol ethers effectively reduce particulate emissions, the fundamental mechanisms of the reduction have not been clearly identified. There has been some work in simulating the ignition and rate mechanism behavior of dimethyl ether in comparison to dimethoxymethane [25]. Also, oxidation mechanisms have been proposed for gaseous forms of DME [38, 94, 95]. More recently, the modeling of DME oxidation has proven consistent with experimental results from jet stirred reactor theory and shock-tube conditions, providing confidence in reaction mechanisms [96].

2.9 Fundamental Property Research on DME

It almost seems like a mythical story. It is true that everyone studying the use of DME refers to this as the beginning of the journey: " New fuel: The lawnmower's tale" [97]. One day, an excited scientist for Haldor Topsøe took some DME home to try in his lawnmower, and had great success. Then, he tried it in a diesel fork lift at the plant, and was astounded when the power was turned off and the fork lift kept running. Again, this supports the finding that DME is a very compressible and ignitable fuel.

Another important aspect of DME that is demonstrated through this tale is the chemical kinetics of the combustion process. It has been demonstrated that the radical reactions during the propagation phase of the combustion process include OH, H and CH_3 [43]. With the presence of the OH radical, the ignition quality is enhanced by making the fuel mixture more reactive, thereby shortening the ignition delay and increasing oxidation rates. When the OH radical was present and DME was provided, the reaction continued. The proposed reaction channels for the presence of the OH radical are equations 2.10 and 2.11 [42]:

$$CH_3OCH_2 + O_2 + M \rightarrow CH_3OCH_2O_2 + M \qquad (2.10)$$

$$CH_3OCH_2 + O_2 \rightarrow 2\ CH_2O\bullet + OH\bullet \qquad (2.11)$$

From other work, the proposed decomposition reactions include the following chain reaction in equation 2.12 [43]:

$$CH_3OCH_3 \rightarrow CH_3\bullet + CH_3O\bullet \qquad (2.12)$$

Then, a CH_3 radical abstracts a hydrogen atom from a second molecule of dimethyl ether by the equation 2.13:

$$CH_3 + CH_3OCH_3 \rightarrow CH_4 + CH_2OCH_3 \qquad (2.13)$$

The resulting CH_2OCH_3 radical then decomposes to formaldehyde and methyl radical, and then finally to formaldehyde and methane, according to the following reactions, equations 2.14 and 2.15 [43]:

$$CH_2OCH_3 + M \rightarrow CH_3 + CH_2O + M \qquad (2.14)$$

$$CH_2OCH_3 + M \rightarrow CH_4 + CH_2O + M \qquad (2.15)$$

Within this study, the author proposed and concluded the following competitive reactions, equation 2.16, through an ab initio study:

$$\begin{aligned} CH_3OCH_3 &\rightarrow CH_3O + CH_3 \\ &\rightarrow CH_3OCH_3 + H \\ &\rightarrow CH_4 + CH_2O \\ &\rightarrow CH_3OH + CH_2 \\ &\rightarrow CH_3OCH + H_2 \end{aligned} \qquad (2.16)$$

Even though there is some experimental and theoretical work for the combustion mechanisms of DME, there is still much work to be done to fully understand the process.

In additon, rate coefficients for the hydroxyl radical reaction have been determined over temperature ranges. This is an important key in preparing a theoretical model of the heat release rate during the combustion of DME. The Arrhenius expression recommended for combustion modelers is in equation 2.17 below:

$$k(295\text{-}650K) = 1.05 \times 10^{-7}\, T^{2.0} \exp[-328/T] \quad (2.17)$$

(in units of cm^3 molecule $^{-1}$ s^{-1})

This study also concluded that the dominant fate of the CH_3OCH_2 radical was the beta bond cleavage between the C-O bond, which finally decomposed to formaldehyde and methyl radicals [98].

Not only has DME been demonstrated theoretically and experimentally to exhibit rapid reaction chemistry, but also DME has been shown to reduce NO and CO emissions [99]. In comparing DME with propane and butane, DME demonstrated reduced CO emissions, and a less striking, NO reduction. It was speculated that this is due to the longer residence time of DME in the flame zone, confirming the speculation about the rapid reaction chemistry.

2.10 Technical Issues with Utilization of DME as a fuel

Much of the early work with DME utilization has been done at the AVL labs in Graz, Austria. The testing concluded that DME does indeed reduce the particulate

emission to zero, and also concluded that the typical diesel fuel injection system does not tolerate DME [79]. Below is a combined list of concerns not only from this testing, but also from other groups who are now working through the fuel property, design and technology issues for utilization of DME:

- DME was leaking past clearances on the injectors and seals. This caused the need for the camshaft housing and crankcase of the engine to be vented [79].
- At high vapor pressure, the DME was cavitating, which caused difficulties in maintaining stable fuel injection .
- While DME is more compressible than diesel fuel, it was found that the compressibility changed with temperature and pressure. Therefore, this made it difficult to inject the maximum fuel quantity at high temperatures and during full load operation using traditional diesel equipment [79].
- DME chemically attacked some seals [79].
- Not much effort has been put towards understanding the environmental impacts of the compound itself or the emissions from the fuel combustion, as compared to other fuels [79].
- A larger fuel tank will be required, as compared to diesel fuel, because of the lower density and heating value of DME [80].
- Since the vapor pressure of DME is low, the fuel vaporizes immediately upon injection into the cylinder. This may or may not be an issue, but further study may be

suggested to confirm how the combustion reaction takes place after the vaporization occurs [80].

- Injection via some fuel pumps causes uncontrollable pressure waves in the entire system [100].
- Predictability of spray behavior and characteristics is important in repeatability of combustion [101].
- Turbulence within the cylinder is important for mixing of the fuel, which in turn reduces emissions [102].

2.11 Health and Safety Concerns

As stated earlier, DME is used as an aerosol propellant. DuPont Fluorochemicals markets DME as Dymel A. With regard to flammability, DME has a higher explosion limit than propane, but it should still be considered extremely flammable and proper caution should be used. DME is a very stable compound, as it does not decompose to peroxides under normal conditions encountered in the aerosol industry. Dimethyl ether is highly soluble in polar and non-polar solvents, which means that it is miscible in water. According to the studies reviewed by DuPont Fluorochemicals, DME has low acute and chronic toxicity. In circumstances of high inhalation levels, the main affect to a person would be of that of a weak anesthetic. From a longer term inhalation study on animals, the exposure level of 20% showed no compound related effects. In summary, DME showed no signs of carcinogenicity, and no evidence of mutagenicity or teratogenicity.

Therefore, it had been given approval for use in consumer products and approved by the DuPont company [103].

Chapter 3

Methodology: Experimental Facility and Combustion Measurements

3.1 Introduction

The key feature of the compression ignition engine is to control the ignition of the fuel to occur at the appropriate time in the 4-stroke process. There is an appropriate point for fuel injection into the engine at which engine power and torque output are optimized in conjunction with minimizing the exhaust emissions [1]. Additionally, this optimal point for fuel injection may change as the engine's speed and load changes. The optimal point for fuel injection is a function of the ignition delay of the fuel, or the time it takes from the moment of injection until a rapid rise in pressure occurs [1]. As changes in fuel composition are made, changes in the ignition delay may occur due to changes in the fuel injection/ mixture preparation process, and changes in the autoignition chemistry of the fuel. To address this conflict between fuel economy and low emissions from a modified fuel, it is important to understand the effect of fuel on the timing of the combustion process, as observed by the emissions, cylinder pressure trace, and heat release rate.

There are many ways to assess the effect of the fuel on the combustion process. In this work, a pressurized fuel delivery system was implemented on a turbodiesel engine to permit operation on DME-diesel blends, and thereby to permit examination of the

impact of DME on the diesel combustion process. Later, information gained from this data will be used to determine how to optimize the engine's operation.

The following discussion provides the specific details of the experimental facility, experimental test procedure, and measurement acquisition. A brief overview of important characteristics of the engine's fuel system will assist in understanding and explaining the information presented in the Results and Discussion section.

3.2 Experimental Design

An experimental facility was designed to permit operation of a Navistar 7.3L "T444E" V-8, direct injection turbodiesel engine on DME-diesel fuel blends, with minimal changes to the fuel system. The following sections describe the engine, modifications to the fueling system and equipment used to quantify the exhaust emissions and effects on ignition delay.

3.2.1 Test Engine

To study the effects of fuel additives on combustion in light-duty to medium-duty diesel engines, a Navistar T444E 7.3L Turbodiesel engine was coupled to a 450 horsepower Eaton (Model AD-1802) eddy-current dynamometer. The specifications of the engine are given in *Table 3–1*. A Pentium PC with Keithley Metrabyte DAS-1800 data acquisition card was connected to the engine to log real-time engine outputs. These outputs included engine crank angle, cylinder pressure, mass air flow, oxygen concentration and engine

load (torque). Additionally, a Modicon Programmable Logic Controller (PLC) was interfaced with the same computer connected to the Kiethly DAS acquisition system. A Visual Basic program was written and used to combine both acquisition system's output into one data collection /storage location, with output streamed into an Excel spreadsheet. The outputs from the PLC included engine speed, torque, and temperatures from the engine. From this data, power was calculated. The Modicon PLC (Programmable Logic Controller) was used to record temperatures from the engine, as well as, from the entire experimental system. Intake airflow rates were measured directly via a Delphi electronic mass air flow sensor (Model No. 25178988; 90.0mm dia. Aluminum inlet and outlet, 74mm dia. throat), which was calibrated using a laminar flow element. Fuel consumption was monitored using a precision Sartorius scale (Model EA60EDE-1), with an accuracy of ± 2 grams. *Figure 3–1* shows the test cell set up, and additional equipment used for emissions monitoring.

Table 3–1: Characteristics of the 1998 Navistar T444E 7.3L Turbodiesel engine [104]

Displacement	444 cu. in. (7.3 Liter)
Bore	4.11 inch (104.39mm)
Stroke	4.18 inch (106.20mm)
Rated Power	190 HP @ 2300 RPM
Peak Torque	485 lbf-ft @ 1500 RPM
Configuration	Turbo charged, Charge air cooled (Air to Air), Direct Injection
Injection Scheme	HEUI- Hydraulically actuated, electronically controlled unit injectors
Low Idle Speed	700 RPM
Features	Split-shot injection (low speed only)
Compression Ratio	17.5:1

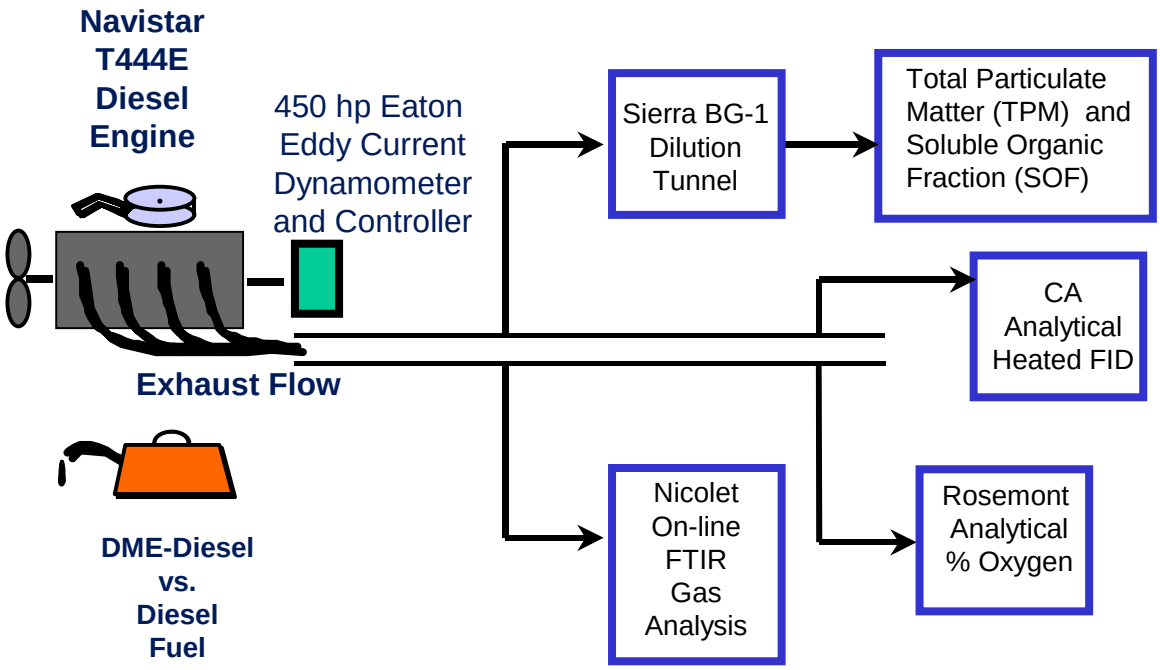

Figure 3–1: Engine Test Cell Set-up, Navistar T444E Turbodiesel

3.2.1.1 Fuel Injection

Most of the modern concepts of fuel injection come from the early developments of Robert Bosch [77]. The Navistar T444E fuel system is based on the unit fuel injector concept. In simple terms, this means that the fuel is pumped from the tank to the fuel gallery that is common (common rail) to a series of injectors. The injector is built so that it times, meters, pressurizes, and atomizes the fuel as it enters the combustion chamber. Additionally, typical systems will use this fuel to cool and lubricate the injectors, while

passing a large portion of the fuel back into the tank. However, the Navistar T444E has a dead head style fuel rail, meaning that no fuel is returned to the tank from the fuel injectors. The fuel remains in the rail until the fuel is used [105].

The T444E engine utilizes a unique fuel injector system developed by Caterpillar, Inc. The injector is commonly referred to as a "HEUI", which means Hydraulically actuated Electronically controlled Unit Injector. A picture of the injector is found below in *Figure 3–2*. The injector is actuated through the use of high pressure engine oil. The pressure intensification is achieved by the design of the injector, as the area of the piston is seven times the area of the plunger. The fuel is injected at pressures from 19 to 120 MPa through a conventional multi-orifice nozzle [29].

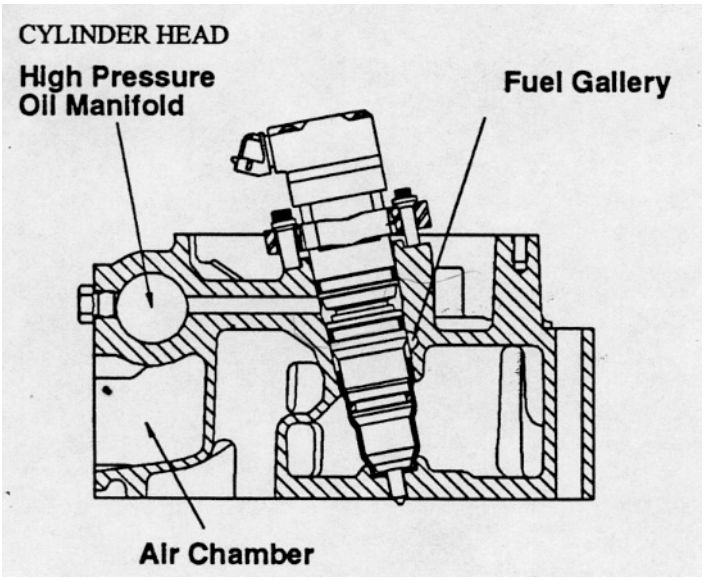

Figure 3–2: Schematic of HEUI Fuel Injector [29]

The injection control pressure is governed by the Electronic Control Module (ECM) through the Injection Pressure Regulator (IPR). As stated above, the pressure is achieved through the use of the engine oil, so the sensors are located in the engine head oil reservoirs. There is a feedback closed loop control on the pressure, accomplished through the use of an Injection Control Pressure Sensor (ICP). The engine control gets information from the ICP on the actual pressure, at all times. The information is then used by the ECM to determine how to adjust the IPR. *Figure 3–3* helps to convey how the ECM operates the injection control system [104]. *Figure 3–4* shows the closed loop operation of the injection pressure control.

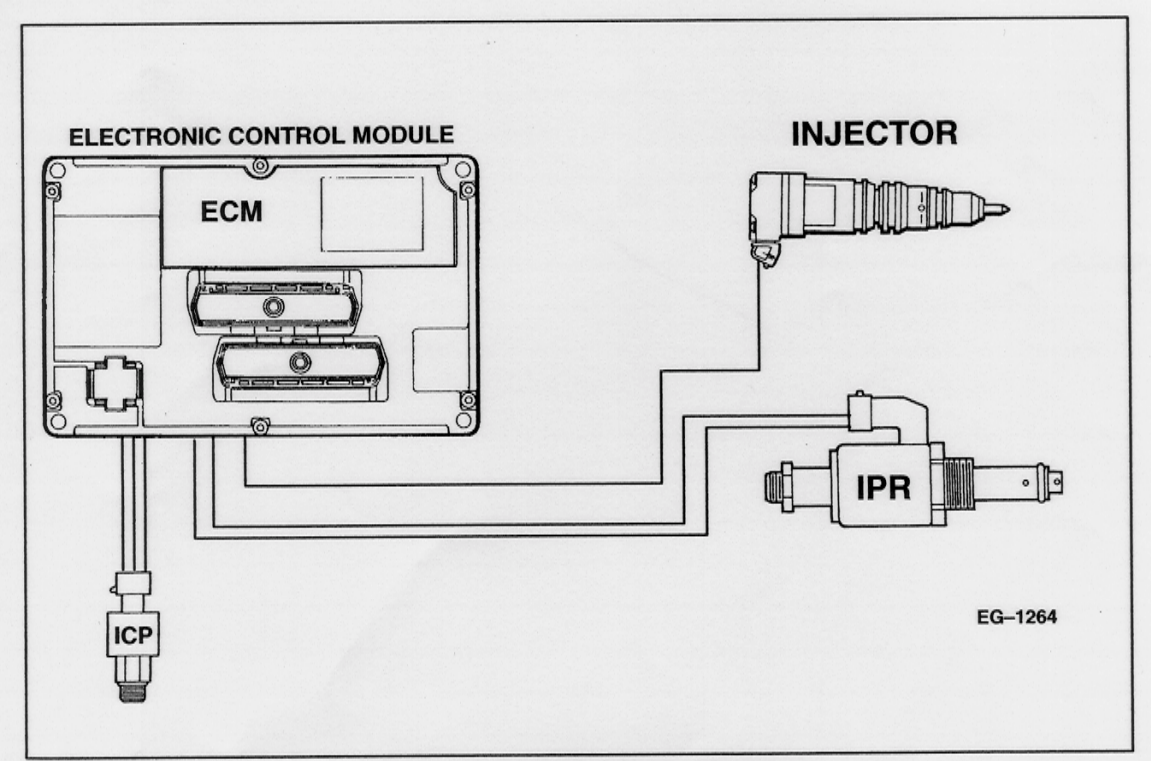

Figure 3–3: Injection Control System [104]

ICP-Injection Control Pressure Sensor

IPR- Injection Pressure Regulator

ECM- Engine Control Module

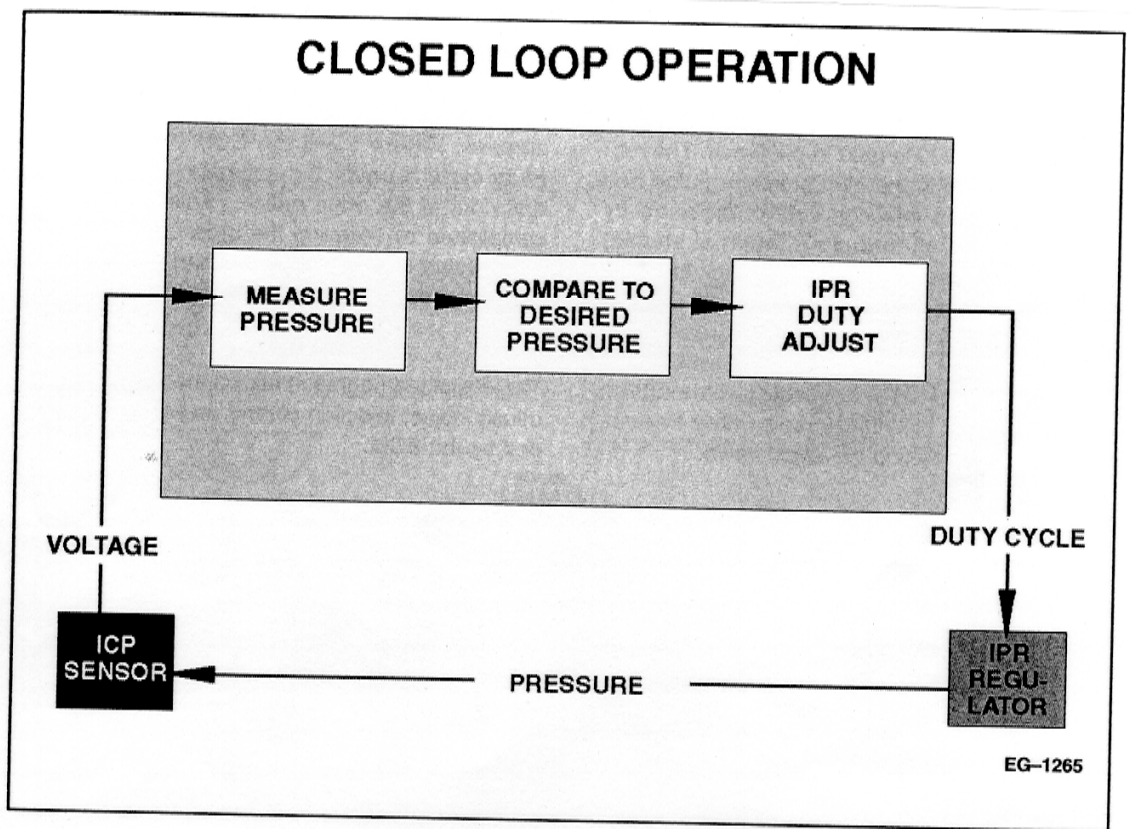

Figure 3–4: Closed Loop Operation [104]

The IPR operates by pulse width modulation (duty cycle %) at a frequency of 400 Hz. The pulse width is modulated from 8-60% to control the pressure from 3.4 to 20 kPa (500 to 3000psi). As the engine demand for pressure increases, the ECM increases the pulse width on the IPR solenoid, which in turn increases the oil pressure. *Figure 3–5* shows how higher injection pressure is commanded [104]. Notice the pulse width in the upper portion of the figure.

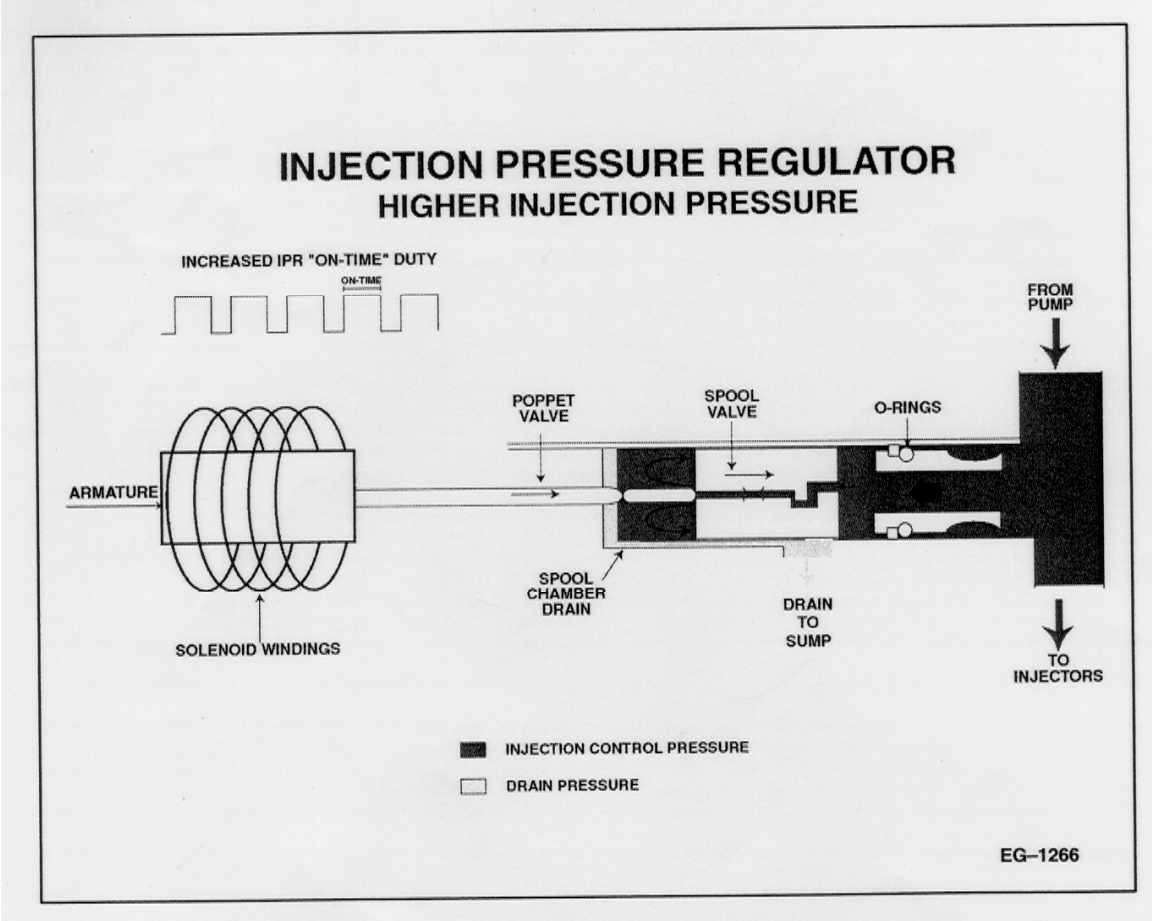

Figure 3–5: IPR Higher Injection Pressure [104]

Figure 3–6 shows how lower injection pressure is commanded. Notice the pulse width duty in the upper portions of the figures. It is the "on time" of the pulse which controls the operation of the armature on the solenoid windings, which in turn opens and closes the spool valve to keep the required pressure. This is the pressure of the injector, in the upper potion above the intensifier plunger. Therefore, this pressure is critical to the injector's operation.

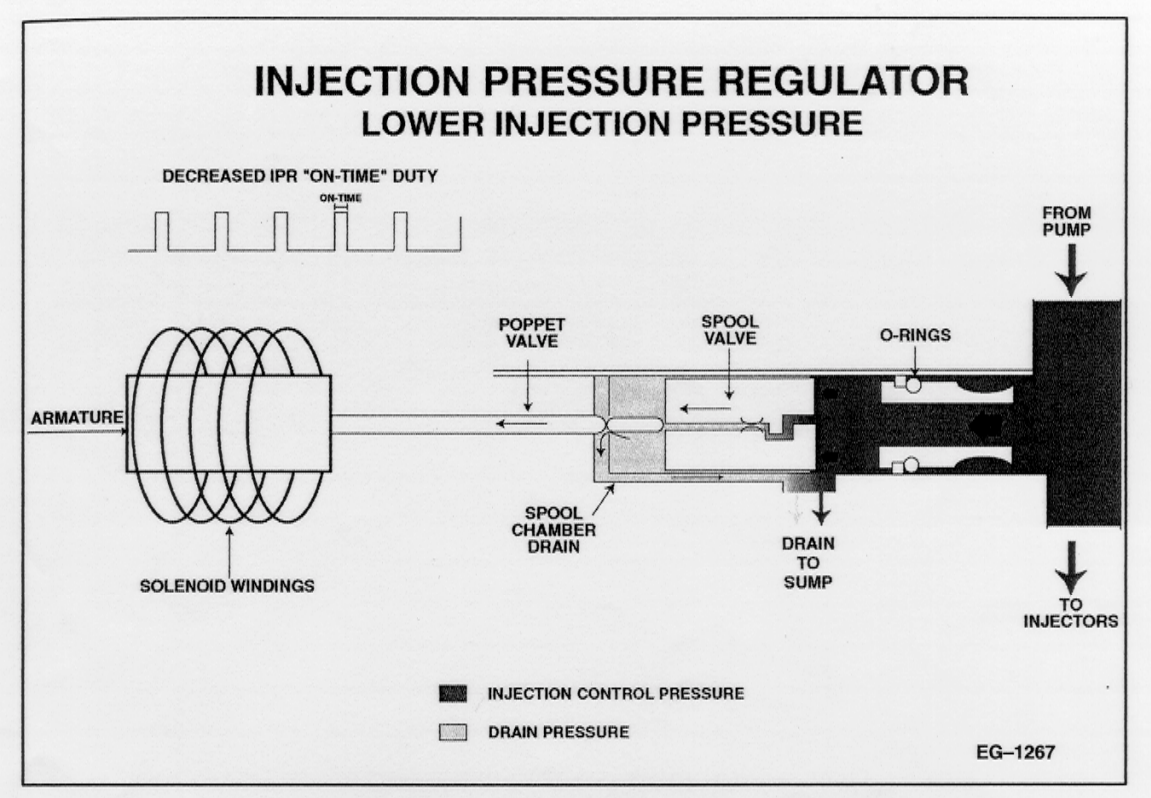

Figure 3–6: IPR Lower Injection Pressure [104]

The operation of the HEUI fuel injector is divided into three stages: fill, injection, end of injection. During the fill stage, the solenoid is de-energized and the poppet valve is in the closed postion, preventing oil from entering the intensifier piston area. Without oil in the intensifier piston area, the piston locates itself in an upper open position, which allows for fuel to flow into the nozzle of the injector. When, the ECM commands injection, the solenoid is energized, which starts the injection stage. The poppet valve is lifted, and high pressure oil enters the intensifier piston area. The pressure is transmitted from the

oil to the fuel and intensified by a factor of 7, creating pressures up to 21,000 psi. This is accomplished by the area of the lower portion being 7 times that of the upper portion. Once the pressure is high enough to lift the needle valve, high pressure fuel is sprayed through the nozzle and atomized into the cylinder. After the injection is complete, the solenoid is de-energized and the high pressure oil leaves the intensifier piston area. The fuel injector returns to the fill stage. *Figure 3–7* shows a pictorial view of the injector and how the stages work [104].

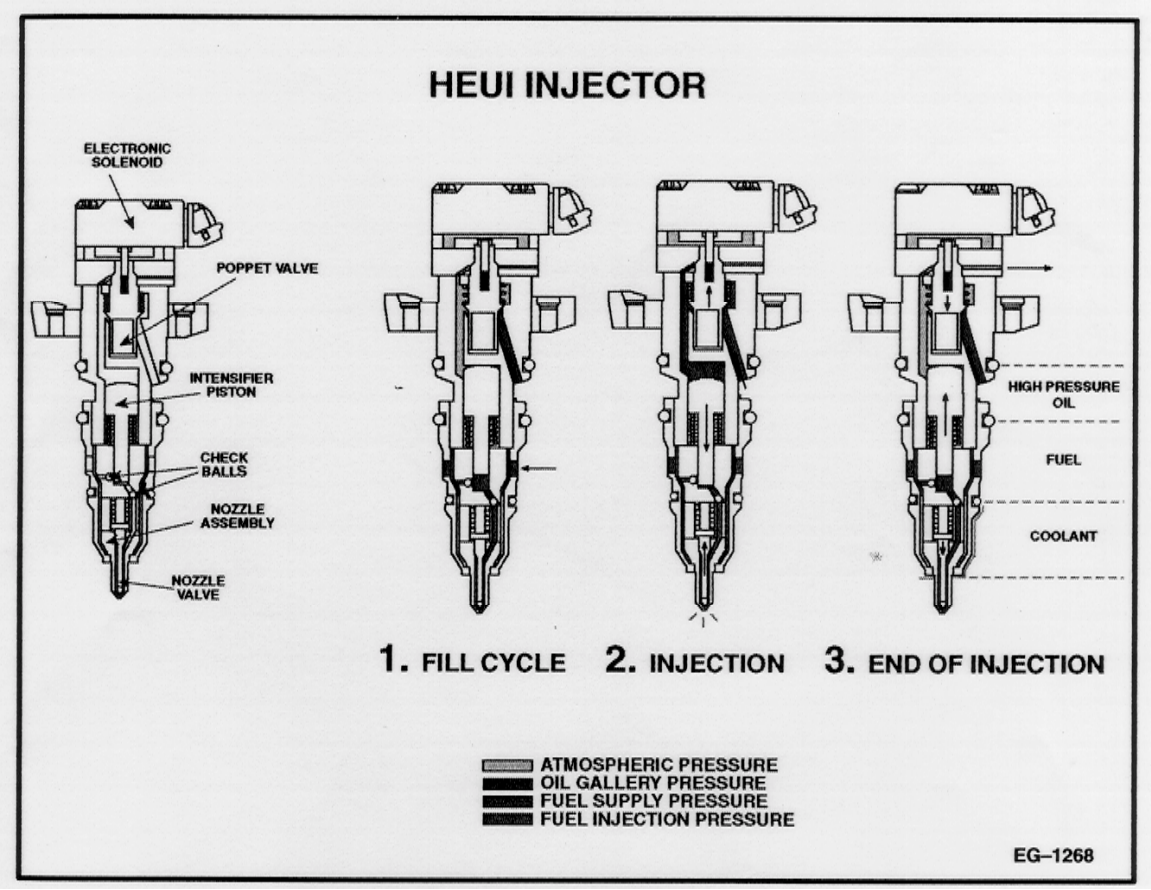

Figure 3–7: HEUI Injector Stages of Operation [104]

3.2.1.2 Turbocharging

The end result of what is known as turbocharging is to increase the mass of air brought into the cylinders of the engine by raising the density of the intake air, and thus allow more fuel to be burnt. The power output of the engine is increased for a given swept

volume of the cylinders. On an engine, a compressor is used to achieve this increase in air density. The system may have either a turbocharger or a supercharger. In a supercharged system, the compressor is driven from the crankshaft of the engine, and thus called "mechanically driven supercharging", or just supercharging [1]. In a turbocharged system, the compressor is driven by a turbine, which is driven by the exhaust gas.

Since the process of compression raises cylinder or charge temperature and pressure, a charge air cooler is used to cool the air between the turbocharger and the intake manifold. This assures that a maximum rise in density is achieved with the pressure increase. *Figure 3–8* shows a comparison between an ideal combustion cycle and a supercharged cycle on a P-V diagram (Pressure- Volume). Supercharing gives the same result as turbocharging, utilizing a different method of compressing the gas. As can be seen, turbocharging causes the inlet and exhaust temperatures to be above ambient, with a total pressure increase throughout the cycle [1]. The figure shows this comparison with what is called a dual combustion cycle. This cycle represents a combination of a constant pressure and constant volume cycle, which is a closer approximation to an actual diesel cycle.

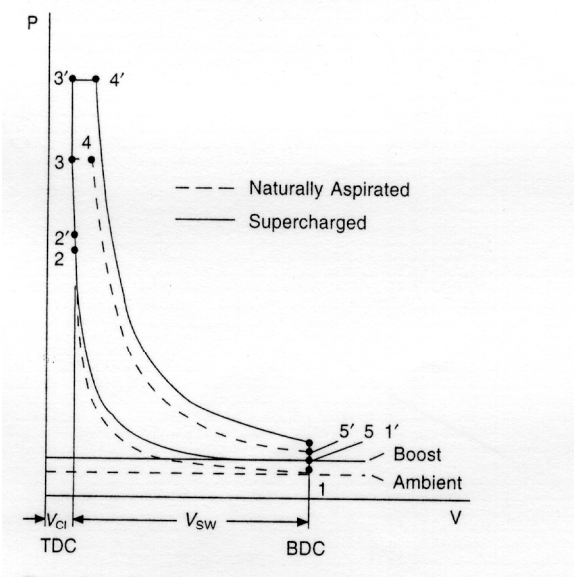

Figure 3–8: Comparison of turbocharged and naturally aspirated air standard dual combustion cycles having the same compression ratio [1]

3.2.1.3 Intercooling

The term intercooling is often used to describe the temperature reduction of the turbocharged charge air. As described above in the turbocharger section, the cooling is necessitated by the increase in temperature associated with the increase in pressure and density of air achieved by the compression effect in the turbocharger. Again, the net goal is to increase the density of intake air, thus providing for more fuel to be combusted [1].

3.2.2 Pressurized Fuel Delivery System for Diesel-DME Blends

Dimethyl ether (DME) is a liquefied gas. At room temperature and atmospheric pressure, it is a gas, but changes to a liquid at a moderate pressure. Dimethyl ether is currently manufactured by DuPont Fluorochemicals under the trade name Dymel A. For the purposes of effective operation of the experimental design, information regarding the vapor pressure, density changes with temperature, viscosity, and miscibility was needed. A portion of this information is reported in *Figure 3–9*, from the DuPont Technical Information (ATB-25) bulletin [103]. However, no experimental data exists for DME-diesel fuel blend properties, which had to be determined experimentally.

Dimethyl ether was found to be miscible with # 2 diesel fuel. Miscibility tests were carried out in a pressurized vessel with a glass observation window [106]. The two fuels were introduced taking care not to physically mix them. Diesel was introduced first into the bottom of the vessel. DME, which has a specific gravity less than diesel fuel, was then introduced on top of the diesel fuel. Thus, initially there were two distinct layers. The two layers were then observed to mix together without physical agitation after a period of 5 to 6 hours to form a homogeneous mixture, at up to 60% DME by mass in the mixture. Furthermore, no separation was observed after standing undisturbed for about 3 days [107].

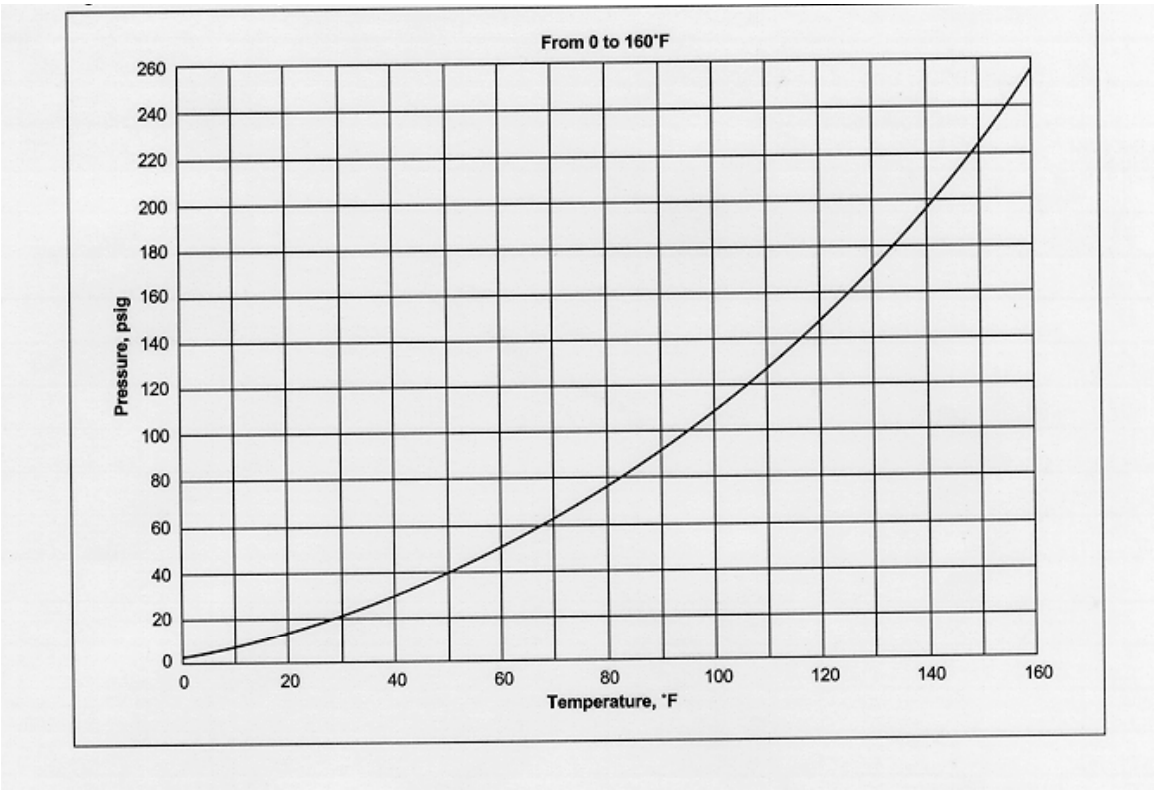

Figure 3–9: Vapor Pressure changes of Dymel A as a function of temperature [103]

Also, *Figure 3–10* shows the changes in density of DME as a function of temperature. This information was used to determine the energy density of the fuel.

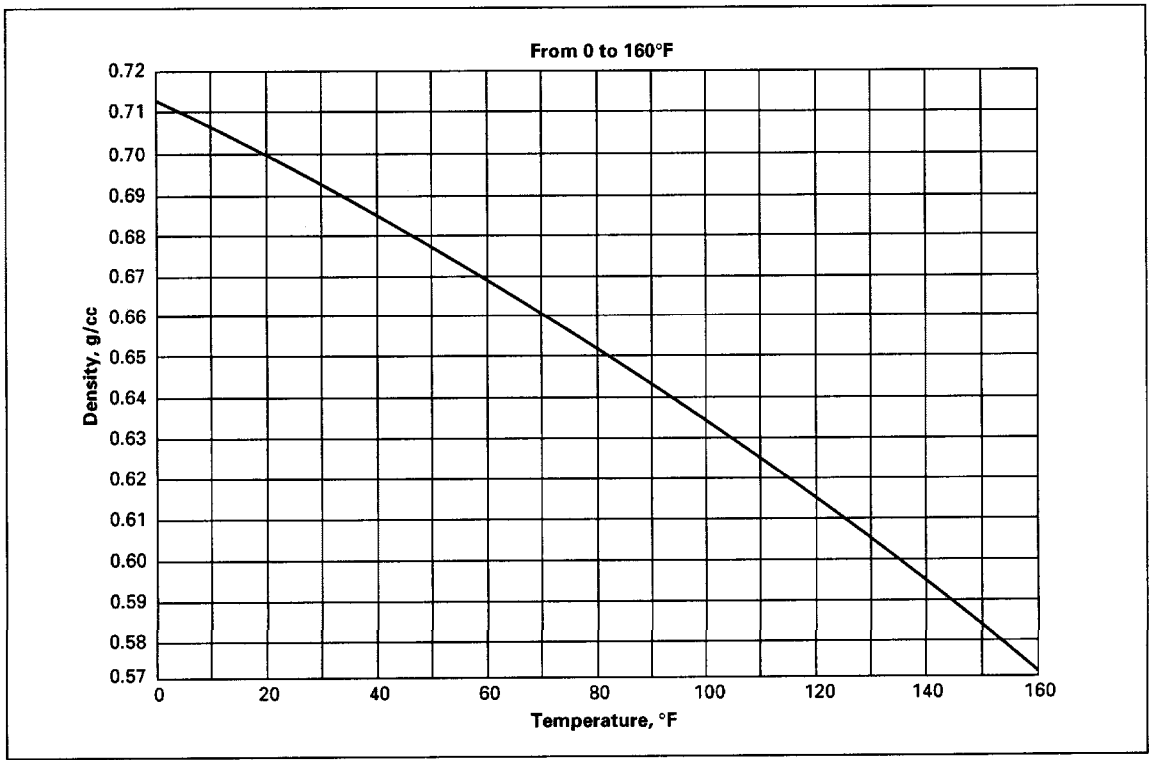

Figure 3–10: Density changes of Dymel A as a function of temperature [103]

A schematic of the modified fuel system is shown in *Figure 3–11* . The fuel system on the T444E engine had to be modified to account for the need to deliver fuel at elevated pressure, because of the vapor pressure of DME at higher temperatures. For the unmodified Navistar T444E engine, the fuel rail in the cylinder head of the engine receives fuel at a pressure of about 70 psi. Fuel from this rail is then fed to the injectors. A study was performed using #2 diesel fuel to measure the temperature rise of the fuel in the fuel rail. This measurement, coupled with the fuel consumption, gave an approximate heat transfer rate between the cylinder head and the fuel in the gallery. A maximum target

temperature of 50°C was chosen for the diesel-DME blend based on the vapor pressure curve of DME and the pressure rating of the fuel rail. This required a change in fuel recirculation flow rate was then calculated based on the above observations. This recirculated fuel was then cooled using a water cooled heat exchanger. The fuel delivery pump was sized based on the required flow that was calculated. Selecting a pump for DME was challenging due to the properties of DME. Gasket material for the pump had to be modified, as common materials such as Viton and buna-N have been found to be unsatisfactory [108]. A fuel filter with a high filter surface area and high pressure capacity was needed. A modified propane filter was selected for the application. The fuel tank consisted of a modified 100 lb capacity LPG cylinder which was pressure tested at 120 psi prior to use.

The fuel delivery system works as follows:

1. The fuel tank is pressurized to between 90 and 100 psi using helium to pressurize the space above the fuel. Therefore, this pressure is the force to drive the fuel from the tank into the engine fuel system which eliminates the need for a fuel transfer pump. The overpressure is necessary to keep the DME in the liquid state. Any inert gas can be used. In this case, helium was chosen because it has a lower solubility in DME than nitrogen.

2. The pressure of the fuel is then boosted by a gear pump to between 120 to 150 psi. A higher pressure allows for the fuel to absorb more heat and still remain in the liquid state. The unmodified rail pressure is 70 psi, provided by the low pressure fuel pump. The fuel injectors fill through a pressure difference created by the rail pressure, regardless of what the pump outlet pressure to the fuel rail is. This higher pressure fuel may be increasing the force present on the fuel o-rings located around the fuel injector. This is important to note because this higher pressure around the sleeve of the injector could cause fuel to leak into the oil portion of the fuel injector line, if after repeated use the o-ring begins to fail.

3. The fuel return loop pressure is held at about 120 to 150 psi, depending on the pressure setting of the back pressure regulator. The regulator is a simple spring loaded valve that regulates the flow to keep the back pressure at the desired setting. A pressure gage was placed upstream and close to the back pressure regulator to verify system pressure.

4. The return fuel then passes through a heat exchanger, where cooling of the fuel after exiting the rail is necessary to keep the temperature of the fuel in the rail below 45 °C.

5. After cooling, the fuel is then fed to a tee in the fuel line, prior to the inlet of the pump. All fuel in this portion of the line is at 100 psi, which is the pressure of the fuel tank.

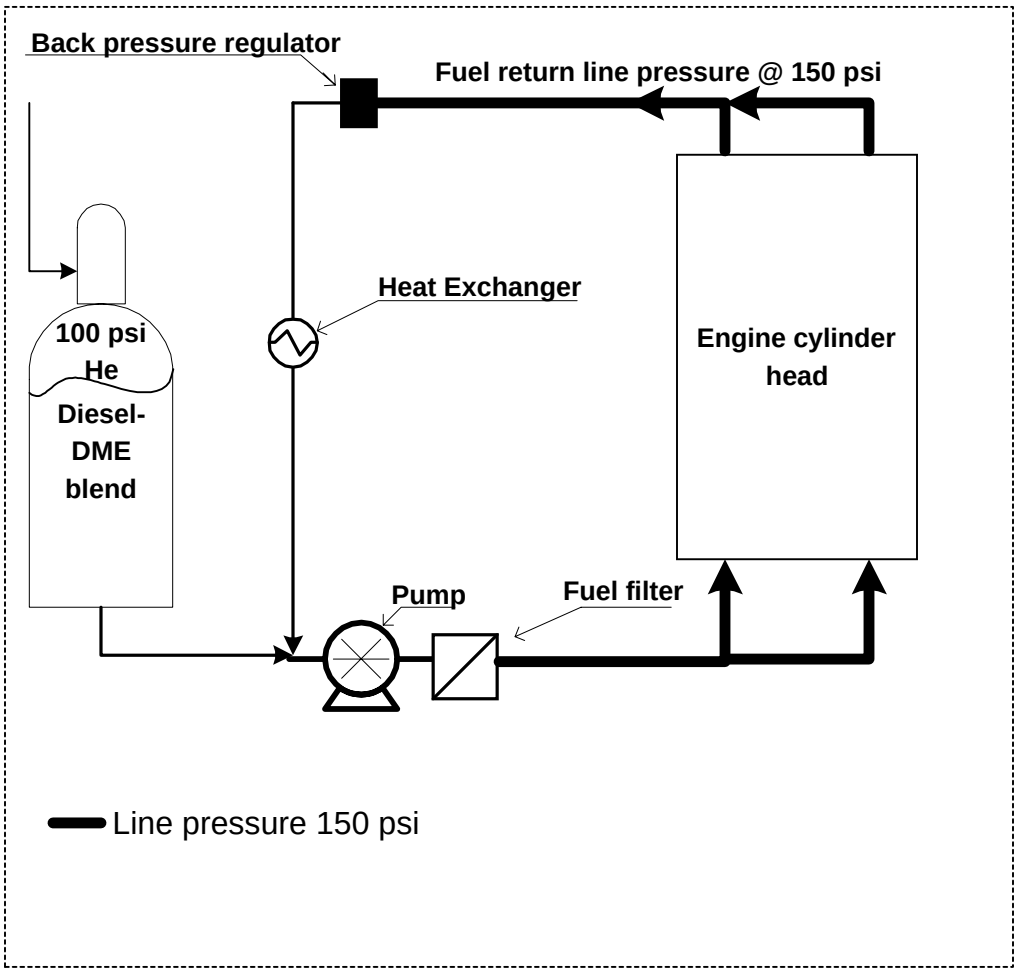

Figure 3–11: Diagram on the pressurized fuel system for the Navistar T444E Turbodiesel engine

3.2.2.1 Pressure, Temperature, and Flow Requirements

At 20°C, the vapor pressure of DME is about 0.52 MPa (75 psia), and is a strong function of temperature. Keeping DME in a liquefied state calls for pressurizing the entire fuel system from the fuel tank up to the fuel injectors. The vapor pressure also changes strongly with temperature. The required pressure of the fuel system is hence dictated by the fuel temperature. The pressure, however, is limited by the pressure rating of the fuel rail. The engine used in the study has a common rail injection system. Both cylinder heads have a fuel rail running along their length, which is the source of fuel for the pressure intensifier in the fuel injectors. In the original fuel system of the engine, the pressure in the rail is maintained at 0.48 MPa (70 psig). This facilitates proper filling of the pressure intensifiers. The fuel rails in the cylinder head form a dead head system. This means that there is no fuel return once the fuel enters the fuel rail. Because of this configuration, the fuel temperature in the rail approaches the engine coolant temperature in the head. This layout of the fuel system was modified to accommodate a fuel return from the cylinder heads.

In designing the experimental facility, a study was performed in which the temperature of the fuel in the fuel rail was recorded in conjunction with the fuel consumption of the engine, for the "AVL 8-mode" test protocol [38]. Approximating values for heat capacities for diesel and DME, a minimum flow rate value was calculated so as to keep the temperature of the fuel in the rail below 50°C. The vapor pressure of DME at this temperature is about 1.0 MPa (150 psi). This pressure, more or less, dictated the allowable temperature rise. The fuel delivery pump was sized based on the above

calculations. Because the cooling provided by the fuel flow rate was not sufficient to keep the fuel in the liquid state, cooling of the returned fuel was necessary to maintain the required fuel temperature. In these tests, a 500 W capacity chiller was used to chill a bath through which the fuel was passed within stainless steel coils. This fuel cooling was insufficient to maintain the fuel temperature below 50°C under some operating conditions, particularly during Mode 8 which is close to rated speed and maximum load of the engine.

The final system has an operating pressure of 150 psi at the back pressure regulator, and the flow rate of the fuel is fixed as it moves through the system. The fuel cooling was insufficient for high load conditions (at the peak load of the engine) at medium and high engine speeds. This indicated further optimization of the system was required.

3.2.2.2 Design Considerations for the Pressurized Fuel System

Dimethyl ether is known to be incompatible with common gasket materials such as Viton and buna-N, used in diesel service, as shown in the Chemical Resistance Guide available at the Dupont-Dow Elastomer website. Data provided by DuPont-Dow, Inc. indicated Kalrez™, a perflouropolymer, (designed and manufactured by DuPont–Dow Inc.) to be the best material for DME. For economic considerations, however, this material was used sparingly for the engine fuel system modifications. Other materials such as butyl rubber, Teflon and neoprene have also been found to be compatible, though

not to the same degree as Kalrez™. Stainless steel was used for the fuel lines as a safeguard against corrosion. All the other components such as valves and regulators were also made of stainless steel.

Selecting a pump for circulating DME was challenging due to the low lubricity and low viscosity of DME. Due to the vapor pressure of DME, the pump housing was required to handle pressures up to 1.7 MPag (250 psig). Positive displacement pumps such as vane pumps, diaphragm pumps and gear pumps were considered. Gear pumps were found to be economical, as well as convenient to operate. With these considerations, a gear pump made by Tuthill Pump Co., California (Model #TXS2.6PPPT3WN00000) was selected. This pump has a magnetically coupled AC motor. This configuration does not have a driveshaft going through the pump housing, which circumvents the need for seals, a potential source of leakage. The gear material is Ryton (Polyphenylene sulphide), which was found to be compatible with diesel and DME as per the data provided by DuPont Fluorochemicals, Inc. The pump body seals are made of Teflon.

The original fuel filters on the engine could not be used because of the high pressure of the modified fuel system. The minimum pressure in the fuel lines was 0.62 MPag (90 psig). This required the use of special filters, which would withstand higher pressure. A diesel water separator was used as a primary filter. This is rated at 0.69 MPag (100 psig). The final filter was an LPG filter rated at 3.4 MPag (500psig). The mesh size of the filter was 2 micron, very near to the engine specification.

The fuel tank was made out of a modified 45 kg (100 lb) capacity LPG cylinder which was pressure tested prior to use. This tank was fitted with a 1/2" NPT fitting at the bottom for liquid exchange.

3.2.2.3 Redesign of the Modified Fuel System

From previous studies on this same engine for the DME-diesel blend providing 2 wt.% oxygen in diesel, the cooling capacity of the heat exchanger and fuel circuit was determined to be insufficient, based on the fuel temperatures recorded, as well as observed engine instabilities [109]. In response to this shortcoming, the system, shown in *Figure 3–11*, was modified by the addition of a second fuel coil in the cooling bath, and a larger chiller unit for cooling the bath. Additionally, the system was pressurized to 150 psi, which then increases the allowable fuel temperature before the DME vaporizes.

Testing with this modified system has continued so as to determine the flow rate and pressure drop through the entire fuel loop. Because the flow conditions in the fuel system are critical, sizing a pump appropriate for maintaining the fuel in a liquid state is essential.

3.2.3 Test Procedure

In this work, an AVL 8-mode test procedure has been utilized as a model for diesel emissions tests. The AVL 8-mode test was designed to correlate to the U.S.

Federal Heavy- Duty Transient Test procedure through a weighted 8-mode steady state test procedure. The 8 modes are a combination of speeds and loads, which when combined with the weighting factors, reports the same emissions output as would be recorded for a transient cycle [38]. For this engine, the test procedure included the speed and load settings shown in *Table 3–2*.

Table 3–2: AVL 8-Mode Test for the Navistar T444E Turbodiesel engine

Mode	**Speed (RPM)**	**Load (ft-lb)**
1	700	0
2	876	84
3	1036	224
4	1212	357
5	2300	77
6	2220	178
7	2220	307
8	2124	409

Another perspective of the testing can be seen in *Figure 3–12*, showing Modes 1-4 within the low speed region and defined by increasing load, and Modes 5-8 within the high speed region of the engine and defined by increasing load.

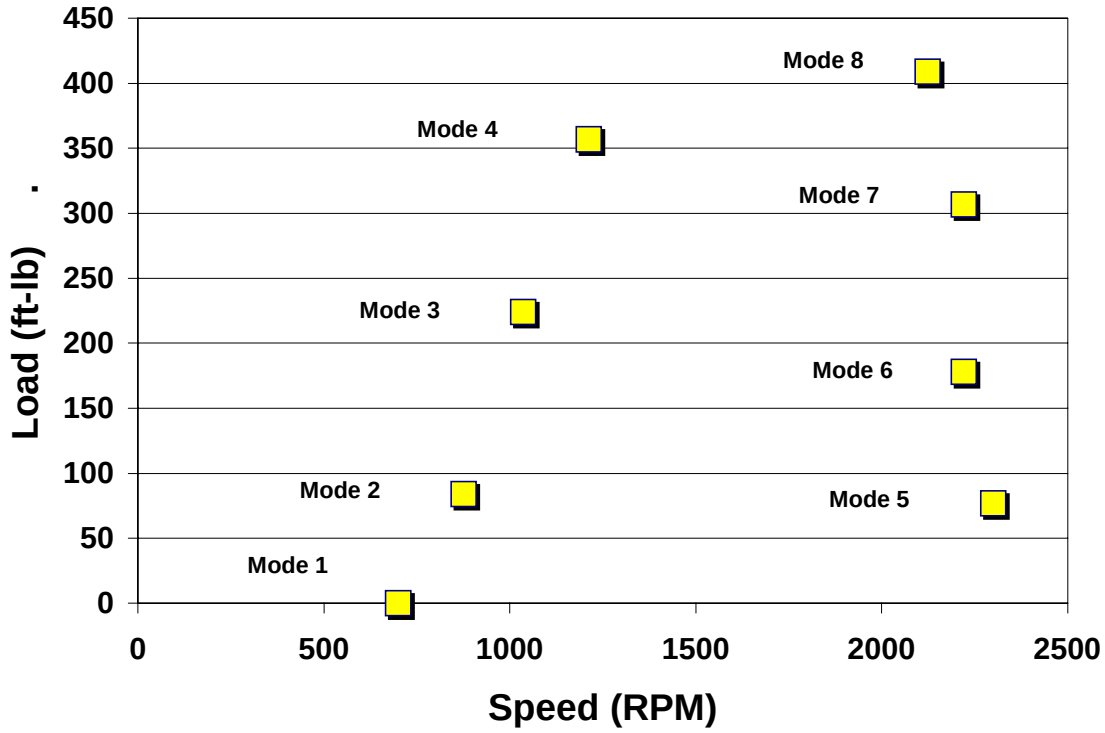

Figure 3–12: AVL 8-Mode Test for the Navistar T444E Turbodiesel engine

3.2.4 Emissions Equipment

An extended warm-up period was used to prepare the engine for testing. The sampling and measurements during each mode commenced when the exhaust temperature reached steady state. During this time, speed and torque were maintained within 2% of the target test conditions. Once steady-state operation was achieved, a

portion of the exhaust gas was passed through a Sierra Instruments BG-1 micro-dilution test stand with a constant dilution air / sample flow ratio of 8:1 and a total flow of 150 liters/min. These settings were chosen in order to maintain the temperature of the particulate sampling below the International Standard (ISO/DIS 8178-1.2) of 52°C [46]. Particulate were collected on Pallflex 90mm filters (Type EMFAB TX40HI20-WW), conditioned in an environmental chamber at 25°C and 45% relative humidity before and after sampling. For reproducibility, five particulate samples were taken for each fuel at each test mode.

Exhaust gas analyses were completed using a Nicolet Magna 550 Fourier Transform Infrared (FTIR) Spectrometer. For each mode, five gas samples were analyzed for CO_2, CO, NO and NO_2. The FTIR has a 2 meter cell, and operating conditions include keeping the cell temperature at 150°C and the cell pressure at 680 mm Hg absolute. The FTIR was calibrated in specific frequency ranges so as to minimize other molecular interferences, especially from water. The species are calibrated for a particular ppm range in the following wave numbers: CO_2 (732.8-766.0), NO_2 (1580.0-1632.0), NO (1850.6-1953.5), and CO (2002.0-2058.8). Also, a Rosemont Analytical on-line O_2 analyzer was used to monitor the oxygen concentration in the exhaust gas. The oxygen readings were used in conjunction with the mass flow sensor to determine and verify the air / fuel ratio. Additionally, total hydrocarbon emissions were monitored using a California Analytical Instruments Model 300 HFID Heated Total Hydrocarbon Gas Analyzer. For the total hydrocarbon measurements, undiluted exhaust gas was collected via a heated sample line, which was maintained at 190°C. Calibration of the

HFID and the Rosemont Analytical on-line O_2 analyzer was completed prior to each day of testing. All other equipment calibrations were checked on a periodic basis.

3.2.5 Pressure Trace Analysis

In order to observe the impact of the oxygenated blends on combustion and heat release, the combustion chamber of Cylinder # 1 of the engine was fitted with a Kistler 6125A pressure probe. The pressure sensor was used with a Kistler 2612 optical crank angle encoder to provide time resolved in-cylinder pressure traces of the combustion event. Pressure, crank angle, and TDC trigger signals were acquired with a Kiethley DAS-1800 data acquisition card operating in a "burst" mode. The pressure traces were analyzed with PTrAn V.02, a software product designed by Optimum Power. The techniques used for the analysis are based on the Rassweiler and Withrow methods, established in 1938 [110]. The methods assess burn rate from measured pressure data by estimating the apparent pressure rise as a result of combustion.

3.2.6 Navistar Engine Control Data

In the process of debugging the engine, it was necessary to purchase the Service Technician Tool which would allow the failure modes of the engine to be observed. The tool allows for communication across the ATA (American Trucking Association) communication lines through one of the established communication languages of the

electronic controls. The tool does allow additional engine parameters to be monitored and for small portions of that information to be logged into the tool itself. The tool has served a great purpose in allowing for the engine to be easily debugged during the start up phase and while operating. It has allowed for understanding of which common failure modes the engine experiences. The tool allows for understanding of the engine operation, so that observations can be made of what may be occurring when the engine will not operate.

3.2.6.1 Automotive Electronic Communication Protocols

In the past, there have been many different types of communication protocols used by automotive and truck manufacturers. Over the past 10 years, a conscientious effort has been made to standardize these methods so as to reduce the proliferation of Service Technician tools, and the amount of software that needs to be programmed into the ECM for the manufacturing facility's test equipment. This in turn helped to reduce the overall cost and complexity of the product by using the least memory necessary. The protocol which is gaining wide acceptance in the industry is called CAN (Controller Area Network). The important aspect of the protocol is that with the correct IC (Integrated Circuit) within the ECM, software can be transmitted serially to the product through the ECM connector. In comparison, in the past, if an ECM needed to be reprogrammed, this was accomplished by sending it back to the factory and programming occurred by probing on the microprosessor pins.

3.2.6.2 Engine Control Module Computer Interfacing

After gaining a brief understanding of the engine control module (ECM) electronics, the complexity of being able to make changes to software calibrations became obvious. Further, after numerous communications with Navistar, the possibility to modify the electronic controls calibration for the DME/diesel fuel blend optimization would cause Navistar a great deal of product liability. Additionally, this would create an open electronic architecture structure, which requires years of research to comprehend. The potential calibration method would potentially cause significant struggle with procuring and building a great deal of expensive hardware to modify only a few parameters. Another option was required.

A compromise was suggested by Navistar which would allow for the minor monitoring and data collection on the engine, while allowing for Navistar to be involved with monitoring modifications and assisting in the development. The suggested course involves using the CAN communication protocol as described earlier. Navistar suggested the purchase of a National Instruments CAN instrumentation board and Labview software. The CAN board allows communication via the ATA data protocol with the ECM. Labview is National Instrument's data acquisition software. It is useful for creating visual instruments, and as one programs the software it operates as if one were assembling simple electrical circuits with inputs and outputs.

Using these two products together, the following was accomplished:

Engine Parameter Programming

The CAN Card together with the modified ECM calibration allows for specific parameters to be modified as the engine is operating. Additionally, the engine control software sends out specific information regarding how the engine is operating.

Parameters Needed for Pressure Trace Analysis

The injection timing is a little more difficult to measure since it is calculated from several tables and is a combination of an internal variable in the ECM as well as the hydraulic delay of the pressurized oil. It cannot be measured directly because the injector firing as given by the ECM lags the initiation of the injector firing due to delays within the fuel injection system that depend on oil temperature and injection pressure. The variable will be logged, but further data will need to be collected to confirm the actual time of the injector firing. The value recorded from the ECM can be used for simple relative comparison.

3.2.6.3 Engine Control Data Acquisition

Because of the throughput on the existing computer at the test cell, another laboratory computer was reallocated to the test cell to serve as the support for the

National Instruments CAN card. A Labview data acquisition program was written with the support of Navistar to send to and to receive data from the ECM.

To gain further insight into the operation of the engine, instrumentation was developed to enable access the engine control signals, and to eventually enable modification of some of them. The following are the signals acquired from the engine control module:

- Volume Fuel desired
- Dynamic Injection timing desired
- Injection Control Pressure
- Manifold Absolute Pressure
- Barometric Absolute Pressure
- Air Intake Temperature
- Engine Speed
- Engine Oil Temperature
- Engine Coolant Temperature

The observation of these signals allowed for an electronic recording of the steady state operation of the engine. Additionally, the CAN system will allow Injection Control Pressure and Dynamic Injection Timing to be adjusted, as programmed by engineers at Navistar. These two parameters are important, because they control the time the fuel injection begins, and the pressure that the injector must build up to force the required fuel

out of the nozzle. Once the correlation between injection pressure, duration and timing are understood, the CAN system can be used to modify the injection for optimization of performance. At this time, the correlation which exists between these parameters is unclear, and will require further work [104, 111, 112].

3.2.7 Test Fuels

Previous work has examined the effects of increasing the percentage of oxygenate mixed with diesel fuels within several types of engines [14-23, 95]. For this work, comparisons are made between a 5 wt. % and 10 wt. % oxygen via blending of DME in diesel fuel. The baseline diesel fuel properties, as well as test fuel properties are given below in *Table 3–3*. Because of the difficulty in obtaining the fuel blend properties for DME as a liquid, the properties available in the literature for neat DME are presented.

Table 3–3: Fuel Properties [30, 38, 77, 78]

Property	**DME**	**Diesel**	**Propane**
Chemical Formula	C_2H_6O	$C_{10.8}H_{18.7}$	C_3H_8
Mole Weight	46.07	148.6	44.11
Critical Temperature- °C	127	-	95.6
Boiling Point- °C	-24.9	71-193	-42.1
Vapor Pressure at 20 °C-kg/m^2	5.1	<0.01	8.4
Critical Pressure-bar	53.7	-	43
Liquid Viscosity- cP	.15	2-4	.10
Liquid Density at 20 °C-kg/m^3	668	800-840	501
Bulk Modulus (N/m^2)	6.37E+08	1.49E+09	
Specific Density,gas	1.59	-	1.52
Solubility in H2O at 20 °C g/l	70	Negligible	.12
Lower Heating Value- kJ/kg	28430	42500	46360
Heat of vaporization- kJ/kg 20°C	410	233	426
Explosion limit in air- vol%	3.4-17	1.0-6.0	2.1-9.4
Ignition temperature at 1 atm- °C	235	250	470
Cetane Number	55-60	40-55	-

3.3 Data Analysis

After all testing was completed, the data were analyzed through the use of several methods. As described above, there are three data collection mechanisms, each handled independently and differently. The following section will briefly describe how each data set is handled and what observations are expected.

3.3.1 Steady State Engine Data

To confirm that the engine was operating in a steady state condition, a variety of data were recorded while the engine was running. These data include:

- Speed
- Torque
- Power,(calculated from speed and torque)
- Ambient temperature
- Coolant Temperature
- Oil Temperature
- Exhaust Temperature
- Dyno Water Temperature
- Charge Air Cooler Temperature
- Fuel In Temperature
- Fuel Out Temperature
- Mass Air Flow

The primary use of these data is to confirm that the engine conditions were similar for each fuel blend tested, or within a range of about 2%. These data can also be used to explain emissions results and how they may be related to changes in fuel properties. Additionally, the fuel temperatures are useful in diagnosing the DME behavior in the injector. Charge Air Cooler exit temperature is monitored before the air goes into the

cylinder, after the turbocharger, which indicates air density into the engine. Other temperatures collected can be compared to the data collected from the engine control, as an indication of the calibrated data algorithm. Of these, the engine oil temperature would be most important to note, as it directly affects the injection timing and pressure.

3.3.2 Engine Control Data from the CAN Communication Line

The primary use of these data is to flight record the engine's steady state operation, as the engine is operated on the different fuel blends. The most important values are injection timing and pressure, and volume of fuel desired. These show how engine operation was changing based on the fuel energy density change. What should also be noted is that changes in oil temperature can also affect the injection timing and pressure. Therefore, it is important to note these and compare at each mode tested. A secondary use for these data will be to determine how to optimize the engine to improve emissions reductions and performance. A final use was to flight record the engine operation when changes were noticed in engine behavior, such as metallic sounds from the injector, and erratic speed changes.

3.3.3 Pressure Trace Analysis

The primary use of pressure trace data is to assess the changes in the combustion process due to the change in fuel type. The changes to be observed include: heat release rate, ignition delay, pressure rise as fuel is injected, and any indication that the fuel may

be leaking past the injector causing pressure pulses where they should not be. The PTrAn software, provided by Optimum Power Technology, will process the data to calculate IMEP (indicated mean effective pressure) and mass fraction burned. The output includes pressure trace and burn rate curves for each cycle of the process, or as an average. Since the processing is for a diesel engine, a double Wiebe function is used to fit a mathematical expression for the mass fraction burned for the two phases of combustion, pre-mixed and diffusion [44, 113]. The general form of the Wiebe function is given in equation 3.1 as:

$$x(\theta) = 1 - e^{-a\left[\frac{\theta - \theta_O}{\Delta\theta}\right]^{m+1}}$$

where $x(\theta)$ is the mass fraction burnt at crank angle θ
θ_o is the crank angle at the start of combustion
$\Delta\theta$ is the duration of combustion
and a and m are constants that can be varied so that a computed P-V diagram can be matched to a particular engine

(3.1)

Heat release analysis is accomplished through the use of the equation 3.2 given below from Heywood [44]:

$$\frac{dQ_n}{dt} = \frac{\gamma}{\gamma - 1} p \frac{dV}{dt} + \frac{1}{\gamma - 1} V \frac{dp}{dt}$$

(3.2)

where γ is the ratio of specific heats c_p/c_v

The contents of the cylinder are modeled as an ideal gas to arrive at this equation. This calculation is performed separate from PTrAn, as the software is not currently capable of this computation.

Chapter 4

Results and Discussion

4.1 Introduction

The objective of the research was to demonstrate that a Navistar T444E engine could be operated with blends of DME in diesel fuel with minimal engine changes. In this study, the engine was shown to operate with blends of 5 and 10 wt. % oxygen, with an appropriate fuel system design. In this section, detailed results are provided for the effect of the oxygen addition on emissions. Through an uncertainty analysis, based on methods described by Moffat, error bars showing the 95% confidence intervals are presented in each figure showing exhaust emissions [114]. A repeatability study was performed on the steady state operation of the engine for a particular mode to confirm the deviations within the data. Fuel injection timing and fuel injection pressure collected from the engine computer are used to explain the emissions data, and complications during engine operation. Additionally, pressure traces and heat release analysis for one mode are used to show how the ignition timing has changed with the addition of DME to the diesel fuel. Finally, general observations of engine operation will be detailed and explained.

4.2 Fuel Property Data

Fuel property data are available in *Table 4–1* to permit comparative analysis of the combustion data. Several data points have been projected as a linear combination because the fuel properties are not able to be determined with available instrumentation.

Table 4–1: Fuel Property Data [30, 41, 92]

Fuel Property	ASTM Method	ASTM Spec.	Base Diesel	Neat DME	25 wt. % DME in Diesel
Viscosity,40°C (cSt)	D445	1.39-4.2	2.2	.25	.92[106]
API Gravity	D287	API 30	35.3		
Cloud Point (°F)	D2500	<0	4		
Pour Point (°F)	D2500	<0	<0		
Flash Point (°F)	D93	125	166	-42	
Calorific Value (BTU/lb)	D2015	19700	19483	12228	17669 *
Boiling Point (°C)			180-370	-24.9	
Critical Pressure(bar)			---	53.7	
Critical Temperature (°C)			---	127	
Ignition Temp. (°C)			250	235	
Vapor Pressure – bar (°C)			<.001	5.1 (20°C)	
Bulk Modulus (N/m^2)			1.49E+9	6.37E+8	
Centane Number	D613	46-48	47	>55	
Density (gm/ml) (20 °C, various P)	D4052	.845-.855	.84	.66	.79 *

* projected

4.3 Particulates

As noted previously, oxygenates traditionally reduce particulate emissions, supposedly through reducing the overall temperatures in the engine, and through chemically changing the composition of the radical pool, thereby inhibiting the formation

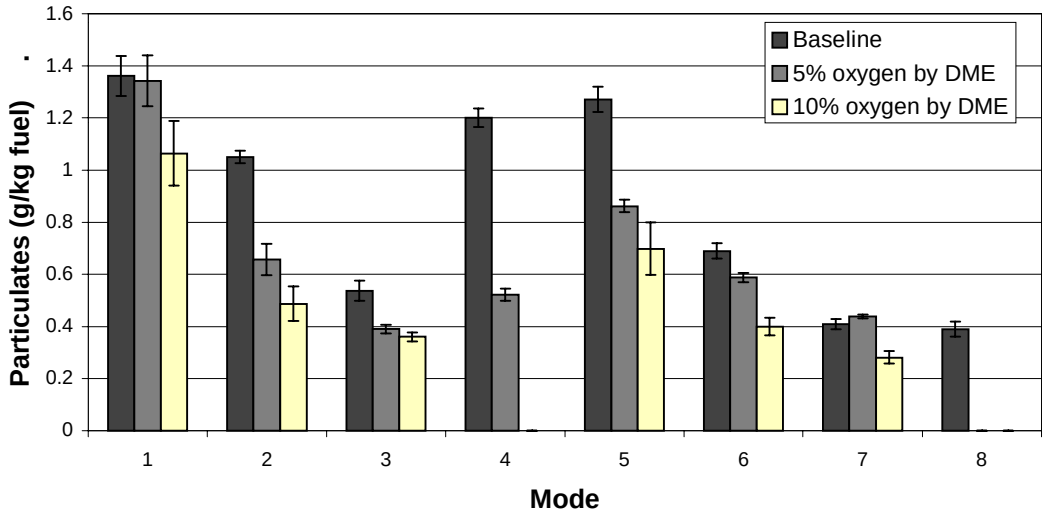

Figure 4–1: Particulate Matter per unit fuel consumed, g/kg fuel

of soot [17]. The data indicate a particulate matter reduction for all test modes, as shown in *Figure 4–1*. Using the AVL 8-mode test protocol, the net particulate emission reductions for each mode are found in *Table 4–2*. Because the engine was not able to be operated for Modes 4 and 8 for each additive, the data is presented in a mode by mode

comparison. For most modes, shown in *Figure 4–1*, particulate reductions were observed on the basis of grams particulate matter emitted per kilogram fuel consumed. As the engine load was increased with increasing engine speed, as in Modes 1 to 4 and Modes 5 to 8, the particulate emission was lowered for each fuel blend as compared to the original baseline diesel fuel, except for Mode 7.

Table 4–2: AVL 8-mode Weighted Emissions Results per mode, Brake Specific Basis

Particulate Emissions Per Mode	**Baseline Diesel (g/bhp-hr)**	**5wt. % oxygen via DME (g/bhp-hr)**	**10wt. % oxygen via DME (g/bhp-hr)**
1	3.36	3.44	2.87
2	.224	.149	.118
3	.091	.069	.082
4	.209	.095	NA
5	.339	.255	.214
6	.137	.128	.092
7	.078	.086	.057
8	.068	NA	NA

The effect seen in Mode 7 by comparing the baseline diesel to the DME-diesel blends may be due to a change in the injection timing. As shown in *Figure 4–2* and *Figure 4–3*, the injection timing and injection pressure were changing as commanded by the engine

control for changing speed and load. This is true for the low as well as the high engine speeds. The trend does not follow what would be expected based on the work by Kajitani and coworkers [85]. Their work showed that as the mean effective pressure increases, which correlates with increasing load for an engine speed of 960 RPM combusting diesel fuel, so do soot emissions based on the Bosch Smoke Number. In their work, the DME emissions were close to zero over the same mean effective pressure range. In the research performed by Ikeda and coworkers on a single cylinder engine operated at 75% of the rated speed, the same pattern was observed for the baseline diesel fuel as in Kajitani's work. For a DME-diesel fuel blend (40% DME), the Bosch Smoke emissions were shown to increase at a faster rate than the diesel fuel, as the mean effective pressure increased [86]. From an additional set of experiments performed by Kajitani and coworkers, again, the Bosch Smoke number increases as mean effective pressure increases [84]. Additionally, the smoke number decreases with increasing oxygen addition via DME [84]. The study was performed with several blend levels of DME and diesel fuel, and is consistent with the trend of particulate reduction in this thesis.

In the research work presented in this thesis, with increasing content of DME, generally, the soot emissions decrease over a range of speed and load conditions. The trend in particulate emissions reduction using the AVL 8-mode test is similar to the trend observed by Hess and coworkers for each mode, even though the research was conducted with a different multicylinder engine [115].

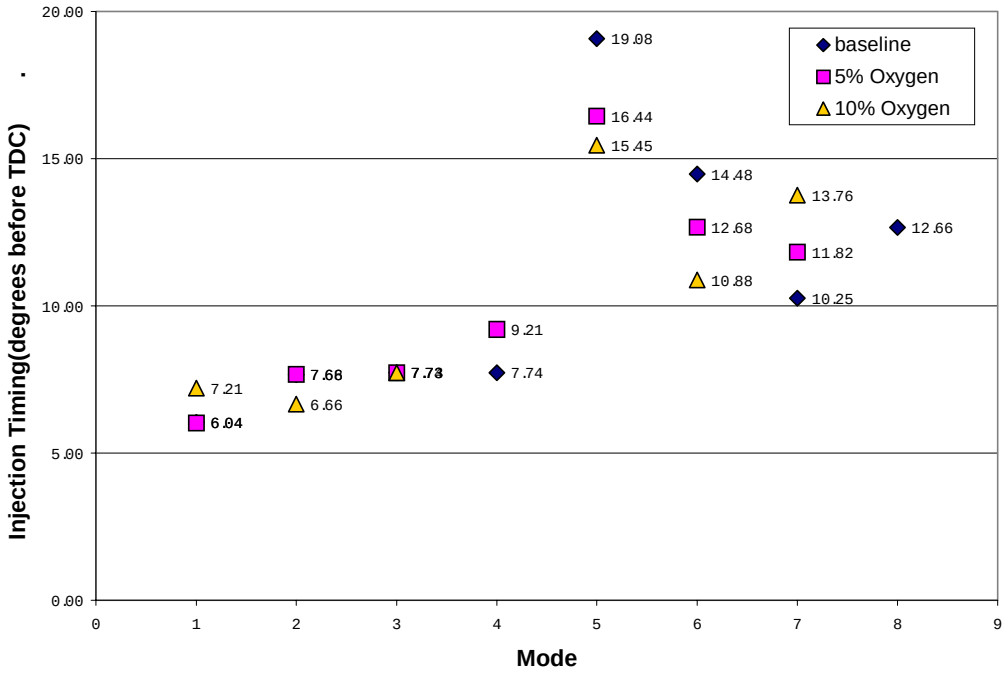

Figure 4–2: Engine Injection Timing

* Injection timing is relative to the number of degrees before 0 degrees: TDC (Top Dead Center)

As has been shown in previous work by Liotta and co-workers, this particulate reduction is due to a reduction in the soot portion of the emission, and would result in a percentage increase in the soluble organic fraction (SOF) portion [11]. This has also been confirmed more recently by Sidhu and coworkers [116], with DME giving the highest SOF.

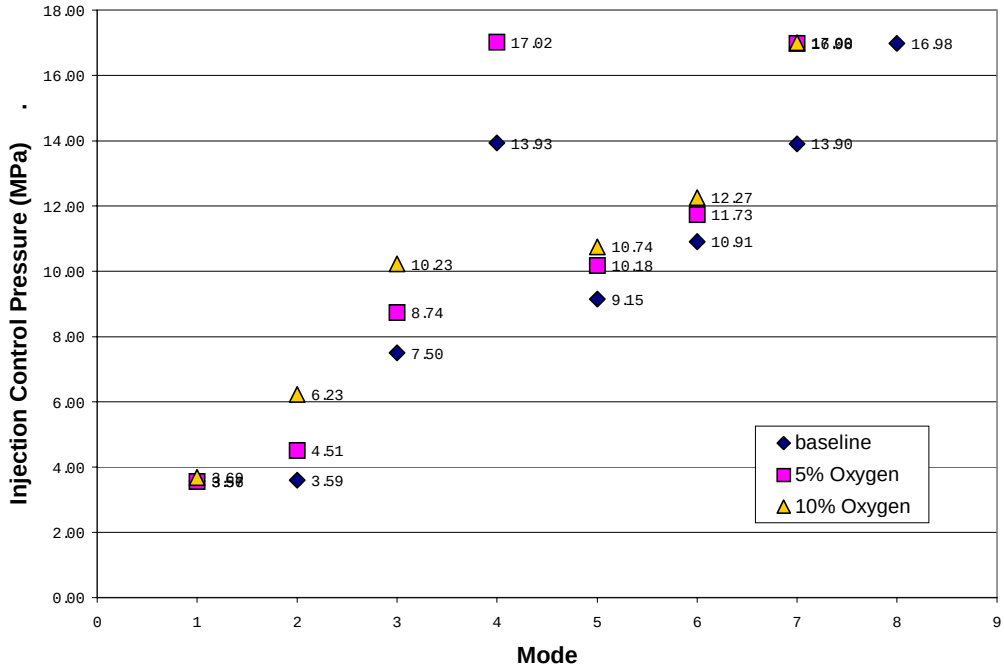

Figure 4–3: Engine Injection Pressure

In this research work, the addition of DME into diesel fuel provided a dilution effect of the sulfur content of the final fuel blend. Therefore, it should be noted that the reduction in PM content may also be due to a reduction in the SOF portion of the total PM.

Figure 4–4 shows the injection pressure versus engine load. A difference in the injection pressure for a specific engine speed and load can be observed. At higher engine loads, the injection pressure reaches its maximum for this specific engine configuration, regardless of the engine speed.

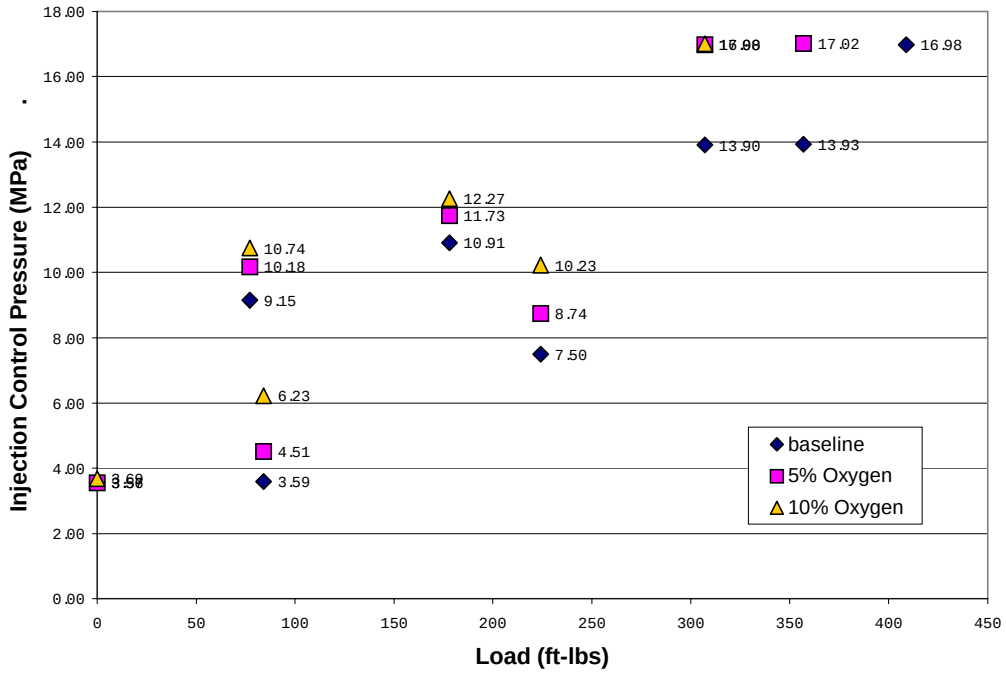

Figure 4–4: Injection Pressure (MPa) versus engine load (ft-lbs)

4.4 Oxides of Nitrogen (NO_x)

Table 4–3 reports the weighted brake specific NO_x ($BSNO_x$) emissions. *Figure 4–5* shows that at lower engine loads, the DME-diesel fuel blend causes a decrease in

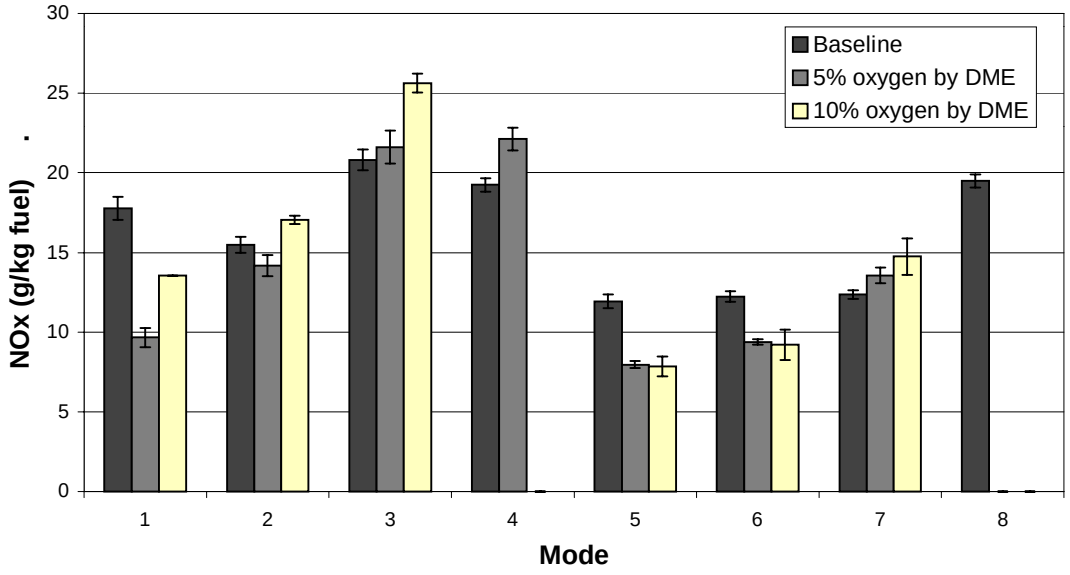

Figure 4–5: NO_x Emission Results per unit fuel consumed, g/kg fuel

NO_x. This is seen in Modes 1,5 and 6, but not for all fuel blends in Mode 2. What is observed in Mode 2 may be the result of an increase in injection pressure without a change in injection timing, causing a change in the fuel plume as it exits the nozzle opening. At higher engine loads (Modes 3, 4 and 7), NO_x increases. Heywood suggests that NO and NO_2 are a function of equivalence ratio [44]. As equivalence ratio approaches 1 from the lean side,the excess of combustion air decreases, combustion

temperature increases, and NO_2 and NO emissions increase. Above an equivalence ratio of 1, the mixture becomes fuel rich, the pool of O and N decreases and the destruction by CH_x increases, thus the NO_x emissions are lower. Equivalence ratio is defined by equation 4.1 below:

$$\phi = \frac{(F/A)_{actual}}{(F/A)_S}$$

where F is fuel

A is air (4.1)

S is stochiometric ratio

Also, $\lambda = \frac{1}{\phi}$

However, NO_x is also a function of temperature and time. It is unclear in the data whether the increase or decrease in NO_x is a function of equivalence ratio, time, temperature, or injection timing.

Table 4–3: AVL 8-mode Weighted Emissions Results per mode, Brake Specific Basis

NO_x Emissions Per Mode	**Baseline Diesel (g/bhp-hr)**	**5wt. % oxygen via DME (g/bhp-hr)**	**10wt. % oxygen via DME (g/bhp-hr)**
1	43.91	24.74	36.54
2	3.31	3.21	4.14
3	3.52	3.85	4.80
4	3.35	4.01	NA
5	3.18	2.36	2.40
6	2.44	2.05	2.11
7	2.37	2.67	2.99
8	3.42	NA	NA

As can be seen in *Figure 4–2*, the injection timing of the engine was changing so as to increase the amount of fuel to meet the speed and load conditions. Mode 3 was the only mode where the injection timing did not change, and shows that the NO_x does increase with DME addition. However, injection pressure was increasing so that the required fuel energy could be injected into the cylinder over the same crank angle timing. This increase in injection pressure, as well as the longer fuel spray duration may explain the increase in NO_x. Because of DME's vapor pressure, as the fuel is injected into the engine, the DME may be acting to break apart the diesel fuel into a finer spray, and entraining more air into the edge of the fuel plume. The blended fuel has a lower density

than the diesel fuel, and the viscosity of the fuel blend has also changed. This may be increasing the premixed phase of combustion, causing less of the combustion process to be diffusion-controlled because the fuel is vaporizing and igniting so quickly, with minimal time for mixing. Additionally, more fuel volume is being injected to maintain speed and load conditions. So, there could be some small increase in NO_x emissions for this reason. In *Figure 4–10,* the brake specific energy consumption shows that the same amount of fuel on an energy basis is used for each mode, except for Mode 1. Since the fuel is less dense and has lower viscosity, this may be affecting the fuel leaving the injector port and modifying the air entrainment into the fuel jet. Kajitani and coworkers' data support the scattered increase or decrease in NO_x emissions depending on engine load [85]. In their work, a comparison of the emissions for various fuel blends was made based on two injection timing points from the engine and showed a significant effect of timing on the emissions for various DME-diesel fuel blends as well as neat DME [85].

However, the data reported here show an interesting phenomenon. The NO_x emission decreases for the 5 wt. % oxygen, and then begins to increase with additional oxygen content, as shown in Modes 1 and 2. The HEUI fuel injectors use a split shot injection at the lower engine speeds, creating two reaction zones and lowering the overall peak temperature, thus reducing the NO_x. Choi and Reitz observed that there is a small penalty on the NO_x emissions when using a split injection strategy (two fuel pulses) with an oxygenated fuel, which could be affecting the results for Mode 1 and 2 for this particular engine [10]. Because the unique multiple fuel injection strategy of the Navistar T444E is especially predominant at lower speeds, the NO_x reduction could occur due to

improved mixing effect in the cylinder during the combustion event. At higher engine speeds, the data show that NO_x is lower for DME-diesel blends at light loads, and NO_x increases more rapidly for the DME-diesel blends as load increases. There are conflicting reports in the literature as to whether oxygenates increase or decrease NO_x emissions [8, 10, 11, 17, 18]. It is also unclear from these data whether there is a true reduction in NO_x, because the injection timing and pressure were changing, both of which have been shown to affect NO_x emissions. Further experiments are needed to determine precisely the effect on NO_x emissions, through maintaining the injection timing or injection pressure constant while varying the other parameter.

Figure 4–6 presents the particulate matter vs. NO_x tradeoff at each test mode. Typically, as PM is reduced, NO_x is increased, thus making the reduction of either emission a tradeoff for the other. As can be seen for modes with lower loads (Modes 2, 5 and 6), as particulates are reduced, NO_x is reduced. However, for Modes 3,4 and 7, an increase in NO_x with decreasing particulates is observed. In some cases, the PM-NO_x emissions point shifts toward the origin, which may demonstrate that oxygen addition is a viable means of simultaneously reducing diesel engine NO_x and particulate matter emissions. However, the changing of the injection timing and injection pressure may also be affecting the reduction or increase in NO_x. This shift in injection parameters is a confounding effect making interpretation of the emissions more difficult.

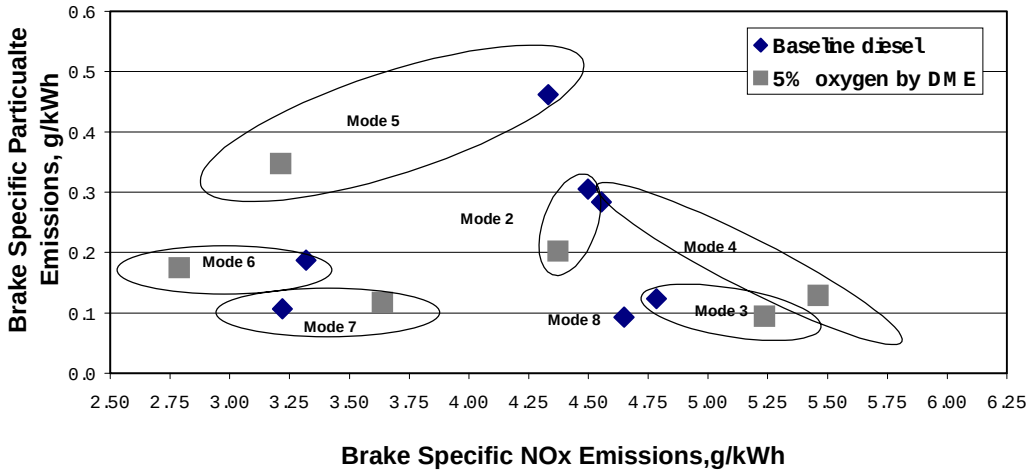

Figure 4–6: PM vs.NO_x Tradeoff

4.5 Carbon Monoxide (CO)

Table 4–4 reports the weighted brake specific CO (BSCO) emissions. On a CO per unit of fuel basis, CO emissions increase as the wt. % oxygen is increased, for each mode, except for Mode 3 for the 5 wt.% and 10 wt.% oxygen by DME-diesel blends. The exception for Mode 3 may be due to the observed change in injection pressure, and a combined effect of the change in the fuel blend properties.

Table 4–4: CO Emissions results per mode, Brake Specific Basis

CO Emissions Per Mode	**Baseline Diesel (g/bhp-hr)**	**5wt. % oxygen via DME (g/bhp-hr)**	**10wt. % oxygen via DME (g/bhp-hr)**
1	40.0	51.8	75.93
2	1.60	1.97	2.75
3	.560	.689	.671
4	8.12	7.63	NA
5	2.33	4.16	6.59
6	.913	1.344	2.10
7	.691	.875	.916
8	.493	NA	NA

In general, CO decreases as load increases, as shown in *Figure 4–7*. Also, the amount of CO increases with oxygen addition, except for the Modes 3 and 7, which seem to be fairly equal. For Mode 4, there is a decrease in the amount of CO in the exhaust. Oxygenates decompose to form extra CO which "freezes" at elevated levels due to bulk gas quenching during the expansion stroke. This may again support the idea that during the low speed and low load conditions, CO formed during early reaction of the fuel is impeded from conversion to CO_2. The mechanism was postulated by Litzinger and coworkers through the following reactions (equations 4.2 and 4.3), scavenging radicals from the soot creation process [17]:

$$H + CO + M \rightarrow HCO + M \qquad (4.2)$$

and

$$H + CO_2 \rightarrow CO + OH \qquad (4.3)$$

As explained by Glassman, the conversion of CO to CO_2 would be a function of the size of the hydroxyl radical pool, which does not grow until after all the original fuel and hydrocarbons have been consumed [52]. Since the concentration of hydroxyl radicals is important in the rate of CO oxidation, the additional oxygen atoms from DME may be playing a role in providing excess CO and CO_2, which continue the creation of the hydroxyl radical pool.

In addition, Flynn and coworkers show through kinetic simulations that the addition of the oxygen in the fuel leads to reduced amounts of soot precursors, and larger amounts of carbon leaving the fuel rich premixed combustion zone as CO [117]. Additionally, the work by Flynn and coworkers considers a model of a mixture of 40 %n-heptane and 60% DME (molar percentages), which indicates smaller amounts of C_2H_2, C_2H_4, and C_3H_3 formation, and this larger amount of CO leaving the premixed zone. At these molar percentages of fuel, the soot precursors almost disappear.

As seen in the present data, the amount of CO increases with oxygen addition, except for Modes 3 and 7, which seem to be fairly equal. For Mode 4, there is a decrease in the amount of CO in the exhaust, which may not be statistically significant. It seems that above a certain oxygen content, there could be a shift in the kinetic mechanisms,

demonstrated through a drop off in CO. For higher engine loads, regardless of speed, this is shown in the data, which indicates high temperatures to oxidize the CO, and the possibility of an extended heat release time. This is an interesting phenomenon which is also demonstrated in the work by Hess and coworkers [28].

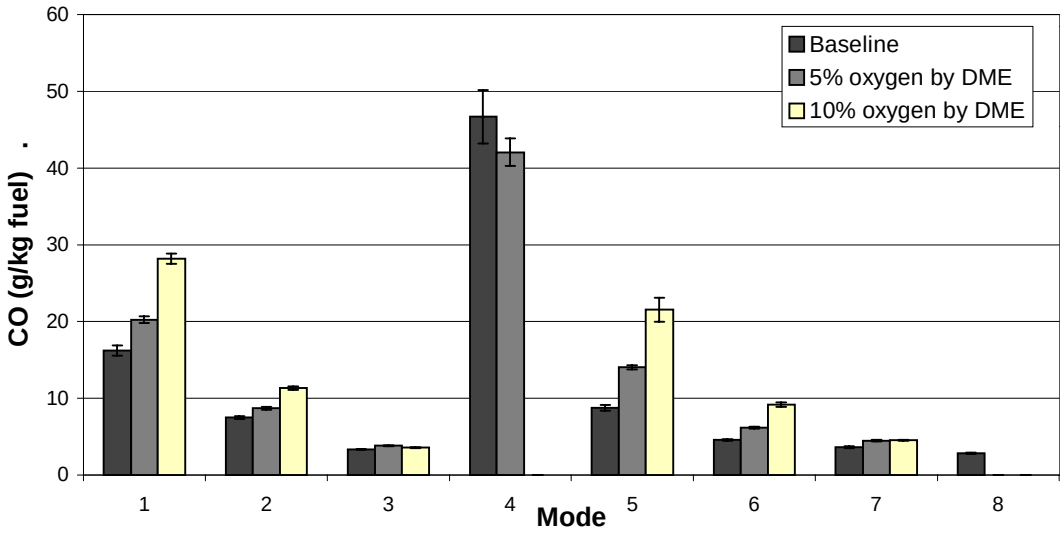

Figure 4–7: CO Emissions per unit fuel consumed, g/kg fuel

The increase in CO has been shown to be a signature of the change in chemical reactions involved in the combustion of an oxygenated fuel. This set of data also shows this to be true. Again, however, changes in the injection timing may be affecting the amount of CO, and skewing the true meaning of the signature. The work by Kajitani shows that the CO emissions actually decrease from the baseline diesel fuel for

increasing amounts of DME in diesel, given an engine speed of 960 RPM and increasing MEP [85].

4.6 Hydrocarbons (HC)

The weighted brake specific hydrocarbon emissions for each mode are reported in *Table 4–5*.

Table 4–5: Hydrocarbon Emissions results per mode, Brake Specific Basis

Hydrocarbon Emissions Per Mode	**Baseline Diesel (g/bhp-hr)**	**5wt. % oxygen via DME (g/bhp-hr)**	**10wt. % oxygen via DME (g/bhp-hr)**
1	34.3	51.4	48.5
2	.707	1.78	1.54
3	.211	.953	1.54
4	.137	.561	NA
5	.549	3.07	3.18
6	.216	1.22	1.28
7	.127	.777	.430
8	.094	NA	NA

In general, the HC emissions decrease with higher engine loads, as the engine combustion efficiency increases. For all modes, HC emissions increase with oxygen addition, and decrease as engine load increases, as seen in *Figure 4–8*. For the lower engine speeds, as the oxygen addition increases, the HC emissions increase. However, because very few data points are involved with this figure, these measurements may not be accurate. These data are inconsistent with what has been observed by some previous engine studies. Ikeda and coworkers testing showed that the total hydrocarbon emissions from the DME fuel tests remained roughly the same as the results from the diesel tests [86]. In this work, the two fuels were mixed in the fuel line prior to injection, which ensured a homogeneous mixture. Ikeda's work also shows that as the DME concentration increases, the exhaust hydrocarbon concentration increases. Kajitani and coworkers testing showed that the HC emissions were roughly the same as the diesel HC emissions, over a range of increasing load and for several injection timings [85]. Therefore, the data in *Figure 4–8* may suggest that there are other fuel parameters and injection effects occurring within the system affecting the hydrocarbon emissions.

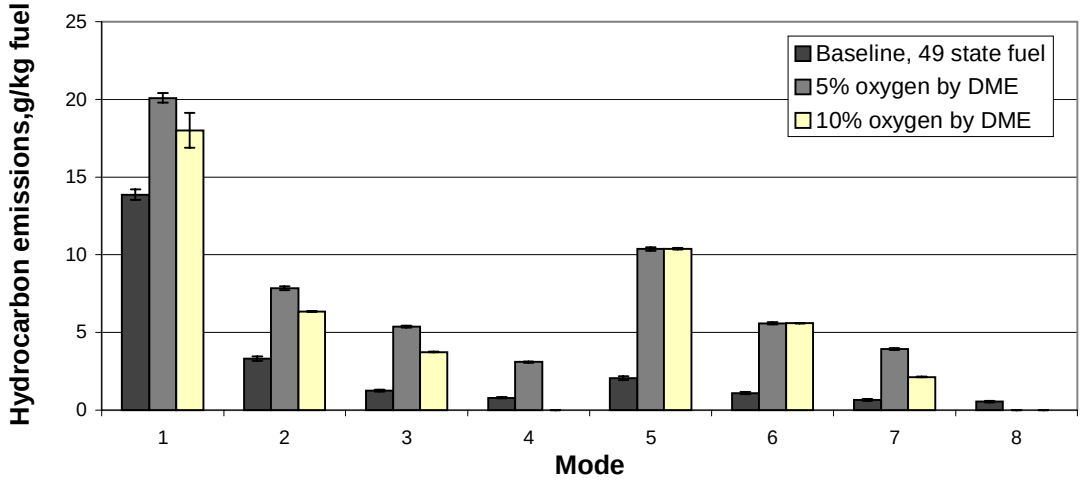

Figure 4–8: Hydrocarbon Emissions per unit fuel consumed, g/kg fuel

4.7 Fuel Consumption

Figure 4–9 reports the brake specific fuel consumption (BSFC) for the DME addition. The general trend shows an increase in the amount of fuel required to maintain the same speed and load. This is due to the slightly lower calorific value of the fuel blend, as shown in the Fuel Properties of *Table 4–1*. However, when fuel consumption is calculated on an energy basis, the energy consumption results are not significantly different.

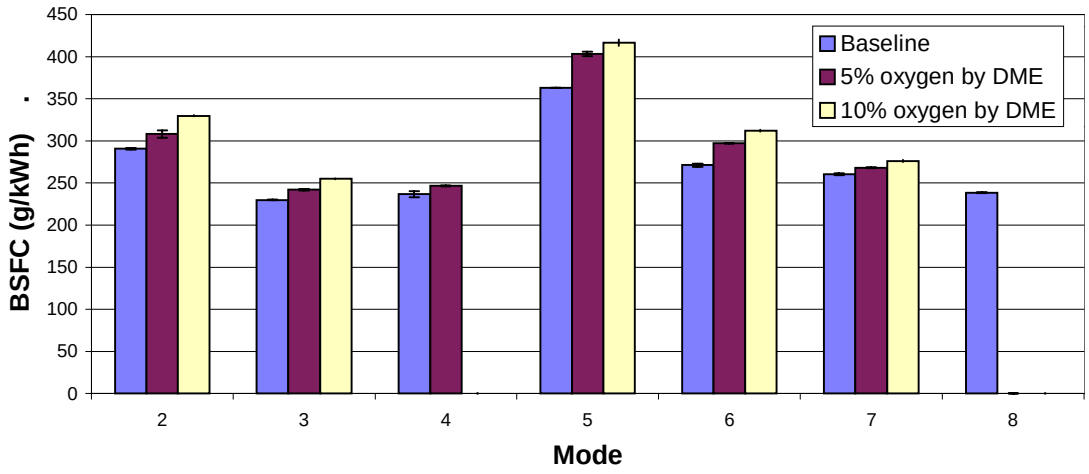

Figure 4–9: Brake Specific Fuel Consumption, g/kWh

Below in *Figure 4–10* the brake specific energy consumption is shown. The energy content of the fuel was calculated based on the Fuel Property Data in Table 4-1. The DME-diesel blends were calculated based on a linear combination of the fuels.

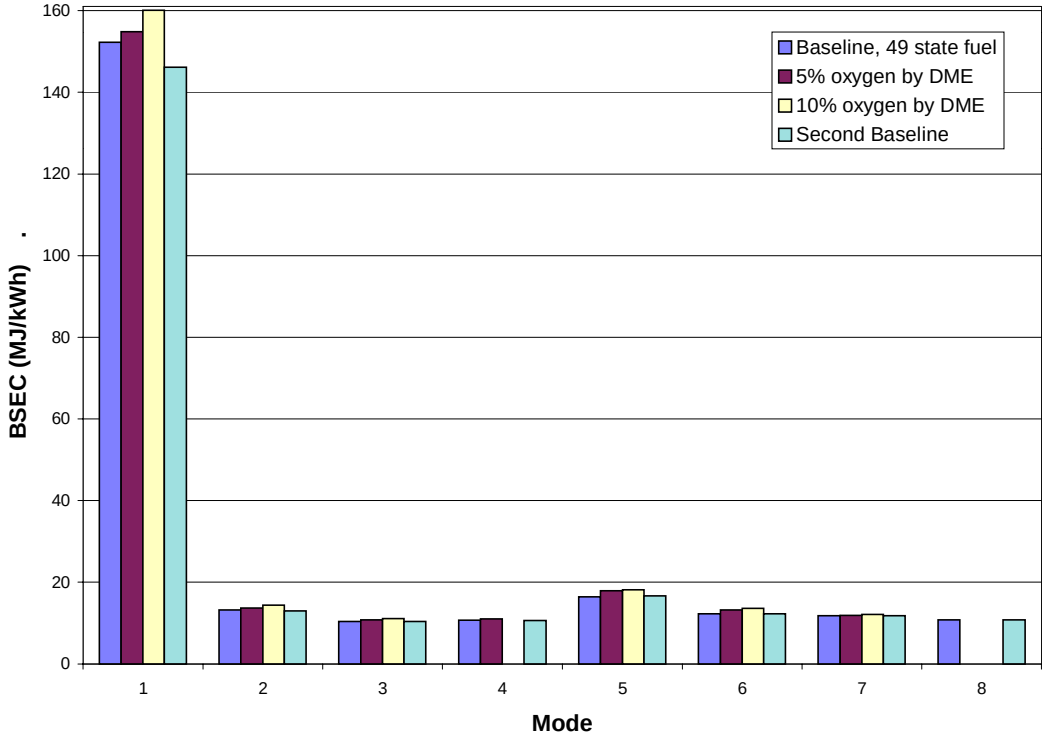

Figure 4–10: Brake Specific Energy Consumption, MJ/kWh

As described before, the engine was commanding more fuel, which caused the fuel injection pressure, as well as the fuel injection timing to shift. The fuel volume required is also confirmed by the engine control signals, shown in *Figure 4–11*.

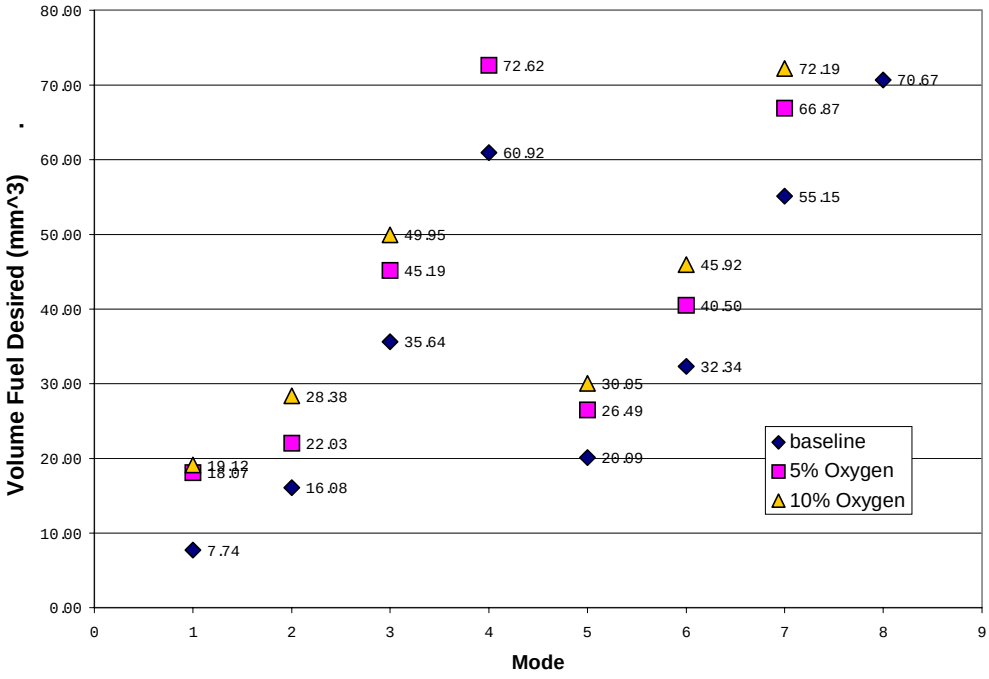

Figure 4–11: Engine control commanded fuel volume desired,mm^3

4.8 Pressure Trace and Heat Release Analysis

Cylinder pressure histories of the combustion cycles were collected for each of the fuel blends. This information was compiled by the analysis software as an average of roughly 50 cycles, and plotted in comparison with other fuel blends at the same mode to determine the effect of the fuel on ignition delay in the combustion process. *Figure 4–12* shows this comparison for Mode 3, which shows that for the 5 wt.% oxygen by DME one observes a very small premixed combustion phase, with a lower pressure rise, and an early heat release.

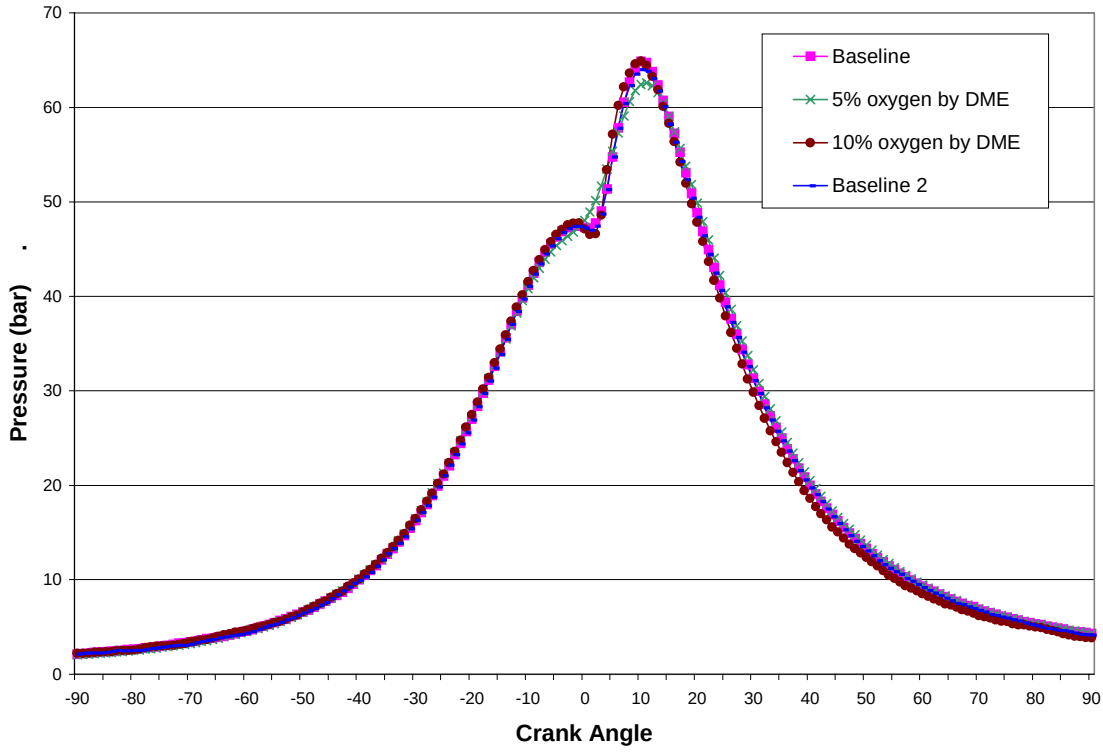

Figure 4–12: Pressure Trace for Mode 3

* 0 degrees is TDC (Top Dead Center)

Additionally, the peak pressure for 5 wt.% oxygen is slightly lower than the baseline diesel fuel. Looking at an expanded view of this pressure trace in *Figure 4–13*, the change in the pre-mixed phase of combustion is noted for the 5% oxygen by DME case.

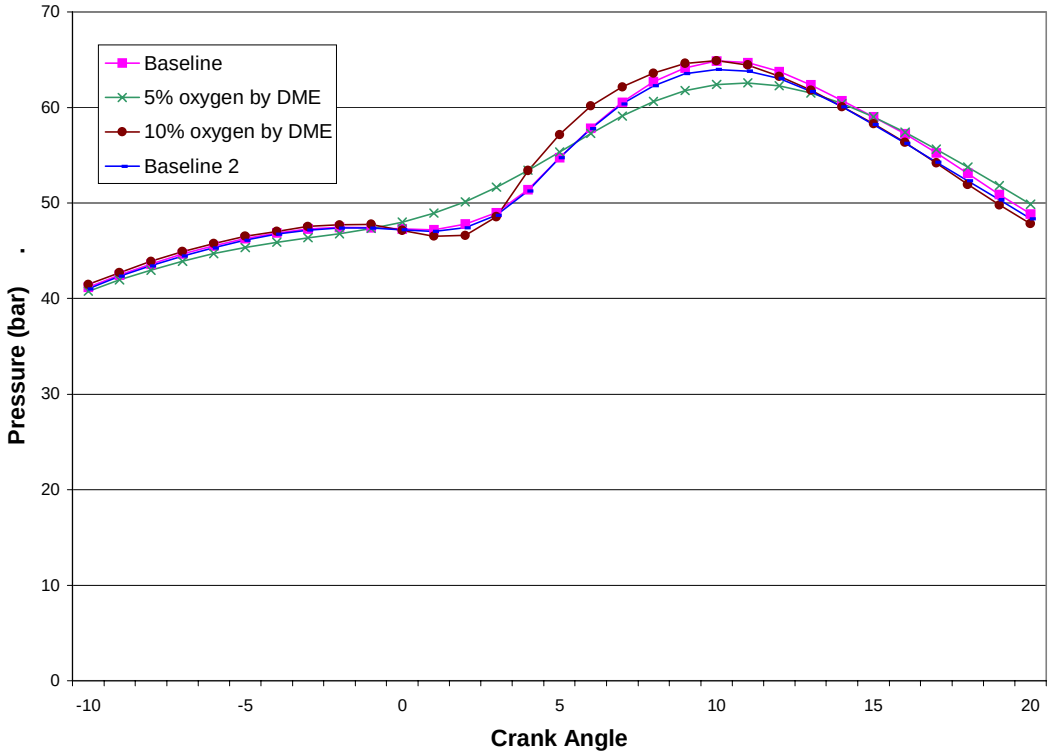

Figure 4–13: Pressure Trace for Mode 3 (Expanded Scale)

* 0 degrees is TDC (Top Dead Center)

However, the 10 wt.% oxygen by DME curve follows the diesel curve very closely. This could show some relationship to the fuel pressure, since for this curve, the fuel injection pressure was significantly increased. Also, since there is more DME in the blend, this could be the result of the compressibility effect on the injection process, with a delay in the fuel being delivered into the cylinder.

Mode 3 is analyzed for this part of the discussion because it was the only mode that had similar injection timing for diesel fuel and the DME-diesel blends, thereby permitting direct comparison. For all other modes injection timing and injection pressure changed as DME was added, making it difficult to determine and attribute the effect of any single mechanical or chemical change specifically.

Additionally, the heat release for these pressure traces was calculated according to equation 4.4 given by Heywood [44].

$$\frac{dQ_n}{dt} = \frac{\gamma}{\gamma - 1} p \frac{dV}{dt} + \frac{1}{\gamma - 1} V \frac{dp}{dt} \qquad (4.4)$$

where γ is the ratio of specific heats c_p/c_v

Figure 4–14 shows the following result of this calculation. An interesting observation is the steep peak associated with the 10% oxygen by DME. This again suggests the injection delay-compressibility effect of the DME by about 1 crank angle degree, and then a quick and steep heat release. Additionally, the heating during the delay period is shown on the 10 % oxygen by DME, as the curve drops below the axis due to the heat transfer to the walls and to fuel vaporization and heating [44]. *Figure 4–2* indicated the injection timing for Mode 3 to be approximately 7 degrees before TDC. Because of other actions occurring in the injector mechanism, specifically the lag time involved with the electronics and the lag time involved with the hydraulic action, it is understood that this is an acceptable number for data analysis and comparison, but not exact. It gives a point of comparison for the chart, in that the ignition delay for the 5 wt.% oxygen by DME

mixture is shorter and the ignition delay for the 10 wt.% oxygen by DME mixture is longer than for the baseline diesel fuel.

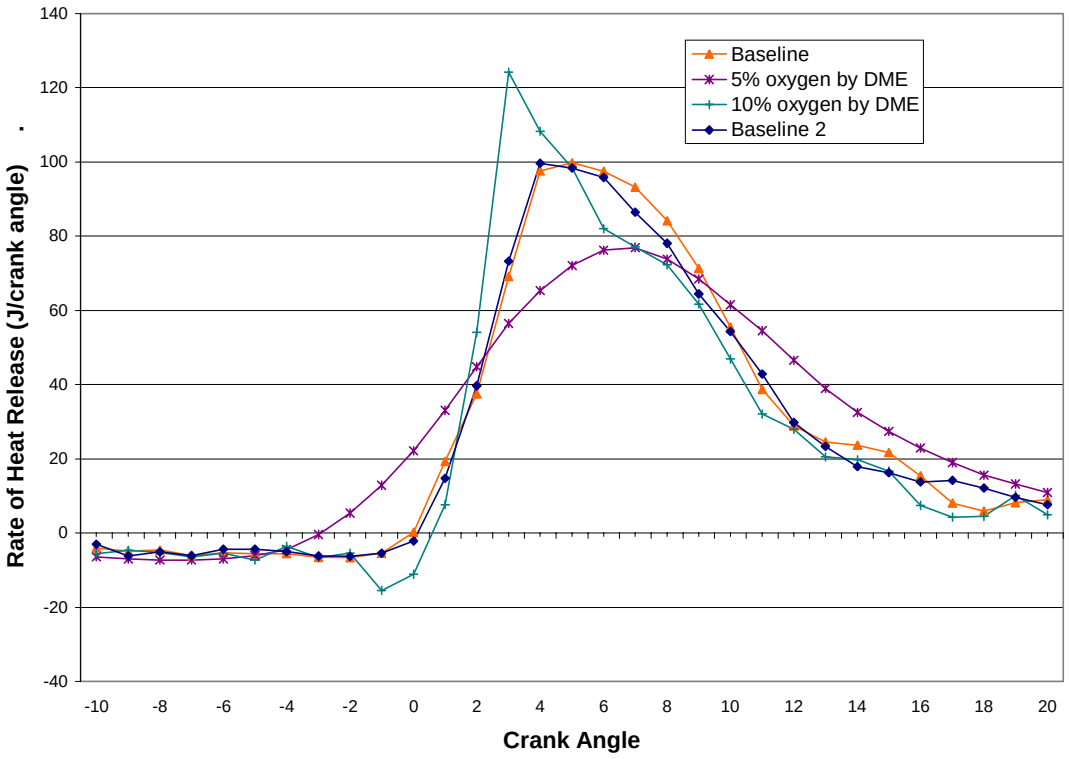

Figure 4–14: Heat Release for Mode 3

* 0 degrees is TDC (Top Dead Center)

Westbrook describes the ignition process of a fuel being dependent on a dominant chain branching reaction that drives the chemical combustion [118]. The ignition process depends on physical, chemical, and mixing and transport dynamics of the situation. To understand the ignition kinetics, it is important to understand the chain branching

mechanisms for the conditions being studied. The most important high temperature reaction for chain branching is the following in equation 4.5:

$$H + O_2 \rightarrow O + OH \qquad (4.5)$$

It is important to note that the specific reactions that provide chain branching are dependent on temperature, pressure, and the composition of the reactants over time. At the beginning of a chemical reaction, sufficient time is needed for a system to progress through low and intermediate temperature kinetic pathways until a critical temperature of the system is reached, and a large pool of OH radicals is produced in the system and the system ignites. From laser diagnostic studies performed by Dec and coworkers, a schematic of diesel ignition and combustion has been provided [117]. After the start of injection, a jet of diesel fuel mixes with hot and compressed air. As the air and fuel mix, the fuel-air equivalence ratio is reduced while at the same time the mixture temperature is increasing. Dec and coworkers determined that the mixture starts to ignite when the equivalence ratio is near ϕ=4. At this point, soot is produced in this fuel-rich pre-mixed ignition flame, and then it is consumed into the diffusion flame. Per the schematic, the diffusion flame is established at the end of the liquid fuel jet. This research supports a direct correlation of soot production to ignition kinetics. Therefore, lowering the post-ignition soot promotion species is a way to reduce soot production.

4.9 General Engine Observations

The engine and fuel system were constructed in such a way as to make sure that the engine would operate as close to steady state as possible. This was important for the comparison of the emission and pressure trace data. The engine seemed to operate, from observed sound and ease of starting, as if pure diesel fuel was being used. However, there were some complications.

From a fuel consumption standpoint, as DME content increased the volume of fuel being commanded from the engine control increased, but reached the maximum limit, as expressed in *Figure 4–11*. This could be the result of the maximum limit, the fuel injection pressure limit and possibly the injection timing limit, within the engine control program.

*Figure 4–15 s*hows the engine oil temperature. It was important to keep this constant so that the injection timing commands would be constant, since the temperature of the oil determined the hydraulic effect during operation of the fuel injector. Injection timing is a function of several factors including the oil temperature, energized solenoid operation, and timing location commanded by the engine control.

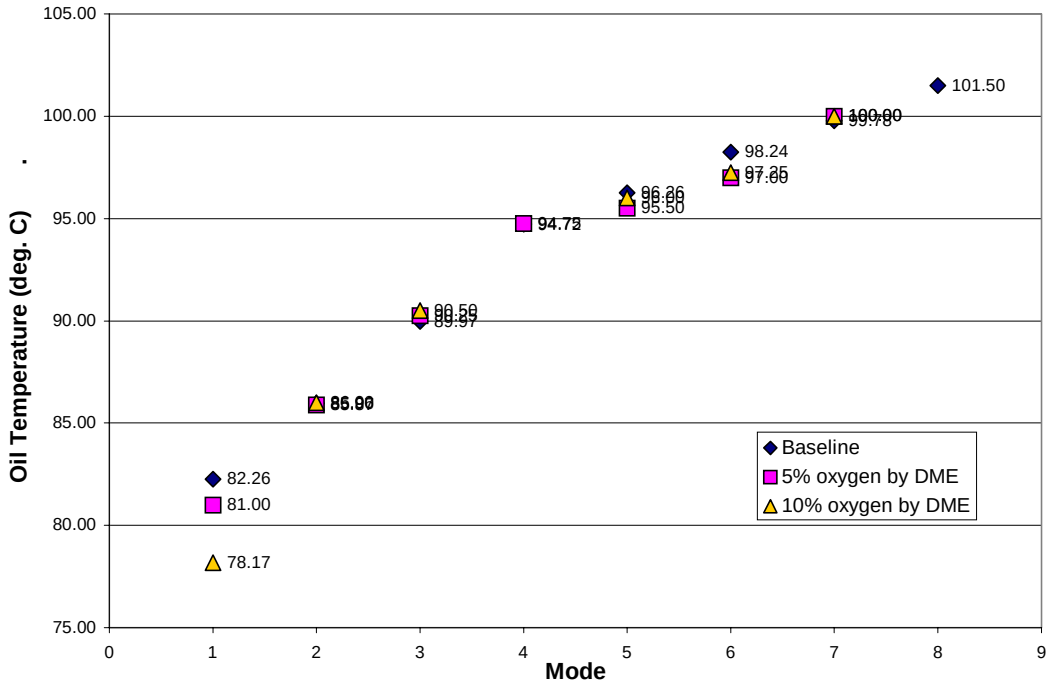

Figure 4–15: Engine Oil Temperature, °C

Additionally, the oil temperature and the engine coolant temperature, in *Figure 4–16,* represent the bulk temperature of the engine. This represents the steady state temperature at each operating mode, and the heat rejection by the engine to the engine coolant and the fuel in the rail.

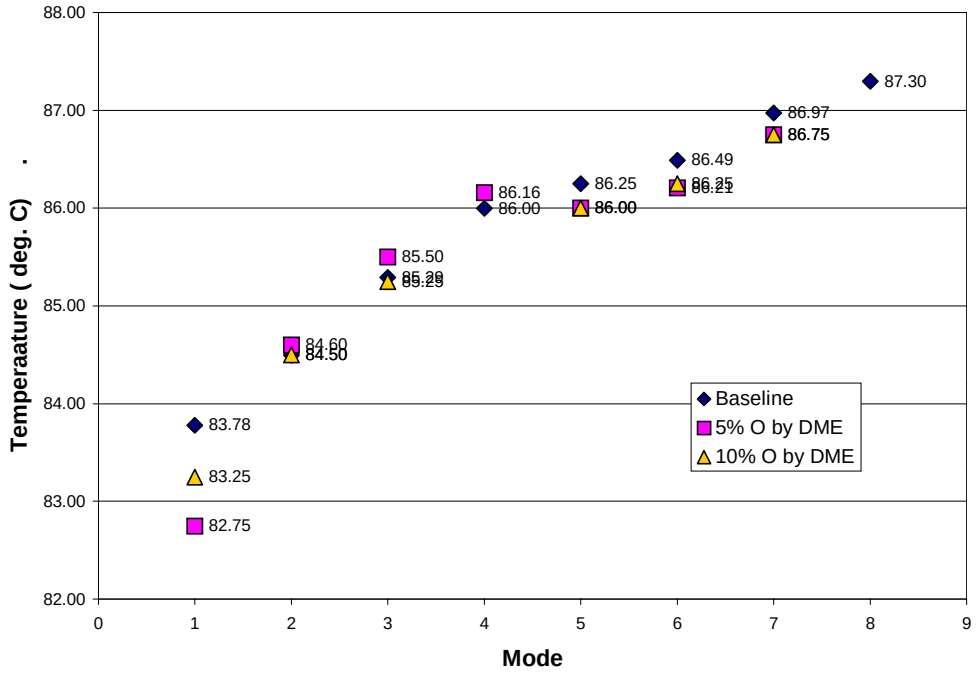

Figure 4–16: Engine Coolant Temperature,°C

Further, it was noted after the testing was completed, that the engine would possibly be using the air temperature information to determine the point on the speed and load map to determine injection timing. The sensor was installed in the wiring harness and recording room air measurements, to confirm the engine control was receiving the required voltage input for proper engine operation. However, the sensor was not installed on the engine in the standard location. *Figure 4–17* shows the test cell ambient air temperature, which is the data the engine control was receiving.

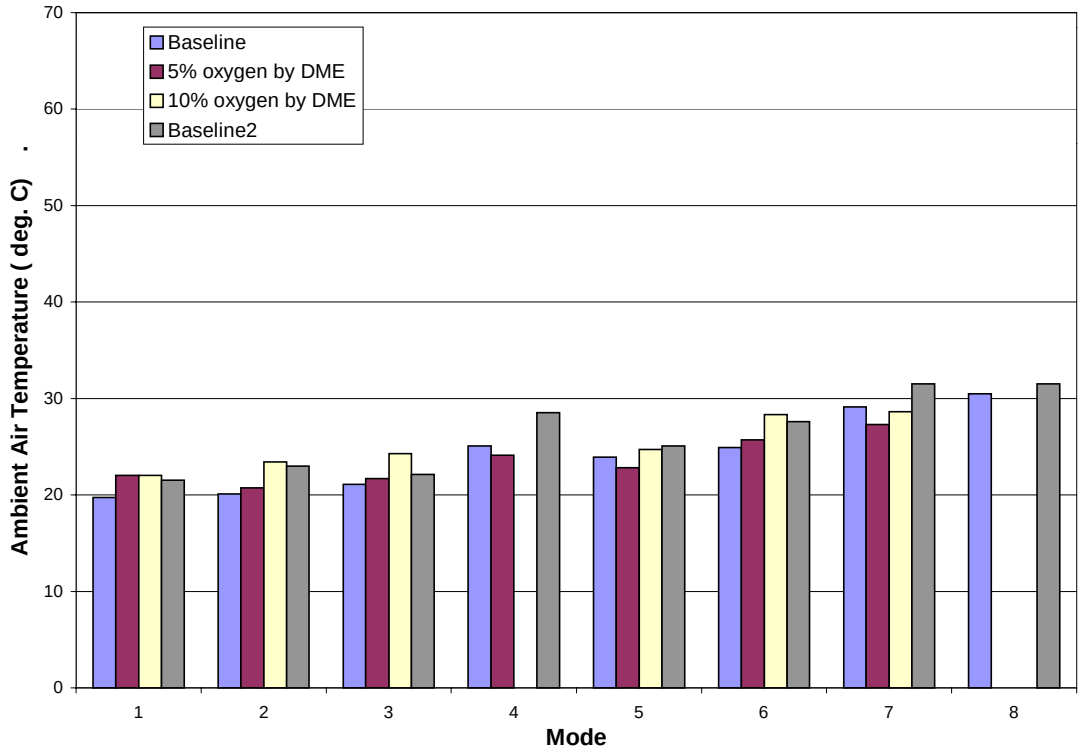

Figure 4–17: Engine Test Cell Ambient Air Temperature,°C

Figure 4–18 shows the actual intake air temperature, measured on the outlet side of the charge air cooler. This would be the temperature most important to the engine control. It would be important to confirm through the engine manufacturer the specific location and requirement for the sensor.

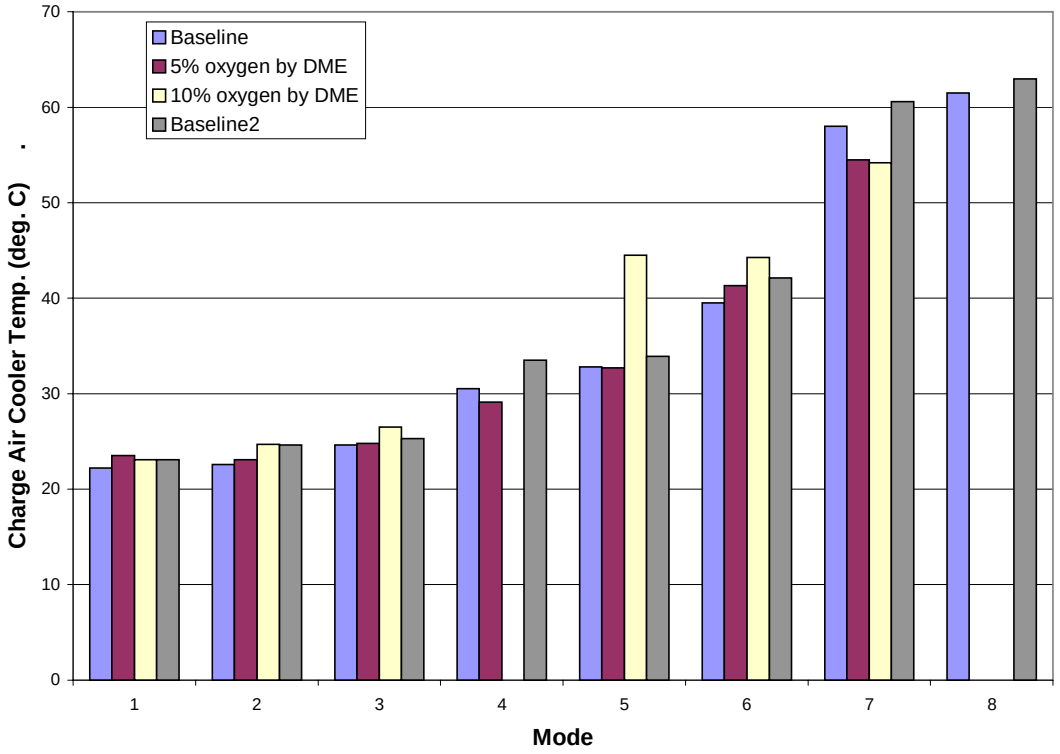

Figure 4–18: Charge Air Cooler Temperature,°C

Finally, a metallic knocking noise was observed from the engine, upon reduction from a high engine speed to a low engine speed, regardless of load. Also, the engine seemed to be close to stall. This could be due to reduced flow rate of fuel in the rail, during a period of high heat rejection from the engine, which could be causing the DME to vaporize in the injectors. Additionally, the viscosity and lubricity of the fuel could be dropping below the ASTM limit, producing a metallic wear "clapping" sound.

4.10 Engine Repeatability Study

A series of data was collected for Mode 4 over the course of several days. The purpose was to confirm that the engine data comparisons were consistent within some error range and to quantify day-to-day variability. *Figure 4–19* and *Figure 4–20* show the particulates and NO_x for Mode 4. The data are consistent within 30%, from center point to center point of the largest and smallest data point.

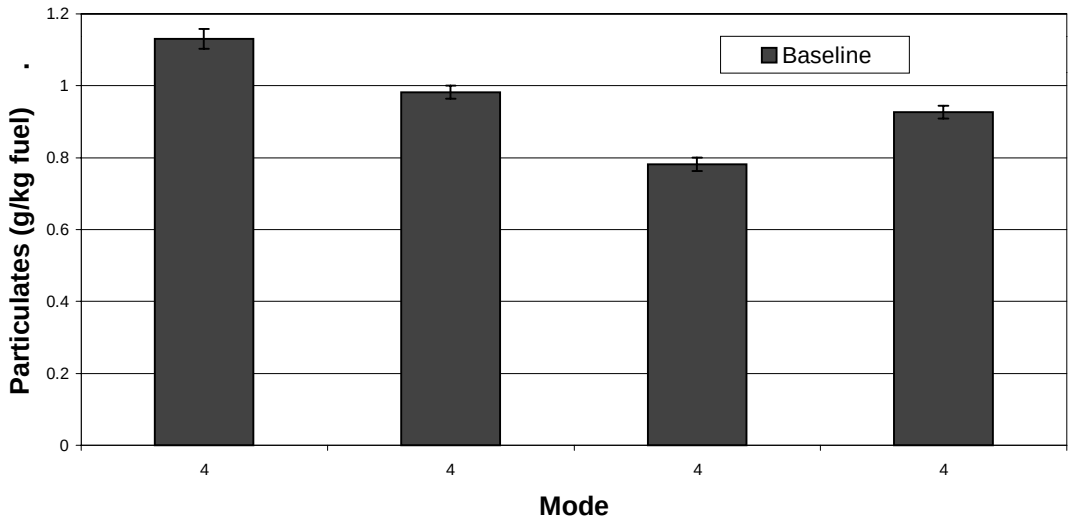

Figure 4–19: Particulates, Mode 4 Comparison, g/kg fuel

Along with the above particulate comparison, all filters were analyzed to determine how much error existed in the filter weighting procedures and the use of the humidity chamber. This statistical analysis is presented in Appendix B. There seems to

be some variability in this system, which yields errors above the fixed errors in the system. The cause was believed to be a function of the unstable humidity in the filter weighing chamber, and led to changes in laboratory procedures for filter weighing.

In *Figure 4–20* , the data are consistent within 3 %, based on the higher point of an error bar to the lowest point of another error bar. From center point to center point of the highest and lowest data point, the error is within 9.5 %.

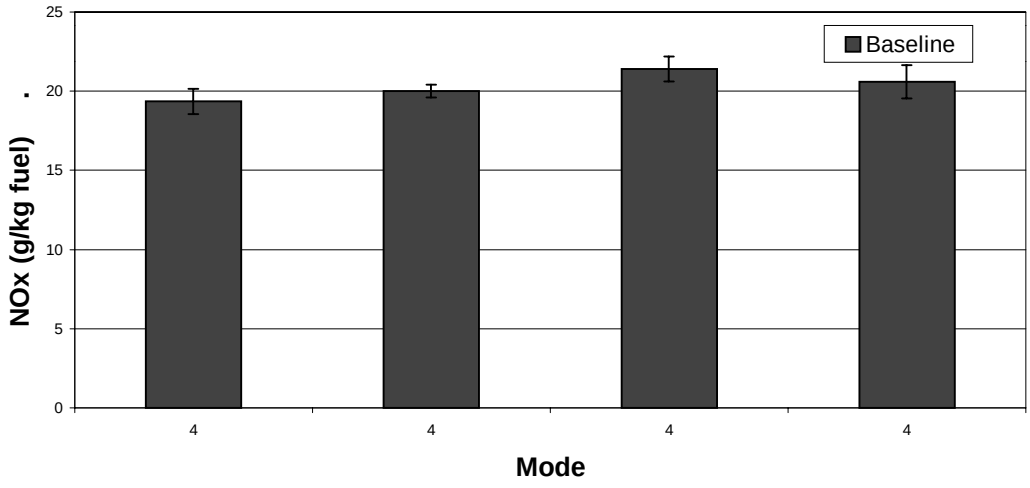

Figure 4–20: NO_x, Mode 4 Comparison, g/kg fuel

Variations in the above data can be explained by the higher air consumption for particular modes, and increased exhaust temperature, as shown in *Figure 4–21.*

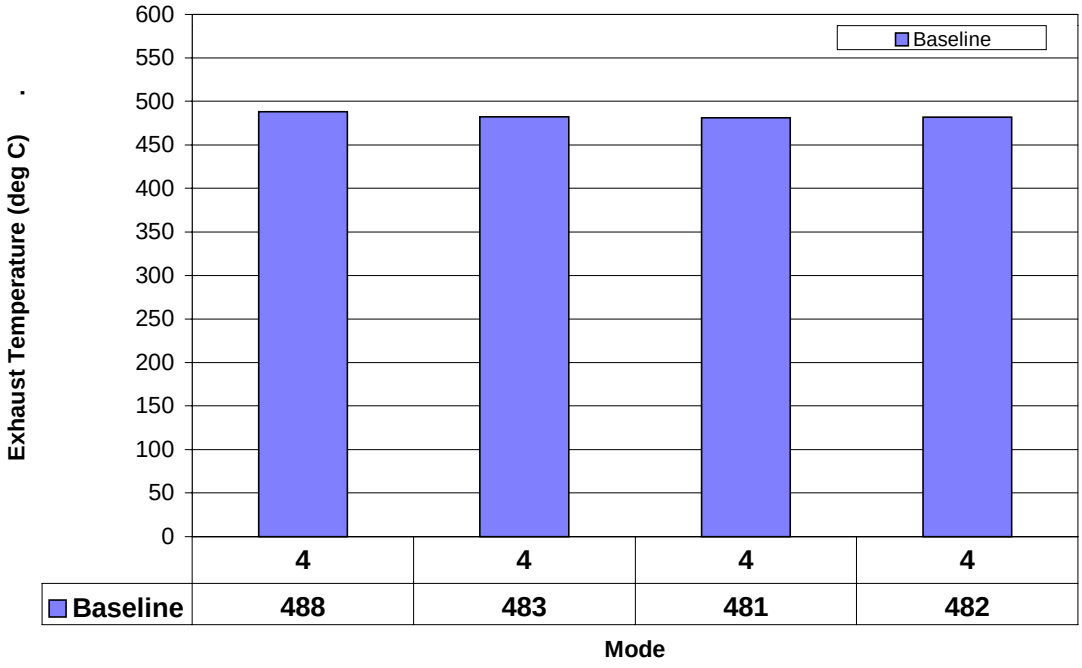

Figure 4–21: Exhaust Temperature, Mode 4 Comparison,°C

Chapter 5

Summary, Conclusions, and Recommendations for Future Research

5.1 Summary and Conclusions

Manufacturers of diesel engines and vehicles are facing continued pressure due to governmental regulations to reduce the engine and vehicle emissions. Regulations set for 2004 and 2007 are currently out of reach with current technology [4, 119]. Therefore, manufacturers are resorting to adapting a total system approach for emissions reductions, implementing pre-combusiton, in-cylinder, and post-combustion technologies to meet these emission levels. The focus of this research involved the study of a pre-combustion approach, via fuel modification.

Dimethyl ether (DME) has been shown to reduce particulate emissions when combusted in a compression ignition engine [86]. Dimethyl ether is considered an oxygenated compound that can be blended with or used as a fuel. However, when using DME as a fuel, there are some challenges that need to be overcome to achieve optimal engine operation. These include changes in fuel injection quantity and timing, as well as reduction in the lubricating properties of the fuel in the injectors.

In order to accommodate the need for lubricity in the fuel injectors, it was theorized that the DME could be mixed with diesel fuel in order to maintain the quality of the fuel

needed by the fuel system. The minimal quality of fuel is established by the ASTM specification for No. 2 diesel fuel. However, what is not known is what the minimal amount of lubricating quality that the fuel injectors, in particular, can accommodate and for what duration of time.

Mixing the DME with the diesel fuel, provides what is typically referred to as an oxygenated fuel blend. Dimethyl ether contains oxygen within its molecular structure. Many researchers have shown that mixing an oxygenate with a diesel fuel will provide reduction of particulate matter in the exhaust [7, 8, 11, 95]. Since DME has been shown to reduce particulate emissions when used in neat form, it was theorized that there would be some emissions reductions when mixed with diesel fuel.

A Navistar 7.3L Turbodiesel engine and fuel system were modified for the purpose of utilizing pressurized DME and diesel fuel blends. Instruments were placed in the engine and fuel system so that data could be flight recorded for real-time observation, as well as, for future analyses. The objective of the data collection was to provide information which could be used to modify the engine from it's production configuration to improve performance and emissions with the various fuel blends.

Research continues in testing and reviewing the effects of oxygenates, specifically DME diesel fuel blends, on the composition of emissions from diesel engines. The results from this research lead to the following conclusions:

- DME-diesel blends can be used to fuel a compression ignition engine, using of a pressurized fuel system. The engine operates in a similar manner with the DME-

diesel fuel as with the diesel fuel, as reviewed in the engine stability data. Changes in combustion peak pressure were not audibly noticed, but were shown using pressure trace analysis.

- DME has been shown to reduce particulate emissions from a DI diesel engine. With the addition of oxygen contained within the fuel, additional CO and CO_2 is present in the combustion process. This has lead researchers to conclude this higher level of CO prevents the formation of soot precursors in the pre-mixed flame, which then reduces the formation of particulates.

- It has also been observed that small NO_x reductions or increases occur over the engine operation map. Multiple injections at lower loads and speeds may explain this data. For higher speeds and loads, this may be explained due to advanced injection timing and injection pressure. No conclusion can be drawn from this data as to the effect of oxygen on the formation of NO_x.

- The engine control module and the calibration for the Navistar 7.3L T444E engine are sensitive to changes in fuel properties, resulting in inconsistent injection timing and injection pressure for each of the fuel blends tested. This can be explained by the changing energy content and density of the fuel blends. The end result makes comparisons in emission results extremely difficult.

- Upon this initial testing, no determinations of the effect of the DME on the durability of the engine can be addressed. None of the data collected suggests that the testing of

the engine has degraded the injector operation. The engine has been operated for about 100 total hours, with at least 5% DME content in the fuel for half of that time.

- Because the pressurized system requires the fuel to enter the injector at a lower temperature than would the production style engine, the effect of the lower temperature fuel may result in a change in the emissions.

- The pressure trace analysis for Mode 3 revealed that there is some effect of DME on the combustion peak pressure. Additionally, the heat release analysis showed potentially some effect of the compressibility of the fuel, as a result of the blends or the temperature of the blends as they enter the cylinder.

The conclusions from the research completed thus far lead to recommendations for future work in order to improve the engine operation, by further separating the variables affecting the performance and emissions of the engine.

5.2 Recommendations for future research

Although it has been shown that DME can be used in combination with diesel fuel in a compression ignition engine, the fuel blend and engine operation can be further optimized for improved emissions and long term durability of the engine. This involves several factors including, increasing the DME content in the blend, up to the point where the engine can still produce acceptable speed and load, with improved emissions for an acceptable lifetime of the engine and fuel injectors. It should be noted that since the fuel

is being used within an engine, there exists not only chemical effects of the fuel and changes in the fuel as the blend is altered, but also mechanical effects by the engine, some which are a result of changing fuel blends. Therefore, further study of the engine emissions are a function of understanding the various chemical and mechanical effects.

This research work aided in identifying many of the chemical and mechanical effects. Some of the mechanical effects are inherent to the engine and cannot be directly altered. The optimization of the engine is influenced by the following factors:

- DME content in diesel fuel blend
- Ignition delay
- Injection pressure and timing for the fuel blend
- Engine emissions
- Internal injector wear
- Injector o-rings
- Compressibility of the fuel blends
- Vaporization of DME in the cylinder/ liquid length of the DME-diesel fuel blend
- Injector nozzle size and flow rate
- Cooling required to maintain the fuel in a liquid state

Changes in the fuel blends relate to changes in the fuel blend properties. Therefore, above a certain blend level, there is a requirement to adjust the engine control system to achieve improved ignition delay in conjunction with the correct engine timing.

To perform this optimization, it would be important to know how the fuel properties are changing that affect the ignition delay. Since the cetane number is increasing with increasing DME content, this would be one factor. Also, and more significantly, the compessibility of the fuel is changing with increasing DME content, which has an unknown relationship to ignition delay. Additionally, the fuel blends have an unknown effect on the engine and injector wear and wear rate, including both metallic and polymeric materials. Therefore, the future work should be divided into several sections:

1. Fuel Property Studies

   To aid in explaining the changes in heat release of the DME-diesel blends, it is important to understand how the DME-diesel fuel blends change in compressibility as the DME content is increased over a range of temperatures. Additionally, it is unclear whether a change in viscosity or lubricity with increasing DME content is affecting the wear and wear rate in the injectors.

2. Engine Optimization for Performance and Emissions

   To determine the optimal conditions for engine operation, an optimal network of conditions should be established to direct the optimization of the engine for performance and emissions. This would be accomplished both experimentally and through computational analysis, and confirmed experimentally.

3. Engine Optimization for Durability

To determine the ability of the engine and fuel system to be durable and label it as durable, two specific types of data should be collected. One, injector o-rings should be tested in the fuel to determine if they are able to withstand the effect of DME. Two, an injector test stand should be used to operate the injectors for an extended period with the DME-diesel fuel blend and inspect them after the testing. Such testing would be comparable to ASTM methods.

BIBLIOGRAPHY

1. Challen, B., Baranescu, R., Diesel Engine Reference Book. 2nd ed. 1999, Warrendale, PA: Society of Automotive Engineers.
2. Eastwood, P., Critical Topics in Exhaust Gas Aftertreatment. 2000, Baldock,Hertfordshire, England: Research Studies Press LTD.
3. Karim, G.A., "*Combustion in Gas Fueled Compression-Ignition Engines." ASME ICE Fall Technical Conference*, 2000. **35**(1) (2000-ICE-299): p. 1-10.
4. Khair, M., Lemaire, J., Fischer, S., "*Achieving Heavy-Duty Diesel NOx/PM Levels Below the EPA 2002 Standards-- An Integrated Solution." Society of Automotive Engineers*, 2000 (2000-01-0187).
5. Walsh, M., "*Global Trends in Diesel Emissions Control- A 1999 Update." Society of Automotive Engineers*, 1999(1999-01-0107).
6. Hallgren, B., and Heywood, J., "*Effects of Oxygenated Fuels on DI Diesel Combustion and Emissions." Society of Automotive Engineers*, 2001 (2001-01-0648).
7. Neeft, J.P.A., Makkee, M., Moulijn, J.A., "*Fuel Proc. Tech."* 1996. **47**: p. 1-69.
8. McCormick, R.L., Ross, J.D., and Grabowski, M.S., "*Effect of Several Oxygenates on Regulated Emission from Heavy-Duty Diesel Engines." Environmental Science and Technology*, 1997. **31**(4): p. 1144-1150.

9. Graboski, M.S., and McCormick,R.L., "*Combustion of Fat and Vegetable Oil Derived Fuels in Diesel Engines." Prog. Energy and Combust. Sci.*, 1998. **24**(2): p. 125-164.

10. Choi, C.Y., Reitz, R.D., "*An Experimental Study on the effects of Oxygenated Fuel Blends and Multiple Injection Strategies on DI Diesel Engine Emissions." Fuel*, 1999. **78**(11): p. 1303-1317.

11. Liotta, F.J., and Montalvo,D.M., "*The Effects of Oxygenated Fuels on Emissions from a Modern Heavy-Duty Diesel Engine." Society of Automotive Engineers*, 1993 (932734).

12. Ullman, T.L., Spreen, K.B., and Mason,R.L., "*Effects of Cetane Number, Cetane Improver, Aromatics, and Oxygenates on 1994 Heavy-Duty Diesel Engine Emissions." Society of Automotive Engineers*, 1994 (941020).

13. Spreen, K.B., Ullman, T.L. and Mason, R.L., "*Effects of Cetane Number, Aromatics, and Oxygenates on Emissions From a 1994 Heavy-Duty Diesel Engine with Exhasut Catalyst." Society of Automotive Engineers*, 1995 (950250).

14. Tsurutani, K., Takei, Y., Fujimoto, Y., Matsudaira, J., and Kumamoto, M., "*The Effects of Fuel Properties and Oxygenates on Diesel Exhaust Emissions." Society of Automotive Engineers*, 1995 (952349).

15. Hess, H.S., Roan, M.A., Bhalla, S., Butnark, S., Zarnescu, V., Boehman, A.L., Tijm, P.J.A., and Waller, F.J., Chemistry of Diesel Fuels. *"The Use of Oxygenated Diesel Fuels for Reduction of Particulate Emissions from a Single-Cylinder*

Indirect Injection Engine," Applied Energy Technology Series, ed. C. Song, Hsu, C., Mochida, I. 2000, New York, NY: Taylor & Francis. 255-268.

16. Stoner, M., and Litzinger, T., "*Effects of Structure and Boiling Point of Oxygenated Blending Compounds in Reducing Diesel Emissions." Society of Automotive Engineers*, 1999 (991475).

17. Litzinger, T., Stoner, M., Hess, H., and Boehman,A., "*Effects of Oxygenated Blending compounds on Emissions from a Turbo-charged Direct Injection Diesel Engine." Int. J. Engine Research*, 2000. **1**: p. 57-70.

18. Beatrice, C., Bertoli, C., D'Alessio, J., Del Giacomo, N., Lazzaro, M. and Massoli, P., "*Experimental Characterization of Combustion Behavior of New Diesel Fuels for Low Emission Engines." Comb. Sci. and Tech.*, 1996. **120**: p. 335-355.

19. Bertoli, C., Del Giacomo, N., and Beatrice, C., "*Diesel Combustion Improvements by the Use of Oxygenated Synthetic Fuels." Society of Automotive Engineers*, 1997 (972972).

20. Beatrice, C., Bertoli, C., and Del Giacomo, N., "*New Findings on Combustion Behavior of Oxygenated Synthetic Diesel Fuels." Comb. Sci. Tech.*, 1998. **137**: p. 31-50.

21. Beatrice, C., Bertoli, C., Del Giacomo, N. and Migliaccio, M., "*Potentiality of Oxygenated Synthetic Fuel and Reformulated Fuel on Emissions from a Modern DI Diesel Engine." Society of Automotive Engineers*, 1999 (993595).

22. Miyamoto, N., Ogawa, H., Nurun, N.M., Obata, K., and Arima, T., "*Smokless, Low NOx, High Thermal Efficiency, and Low Noise Diesel Combustion with Oxygenated Agents as Main Fuel." Society of Automotive Engineers*, 1998 (980506).

23. Nabi, M.N., Minami, M., Ogawa, H., and Miyamoto, N., "*Ultra Low Emission and High Performance Diesel Combustion with Highly Oxygenated Fuel." Society of Automotive Engineers*, 2000 (2000-01-0231).

24. Edgar, B.L., Dibble, R.W. and Naegeli, D.W., "*Autoignition of Dimethyl Ether and Dimethoxy Methane Sprays at High Pressures." Society of Automotive Engineers*, 1997 (971677).

25. Murayama, T., Zheng, M., Chikahisa, T., Oh, Y.-T., Fujiwara, Y., Tosaka, S., Yamashita, M., and Yoshitake, H., "*Simultaneous Reductions of Smoke and NOx from a DI Diesel Engine Using EGR and Dimethyl Carbonate." Society of Automotive Engineers*, 1995 (952518).

26. Rubino, L., Thompson, M.J., "*The Effect of Oxygenated Additives on Soot Precursor Formation in a Counterflow Diffusion Flame." Society of Automotive Engineers*, 1999 (993589).

27. Song, C., Hsu, C., Mochida, I., ed. Chemistry of Diesel Fuels. 2000, Taylor & Francis: New York, NY.

28. Hess, H., Szybist, J., Boehman, A., Tijm, P., and Waller, F.J. "*Impact of Oxygenated Fuel on Diesel Engine Performance and Emissions"*. Proceedings in

35th National Heat Transfer Conference-American Society of Mechanical Engineers, 2001. Anaheim, CA.(NHTC01-11462).

29. Hower, M.J., "*The New Navistar T 444E Direct-Injection Turbocharged Diesel Engine." Society of Automotive Engineers*, 1993 (930269).

30. Sorenson, S.C., Mikkelsen S., "*Performance and Emissions of a DI Diesel Engine Fuelled with Neat Dimethyl Ether." Society of Automotive Engineers*, 1995 (950064).

31. McCandless, J., Li, Shurong, "*Development of a Novel Fuel Injection System (NFIS) for Dimethyl Ether – and Other Clean Alternative Fuels." Society of Automotive Engineers*, 1997 (970220).

32. EPA, *Final Emission Standards for 2004 and Later Model Year Highway Heavy-Duty Vehicles and Engines (EPA 420-F-00-026)*. 2000, United States Environmental Protection Agency.

33. EPA, *Heavy-Duty Engine and Vehicle Standards and Highway Fuel Sulfur Control Requirements (EPA420-F-00-057)*. 2000, United States Environmental Protection Agency.

34. Cheney, D., Powell, C., O'Neill, P., Norton, G., Veneman, A., Evans, D., Mineta, N., Abraham, S., Allbaugh, J., Whitman, C.T., Bolten, J., Daniels, M., Lindsey, L., Barrales, R., Lundquist, A., *"National Energy Policy: Reliable, Affordable, and Environmentally Sound Energy for America's Future"*. 2001, National Energy Policy Development Group, U.S. Government: Washington, D.C.

35. Verbeek, R., Van der Weide, J., "*Global Assessment of Dimethyl Ether : Comparison with Other Fuels." Society of Automotive Engineers*, 1997 (971607).

36. Wakai, K., Nishida, K.,Yoshizaki,T., Hiroyasu, H., "*Ignition Delays of DME and Diesel Fuel Sprays Injected by a DI Diesel Injector." Society of Automotive Engineers*, 1999 (1999-01-3600).

37. Phillips, J.G., Reader, G. T., "*The Use of DME as a Transportation fuel - A Canadian Perspective." ASME Fall Technical Conference*, 1998. **31-3** (98-ICE-152): p. 65-71.

38. Fleisch, T., McCarthy, C., Basu, A., Udovich, C., Charbonneau, P., Slodowske, W., Mikkelsen, S., McCandless, J., "*A New Clean Diesel Technology: Demonstration of ULEV Emissions on a Navistar Diesel Engine Fueled with Dimethyl Ether." Society of Automotive Engineers*, 1995 (950061).

39. Kapus, P.E., Cartellieri, W.P, "*ULEV Potential of a Car Engine Operated on Dimethyl Ether." Society of Automotive Engineers*, 1995 (952754).

40. Tijm, P., Waller, F., Toseland, B., and Peng, X. "*'Liquid Phase Di-Methyl Ether ™' A promising New Diesel Fuel"*. Proceedings in *Energy Frontiers International Conference, Alaska*, 1997.

41. Hansen, J.B., Voss, B., "*Large Scale Manufacture of Dimethyl Ether –a New Alternative Fuel from Natural Gas." Society of Automotive Engineers*, 1995 (950063).

42. Maricq, M.M., Szente, J.J., Hybl, J.D., "*Kinetic Studies of the Oxidation of Dimethyl Ether and Its Chain Reaction with Cl2." J. Phys. Chem. A*, 1997. **101**(28): p. 5155-5167.

43. Nash, J.J., Francisco, J.S., "*Unimolecular Decomposition Pathways of Dimethyl Ether: An Ab Initio Study." J. Phys. Chem. A*, 1998. **102**(1): p. 236-241.

44. Heywood, J.B., Internal Combustion Engine Fundamentals. 1988, New York: McGraw-Hill.

45. Obert, E., Internal Combustion Engines: Analysis and Practice. 2nd ed. 1950, Scranton, PA: International Textbook Company.

46. ISO, *ISO/DIS 8178-2.2 Reciprocating internal combustion engines- Exhaust emission measurement Part 2: Measurement of gaseous and particulate emissions at site*, in *International Organization for Standardization Draft International Standard*. 1995, International Organization for Standarization.

47. Richter, H., and Howard, J., "*Formation of Polycyclic Aromatic Hydrocarbons and Their Growth to Soot-- A Review of Chemical Reaction Pathways." Prog. Energy and Combust. Sci.*, 2000(26): p. 565-608.

48. Warnatz, J., Maas, U., and Dibble, R.W., Combustion: Physical and Chemical Fundaemntals, Modeling and Simulation, Experiments, Pollutant Formation. 1996, Berlin: Springer-Verlag.

49. Garrett, T.K., Automotive Fuels and Fuel Systems, Vol 2:Diesel. 1994, London: Pentech Press Limited.

50. Edgar, B.L., *Ph.D Thesis,"Dimethyl Ether and Other Oxygenated Fuels for Low Emission Diesel Engine Combustion"*, in *Mechanical Engineering*. 1997, University of California-Berkley: Berkley,CA.

51. Soteriou, C., and Smith, M. "*Some characteristics of variable orifice nozzle geometries for diesel injection"*. Proceedings in *IMechE Seminar Publication*, 1999. 1-2 Dec. 1999, IMechE, London, UK: Professional Engineering Publishing Limited.

52. Glassman, I., Combustion. 2nd ed. 1987, Orlando, FL.: Academic Press.

53. Khair, M., Diesel Engine Technology. Society of Automotive Engineers Seminar Series. 1998, Warrendale, PA: Society of Automotive Engineers.

54. Khair, M., Lemaire, J., Fischer, S., "*Integration of Exhaust Gas Recirculation, Selective Catalytic Reduction, Diesel Particulate Filters, and Fuel-Borne Catalyst for NOx/PM Reduction." Society of Automotive Engineers*, 2000(2001-01-1933).

55. Khair, M., et al, "*Achieveing Heavy-Duty Diesel NOx/PM Levels Below the EPA 2002 Standards-- An Integrated Solution." Society of Automotive Engineers*, 2000(2000-01-0187).

56. Turns, S., An Introduction to Combustion: Concepts and Applications. 1996, New York: McGraw-Hill, Inc.

57. Morris, J.D., Wallace, G.M., "*Evaluation of Impact of a Multifunctional Additive Package on Eurpoean Diesel Passenger Car Emission Performance." Society of Automotive Engineers*, 1990 (904212).

58. Baranescu, R., "*Influence of Fuel Sulfur on DIesel Particualte Emissions." Society of Automotive Engineers*, 1998 (881174).

59. Lee, R., Pedley, J., Hobbs, C., "*Fuel Quality Impact on Heavy Duty Diesel Emissions:- A Literature Review." Society of Automotive Engineers*, 1998 (982649).

60. Schmidt, D., Wong, V., Green, W., Weiss, M., Heywood, J., "*Review and Assessment of Fuel Effects and Research Needs in Clean Diesel Technology." ASME Spring Technical Conference*, 2001. **36-1**: p. 23-37.

61. Johnson, J., Bagley, S., Gratz, L., Leedy, D., "*A Review of Diesel Particulate Control Technology and Emissions Effects- 1992 Horning Memorial Award Lecture." Society of Automotive Engineers*, 1994 (940233).

62. Barbour, R.H., Elliott, N.G., Rickeard, D.J., "*Understanding Diesel Lubricity." Society of Automotive Engineers*, 2000 (2000-01-1918).

63. Anastopoulos, G., Lois, E., Serdari, A., Zanikos, F., Stournas, S., Kalligeros, S., "*Lubrication Properties of Low-Sulfur Diesel Fuels inthe Presence of Specific Types of Fatty Acid Derivatives." Energy & Fuels*, 2001. **15**: p. 106-112.

64. Tucker, R., Stradling, R., Wolveridge, P., Rivers, K., Ubbens, A., "*The Lubricity of Deeply Hydrotreated Diesel Fuels- The Swedish Experience." Society of Automotive Engineers*, 1994(942016).

65. Lacey, P., and Westbrook, S., "*Diesel Fuel Lubricity." Society of Automotive Engineers*, 1995(950248).

66. CARB, *Report of the Diesel Fuel Task Force*. 1994, California Air Resources Board/ Governor of California: CA.

67. Ryan, T.W., III, Buckingham, J.P., Olikara, C., "*The Effects of Fuel Properties on Emissions from a 2.5gm NOx Heavy-Duty Diesel Engine." Society of Automotive Engineers*, 1998 (982491).

68. Siebers, D., "*Scaling Liquid-Phase Fuel Penetration in Diesel Sprays Based on Mixing-Limited Vaporization." Society of Automotive Engineers*, 1999(1999-01-0528).

69. Higgins, B., Mueller, C., and Siebers, D., "*Measurement of Fuel Effects on Liquid-Phase Penetration in DI Sprays." Society of Automotive Engineers*, 1999(1999-01-0519).

70. Canaan, R., Dec, J., Green, R., Daly, D., "*The Influence of Fuel Volatility on the Liquid-phase Fuel Penetration in a Heavy Duty DI Diesel Engine." Society of Automotive Engineers*, 1998 (980510).

71. ASTM, *Test Method D86 Standard Test Method for DIstillation of Petroleum Products*, in *ASTM Standards Volume 05.01*. 2000, American Society for Testing and Materials: West Conshohocken, PA.

72. ASTM, *Test Method D976 Standard Test Methods for Calculated Cetane Index of Distillate Fuels*, in *ASTM Standards Volume*. 2000, American Society for Testing and Materials: Wes Conshohocken,PA.

73. ASTM, *Test Method D4737 Standaard Test Method for Calculated Cetane Index by Four Variable Equation*, in *ASTM Standards Volume*. 2000, American Society for Testing and Materials: West Cohohocken, PA.

74. Fox, R., and McDonald, A., Introduction to Fluid Mechanics. 1985, New York: John Wiley & Sons, Inc.

75. McMurry, J., Organic Chemistry, 4th ed. 1995, Pacific Grove, CA: Brooks/Cole Publishing Company.

76. Marchionna, M., Patrini, R., Giavazzi, F., Pecci, G. "*Linear Ethers as High Quality Components for Reformulated Diesel Fuels"*. Proceedings in *Symposium on Removal of Aromatics, Sulfur and Olefins from Gasoline and Diesel presented at the 212th National Meeting (Aug 25-29), American Chemical Society*, 1996. Orlando, FL. 585-589.

77. Riesenberg, K.O., Faupel, W., Blaich, B., Stumpp, G., Ungerer, G., Polach, W., Leonard, R., Schneider, V., Ritter, E., Tschoke, H., Dieter, W., Warga, W., Kaczynski, B., Bauer, H., Diesel Fuel Injection. 1st ed. 1994, Stuttgart, Germany: Robert Bosch.

78. Kapus, P., Ofner, H., "*Development of Fuel Injection Equipment and Combustion Systems for DI Diesels operated on Dimethyl Ether." Society of Automotive Engineers*, 1995 (950062).

79. Ofner, H., Gill, D.W., Krotscheck, C., "*DME as Fuel for CI engines - A New Technology and its Environmental Potential." Society of Automotive Engineers*, 1998 (981158).

80. Glensvig, M., Sorenson, S.C., Abata, D. L., "*An Investigation of the Injection Characteristics of Dimethyl Ether." ASME Fall Technical Conference*, 1997. **29-3** (97-ICE-67): p. 77-84.

81. Nielsen, K., Sorenson, S., "*Lubricity Additive and Wear with DME in Diesel Injection Pumps." American Society of Mechanical Engineers, ICE Fall Technical Conference*, 1999. **33-1**(99-ICE-217): p. 145-153.

82. Nikanjam, N., "*Diesel Fuel Lubricity: On the Path to Specifications." Society of Automotive Engineers*, 1999(1999-01-1479).

83. Bechtold, R., Alternative Fuels Guidebook: Properties, Storage, Dispensing, and Vehicle Facility Modifications. 1997, Warrendale, PA: Society of Automotive Engineers.

84. Chen, Z., Kajitani, S., Minegisi, K., Oguma, M., "*Engine Performance and Exhaust Gas Characteristics of a Compression Ignition Engine Operated with DME blended Gas Oil Fuel." Society of Automotive Engineers*, 1998(982538).

85. Kajitani, S., Chen, Z. L., Konno M., Rhee, K.T., "*Engine performance and Exhaust Characterestics of DI Diesel Engine Operated with DME." Society of Automotive Engineers*, 1997 (972973).

86. Ikeda, M., Mikami, M., Kojima, N., "*Exhaust Emission Characteristics of DME/Diesel Fuel Engine." Society of Automotive Engineers*, 2000 (2000-01-2006).

87. Clifford, T., Fundamentals of Supercritical Fluids. 1999, New York: Oxford University Press.

88. *ESDU Engineering Data*. 1995.

89. Kikkawa, Y., and Aoki, I., "*Dimethyl Ether Fuel Proposed as an Alternative to LNG." Oil & Gas Journal*, 1998(Apr. 6): p. 55-59.

90. Tijm, P., Brown, W., Heydorn, E., Moore, R. "*Overview of the Liquid Phase Methanol (LPMEOH ^{TM}) Technology"*. Proceedings in *American Institute of Chemical Engineers Spring Meeting (March 9-13)*, 1997. Houston, TX.

91. Mikkelsen, S., Hansen, J., Sorenson, S., *Dimethyl Ether as an Alternate Fuel for Diesel Engines*, in *Application of Powertrain and Fuel Technologies to Meet Emissions Standards*, J. Mardell, Parsons, M., Read, J., Lemon, D., Editor. 1996, Professional Engineering Publishing Limites for IMechE: London, UK. p. 289.

92. Christensen, R., Sorenson, S.C., "*Engine Operation on DME in a Naturally Aspirated DI Diesel Engine." Society of Automotive Engineers*, 1997 (971665).

93. Hupperich, P., Dürnholz, M., Hüchtebrock, B., "*Diesel Oil, Water in Carbon Fuel Emulsion, DME or Natural gas? - Comparative tests on a Single Cylinder Engine." ASME Fall Technical Conference*, 1997. **29-3** (97-ICE-65): p. 61-67.

94. Amano, T., Dryer, F. L., "*Effect of DME, NOx, And Ethane or CH4 Oxidation : High Pressure, Intermediate - Temperature Experiments And Modelling." Twenty Seventh International Combustion Symposium Proceedings*, 1998: p. 397-404.

95. Hess, H., Boehman, A., Tijm, P., and Waller, F.J., "*Experimental Studies of the Impact of CETANER (TM) on Diesel Combustion and Emissions." Society of Automotive Engineers*, 2000 (2000-01-2886).

96. Curran, H., Pitz, W., Westbrook, C., Dagaut, P., Boettner, J-C., Cathonnet, M., "*A Wide Range Modeling Study of Dimethyl Ether Oxidation." Inter. Journal of Chemical Kinetics*, 1998. **30**(3): p. 229-241.

97. "*New fuel: The Lawnmower's tale." Economist*, 1995. **33**(7905): p. 79-82.

98. Arif, M., Dellinger, B., Taylor, P.H., "*Rate Coefficients of Hydroxyl Radical Reaction with Dimethyl Ether and Methyl tert-Butyl Ether over and Extended Temperature Range." J. Phys. Chem. A*, 1997. **101**(13): p. 2436-2441.

99. Frye, C., Boehman, A., Tijm, P.J.A., "*Comparison of CO and NO Emissions from Propane, n-Butane, and Dimethyl Ether Premixed Flames." Energy & Fuels*, 1999. **13**(3): p. 650-654.

100. Sorenson, S.C., Glensvig M., Abata Duane L, "*Dimethyl Ether in Diesel Fuel Injection Systems." Society of Automotive Engineers*, 1998 (981159).

101. Wakai, K., Yoshizaki, T., "*Numerical and Experimental Analyses of the Injection Characteristics of Dimethyl Ether with a DI Diesel Injection System." Society of Automotive Engineers*, 1999 (1999-01-1122).

102. Konno, M., Kajitani, S., Oguma, M., Iwase, T., Shima, K., "*NO Emission Characteristics of a CI Engine Fueled with Neat Dimethyl Ether." Society of Automotive Engineers*, 1999 (1999-01-1116).

103. DuPont, *Dymel Aerosol Propellants: Dymel A*, in *Technical Information ATB-25*. 1992, Fluorochemicals Laboratory, E.I. duPont de Nemours and Company.

104. Navistar, T444E Diesel Engine/Vehicle Diagonostic Manual for International Trucks EGES-190. 1997, Melrose Park, IL: Navistar International Transportation Corp.

105. Navistar, *Loss of Power and Engine Knock on International T444E Built January 1997 and Later with Split Shot Fuel Injectors*. 1997, Navistar International Transportation Corp.: Melrose Park, IL.

106. Bhide, S., Boehman, A., and Perez, J. "*Viscosity of DME-Diesel Fuel Blends"*. Proceedings in *222nd ACS National Meeting, Preprints of Symposia, Division of Petroleum Chemistry*, 2001. Chicago,IL. 400-401.

107. Bhide, S., *MS Thesis (Work In Progress)*, in *Department of Mechanical Engineering*. 2002, Pennsylvania State University: University Park, PA.

108. Sivebaek, I., Sorenson, S., Jakobsen, "*Dimethyl Ether (DME)- Assessment of Viscosity Using the New Volatile Fuel Viscometer (VFVM)." Society of Automotive Engineers*, 2001 (2001-01-2013).

109. Chapman, E., Bhide, S., Boehman, A., Tijm, P.J.A., Waller, F.J., "*Emission Characteristics of a Navistar 7.3L Turbodiesel Fueled with Blends of Oxygenates and Diesel." Society of Automotive Engineers*, 2000 (2001-01-2887).

110. Rassweiler, G., and Withrow, L., "*Motion Pictures of Engine Flames Correlated with Pressure Cards (Reprint of original: Jan 14, 1938)." Society of Automotive Engineers*, 1980(800131).

111. Glassey, S., Stockner, A., Flinn, M., "*HEUI- A New Direction for Diesel Engine Fuel Systems." Society of Automotive Engineers*, 1993(930270).

112. Stockner, A., Flinn, M., Camplin, F., "*Development of the HEUI Fuel System Integration of Deisgn, Simulation, Test, and Manufacturing." Society of Automotive Engineers*, 1993(930271).

113. Stone, R., Introduction to Internal Combustion Engines; 2nd edition. 2nd ed. 1992, Warrendale, PA: Society of Automotive Engineers.

114. Moffat, R.J., "*Describing the Uncertanties in Experimental Results." Experimental Thermal and Fluid Science*, 1988. **1**: p. 3-17.

115. Hess, H., Szybist, J., Boehman, A., Tijm, P., Waller, F. "*The Use of CETANER™ for the Reduction of Particulate Matter Emissions in a Turbocharged Direct Injection Medium-Duty Diesel Engine"*. Proceedings in *Seventeenth Annual International Pittsburgh Coal Conference, September 11-15*, 2000. Pittsburgh, PA.

116. Sidhu, S., Graham, J., Striebich, R., "*Semi-volatile and Particulate Emissions from the Combustion of Alternative Diesel Fuels." Chemosphere*, 2001. **42**: p. 681-690.

117. Flynn, P.F., DUrrett, R.P., Hunter, G.L., Loye, A.Z., Akinyemi, O.C., Dec, J.E., Westbrook, C.K., "*Diesel Combustion: An Integrated View Combining Laser Diagnostics, Chemical Kinetics, and Empirical Validation." Society of Automotive Engineers*, 1999 (990509).

118. Westbrook, C. "*Chemical Kinetics of Hydrocarbon Ignition in Practical Combustion Systems"*. Proceedings in *Twenty Eighth International Combustion*

Symposium, 2002. Edinburgh, Scotland: The Combustion Institute, Pittsburgh, PA. 1563-1578.

119. Moser, F., Sams, T. and Cartellieri, W., "*Impact of Future Exhaust Gas Emission Legislation on the Heavy Duty Truck Engine." Society of Automotive Engineers*, 2001 (2001-01-0186).

120. Holman, J.P., Experimental Methods for Engineers. 4th ed. 1984, New York: McGraw-Hill Book Company.

121. Devore, J.L., Probability and Statistics for Engineering and the Sciences. 5th ed. 2000, Pacific Grove, CA: Duxbury: Thomson Learning.

122. Bauer, H., ed. Automotive Handbook, 4th ed. 1996, Robert Bosch GmbH: Stuttgart, Germany.

123. Ekiz, H., Kutlu, A., Baba, M., Powner, E. "*Performance Analysis of a CAN/CAN Bridge"*. Proceedings in *IEEE ICNP'96 Conference,29 Oct-1 Nov*, 1996. Ohio, USA.

Appendix A

Statistical Control and Analysis of Performance and Emissions Experimental Data

A.1 Introduction

The following section describes the statistical controls and statistical analysis of the data collected for this research. A basic overview of experimental error will be discussed, followed by a generic description of statistical analysis concepts. Finally, a discussion of the experimental analysis techniques specific to this research will be discussed, divided into two parts. The first part will describe the data sample collection from the pieces of equipment used, and how they were programmed to collect samples to provide a statistical normal distribution of the data. The second part will describe the spreadsheet used to produce the graphs of the emissions data, including the error bars for the data. Some assumptions that were made to compile this data will be explained.

A.2 Causes and Types of Experimental Error

Some form of experimental analysis must be performed on all data. The analysis may be simplistic, or a more complex analysis of the errors involved, in an effort to match results with fundamental physical principles. In the process of setting up any

experimental equipment, an analysis of the data is important for several reasons. These reasons include:

- to determine and quantify the errors and establish areas where maximum reductions can be achieved,
- to establish an appropriate number of samples needed to reduce standard deviations to the acceptable confidence level and gain precision, and
- to give validity to experimental measurements [120].

Typical types of errors which cause uncertainty in experiments include apparatus or instrumentation error, fixed errors (systematic errors), human error, and random errors. Instrumentation errors are those involved with setup and design mistakes. Fixed errors are considered errors which occur for unknown reasons, with the error being roughly the same amount for each repeated reading. Human error would involve a mistake being made in reading and recording a direct observation, and could be considered a reproducibility issue if various people are involved in data collection. Random errors involve random events, which may or may not be attributed to the other three types of errors [120].

A.3 Basic Statistical Analysis Concepts

To be able to draw conclusions from a data set, a quantitative description of the data is needed. The first step is to determine the uncertainty involved with the data, as a function of the results and independent variables which make up the data set. This

method is also know as Root Sum Square analysis. Next, these results would be used, in addition to the standard deviations and means for the individual data sets, to create the error bars describing the error in the experimental results. The following section will further explain the equations involved.

A.3.1 Uncertainty Analysis

When trying to determine the uncertainty in a set of measurements, the odds for the particular uncertainty would also be an important factor to add further specification to the uncertainty estimate. For example, knowing the calibration history of a device versus not knowing the calibration history may change the precision odds for the measurement. If a set of measurements is made and the odds for the uncertainty in the primary measurements are known, uncertainties in the calculated results can be estimated. This result is sometimes referred to as the Root Sum Square method. The result R is a given function of the independent variables x_1, x_2, x_3, ….x_n. Then, the following is true in equation A.1.

$$R=R(x_1, x_2, x_3, \ldots.x_n) \qquad (A.1)$$

If w_r is the uncertainty in the result and $w_1,w_2,w_3,\ldots w_n$ is the uncertainty in the independent variables, given that the uncertainties in the independent variables are given with the same odds, then the uncertainty in the result having these odds would be given in

equation A.2. The relationship from this equation can be used to calculate the percent uncertainty [120] [114].

$$w_r = \left[\left(w_1\frac{\partial R}{\partial x_1}\right)^2+\left(w_2\frac{\partial R}{\partial x_2}\right)^2+\cdots+\left(w_n\frac{\partial R}{\partial x_3}\right)^2\right]^{1/2} \qquad (A.2)$$

A.3.2 Statistical Analysis and Confidence Interval

Typically, a 95% confidence level is utilized during error analysis testing. This means that the $\alpha/2$ (α, the confidence interval) equals .025 and is used in the hypothesis test. Depending on the number of data points collected, the Central Limit Theorem may or may not be valid. In the case where it is not valid (sample size less than 30 samples) , a "t" test approximation is used. The "t" test establishes a bell shaped approximation of the data, based on the degrees of freedom present in the data. Using the "t" test yields equations to calculate the confidence intervals and the error, given in A.3. The error involves one side of the interval divided by the sample mean.

$$\bar{x} \pm t_{\alpha/2,n-1} \bullet s/\sqrt{n} \qquad (A.3)$$

Where:

$t_{\alpha/2,n-1}$ is the number on the measurement axis for which the area under the t curve with ν degree of freedom to the right of $t_{\alpha/2,n-1}$ is α, and ν is n-1.

ν is the degrees of freedom, n-1

s is the standard deviation of the sample population

n is the number of data points

$\bar{x}$ is the average sample population

The value of the t test varies depending on the value of α, the confidence interval, and the degrees of freedom, ν [121]. A typical t curve is shown below in *Figure A–1*

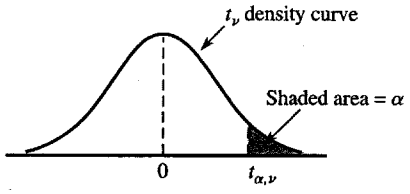

Figure A–1: t-curve

If several data groups have been collected, an analysis of variance (ANOVA) can be used to determine the qualitative response from the data. A Single-Factor ANOVA is used to compare more than two populations or treatment means. If the comparison yields nothing significant, a multiple comparison procedure is then used [121]. This will

become important when performing the comparison on the Mode 4 engine data found in Appendix C.

A.4 Summary of Experimental Error Analysis

The list of equipment used in this experiment is given in *Table A–1* with the manufacturer's listed error, or allowed minimum calibrated error. Additionally, the table shows how the data is collected and how many samples are collected for each variable monitored. The data collected by the Windows-based computer connected to the Modicon PLC sampled the data 33 times, and used the average of the samples for each data point. This allowed for the assumption of a normal distribution for a sample size above 30 samples, and the use of the standard normal curves for determining confidence intervals. The data points were collected throughout the entire engine operation for each mode, which was usually 60 to 80 minutes of data per mode. From this group of data points, the average of every 30 points were used in the excel spreadsheet, giving 5 points from which the standard deviation and 95 % confidence interval was calculated.

Table A–1: Engine Laboratory equipment

Equipment Type	Variables Collected	Error in Data Point	Number of data points per time	Assumptions
Sierra Instruments BG-1 Micro Dilution Test Stand	Particulate Filters	Standard Deviation between Filter samples; causes unknown	1 sample each 5 minutes; 5 samples total each engine mode	Dilution flow is constant, Temperature difference between filters and modes is negligible; Temp. maintained below 52°C
Sartorius M3P Precisions Microbalance (located in environmental chamber)	Weight Particualte Filters	± 0.005 gm	Filters weighted 3 times pre- and post collection	Humidity chamber is constant 45% relative humidity
Nicolet Magna 550 FTIR Spectrometer	NO,NO_2,CO,CO_2	Calibration curve for 1% or less error	5 samples throughout engine test run	Stable gas flow rate, clean spectrometer windows; negligible interferences at wavelengths; cell temp. and pressure constant
California Analytical HFID 300 THC analyzer	Total Hydrocarbons	Resolution 0.01ppm, Repeatability ± .05% of full scale	2 per engine mode	Constant clean sample flow
Rosemont Analytical Oxygen analyzer	Percent Oxygen	± 1% per daily calibration; Resolution 0.01%	5 per engine mode	Constant flow through system
450 hp Eaton eddy current dynamometer	Engine Load control	Zero:1% of rated Repeatable:0.05% of FS; temp.effect 0.002% of FS/°F		Coolant temp. causes no variability in load; Non-linear 0.03% of FS* calib.; Hysteresis 0.04% of FS
Navistar Engine Computer connected to National Instruments CAN (Controller Area Network) board	Injection timing and pressure, temperatures, volume fuel desired	Unknown	800 per 10 seconds; using average of 800 points	Engine is steady state, so that data is steady state
Kistler 6125 Pressure sensor , charge amplifier, Visual Basic program	Pressure, crank angle and TDC trigger	Sensitivity :–15 pC/bar; Linearity: <0.5%FSO	1 data point per crank angle, average of 50	
Torque meter	Torque load on engine	Repeatability 0.05% of full scale	Average of 33 cycles/data point, appx. 1 point/ min	Load created by water flowing over dyno at zero load factor is negligible.
Modicon (PLC) Programmable Logic Controller; Visual Basic program by DDE (Dynamic Data Exchange)	Engine and fuel temperatures, speed, load,,mass air flow	Resolution of 0.25°C; Error of 0.4% over the range of 0 - 60 °C	Average of 33 cycles per data point, appx. 1 data point per minute	PLC is adequately providing temperature reference
MPSI Prolink Service tool	Turbo Boost Pressure	Unknown sampling rate	5 per engine mode test	
Delphi Mass Air Flow (MAF) meter calibrated with a Marion Laminar Flow Element	Voltage signal converted to MAF	Calibration curve has R^2 of 1	5 per engine mode	
Omega K type Thermocouples	Temperature	2.2°C Error or 0.75% above 0°C	Average of 33 cycles/data point, appx. 1 point/ min	
Sartorius Scale	Fuel	Resolution 0.2gm	5 /engine mode, for 5 minutes each	Fuel reading taken when scale reading changed

* FS- Full Scale

A.5 Summary of Excel Spreadsheet Calculations

The following section will describe the equations used to analyze the emissions data, including any assumptions used. Additionally, a description of how the error bars for the data sets were created will be discussed.

To aid in simplifying the analysis process, some assumptions are made regarding the exhaust. First, since the dilution ratio for the particulate sampling with the BG-1 was 8:1 at 150 SLPM (standard liter per minute) total flow rate, the true flow of exhaust particulate was 150 divided by 9, or 16.667 l/min of exhaust. This factor, which represents the flow of exhaust for the particulate measurement at that mode, was the divisor of the total exhaust flow in l/min, and was used to obtain a multiplier to calculate the total particulate in grams per hour. All other emissions measurements used the density of the measured gas divided by the total exhaust flow for the mode to get the measured gas in grams per hour. The density for each measured gas was calculated using the exhaust gas temperature. The density of the exhaust gas was assumed to be 1.2 kg/m^3 at 300 K, and corrected for the specific measured exhaust temperature for the mode.

Primarily, the data sets establishing the steady state operation of the engine for each mode consist of 5 groups. Within these five groups, which includes engine speed, power, torque, and various temperatures, are 30 or more data points which have been collected from the data acquisition system. Each of these data points is from an average of 33 points collected by the system. The standard deviation across the points for each of the five groups is determined from the set of 30 points. This data is used to create the error bars, and consists of items such as speed, load and air flow. The emissions data is

collected 5 times for each mode. Therefore, the “t” test is set up for a 95% confidence interval, with a sample size of 5. The error interval is then created based on the standard deviation in the data, and a root sum square of the equipment error for the steady state operation of the engine.

Appendix B

Statistical Analysis of the Particulate Matter Data Collection

The following section describes the process by which the particulates were measured and evaluated in this research. Extra attention was placed on this portion of the experiment, to provide for quality and repeatability in the data collection. This section contains a description of the procedure, the raw data, and general comments and recommendations about the data.

Particulate samples were collected for each AVL-8 mode, and each fuel blend. Test protocol requires that 5 particulate samples be collected, for statistical quality of the data. The spreadsheet used to analyze the data calculates error bars based on 95% confidence intervals, for a five sample set.

ISO 8178 Part 2 calls for the particulate filters to be pre-conditioned and weighed prior to use, in a controlled environment which is kept to 45% humidity, ± 2%. The scale used to weigh the filters gives a standard deviation across six weighing trials of .005 gm.

It has been the typical procedure in the lab to weigh the filters one time before and one time after particulate collection. For the purpose of trying to minimize the error in the weight of the particulate filters, since the fuel blends were expected to reduce the amount on the filters, the filters were weighed three times before and three times after the collection. The same person weighed the filters, and waited for the scale to stabilize for

10 seconds between each weighing. Also, the scale was tared for each weighing. The average weight was used as the result of the analysis.

The data from this project was collected and put into a spreadsheet for some basic statistical analysis. Preliminarily, the difference between the three samples before and after were compared against the .005 gm standard deviation for the scale weighing range. The spreadsheet gives a True or False indication that the difference is within the standard deviation constraint. The .005 gm was determined by the manufacturer to be the standard deviation from the weighing of the same filter six times. *Figure B–1*, on the following pages, shows the filter weightings before the particulate collection. BF refers to the before weighing. AF refers to weighing after sample collection. The "Problem" column is used to indicate that the standard deviation being above .005 . True in the column would indicate that it is above .005.

Many True indications were observed. This could indicate that there are some other aspects contributing to the error of the data than the scale. The .005 number is much lower than the true error of the entire process.

There are several reasons to explain the results of this data. Since the humidity chamber is to be kept at the designated humidity, the humidifier had to be cycled to keep the humidity constant. The affect of the humidity on the filter is unknown, and not quantified. Another explanation could be malfunction of the humidity sensor. Additionally, particulates could be blown off or somehow removed by static electricity, reducing the weight of the filters.

As recommendations, the following are a few suggestions which may improve the accuracy of this data, even though the source of the inaccuracies has not been quantified. The first effort should be to determine how the standard deviation affects the accuracy of the particulate measurements, to further determine the range in which there is 95% confidence based on the sample size. Some effort should be made to quantify the moisture absorption tendency of the filters, to determine the effect on the filter weight. Also, the humidity chamber environmental controls should be inspected, as well as to confirm the correct operation of the chamber sensors. Further, the device to remove static electricity should be regularly replaced. Also, a ground strip connected from the operator's wrist to bench top could be put in place as an additional method to remove any possibility of static build up on the filter and in the chamber.

Test number	Filter No.	BF weight 1	BF weight 2	BF weight 3	Std dev BF	Problem	Af weight 1	AF weight2	AF weight 3	Std dev AF	Problem
bd349m 1	1	330.304	330.276	330.274	0.0168	TRUE	331.123	331.129	331.13	0.0038	FALSE
bd349m 1	2	330.65	330.688	330.704	0.0277	TRUE	331.502	331.506	331.483	0.0123	TRUE
bd349m 1	3	327.959	327.985	327.973	0.0130	TRUE	328.805	328.825	328.82	0.0104	TRUE
bd349m 1	4	330.761	330.77	330.76	0.0055	TRUE	331.586	331.602	331.597	0.0082	TRUE
bd349m 1	5	330.749	330.753	330.742	0.0056	TRUE	331.581	331.588	331.598	0.0085	TRUE
bd349m 2	1	330.895	330.881	330.872	0.0116	TRUE	332.119	332.134	332.129	0.0076	TRUE
bd349m 2	2	327.67	327.663	327.646	0.0123	TRUE	328.924	328.914	328.916	0.0053	TRUE
bd349m 2	3	329.808	329.83	329.83	0.0127	TRUE	331.054	331.042	331.043	0.0067	TRUE
bd349m 2	4	331.92	331.982	331.961	0.0315	TRUE	333.257	333.251	333.235	0.0114	TRUE
bd349m 2	5	324.71	324.749	324.751	0.0231	TRUE	326.083	326.077	326.065	0.0092	TRUE
bd349m 3	1	333.992	333.98	333.982	0.0064	TRUE	334.848	334.851	334.843	0.0040	FALSE
bd349m 3	2	333.291	333.277	333.304	0.0135	TRUE	334.375	334.371	334.366	0.0045	FALSE
bd349m 3	3	331.079	331.083	331.075	0.0040	FALSE	332.18	332.182	332.178	0.0020	FALSE
bd349m 3	4	334.197	334.2	334.193	0.0035	FALSE	335.197	335.2	335.205	0.0040	FALSE
bd349m 3	5	333.296	333.294	333.288	0.0042	FALSE	334.166	334.159	334.162	0.0035	FALSE
bd349m 4	1	332.581	332.574	332.57	0.0056	TRUE	335.218	335.214	335.209	0.0045	FALSE
bd349m 4	2	335.25	335.25	335.248	0.0012	FALSE	337.789	337.789	337.789	0.0000	FALSE
bd349m 4	3	335.244	335.244	335.245	0.0006	FALSE	337.735	337.726	337.723	0.0062	TRUE
bd349m 4	4	333.935	333.937	333.934	0.0015	FALSE	336.379	336.371	336.377	0.0042	FALSE
bd349m 4	5	335.832	335.825	335.814	0.0091	TRUE	338.55	338.548	338.543	0.0036	FALSE
bd349m 1	a	331.423	331.425	331.425	0.0012	FALSE	331.935	331.935	331.935	0.0000	FALSE
bd349m 1	b	332.255	332.244	332.243	0.0067	TRUE	332.779	332.768	332.775	0.0056	TRUE
bd349m 2	a	324.489	324.485	324.49	0.0026	FALSE	325.558	325.546	325.55	0.0061	TRUE
bd349m 2	b	323.818	323.812	323.81	0.0042	FALSE	324.959	324.965	324.95	0.0075	TRUE
bd349m 3	a	329.9	329.897	329.892	0.0040	FALSE	330.823	330.823	330.817	0.0035	FALSE
bd349m 3	b	332.199	332.176	332.172	0.0146	TRUE	333.038	333.038	333.034	0.0023	FALSE
bd349m 4	a	330.871	330.857	330.869	0.0076	TRUE	333.42	333.41	333.415	0.0050	FALSE

Figure B–1: Particulate Filters

bd349m 5	1	322.767	322.761	322.754	0.0065	TRUE	324.328	324.321	324.322	0.0038	FALSE
bd349m 5	2	325.301	325.279	325.276	0.0137	TRUE	326.626	326.627	326.62	0.0038	FALSE
bd349m 5	3	325.932	325.929	325.935	0.0030	FALSE	327.323	327.32	327.308	0.0079	TRUE
bd349m 5	4	321.957	321.967	321.947	0.0100	TRUE	323.371	323.366	323.38	0.0071	TRUE
bd349m 5	5	327.796	327.79	327.79	0.0035	FALSE	329.198	329.194	329.187	0.0056	TRUE
bd349m 6	1	324.783	324.766	324.771	0.0087	TRUE	325.724	325.724	325.72	0.0023	FALSE
bd349m 6	2	322.305	322.292	322.299	0.0065	TRUE	323.15	323.148	323.144	0.0031	FALSE
bd349m 6	3	326.338	326.332	326.324	0.0070	TRUE	327.33	327.319	327.32	0.0061	TRUE
bd349m 6	4	333.644	333.648	333.633	0.0078	TRUE	334.634	334.632	334.627	0.0036	FALSE
bd349m 6	5	324.42	324.394	324.394	0.0150	TRUE	325.421	325.407	325.413	0.0070	TRUE
bd349m 7	1	330.998	330.991	331.002	0.0056	TRUE	331.605	331.599	331.599	0.0035	FALSE
bd349m 7	2	326.61	326.6	326.592	0.0090	TRUE	327.198	327.194	327.194	0.0023	FALSE
bd349m 7	3	329.253	329.249	329.246	0.0035	FALSE	329.896	329.893	329.886	0.0051	TRUE
bd349m 7	4	329.331	329.325	329.32	0.0055	TRUE	330.01	330.023	330.014	0.0067	TRUE
bd349m 7	5	323	322.989		0.0078	TRUE	323.703	323.696	323.702	0.0038	FALSE
bd349m 8	1	324.552	324.545	324.538	0.0070	TRUE	325.157	325.156	325.152	0.0026	FALSE
bd349m 8	2	324.181	324.16	324.179	0.0116	TRUE	324.908	324.981	324.888	0.0490	TRUE
bd349m 8	3	333.418	333.406	333.4	0.0092	TRUE	334.029	334.016	334.021	0.0066	TRUE
bd349m 8	4	333.554	333.544	333.548	0.0050	TRUE	334.343	334.345	334.342	0.0015	FALSE
bd349m 8	5	329.385	329.36	329.367	0.0129	TRUE	330.038	330.037	330.032	0.0032	FALSE
bd549m 1	1	331.925	331.921	331.915	0.0050	TRUE	332.735	332.737	332.735	0.0012	FALSE
bd549m 1	2	329.355	329.357	329.351	0.0031	FALSE	330.18	330.18	330.172	0.0046	FALSE
bd549m 1	3	327.512	327.52	327.512	0.0046	FALSE	328.353	328.356	328.37	0.0091	TRUE
bd549m 1	4	332.925	332.927	332.927	0.0012	FALSE	333.75	333.75	333.747	0.0017	FALSE
bd549m 1	5	328.435	328.443	328.442	0.0044	FALSE	329.151	329.151	329.158	0.0040	FALSE
bd549m 2	1	332.12	332.117	332.111	0.0046	FALSE	333.303	333.296	333.293	0.0051	TRUE
bd549m 2	2	330.923	330.925	330.918	0.0036	FALSE	332.114	332.114	332.11	0.0023	FALSE
bd549m 2	3	333.847	333.839	333.852	0.0066	TRUE	334.992	334.997	334.989	0.0040	FALSE
bd549m 2	4	326.623	326.611	326.612	0.0067	TRUE	327.734	327.727	327.723	0.0056	TRUE
bd549m 2	5	334.447	334.441	334.44	0.0038	FALSE	335.565	335.559	335.56	0.0032	FALSE

(cont.)

bd549m 3	1	333.441	333.438	333.426	0.0079	TRUE	334.317	334.313	334.306	0.0056	TRUE
bd549m 3	2	332.841	332.835	332.828	0.0065	TRUE	333.697	333.697	333.688	0.0052	TRUE
bd549m 3	3	332.067	332.066	332.059	0.0044	FALSE	332.879	332.875	332.869	0.0050	TRUE
bd549m 3	4	333.26	332.266	333.273	0.5777	TRUE	334.059	334.06	334.054	0.0032	FALSE
bd549m 3	5	334.587	334.588	334.585	0.0015	FALSE	335.421	335.425	335.422	0.0021	FALSE
bd549m 4-1	1	332.162	332.153	332.154	0.0049	FALSE	334.634	334.641	334.639	0.0036	FALSE
bd549m 4	2	331.978	331.977	331.973	0.0026	FALSE	334.438	334.437	334.433	0.0026	FALSE
bd549m 4	3	329.826	329.823	329.807	0.0102	TRUE	332.236	332.229	332.223	0.0065	TRUE
bd549m 4	4	331.007	331.007	331.003	0.0023	FALSE	333.454	333.466	333.456	0.0064	TRUE
bd549m 4	5	333.156	333.149	333.141	0.0075	TRUE	335.507	335.503	335.508	0.0026	FALSE
bd549m 4-2	1	331.518	331.524	331.522	0.0031	FALSE	333.59	333.587	333.58	0.0051	TRUE
bd549m 4	2	334.752	334.752	334.749	0.0017	FALSE	336.806	336.805	336.813	0.0044	FALSE
bd549m 4	3	333.824	333.814	333.813	0.0061	TRUE	335.823	335.816	335.812	0.0056	TRUE
bd549m 4	4	333.517	333.516	333.505	0.0067	TRUE	335.601	335.588	335.58	0.0106	TRUE
bd549m 4	5	334.929	334.929	334.922	0.0040	FALSE	337.092	337.082	337.076	0.0081	TRUE
bd549m 4-3	1	334.32	334.317	334.31	0.0051	TRUE	336.088	336.082	336.079	0.0046	FALSE
bd549m 4	2	318.452	318.445	318.435	0.0085	TRUE	320.11	320.11	320.106	0.0023	FALSE
bd549m 4	3	328.788	328.783	328.782	0.0032	FALSE	330.398	330.389	330.387	0.0059	TRUE
bd549m 4	4	327.661	327.657	327.646	0.0078	TRUE	329.322	329.308	329.309	0.0078	TRUE
bd549m 4	5	330.163	330.175	330.166	0.0062	TRUE	331.797	331.791	331.79	0.0038	FALSE
bd549m 4-4	1	320.965	320.962	320.955	0.0051	TRUE	322.985	322.97	322.969	0.0090	TRUE
bd549m 4	2	331.999	332.001	331.995	0.0031	FALSE	334.016	334.007	334.008	0.0049	FALSE
bd549m 4	3	325.225	325.217	325.217	0.0046	FALSE	327.095	327.091	327.093	0.0020	FALSE
bd549m 4	4	326.864	326.863	326.856	0.0044	FALSE	328.801	328.807	328.802	0.0032	FALSE
bd549m 4	5	328.859	328.855	328.838	0.0112	TRUE	330.809	330.816	330.812	0.0035	FALSE
bd549m 5-2	1	330.31	330.312	330.283	0.0162	TRUE	331.63	331.618	331.63	0.0069	TRUE
bd549m 5	2	331.354	331.634	331.34	0.1658	TRUE	332.72	332.729	332.724	0.0045	FALSE
bd549m 5	3	331.631	331.634	331.622	0.0062	TRUE	333.023	333.014	333.01	0.0067	TRUE
bd549m 5	4	333.781	333.773	333.777	0.0040	FALSE	335.108	335.105	335.092	0.0085	TRUE
bd549m 5	5	331.068	331.068	331.062	0.0035	FALSE	332.405	332.415	332.412	0.0051	TRUE

(cont.)

bd549m 5-1	1	332.873	332.871	332.864	0.0047	FALSE	334.163	334.159	334.152	0.0056	TRUE
bd549m 5	2	331.405	331.398	331.4	0.0036	FALSE	332.7	332.694	332.682	0.0092	TRUE
bd549m 5	3	331.405	331.403	331.4	0.0025	FALSE	332.767	332.768	332.758	0.0055	TRUE
bd549m 5	4	330.918	330.922	330.916	0.0031	FALSE	332.333	332.326	332.323	0.0051	TRUE
bd549m 5	5	328.841	328.835	328.834	0.0038	FALSE	330.253	330.261	330.253	0.0046	FALSE
bd549m 6	1	329.91	329.899	329.899	0.0064	TRUE	330.887	330.885	330.881	0.0031	FALSE
bd549m 6	2	332.788	332.782	332.776	0.0060	TRUE	333.757	333.75	333.75	0.0040	FALSE
bd549m 6	3	330.759	330.757	330.753	0.0031	FALSE	331.797	331.799	331.792	0.0036	FALSE
bd549m 6	4	333.169	333.175	333.166	0.0046	FALSE	334.145	334.145	334.141	0.0023	FALSE
bd549m 6	5	330.938	330.933	330.931	0.0036	FALSE	331.852	331.845	331.842	0.0051	TRUE
bd549m 7	1	332.278	332.298	332.292	0.0103	TRUE	333.169	333.163	333.16	0.0046	FALSE
bd549m 7	2	333.95	333.943	333.944	0.0038	FALSE	334.796	334.797	334.798	0.0010	FALSE
bd549m 7	3	330.844	330.833	330.841	0.0057	TRUE	331.645	331.629	331.621	0.0122	TRUE
bd549m 7	4	332.629	332.638	332.627	0.0059	TRUE	333.389	333.384	333.377	0.0060	TRUE
bd549m 7	5	331.378	331.365	331.383	0.0093	TRUE	332.054	332.044	332.042	0.0064	TRUE
bd549m 8	1	331.672	331.671	331.66	0.0067	TRUE	332.155	332.175	332.154	0.0118	TRUE
bd549m 8	2	334.69	334.709	334.697	0.0096	TRUE	335.284	335.287	335.276	0.0057	TRUE
bd549m 8	3	330.917	330.905	330.903	0.0076	TRUE	331.776	331.771	331.766	0.0050	FALSE
bd549m 8	4	334.478	334.501	334.489	0.0115	TRUE	335.151	335.15	335.151	0.0006	FALSE
bd549m 8	5	332.351	332.344	332.342	0.0047	FALSE	333.024	333.019	332.999	0.0132	TRUE
dd349m 1	1	331.747	331.756	331.728	0.0143	TRUE	332.585	332.598	332.592	0.0065	TRUE
dd349m 1	2	334.345	334.35	334.345	0.0029	FALSE	335.161	335.173	335.166	0.0060	TRUE
dd349m 1	3	331.26	331.273	331.264	0.0067	TRUE	332.076	332.075	332.074	0.0010	FALSE
dd349m 1	4	333.69	333.693	333.693	0.0017	FALSE	334.562	334.562	334.544	0.0104	TRUE
dd349m 1	5	330.927	330.917	330.913	0.0072	TRUE	331.747	331.753	331.748	0.0032	FALSE
dd349m 1-1	1	331.023	331.027	331.011	0.0083	TRUE	331.936	331.929	331.926	0.0051	TRUE
dd349m 1	2	327.649	327.659	327.654	0.0050	FALSE	328.553	328.547	328.542	0.0055	TRUE
dd349m 1	3	331.351	331.356	331.356	0.0029	FALSE	332.299	332.287	332.287	0.0069	TRUE
dd349m 1	4	326.192	326.217	326.191	0.0147	TRUE	326.967	326.96	326.96	0.0040	FALSE
dd349m 1	5	330.696	330.696	330.695	0.0006	FALSE	331.639	331.646	331.639	0.0040	FALSE

(cont.)

dd349m 2	1	324.967	324.96	324.956	0.0056	TRUE	326.152	326.151	326.142	0.0055	TRUE
dd349m 2	2	333.509	333.524	333.515	0.0075	TRUE	334.473	334.475	334.478	0.0025	FALSE
dd349m 2	3	332.939	332.938	332.929	0.0055	TRUE	333.899	333.896	333.891	0.0040	FALSE
dd349m 2	4	329.147	329.142	329.134	0.0066	TRUE	330.053	330.053	330.045	0.0046	FALSE
dd349m 2	5	332.742	332.744	332.733	0.0059	TRUE	333.604	333.605	333.603	0.0010	FALSE
dd349m 3	1	327.611	327.612	327.619	0.0044	FALSE	328.451	328.466	328.458	0.0075	TRUE
dd349m 3	2	331.672	331.666	331.666	0.0035	FALSE	332.432	332.437	332.434	0.0025	FALSE
dd349m 3	3	330.07	330.088	330.076	0.0092	TRUE	330.802	330.803	330.806	0.0021	FALSE
dd349m 3	4	330.311	330.314	330.307	0.0035	FALSE	331.026	331.025	331.02	0.0032	FALSE
dd349m 3	5	334.452	334.44	334.46	0.0101	TRUE	335.175	335.178	335.181	0.0030	FALSE
dd349m 4	1	333.77	333.765	333.755	0.0076	TRUE	335.123	335.116	334.937	0.1054	TRUE
dd349m 4	2	330.727	330.723	330.727	0.0023	FALSE	331.832	331.841	331.834	0.0047	FALSE
dd349m 4	3	322.915	322.897	322.903	0.0092	TRUE	324.027	324.025	324.022	0.0025	FALSE
dd349m 4	4	324.815	324.811	324.795	0.0106	TRUE	325.992	325.99	325.982	0.0053	TRUE
dd349m 4	5	330.382	330.379	330.381	0.0015	FALSE	331.361	331.358	331.358	0.0017	FALSE
dd349m 5	1	324.767	324.766	324.75	0.0095	TRUE	325.749	325.75	325.735	0.0084	TRUE
dd349m 5	2	330.651	330.651	330.649	0.0012	FALSE	331.633	331.62	331.623	0.0068	TRUE
dd349m 5	3	331.167	331.172	331.17	0.0025	FALSE	332.228	332.245	332.238	0.0085	TRUE
dd349m 5	4	329.077	329.078	329.075	0.0015	FALSE	330.124	330.137	330.136	0.0072	TRUE
dd349m 5	5	333.846	333.837	333.832	0.0071	TRUE	334.886	334.889	334.884	0.0025	FALSE
dd349m 6	1	328.616	328.609	328.605	0.0056	TRUE	329.406	329.404	329.404	0.0012	FALSE
dd349m 6	2	317.999	317.998	317.989	0.0055	TRUE	318.9	318.898	318.892	0.0042	FALSE
dd349m 6	3	320.29	320.292	320.29	0.0012	FALSE	321.178	321.181	321.17	0.0057	TRUE
dd349m 6	4	317.569	317.585	317.583	0.0087	TRUE	318.442	318.454	318.446	0.0061	TRUE
dd349m 6	5	319.57	319.58	319.564	0.0081	TRUE	320.46	320.456	320.447	0.0067	TRUE
dd349m 7	1	323.202	323.217	323.205	0.0079	TRUE	324.259	324.263	324.257	0.0031	FALSE
dd349m 7	2	327.618	327.61	327.621	0.0057	TRUE	328.356	328.345	328.351	0.0055	TRUE
dd349m 7	3	329.36	329.363	329.368	0.0040	FALSE	330.129	330.128	330.12	0.0049	FALSE
dd349m 7	4	330.078	330.088	330.085	0.0051	TRUE	330.809	330.814	330.81	0.0026	FALSE
dd349m 7	5	329.443	329.443	329.443	0.0000	FALSE	330.201	330.204	330.204	0.0017	FALSE

(cont.)

dd449m 1	1	321.024	321.027	321.016	0.0057	TRUE	321.75	321.754	321.747	0.0035	FALSE
dd449m 1	2	328.891	328.89	328.88	0.0061	TRUE	329.648	329.634	329.642	0.0070	TRUE
dd449m 1	3	331.501	331.517	331.506	0.0082	TRUE	332.195	332.19	332.187	0.0040	FALSE
dd449m 1	4	324.079	324.07	324.074	0.0045	FALSE	324.814	324.808	324.801	0.0065	TRUE
dd449m 1	5	322.747	322.749	322.749	0.0012	FALSE	323.482	323.469	323.473	0.0067	TRUE
dd449m 2	1	334.338	334.326	334.325	0.0072	TRUE	335.079	335.082	335.065	0.0091	TRUE
dd449m 2	2	321.837	321.829	321.83	0.0044	FALSE	322.521	322.517	322.518	0.0021	FALSE
dd449m 2	3	327.518	327.511	327.505	0.0065	TRUE	328.178	328.176	328.171	0.0036	FALSE
dd449m 2	4	327.5	327.497	327.485	0.0079	TRUE	328.123	328.129	328.123	0.0035	FALSE
dd449m 2	5	324.737	324.731	324.728	0.0046	FALSE	325.403	325.398	325.4	0.0025	FALSE
dd449m 3	1	333.535	333.532	333.539	0.0035	FALSE	334.427	334.433	334.429	0.0031	FALSE
dd449m 3	2	335.459	335.461	335.454	0.0036	FALSE	336.141	336.143	336.143	0.0012	FALSE
dd449m 3	3	335.211	335.193	335.2	0.0091	TRUE	335.928	335.928	335.927	0.0006	FALSE
dd449m 3	4	330.493	330.486	330.485	0.0044	FALSE	331.145	331.144	331.146	0.0010	FALSE
dd449m 3	5	331.24	331.252	331.252	0.0069	TRUE	332.016	332.022	332.004	0.0092	TRUE
dd449m 5	1	323.961	323.954	323.959	0.0036	FALSE	324.809	324.8	324.799	0.0055	TRUE
dd449m 5	2	322.117	322.111	322.116	0.0032	FALSE	323	322.989	323	0.0064	TRUE
dd449m 5	3	330.464	330.467	330.464	0.0017	FALSE	331.382	331.37	331.376	0.0060	TRUE
dd449m 5	4	334.549	334.556	334.55	0.0038	FALSE	335.422	335.409	335.426	0.0089	TRUE
dd449m 5	5	327.562	327.558	327.546	0.0083	TRUE	328.387	328.398	328.381	0.0086	TRUE
dd449m 6	1	333.945	333.933	333.931	0.0076	TRUE	334.497	334.491	334.492	0.0032	FALSE
dd449m 6	2	331.741	331.737	331.73	0.0056	TRUE	332.298	332.293	332.288	0.0050	TRUE
dd449m 6	3	331.121	331.119	331.122	0.0015	FALSE	331.746	331.74	331.738	0.0042	FALSE
dd449m 6	4	330.745	330.74	330.737	0.0040	FALSE	331.386	331.38	331.378	0.0042	FALSE
dd449m 6	5	332.185	332.182	332.181	0.0021	FALSE	332.818	332.818	332.824	0.0035	FALSE
dd449m 7	1	334.567	334.569	334.581	0.0076	TRUE	335.062	335.064	335.056	0.0042	FALSE
dd449m 7	2	334.411	334.412	334.4	0.0067	TRUE	334.875	334.866	334.87	0.0045	FALSE
dd449m 7	3	331.035	331.035	331.027	0.0046	FALSE	331.547	331.549	331.551	0.0020	FALSE
dd449m 7	4	333.396	333.398	333.397	0.0010	FALSE	333.973	333.967	333.967	0.0035	FALSE
dd449m 7	5	334.197	334.192	334.183	0.0071	TRUE	334.702	334.699	334.697	0.0025	FALSE

In summary, the particulate data collection distinguished the following:

- there is variability between the weight of each of the same sample, and the causes at this time are unclear
- reducing error in the measurements may not be improved by increasing particulate collection time to increase particulate quantity, or reducing raw filter weight, but may be improved by increasing scale resolution and improving control over the weighing environment.

Appendix C

Mode 4 Repeatability Study

The following section presents all charts and graphs from the data analyzed as part of the repeatability study of Mode 4. This repeatability study was performed in order to quantify the variance of the data, day to day, for the same test conditions. The data was statistically analyzed as described in Appendix A. A portion of the figures were shown in Chapter 4 Results and Discussion, and will be repeated here for a complete picture of the data. Analysis of variance will be used to determine if there is statistical significance to the differences in data points. Some comments and general recommendations from the data will be presented.

Figure C–1 shows the particulate emissions in grams per kilogram fuel consumed.

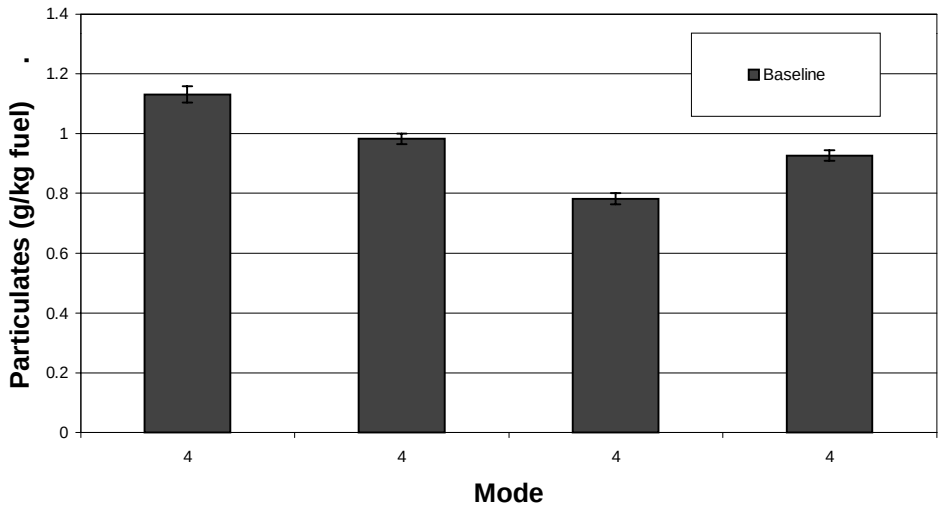

Figure C–1: Particulate Emissions, Mode 4 comparison, g/kg fuel

Even though the error bars are small, this chart indicates that there are some deviations between the samples. The relative error was 1.8 to 2.4 % across the samples in the figure above. Mode 4 was chosen because it is the mode which produces the most particulate emissions for the 5 minute sampling time, and could have the greatest chance of reducing the number of significant figures needed for measurement by the scale. However, the measurements of fuel and air consumption, show some instabilities as well. The particulate measurement is directly impacted by the accuracy of the fuel measurement.

Figure C–2 shows the NO_x emissions in grams per kilogram fuel consumed.

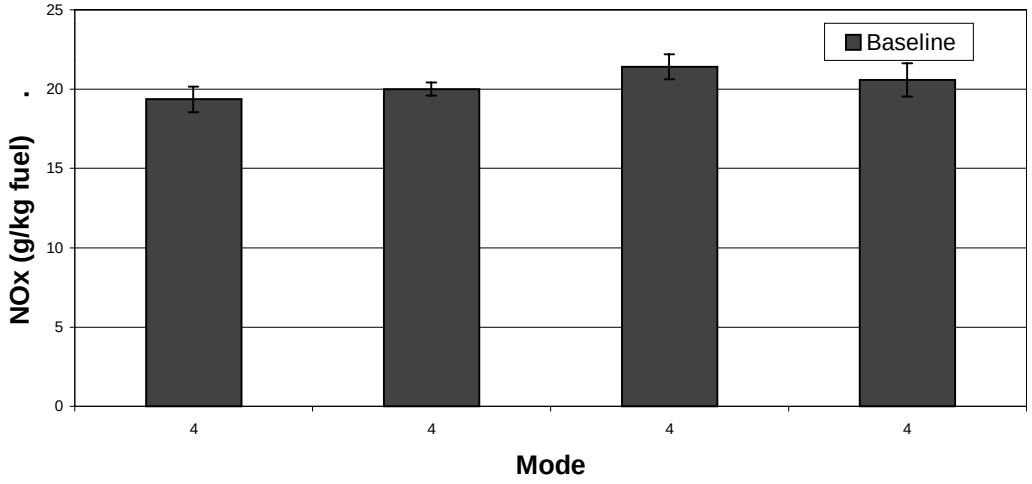

Figure C–2: NO_x Emissions, Mode 4 comparison, g/kg fuel

The NO_x data seems to be fairly stable, and within the range of error bars for the other samples. The relative error was 2-5% for the samples in the figure above. The NO and NO_2 calibration curves for the FTIR were fit with a 1% or less error. Again, error in the fuel measurement contributes to the error in the NO_x results.

Figure C–3 shows the CO emissions in grams per kilogram fuel consumed.

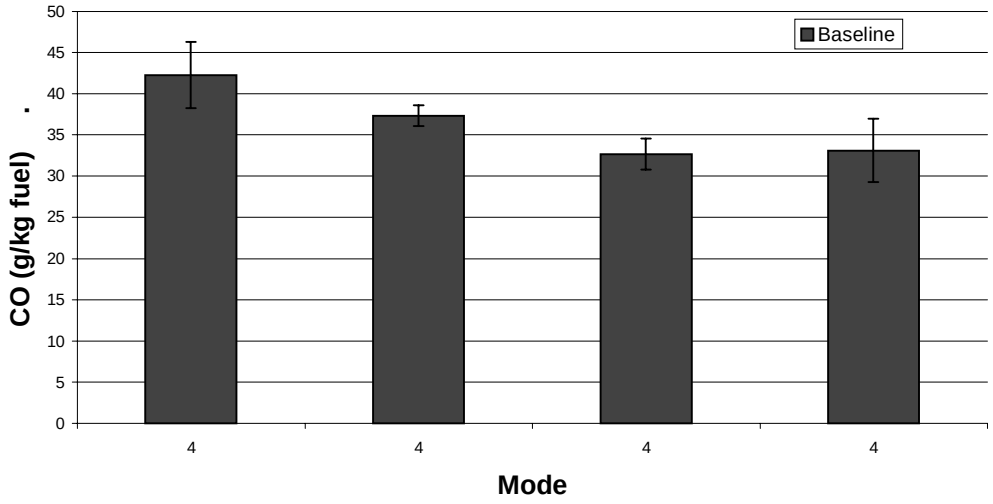

Figure C–3: CO Emissions, Mode 4 comparison, g/kg fuel

The CO calibration curve from the FTIR was fit with less than 1% error. Based on the data in the chart, it seems that some variability exists with the CO reading from the FTIR, but taking into account the error bars, the CO value seems to be consistent. The relative error in the above figure is 3.4 to 11.5% across the samples.

Figure C–4. shows the hydrocarbon emissions in grams per kilogram fuel consumed.

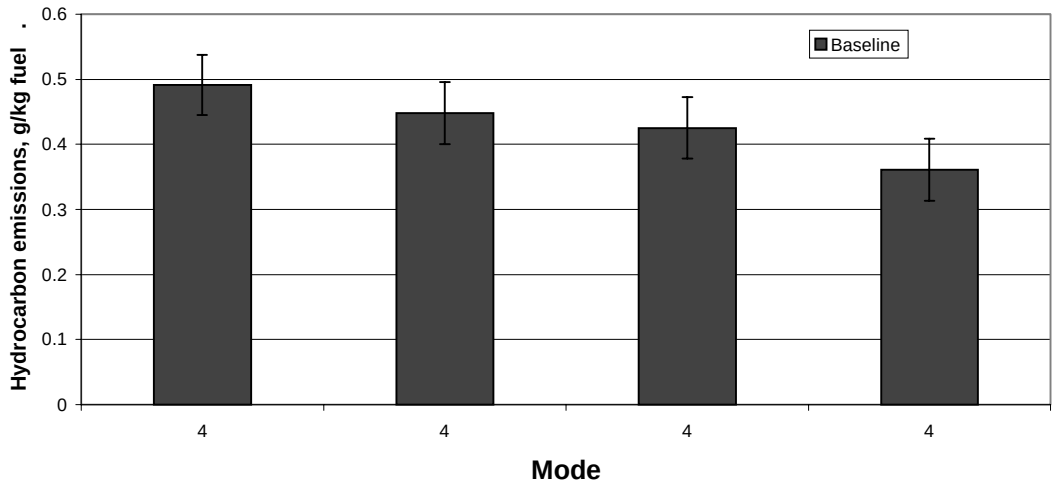

Figure C–4: Hydrocarbon Emissions, Mode 4 comparison, g/kg fuel

The hydrocarbon data is based on only the average of two to three samples per mode, which were collected as average numbers from the Heated FID analyzer. The ability to only collect two to three samples was a function of the heavy particulates of Mode 4 clogging the sample lines. Changes in the sampling systems would be recommended so that a greater surface area exists to allow for sampling over a longer time, and therefore giving a more stable reading of hydrocarbons. The relative error in the above figures was 9.4 to 13% across the samples.

Figure C–5 shows the Brake Specific Fuel Consumption in grams per kilowatt-hour.

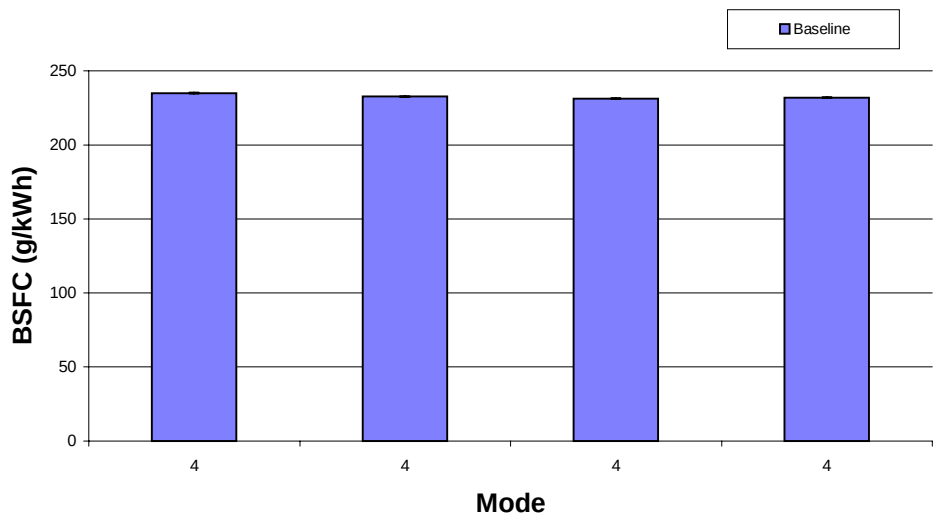

Figure C–5: Brake Specific Fuel Consumption, Mode 4 comparison, g/kWh

It is difficult to determine from *Figure C–5* whether the error in the BSFC arises from the fuel consumption measurement or the engine's operation. The fuel scale being used for this experiment has a resolution of 0.2 kg. During the experiment, the readings were taken so that when the scale changed to the next division, time and fuel were recorded. The error bars in *Figure C–5* refer to measurement variability only. The accuracy of the scale has not been included. The relative error is less than 0.1% for the samples in the figure. However, the raw error in the fuel consumption in grams/hour was 8-25%.

Figure C–6 shows the air consumption in grams per minute. The air consumption trend seems as constant as the fuel consumption trend.

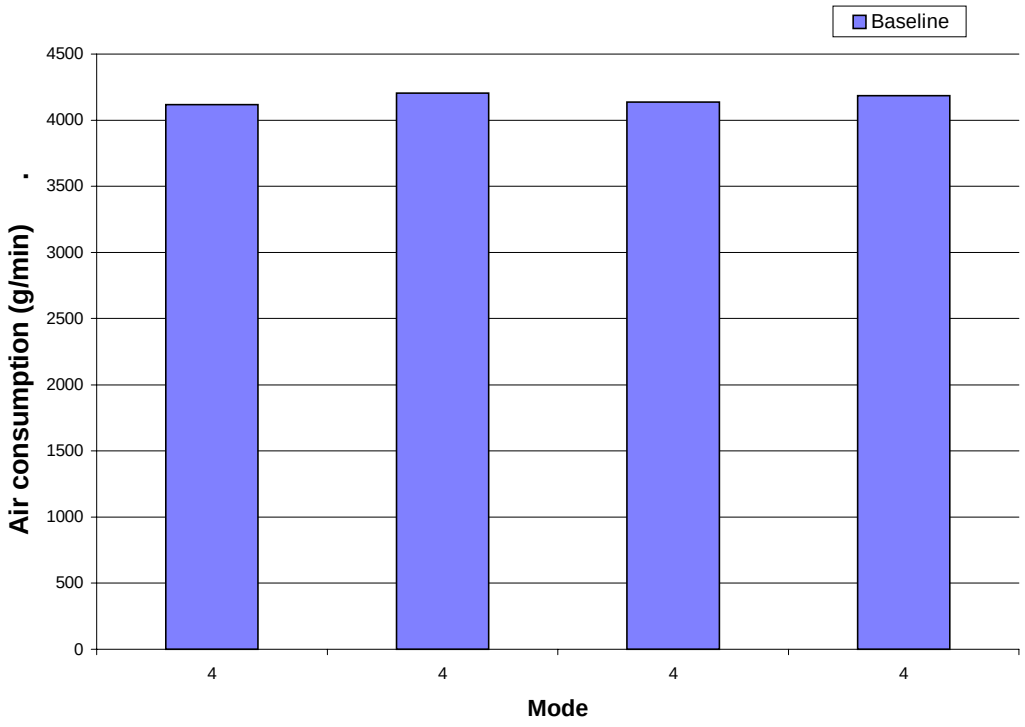

Figure C–6: Air Consumption, Mode 4 comparison, g/min

The air consumption is based on a voltage signal from a mass air flow (MAF) device. The device was calibrated with a laminar flow element (LFE). Due to errors in the device generating a voltage signal into the main computer logging system, the data was recorded 5 times during each mode. The voltage was recorded from a digital voltmeter, giving a reading up to two decimal places for a voltage value between 6 and 10 volts.

The voltage signal was converted to the flow rate, via the calibration. The mass air flow calibration was fit very well, with a correlation coefficient R^2 close to 1. An additional source of error exists between the LFE and the MAF device, in that the LFE which is intended to straighten the air flow may also be blocking the air flow, and thus reducing the signal from the MAF device. The LFE is used for calibration only, and does not reside in the flow passage during engine testing.

Figure C–7 shows the exhaust temperatures. The exhaust temperature follows the same consistent trend that the fuel consumption does.

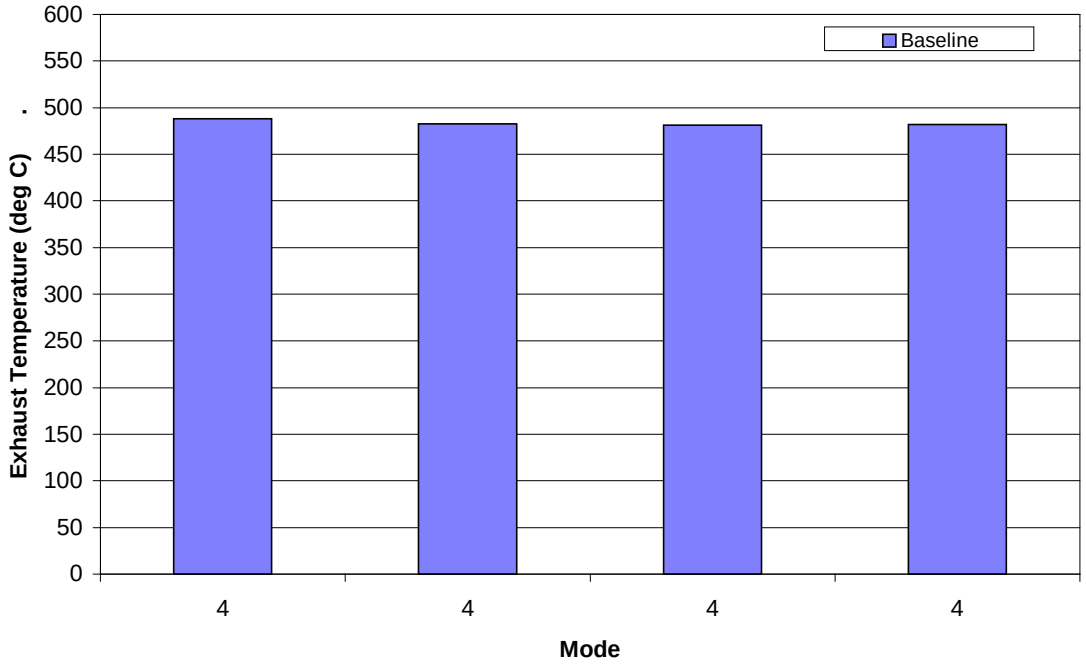

Figure C–7: Exhaust Temperature, Mode 4 comparison, °C

Finally, the data indicates that further investigation of the data to confirm the stability of the engine throughout the time the data was collected, which includes speed and load. Additionally, ambient temperature and humidity should be recorded to assess correlation with variations in the engine measurements. Comparisons between the ambient air temperature and charge air cooler temperature could also be helpful in determining factors which could reduce error in the experimental set-up.

Appendix D

Controller Area Network (CAN) Data

The following section briefly discusses the principles of the Controller Area Network. In addition, this section will show the types of data are collected from the Navistar engine control (Part Number : 1807349C4).

D.1 Definition of Controller Area Network

CAN, Controller Area Network, is a recommended practice intended for light and heavy duty vehicles for on and off-road applications. The purpose of CAN is to provide an open interconnect system for electronic systems, which then allow Electronic Control Units to communicate with each other using standard architecture. The network management structure is outlined in SAE J1939 and several associated documents. This higher level architecture assigns priority to engine functions, and alert status to changes in engine operation, and engine faults. The documents describe message types, lengths, and structures, in an attempt to provide consistency for programmers. The standard messages can then be used to provide generic service diagnostic tools [122, 123].

For the purpose of these experiments, it was important to understand the basics of CAN operation, so that the message information could be decoded. The CAN system for this experiment was developed by Navistar engineers. It was designed to send out information packages when triggered with a signal message. Also, it was set up for

messages to be sent via the CAN to the microprocessor. These messages contain instructions to update the set point values for engine operation, specifically, injection timing and injection pressure.

D.2 CAN Data

The data collected by the CAN bus is discussed in Chapter 3, and several charts are shown in Chapter 4. In this section, several other charts will be shown with the balance of the data collected. As discussed in Chapter 3, the CAN data was collected for 10 seconds, with approximately 800-900 points of data for each logged CAN channel being collected in that time frame. (The list of CAN channels is found in Chapter 3.) The charts that were created constituted the average values during that time frame. However, maximum and minimum values were also calculated for each engine setting, as seen in *Table D–1*

Table D–1: CAN data table: Baseline Diesel tests

bd349m1-1									
Time stamp	Engine Coolant Tem	Volume Fuel Desire	Dynamic Injection T	Injection Control Pre	Manifold Absolute P	Barometric Absolut	Air Intake Temp	Engine Speed	Engine Oil Temp
Max	84.00	8.50	6.17	3.63	99.75	98.75	25.25	709.75	82.50
Min	83.75	7.06	5.88	3.50	98.00	98.75	25.25	689.50	82.25
Average	83.78	7.74	6.04	3.57	98.85	98.75	25.25	700.33	82.26
bd349m2-1									
Time stamp	Engine Coolant Tem	Volume Fuel Desire	Dynamic Injection T	Injection Control Pre	Manifold Absolute P	Barometric Absolut	Air Intake Temp	Engine Speed	Engine Oil Temp
Max	84.50	16.38	7.83	3.63	100.50	98.75	26.00	879.25	86.00
Min	84.00	7.69	6.14	3.52	98.50	98.75	25.25	699.75	81.25
Average	84.50	16.08	7.66	3.59	99.65	98.75	26.00	873.59	85.96
bd349m3-1									
Time stamp	Engine Coolant Tem	Volume Fuel Desire	Dynamic Injection T	Injection Control Pre	Manifold Absolute P	Barometric Absolut	Air Intake Temp	Engine Speed	Engine Oil Temp
Max	85.50	36.06	7.88	7.56	106.50	98.75	27.50	1041.75	90.00
Min	84.50	16.38	7.55	3.59	99.25	97.50	26.25	874.00	85.75
Average	85.29	35.64	7.73	7.50	105.90	97.51	27.49	1036.54	89.97
bd349m4-1									
Time stamp	Engine Coolant Tem	Volume Fuel Desire	Dynamic Injection T	Injection Control Pre	Manifold Absolute P	Barometric Absolut	Air Intake Temp	Engine Speed	Engine Oil Temp
Max	86.00	61.44	7.92	14.06	120.00	97.75	35.00	1220.75	94.75
Min	85.50	35.63	7.61	7.51	106.00	97.25	28.25	1039.50	90.25
Average	86.00	60.92	7.74	13.93	118.92	97.50	34.96	1211.85	94.72
bd349m5-1									
Time stamp	Engine Coolant Tem	Volume Fuel Desire	Dynamic Injection T	Injection Control Pre	Manifold Absolute P	Barometric Absolut	Air Intake Temp	Engine Speed	Engine Oil Temp
Max	86.25	61.88	20.00	14.31	119.75	97.75	35.50	2309.75	96.50
Min	86.25	18.81	7.61	9.05	110.75	97.25	33.75	1212.00	94.75
Average	86.25	20.09	19.08	9.15	111.43	97.75	35.49	2292.85	96.26
bd349m6-1									
Time stamp	Engine Coolant Tem	Volume Fuel Desire	Dynamic Injection T	Injection Control Pre	Manifold Absolute P	Barometric Absolut	Air Intake Temp	Engine Speed	Engine Oil Temp
Max	86.50	33.25	19.38	10.99	129.25	98.75	36.50	2299.00	98.25
Min	86.00	20.00	14.36	9.12	112.50	98.75	33.00	2217.25	96.25
Average	86.49	32.34	14.48	10.91	128.62	98.75	36.27	2225.19	98.24
bd349m7-1									
Time stamp	Engine Coolant Tem	Volume Fuel Desire	Dynamic Injection T	Injection Control Pre	Manifold Absolute P	Barometric Absolut	Air Intake Temp	Engine Speed	Engine Oil Temp
Max	87.00	56.00	14.48	13.99	159.50	98.75	38.75	2236.25	100.00
Min	86.50	32.94	10.13	10.96	129.00	98.75	37.25	2217.50	98.25
Average	86.97	55.15	10.25	13.90	158.00	98.75	38.74	2224.24	99.78
bd349m8-1									
Time stamp	Engine Coolant Tem	Volume Fuel Desire	Dynamic Injection T	Injection Control Pre	Manifold Absolute P	Barometric Absolut	Air Intake Temp	Engine Speed	Engine Oil Temp
Max	87.50	71.63	12.80	17.03	167.25	98.75	43.50	2224.50	101.50
Min	87.25	55.56	10.20	13.93	157.75	98.75	40.25	2117.25	101.25
Average	87.30	70.67	12.66	16.98	166.60	98.75	40.27	2125.56	101.50

Most of the data categories are presented in Chapter 4. The rest of the data tables are presented below:

Manifold Absolute Pressure is shown below in *Figure D–1*.

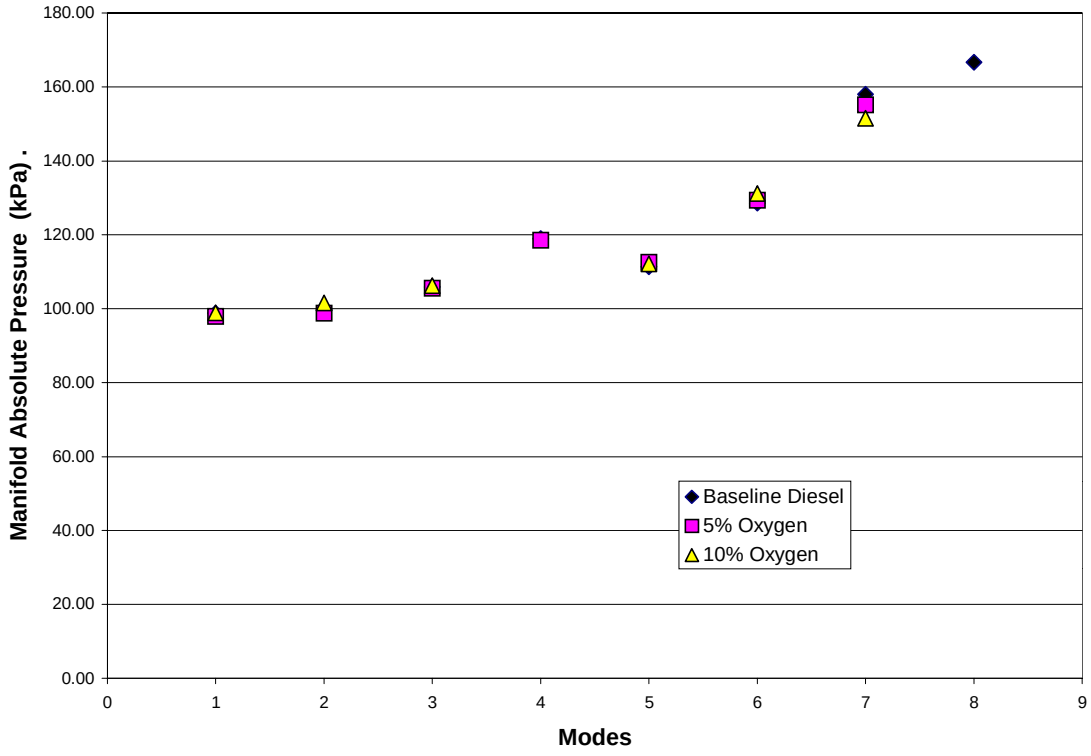

Figure D–1: Manifold Absolute Pressure, kPa

Barometric Absolute Pressure is shown below in *Figure D–2.*

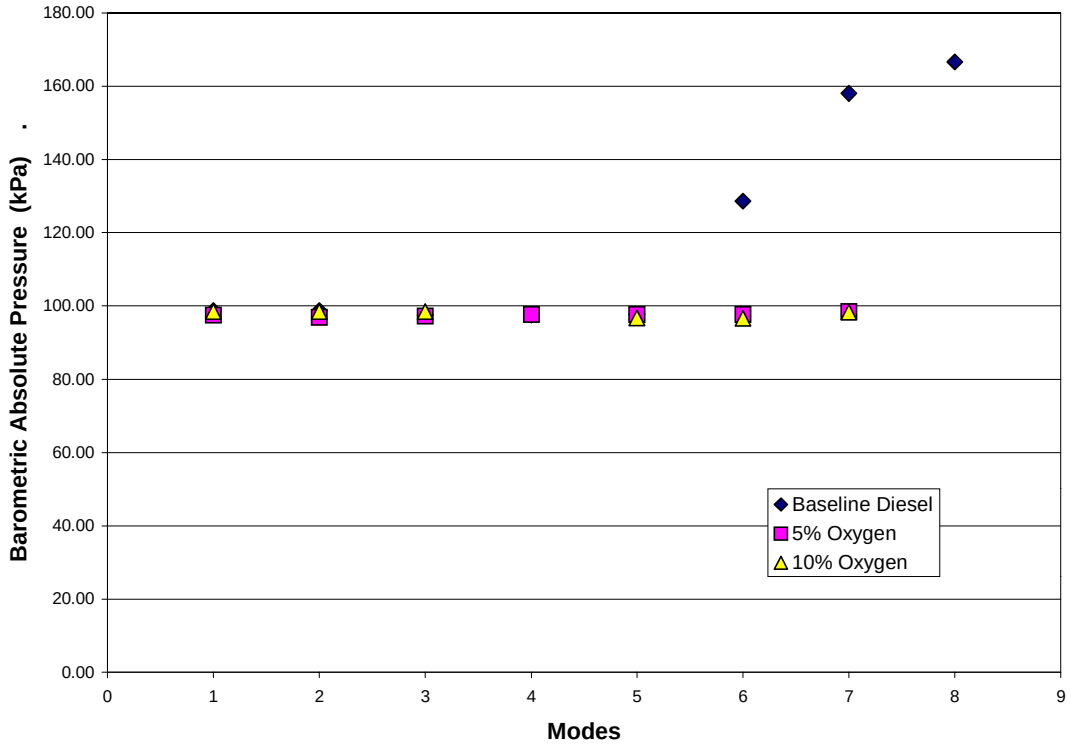

Figure D–2: Barometric Absolute Pressure, kPa

Air Intake Temperature is shown below in *Figure D–3.*

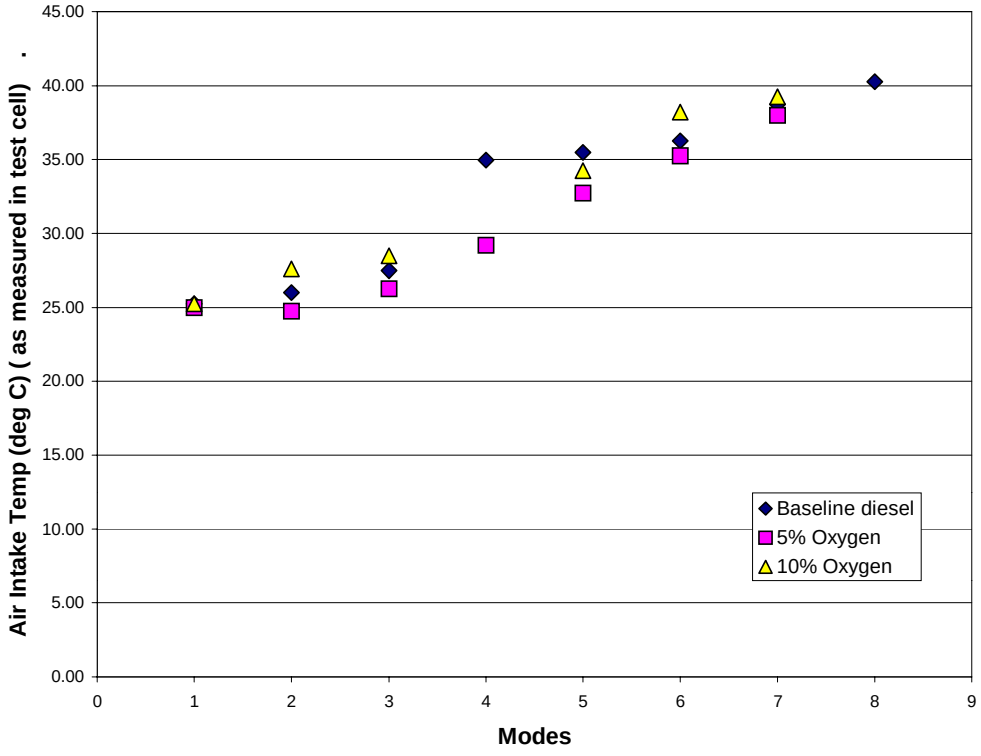

Figure D–3: Air Intake Temperature, °C

Engine Speed is shown below in *Figure D–4.*

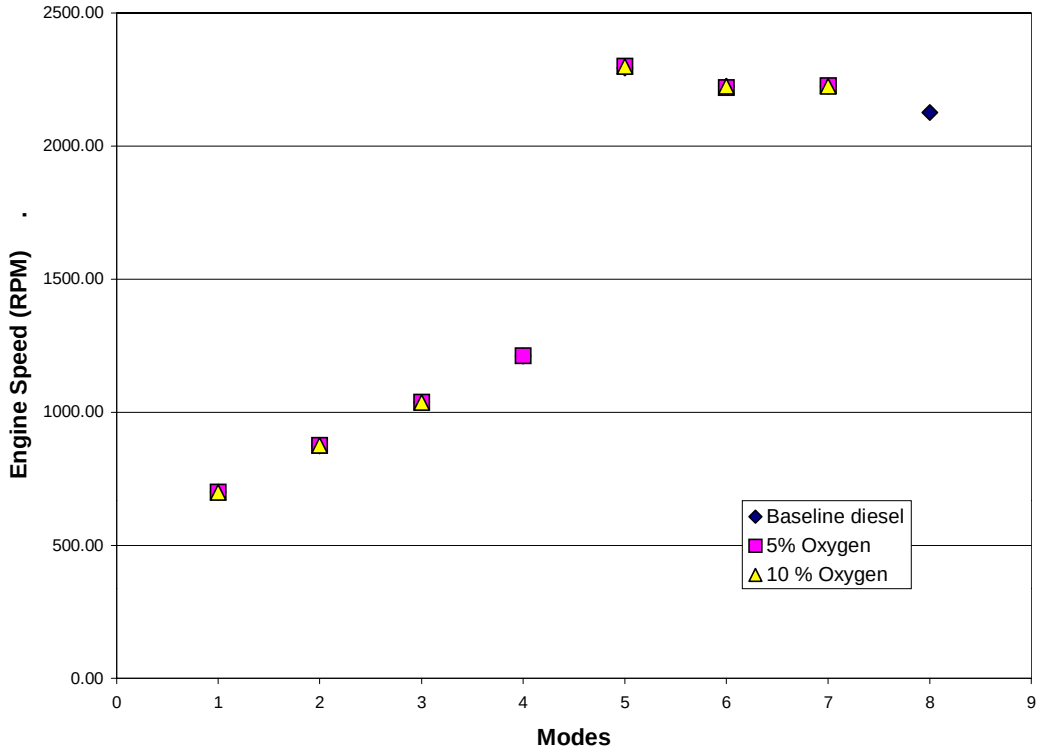

Figure D–4: Engine Speed, revolutions/ minute

Elana M. Chapman

TABLE OF CONTENTS

LIST OF FIGURES

ABSTRACT

The use of Dimethyl Ether (DME) blended with diesel fuel was investigated as an alternative fuel for diesel engines. A pressurized fuel delivery system was designed and built. A Navistar T444E, turbocharged direct injection diesel engine was modified to accommodate the pressurized fuel delivery system and enable operation with a blend of diesel fuel and DME. The engine was operated on a diesel fuel-DME blend containing 2% oxygen by mass and cylinder pressure traces were compared with baseline operation with diesel fuel. An eight mode, AVL steady state dynamometer test was adhered to for this comparison.

Miscibility of diesel fuel and DME was examined in various blend ratios. A methodology was developed to utilize a high pressure capillary viscometer to measure the viscosity of pure DME and blends of DME and diesel fuel in varying proportions and at pressures up to 2500 psig.

The comparison of an analysis of the cylinder pressure traces did not indicate any differences in the combustion characteristics of diesel fuel and a blend of diesel fuel and DME with 2% oxygen content. The engine could not be operated at the highest power mode in the AVL eight mode test. Boiling of DME inside the injectors was believed to be the reason. Diesel fuel and DME were found to be completely miscible in all blend ratios. The viscosity-pressure relationship of DME and blends was found to be logarithmic in nature.

Chapter 1

INTRODUCTION

Dimethyl Ether (DME) is gaining increasing importance as an alternative fuel for Diesel engines. Properties of DME such as its high cetane number and undetectable smoke emissions have made it an excellent fuel for use in compression ignition (CI) engines. Moreover, due to the presence of an oxygen atom, the absence of a carbon-carbon bond in the DME molecule and its high Cetane number, the oxides of nitrogen (NOx) – particulates tradeoff that plagues the traditional CI engine running on diesel fuel, no longer seems to threaten the CI engine operated on DME. The high Cetane number of DME also helps in reducing the combustion noise, which is another drawback of the diesel fuel fired CI engine [3, 8, 20, 25, 26, 28, 29]

The work done for this thesis was the first part of a project, whose final goal is to modify a shuttle bus that runs on the Pennsylvania State University campus at University Park, PA, to operate on an optimized blend of DIESEL-DME. The first part of the project was to modify the fuel system of the engine to be able to use DIESEL-DME blends in a laboratory environment, under controlled testing conditions. A fuel delivery system was designed and developed to take into account the higher vapor pressure of DME along with its lower lubricity and viscosity. The objective here was to do as few modifications as possible and still be able to use

DME to operate the engine. The lack of lubricity of DME is a major hurdle in using the existing diesel injection equipment, which utilizes the lubricity of diesel fuel to lubricate the parts machined with close tolerances. With this in mind, it was decided to blend DME and diesel fuel to provide lubricity to the blend.

A study was performed to measure the viscosity of DME and various blend ratios of Diesel-DME at pressures up to 2500 psig. A high pressure capillary viscometer was used for this purpose. This viscometer was designed and developed at the Pennsylvania State University [1]. Modifications were made to the viscometer taking into consideration the physical and chemical characteristics of DME and the need to charge the viscometer under pressure.

1.1 What is Dimethyl Ether (DME)?

DME is the simplest ether compound (chemical formula C_2H_6O). Some physical and chemical characteristics of DME are given in *Table 1-1*. At standard temperature and pressure it is a gas, but can be liquefied under a moderate pressure. This makes DME quite similar to propane and liquefied petroleum gas for handling purposes. DME was first used as an aerosol propellant because of its environmentally benign characteristics. It is not harmful to the ozone layer as the CFCs that it replaced. DME is also easily degraded in the troposphere [4]. A technical information bulletin [2] gives a good overview of the physical and chemical properties of DME.

Table 1–1: Physical and Chemical Properties of DME [2]

Chemical formula	$H_3C\text{-}O\text{-}CH_3$
Molecular weight	46.07
Oxygen content by mass	34.8 %
CAS Registry number	115-10-6
Boiling point @ 1 atmosphere	-24.825 ^{O}C
Critical temperature	126.85 ^{O}C
Critical pressure	5370 kPa
Liquid density @ 25 ^{O}C	656.62 kg/m^3
Vapor pressure @ 20 ^{O}C	516.76 kPa
Flammability limits in air by volume %	3.4 – 18

1.2 DME in Diesel Engines

A high Cetane number makes DME an attractive fuel for compression ignition (CI) engines. In CI engines running on a single fuel, the fuel has to be injected at the precise moment just before the firing TDC. This point is called the start of injection (SOI), which varies depending on factors like the load on the engine, speed and ambient conditions. Most modern engines usually have the ability to vary the SOI depending on the above parameters. To be able to meet the above injection requirements and also to be able to end the injection in a certain amount of crank angle degrees, injection of liquid fuel is a necessity. As DME has a high vapor pressure, the fuel system needs to be pressurized to maintain DME in a liquid state. Moreover, the fuel system has to be modified considering the physical and chemical properties of DME.

Another important consideration in the use of DME is that of the physical properties like viscosity and compressibility. Diesel fuel injection systems are designed for diesel fuel, which has a kinematic viscosity an order of magnitude higher than that of pure DME.

Taking the above properties of DME into consideration a modified fuel delivery system was designed and built. A Turbocharged Direct Injection Diesel engine was operated with this modified fuel delivery system on a DIESEL-DME blend. The engine used was a Navistar T444E diesel engine. Detail specifications of this engine can be found in Table 3-1. This engine was operated at steady state on an eddy current dynamometer. An AVL 8-Mode test schedule was followed to compare the performance of the engine when fired by diesel fuel and DIESEL-DME blend.

Chapter 2

LITERATURE REVIEW

For the past few years, many investigators have studied the use of DME in diesel engines. As with every other alternative fuel, all aspects of using this fuel have been studied. Alternatives to the fuels presently used, are often considered for a couple of important reasons:

- To make use of a previously unutilized energy source (as in natural gas) in transportation systems
- to face the ever-increasing challenge of emissions regulations.

DME appears to satisfy both the above criteria. With the present technology, natural gas in remote locations can be converted to DME, enabling economical transportation to markets and consumers; thus better utilizing the remote natural gas. The clean burning characteristics of DME, i.e., extremely low particulate emissions and low NOx with injection optimization, also help in meeting the emissions regulations.

When studying the viability of any alternative fuel, the mass production process of that fuel is always compared to that of fuels currently being used. The well to wheel efficiency, which is an important aspect in the long term success of any fuel, goes hand in hand with the production process. Combustion characteristics of

the alternative fuel are another aspect subject to investigation. More often that not, in this age, the alternative fuel is cleaner burning than the standard fuels. Finally, the compatibility of the fuel with the materials used in the fuel injection system is under scrutiny. These aspects of DME studies are examined in the following discussion of literature.

2.1 Production Process of DME and its Efficiency

The use of DME as a fuel for the compression ignition (CI) engine started in 1995 with the work done by Sorenson and Mikkelsen [3]. Prior to this, DME was used as a fuel additive to improve the ignition quality of methanol in CI engines. It was also used on a larger scale as an aerosol propellant to replace CFCs as it does not harm the ozone layer.

Hansen et al [4] reported a number of 150,000 metric tons per day as the production capacity of DME. It was solely manufactured from the dehydration of methanol. This paper presents the laboratory and pilot test carried out for large scale manufacture of DME. A single step production process is discussed which will directly convert synthesis gas into DME. This being simpler than the dehydration of methanol, is a cheaper process of DME production. To achieve a production capacity close to what will be required for an alternative for diesel fuel, different types of DME plant setups are discussed. A slow transition from methanol dehydration to stand-alone DME plants is preferred. Direct dehydration of methanol, revamping

existing methanol plants to co-produce DME and stand-alone DME plants for large scale DME production are the methods discussed and compared for their investment and convenience aspects. Direct dehydration is cited as the most convenient route for the introduction of DME as a fuel. For large scale production, however, stand-alone DME plants are most economical.

Verbeek and Van der Weide [5] have carried out an overall study of various aspects of DME as an alternative fuel. An important aspect in the use of any alternative fuel, namely its energy supply and energy security, is discussed in connection with DME. As DME can be produced by synthesis gas conversion, almost any source capable of producing synthesis gas can be used to produce DME. A reason, more important than any other, is discussed for encouraging research and development of DME as an automotive fuel. That is the long term energy security achieved by making use of a variety of energy sources such as remotely located natural gas, coal and biomass. These energy sources combined together are likely to outlast crude oil. Well to wheel efficiencies for various standard and alternative fuels are compared. In a group consisting of diesel, DME, LPG, CNG, LNG, gasoline and methanol, surprisingly enough, DME comes second after diesel in the well to wheel efficiency. This projected efficiency is more than that of gasoline despite the fact that the production efficiency for DME is the second lowest in the group. For the well to wheel CO_2 emissions, the study shows that DME again comes in second after diesel fuel. Interestingly, if the source of DME is renewable, this cuts down the net CO_2 emissions.

Ofner et al. [6] present a good overview of the use of DME in automotive engines. With alternative fuel research being quite common in the past few decades, they emphasize the importance of a global point of view when studying alternative fuels. Besides the well to wheel efficiency, another concept of the “Sustainable Process Index” (SPI) is used in evaluating the environmental impact of DME. SPI compares the mass and energy flow due to a technical process to the natural flows or cycles in the environment. The SPI of various fuels, alternative and traditional, are calculated. The SPI of DME from renewable sources is shown to be the lowest in the group. Simply put, the SPI can be said to be the effect the lifecycle of a particular fuel has on the environment. A low SPI for DME means that DME is the least taxing to the environment amongst the group of fuels discussed.

Phillips et al. [7] give a Canadian perspective of DME as an alternative fuel. The vast natural gas resources in Canada play an important role in the viability of DME as a fuel. The authors have shown that the end user cost for DME per unit volume could be comparable to diesel and lower than gasoline. However, as the energy density of DME is lower that diesel, more DME (in volume and in mass) will be required to complete a specific journey. In the end DME would still end up about 30% more expensive than diesel.

2.2 DME Injection Systems and Injection Characteristics

The earliest work done on pure DME injection were studies in which unmodified diesel injection equipment was used for DME injection with an objective of identifying the areas where modifications would be necessary to successfully use DME and then to optimize that equipment for further improving the injection process.

Kapus and Ofner [8] talk about modifying and optimizing an existing diesel fuel injection system to account for the properties of DME. This is a study of DME injection using standard diesel injection equipment. Physical property data for DME, such as compressibility and velocity of sound were estimated using modeling techniques. A test rig was configured, which measured the pressure oscillations in a tube placed between two injection nozzles. The properties like viscosity and velocity of sound were estimated using these pressure traces. A flow visualization study was also carried out using a glass nozzle. Initiation of cavitation and its effect on the spray development was studied. Different characteristic parameters of the fuel injection equipment (FIE) were varied and the effects of such changes on combustion noise, fuel consumption and NOx emissions were recorded. FIE used on DI diesel engines, was found to be generally more suitable for DME injection than FIE on IDI engines.

McCandless and Li [9] present a “Novel Fuel Injection System” (NFIS) for DME and other alternative fuels. The NFIS was designed to retrofit existing diesel

engines. Low cost was also a major consideration. The design process for a NFIS was initiated by taking into consideration the technical and economic requirements of the customer. Various existing FIE were compared to find the most suitable for modifications. A common rail system was selected as the most suitable. The bw viscosity of DME caused a lot of leakage past the solenoid valve and the nozzle. A clever design of equipment, however, enabled the containment of the leakage. The NFIS was also capable of rate shaping, which is a very important control strategy for lower NOx and combustion noise. The pump used to pressurize the DME to injection pressures was an axial piston pump with special shaft seals and wear resistant pumping elements. The fuel injector used, was a modification of a commercially available injector. The nozzle spring and the inclusion of a large volume behind the plunger were the modifications made. Flow bench tests were carried out which showed that the goals such as controllable initial injection rate and system durability were met.

McCandless et al. [10] describe the design and performance of a 275 bar DME pump with variable displacement and variable output pressure. The leakage of DME past the pumping element, which is very common given the extremely low viscosity of DME, was reduced by introducing a “hydraulically long” flow path for the leakage flow. This pump was found to be overall satisfactory in terms of performance and durability. Additionally, it can also be used for other alternative fuels such as methanol, and liquid propane.

Ofner et al. [11] present an injection concept for DME injection. They have included a low pressure “purge” circuit. This purge circuit absorbs all leakages and the DME released from purging the injectors. This system includes a compressor, which then pushes the DME vapors back to the fuel tank. Since this is one of the earlier works on DME injection, a greater emphasis was given on the safety aspect and seals. Contact seals were used. There were two sealing elements in series with the space in between connected to a purge tank to collect any leakage.

Sorenson and Nielsen [12] performed an important study of the wear of plunger type diesel injection pumps pumping DME. A test rig was made out of standard diesel injection equipment, as ASTM standard lubricity test rigs are not suitable for compressed liquids. Several lubricity additives were tested. The tests were run for typically 80 hours. The pumping elements showed wear even after a relatively short time of 80 hours, showing the difficulty in using DME in conventional diesel injection systems. The location and severity of the wear, however, could not be characterized. The drawback of this test was that the areas selected for wear analysis samples were not representative of maximum wear. Also most of the wear observed was the polishing of the plunger due to metal to metal contact. Even though the wear could not be characterized, it was important that DME with all the additives showed some amount of wear. It proved that none of the additives used were effective. Also, no wear whatsoever was observed when the injection equipment was run with standard diesel fuel.

Another important aspect in DME fuel injection is the behavior of DME as it leaves the injection nozzle and enters the high temperature and pressure environment in the combustion chamber towards the end of the compression stroke. The critical point of DME at 127 ^{O}C is well below the conditions in the combustion chamber at the instance of injection. This fact makes DME behave differently than diesel fuel once injected into the cylinder.

Glensvig et al. [13] performed a comparative study of the injection properties of diesel fuel and DME. Here, the two fuels were injected into a transparent chamber filled with Nitrogen to a desired pressure and ambient temperature. The penetration rate and the spray angle were the objects of study. As expected, the diesel fuel spray was found to have a faster penetration than DME. The correlations developed for diesel fuel sprays however, gave incorrect results for DME sprays. The spray angle for DME was also found to be almost twice as wide as that for diesel fuel at the same distance from the nozzle tip. The spray angle correlation again was found to give incorrect results in predicting the difference for the two fuels.

Upto this point, all the studies done with Diesel fuel-DME blends have been with premixed solutions of the two fuels. A different approach would be to introduce DME as a liquid or a gas at the very last moment before injection. Recent studies by Sovani et al [14, 15] regarding effervescent Diesel injectors present an idea that may be well suited for injection of Diesel fuel – DME blends. Here, a study of the fuel spray was done by introducing an atomizing gas into the fuel stream before it is discharged from the injectors. It was found that the droplet size of the fuel spray

could be reduced to about 5μm at injection pressures that were about 5 to 7 times smaller than those used in modern diesel injection systems. This concept can be incorporated for use with DME injection. The atomizing gas in this case would be DME. DME could be mixed just before the fuel enters the injectors. This setup would obviate the necessity of a complicated pressurized fuel delivery system used with a mixture of diesel – DME. This method would however limit the maximum percentage of DME in the blend.

The study of literature has shown that the fuel delivery system discussed in the next chapter is the best way to modify the fuel system of the Navistar T444E engine. This attempt to mix diesel and DME will also try to solve the lubricity issues when using pure DME in diesel engines.

Chapter 3

EXPERIMENTAL SETUP

The present study is an investigation of the use of Dimethyl Ether (DME) as a fuel in diesel engines. The study consists of design and installation of an engine testing facility including an engine, dynamometer, control system and instrumentation for exhaust emissions monitoring, as well as configuration of a high-pressure viscometer instrument for measuring the viscosity of blends of diesel-DME. Moreover, the existing fuel system on the engine was modified to enable operation at higher fuel delivery pressures required for the fuel blend.

3.1 Engine-Dynamometer Setup

The engine-dynamometer was installed in a sound reducing test cell. The engine and the dynamometer were mounted on a concrete pad with adequate vibration isolators (Mtech #X pads) between the floor of the test cell and the concrete pad. Heat exchangers were installed for cooling the engine and the dynamometer. An air handling system was also installed to maintain near ambient conditions in the test cell. Care was taken to do a proper alignment of the engine and the dynamometer. The engine flywheel and the dynamometer hub were held parallel to

each other. The driveshaft was kept at an angle of 1.5 degrees. This was in accordance with a driveshaft installation guide. The driveshaft has a rubber damper to dampen driveline vibrations.

3.1.1 Engine

The engine used for the study was the Navistar T444E, 7.3 liter, 4 stroke cycle turbocharged direct injection diesel engine. The selection of this particular engine was based on several important factors. The bus, which was to be modified later, had the same engine model, with the same Engine Control Module (ECM). Secondly, this engine was used in previous studies involving DME. The reason for the popularity of this engine is its fuel injection system. This engine has the common rail Hydraulic Electronic Unit Injector (HEUI) fuel injection system. This system being electronically controlled is highly flexible in operation and hence suitable for developmental work. The relevant specifications for the T444E engine are shown in *Table 3–1*.

Table 3–1: T444E Engine Specifications [16]

Engine Type	Diesel, 4 stroke cycle
Configuration	Over Head Valve V – 8
Displacement	444 cu.in.
Bore and Stroke	4.11*4.18 in.
Compression ratio	17.5:1
Air Aspiration	Turbocharged and air-to-air intercooled
Rated power	190 bhp @ 2300 rpm
Governed speed	2500 rpm
Peak torque	485 lb-ft @ 1500 rpm
Combustion system	Direct injection
Fuel Injection System	HEUI; Common rail

Hower et al. [17] give a detailed description of the engine development process and describe the various important aspects such as the combustion system, fuel injection system and the electronic engine management system for the Navistar T444E.

The engine has two valves per cylinder. The fuel injection system is a state of the art, electronically controlled system that was developed by Caterpillar Inc. Stockner et al. [18] and Glassey et al. [19] describe the HEUI fuel injection system in great detail. Increasingly stringent emissions regulations were the impetus behind the development of this completely new concept in diesel fuel injection systems. This system uses engine oil to activate the injectors. The injection pressure, that can reach as high as 18000 psig (1240 bar), is achieved by using a pressure intensifier. This pressure intensifier is integral to the injector, resulting in the overall compactness of

the system. The electronic control with feedback gives a precise control over the air/fuel ratio, which is very important in controlling exhaust emissions. Another important aspect is the flexible injection timing. Start of injection is critical in minimizing emissions, as well as, fuel consumption. Due to the hydraulic-electronic activation, the injection timing can be tailored for each engine operating condition. Injection timing is decided by the electrical actuation signal that is sent to the injector solenoid. Another concept of "split shot" injection, which is a part of the HEUI fuel injection system, has been shown to reduce combustion noise as well as NOx emissions during idling and low loads.

3.1.2 Dynamometer

The dynamometer that was used was an eddy current absorption dynamometer (Dynamatic Corporation Model # AD-8102). The torque arm is 15.375 inches. The rated capacity is 450 HP between shaft speeds of 3100 to 6000 rpm. The excitation is achieved by a 45V, 14A DC power supply. The dynamometer is water-cooled and requires a cooling water supply of 45 GPM at or below 32 ^{O}C. A Lebow tension and compression load cell (model # 3132–500), with a capacity of 500 lbs, measures the load. This load cell was calibrated using free weights as described in the dynamometer operations manual.

3.1.3 Cooling Systems

Three separate cooling systems were used in the test cell. Water to water heat exchangers were utilized for engine and dynamometer cooling. The cooling water source is the same for the engine and dynamometer heat exchangers. The sequence of the heat exchangers in the cooling water line was critical, as the output temperature requirements were very different in both cases. The dynamometer requires coolant at a temperature less than or equal to 32 ^{O}C. There is no such requirement for the engine. Thus the dynamometer heat exchanger had to be put upstream of the engine heat exchanger to provide maximum cooling. An air handling system was used to constantly replace the hot air in the test cell with cooler ambient air. A schematic of the cooling systems is shown in *Figure 3-1*.

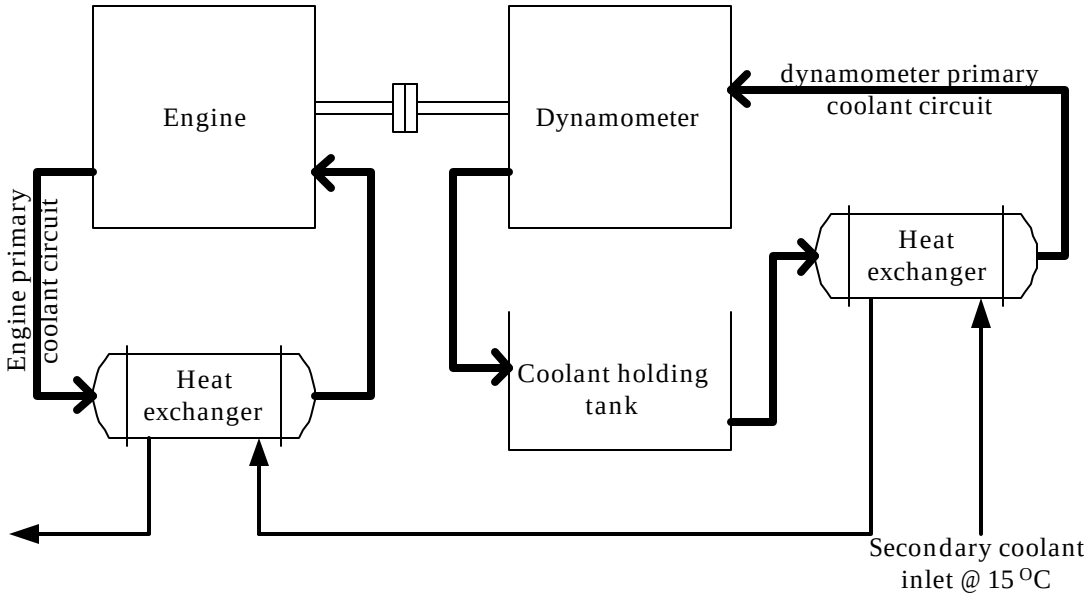

Figure3–1 **Cooling Systems**

3.1.3.1 Engine Cooling

A water-to-water shell-tube type heat exchanger was used for engine cooling (Young Radiator Company model # F-504-EY-2P). The engine coolant, a 50-50 mixture of ethylene glycol and distilled water, flows through the shell side while treated cooling water flows through the tubes. The engine coolant temperature is maintained at a preset level in the engine block and head by a thermostat valve. There is no external temperature control for engine cooling.

3.1.3.2 Dynamometer Cooling

The dynamometer is water-cooled. A water to water heat exchanger (Affinity Industries Inc., model # 3100) was also used in this case. This heat exchanger has a modulating valve on the cooling water side which is used to control the output temperature. This valve, however, had to be disabled in order to provide the engine heat exchanger with a constant flow. Constant flow was also the requirement of the source of the cooling water.

3.1.3.3 Test Cell Cooling System

An induced draft fan arrangement was used to keep a constant airflow through the test cell. This fan has a Cutler-Hammer adjustable frequency drive to

adjust the fan speed. Constant airflow was important to keep the ambience in the test cell at a steady state. The air is introduced into the test cell from the front end. This also helps maintain an adequate airflow over the charge air cooler, which has a bank of fans to drive air through it. Maintaining the test cell temperature was also important for the operation of exhaust analysis equipment. The Micro-dilution tunnel in particular is very temperature sensitive. The temperature of the diluted exhaust gases should be at or below 52 ^{O}C. The test cell air handling system also helps in maintaining this temperature.

3.1.4 Engine flow systems: intake air, fuel

Source of intake air and fuel to the engine are important. The conditions of air and fuel such as the temperatures, humidity and presence of impurities can have a profound effect on the repeatability of engine performance. Close monitoring and control of these variables would be ideal. No control was used on the conditions of air and fuel, but they were monitored and recorded.

3.1.4.1 Intake Air System

Clean filtered air was provided to the engine using standard automotive filters. The temperature of the intake air was close to a temperature of 20 ^{O}C, as room air outside the test cell was used for this purpose. Large diameter ducting was used to ensure adequate flow capacity for the engine size. The engine being turbocharged

and intercooled, an air to air intercooler was used to cool the charge air. Cooling air was blown over the charge air cooler using a bank of fans, which in turn was aided by the air draft from the test cell air handling system. The intake air consumption was measured using an electronic mass air flow meter. This meter is based on the hot wire anemometer principle. The meter is placed between the air filter and a plenum chamber, which dampens out any pulsation in the air flow. This is an important consideration in getting an accurate reading from the mass flow meter. The mass flow meter was calibrated using a laminar flow element. The output from the flow meter is a frequency signal, which was then converted to a voltage signal for ease of measurement. This signal was logged using a computer to give a real time air consumption reading.

3.1.4.2 Fuel Supply System

The fuel tank supplying fuel to the engine is a modified LPG tank that sits outside the test cell. Stainless steel tubes are used to supply fuel from the fuel tank to the engine and return the excess fuel to the tank. High pressure fittings were used with the future application of a pressurized fuel system in mind. The standard fuel filter provided with the engine was used for the baseline runs. For the DME test run, however a modified liquid propane filter was used to handle the high system pressure. In all cases, fuel consumption was measured by using a weighing scale

with a readability of 2 grams. The time was measured accurately by a stopwatch to a hundredth of a second.

3.1.5 Pressurized Fuel Delivery System for Diesel-DME Blend

DME is a liquefied gas. At standard temperature and pressure, it is a gas, but liquefies under a moderate pressure. The vapor pressure and density changes with temperature are characterized in the Technical Information (ATB-25) bulletin. The fuel delivery system was designed keeping in mind the following important points:

- The vapor pressure of DME and related temperature requirements.
- Material compatibility of the various components in the fuel system with DME
- Lack of lubricity of pure DME.

A schematic of the fuel delivery system is shown in *Figure 3–3*. The working of the fuel delivery system can be explained as follows:

1. The fuel is delivered from the fuel tank at a pressure of about 90 psig. This overpressure is necessary to keep the DME in a liquid state. Any inert gas is suitable for this purpose. Helium was used as it has a lower solubility in DME than nitrogen.
2. The pressure is then boosted by a gear pump to about 150 psig, depending on the pressure rating of the fuel rail. The rail pressure is maintained at 70 psig in the original fuel system of the engine.

3. The fuel return line pressure is held at about 150 psig by the backpressure regulator. The regulator is a simple spring loaded valve that regulates the flow to keep the backpressure at the desired pressure.
4. This fuel then passes through a heat exchanger, where it is cooled down.
5. After cooling, the fuel is then fed to the inlet of the pump.

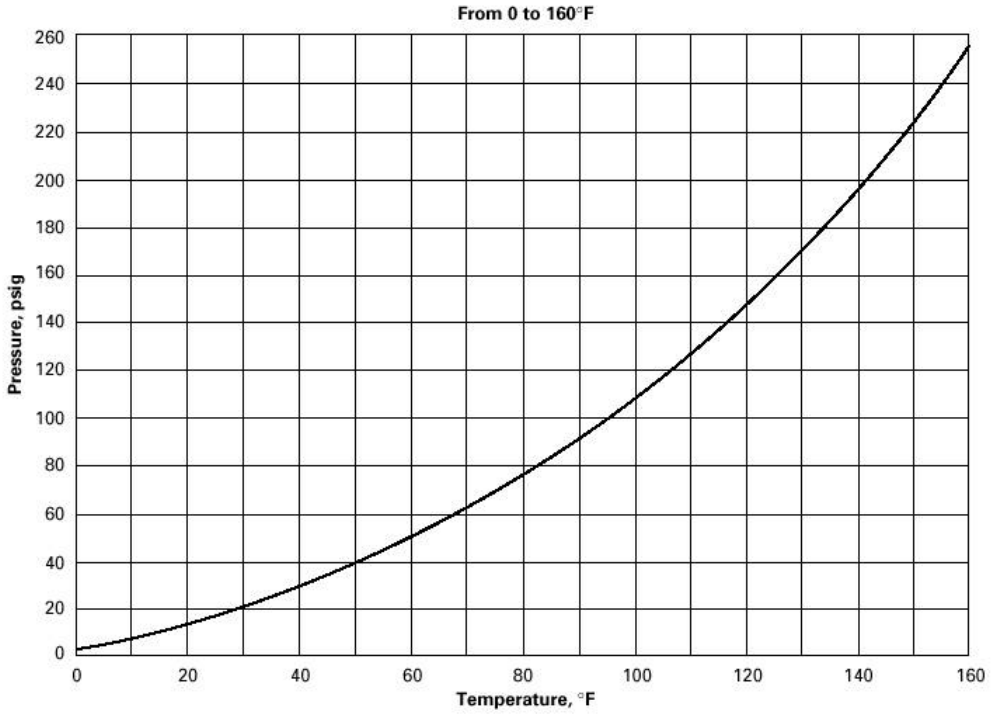

Figure 3-2: Vapor pressure curve for DME (Dymel A) [2]

3.1.5.1 Fuel Pressure and Flow Requirements

At 20 ^{O}C the vapor pressure of DME is about 62 psig. Keeping DME in a liquefied state calls for pressurizing the entire fuel system from the fuel tank up to

the fuel injectors. The vapor pressure also changes rapidly with temperature. The vapor pressure curve for DME is shown in *Figure 3-2*. The pressure of the fuel system is hence dictated by the fuel temperature. The upper limit of pressure, however, is decided by the pressure rating of the fuel rail. The engine used in the study has a common rail injection system. Each cylinder head has a fuel rail running along its length, which is the source of fuel for the pressure intensifier in the fuel injectors. In the original fuel system of the engine, the pressure in the rail is maintained at 70 psig. This facilitates proper filling of the pressure intensifier. The fuel rails in the cylinder head form a dead head system. This means that there is no fuel return once the fuel enters the fuel rail. It is because of this that the fuel temperature in the rail approaches the engine coolant temperature in the head. This layout of the fuel system was modified to accommodate a fuel return from the cylinder heads. A study was performed in which the temperature of the fuel in the fuel rail was recorded in conjunction with the fuel consumption of the engine, for the 8 modes of the AVL test. The temperature of the fuel in the fuel rail, which was about 80 ^{O}C, would be too high for the DME to remain in the liquid state at the operational pressure of 150 psig. A minimum flow rate value was calculated so as to keep the temperature of the fuel in the rail below 50 ^{O}C. The vapor pressure of DME at this temperature is about 150psi. This pressure, more or less dictated the final fuel temperature as it exited the fuel rail. The fuel delivery pump was sized based on the above calculations. In addition to excess flow rate, cooling of the returned fuel was resorted to, to maintain the required fuel temperature.

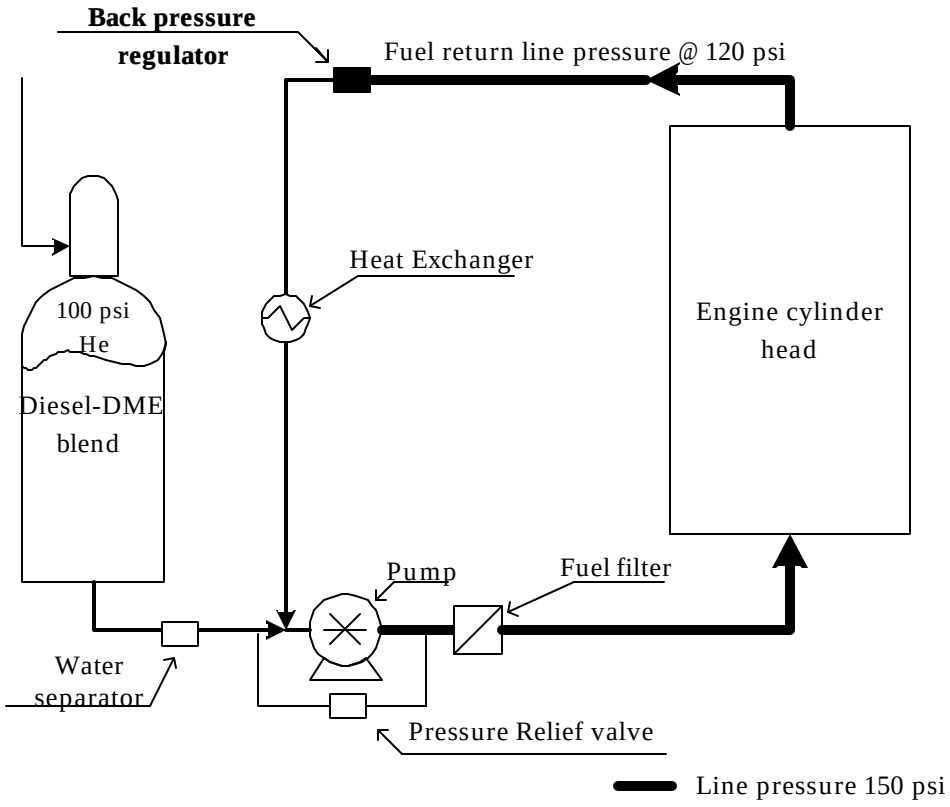

***Figure3–3*: Pressurized Fuel Delivery System**

3.1.5.2 Design Considerations for Fuel System

DME is known to be incompatible with the common gasket materials such as Viton and buna-N, used in diesel service. Data provided by DuPont Inc. indicated Kalrez to be the best material for DME in terms of compatibility. For economic considerations however, this material was used sparingly. Other materials such as butyl rubber, Teflon and neoprene have also been found to be compatible, though not to the same degree as Kalrez. Stainless steel was used for the fuel lines as a safeguard against corrosion. All the other components such as valves and regulators were also made of stainless steel.

Selecting a pump for pumping DME was challenging due to the properties of DME such as its low lubricity and low viscosity. Due to the vapor pressure of DME, the pump housing is required to handle pressures upto 250 psig. Positive displacement pumps such as vane pumps, diaphragm pumps and gear pumps were considered. Gear pumps were found to be economical as well as convenient to operate. With these considerations, a gear pump (Tuthill Pump CO, California model #TXS2.6PPPT3WN00000) was selected. This pump has a magnetically coupled AC motor. This configuration does not have the driveshaft going through the pump housing, which in turn, obviates the need for seals. The gear material is Ryton (Polyphenylene sulphide), which was found to be compatible with diesel and

DME as per the data by provided DuPont Inc. The pump body seals are made of Teflon.

The fuel filters on the engine could not be used because of the high pressure of the fuel. The minimum pressure in the fuel lines was 90 psig. This required the use of special filters, which could withstand higher pressure. A diesel water separator was used as a primary filter. This is rated at 100 psig. The final filter was a LPG filter rated at 500psig. The mesh size of the filter was matched to the engine specifications of 3 micron.

The fuel tank was made out of a modified 100 lb capacity LPG cylinder which was pressure tested prior to use. This tank was fitted with a 1/2" NPT fitting at the bottom for liquid exchange.

3.1.5.3 Engine Operation Procedure With the Pressurized Fuel Delivery System.

The pressurized fuel delivery system made it essential for a particular operating procedure to be followed. The pressurized fuel delivery system was controlled using separate controls from the engine. A particular procedure was followed while charging the fuel tank with diesel and DME to guarantee a reasonable accuracy in mixture preparation. Studies showed that diesel and DME are miscible in any proportion. Taking this fact into consideration, no mixing apparatus was used. The tank filling procedure is as follows:

- The fuel tank is purged with Helium to get rid of any air present in it.

- The tank is placed on a weighing scale and the initial reading is noted.
- A predetermined quantity of diesel is introduced in the tank under gravity.
- Care is taken to note the reading before and after filling, with the hoses on or off, but always the same way.
- The fuel tank is then pressurized with helium to about 50 psig or to about 10 psig less that the DME cylinder pressure. This pressure differential is sufficient to force DME with a sufficient high velocity into the fuel tank to aid the mixing of diesel and DME.
- The quantity of DME is again predetermined by the ratio of diesel to DME required.
- Additional helium is now introduced in the fuel tank to raise the pressure to about 90 psig.
- In addition to the entering velocity of DME, the blend is allowed to stand for about 6 hours, by which time the blend is assumed to be completely homogeneous.
- The fuel pump in this case is electric driven. For this reason it is turned ON and the backpressure regulator is set to 150 psig before the engine is fired.
- During engine operation, the temperature of the fuel exiting the rail needs to be monitored to prevent it from going above a certain limit.

3.1.6 Data Logging and Test Cell Control

One of the main purposes of an engine test cell is to produce data for various experimental settings. Real time data acquisition is very important to ascertain the steadiness of the engine operating parameters during a steady state test. This also helps in making a statistical interpretation of the data to get an estimate of the variation of the parameters during testing. Control systems on the other hand, help in maintaining desired conditions in the test and also act as safety checks for various aspects in test cell operation. Together these two systems help in the day to day activity of a test cell. A Programmable Logic Controller made by Modicon was used for data acquisition as well as test cell control. In addition to this a data acquisition card by Kiethley Instruments was also used.

3.1.6.1 Data Acquisition System

A PC based system was used for acquisition and logging of the various data output from the engine and the dynamometer. Type K thermocouples were used to record various temperatures. *Table 3-2* shows the measurement equipment used for each type of measurement done.

Table 3–2*:* Data Acquisition

Data type	Sensing instrument	Recording instrument
Temperature	Type K thermocouples	PC based Modicon PLC
Cylinder pressure	Kistler pressure transducer (6125A non-cooled)	PC based DAS 1800 data acquisition card
Engine control module data	Engine sensors	PC based National Instruments CAN card
Engine speed	Hall effect sensor.	PC based Modicon PLC
Engine load	Lebow load cell (model # 3132–500)	PC based Modicon PLC
Air Flow	Mass Air Flow	PC based DAS 1800 data acquisition card
Fuel Flow	Electronic Mass Scale	Manual observation

3.1.6.2 Test Cell Control

The engine and dynamometer operation was controlled using a Programmable Logic System (Modicon). The PLC had some shut off limits for various temperatures and engine speed. The OEM Accelerator Position Sensor (APS) was used to control engine fueling. No feedback control was deemed necessary for

engine speed as the dynamometer and OEM APS were able to keep the engine speed to within a few rpm of the desired value. The air handling and cooling systems and the pressurized fuel delivery system had separate controls of their own.

3.1.7 Engine Testing and Exhaust Emissions sampling strategy

One of the main objectives of this project was to demonstrate the operation of the T444E engine on a blend of diesel and DME. Due to the nature of combustion in a diesel engine, particulates and NOx are the main pollutants formed in the exhaust. CO, CO_2 and hydrocarbon emissions are usually less that its counterpart, the spark ignited engine due to leaner air fuel mixtures and high thermal efficiency.

3.1.7.1 Engine Testing Procedure.

A steady state dynamometer testing strategy was adopted to examine the engine performance and emissions with different fuels. The AVL 8 mode steady state test was followed as it closely approximates the US-FTP heavy duty engine testing procedure. This test was also used in previous studies involving the T444E engine and DME [20]. The AVL 8 mode test is shown in the *Table 3-3*

Table 3–3*:* AVL 8 Mode Test

Mode	RPM (%)*	Actual rpm	Load (%)**	Actual load (ft-lb)	Wt. Factor %	Engine HP
1	0	700	0	0	35	0
2	11	876	25	84	6.34	13.97
3	21	1036	63	224	2.91	44.12
4	32	1212	84	357	3.34	82.38
5	100	2300	18	77	8.4	33.90
6	95	2220	40	178	10.45	75.24
7	95	2220	69	307	10.21	129.79
8	89	2124	95	409	7.34	165.20

The AVL 8 mode test dictates the speed of each mode in relation to the idle and rated speed. The load is fraction of the maximum brake torque at that speed.

The speed and load for the 8 modes can be calculated as follows:

***Speed** (rpm) = Low idle + %speed *[(rated – low idle) / 100]

where,

low idle = 700 rpm

rated speed = 2300 rpm

****Load** % = is the percentage at each speed as per the torque curve.

The torque curve provided by the engine manufacturer was used to calculate the load, though it was also verified during testing. Exhaust emissions were measured and quantified at each of the 8 modes after allowing sufficient time to attain a steady state. The exhaust temperature, as well as the oil and coolant temperatures, were closely monitored to decide whether the engine has reached a steady state or not. The speed of the engine was precisely controlled with an accelerator position sensor (APS/IVS) switch. This, along with a precise load control, helped in maintaining the steady states repeatable and close to that required by the modes.

3.1.7.2 Exhaust Sampling Strategy.

As discussed earlier, the exhaust was collected and characterized for particulates, NOx, CO, CO_2 and hydrocarbons. The same sampling and characterization procedure was followed to ensure consistency for all the fuels used.

3.1.7.2.1 Sampling of Particulate Emissions.

The BG1 microdilution test stand was used to measure the particulate emissions. A detailed description of the instrument can be found in the operations manual [21]. The raw exhaust passes through a micro dilution tunnel, where it is mixed with shop air in a predetermined dilution ratio. This diluted exhaust then passes through a Pallflex membrane filter (Emfab ™). The filters are 90mm in diameter. The particulates are collected on the filter as the gas passes through it.

These filters are preconditioned in a humidity controlled environment for 24 hours before and after collection of particulates. The temperature of the gas stream and the filter is kept at or below 52^{O}C. The selection of operational parameters such as the dilution ratio, the total flowrate and the sampling time was done based on a trial and error method. These conditions were adjusted so as to collect sufficient sample during a sampling duration of 5 minutes. With the sampling time fixed, the dilution ratio and total flow were adjusted. It was found that as the total flow increased above 150 SLPM the mass of particulates collected in a particular amount of time actually decreased. This was attributed to a very high face velocity. The dilution ratio is an important parameter. Lapuerta et al [22] have shown the effect of dilution ratio and other sampling conditions such as filtering temperature and pre and post processing of the filters on the measured specific particulate emissions. The effect of filter temperature and the dilution ratio on the specific particulate emissions is discussed. It is shown from data gathered, that the dilution ratio has a more profound effect on the mass of particulates collected, than the filter collection temperature (12% reduction for a dilution ratio change from 5 to 25 as opposed to a 3.7% reduction for the filter temperature change from 25 ^{O}C to 45 ^{O}C). Keeping this in mind it was decided to keep the dilution ratio for collection constant and allow the collection temperature to vary. The range of dilution ratios in our case was bound by the amount of particulates collected within 5 minutes, on the higher side and the filter temperature on the lower side. By trial and error, 8:1 ratio was found to be suitable. A higher dilution gave an insufficient sample mass, while a lower

dilution ratio resulted in higher filter temperatures. The 8:1 dilution ratio was used throughout all the testing done i.e. for all modes of all tests with different fuels. This removed the variation due to sampling conditions from the results. As cooling of the gas sample was unavailable, the collection temperature varied from mode to mode. To account for the sample to sample variation, 5 samples were taken for every mode in every test. The filters were weighed before and after sampling, every time after equilibration. The humidity controlled chamber is Electro-tech Systems, Inc. (Model # 506A). The humidity controller was by the same manufacturer (model # 514). The humidity in the chamber was maintained at a relative humidity of 45%. The scale used for weighing the samples was a Sartorius microbalance with a resolution of 1µg.

Another instrument that was used for particulate analysis is the Series 5100 Diesel Particulate Measurement System (Rupprecht and Patashnick Co., Inc.) A detailed description of this can be found in the Operating manual. Okrent [23] also gives a description of the instrument as well as a sample application. This instrument samples the raw exhaust gas. The sampling line was heated to keep any condensation from taking place. The ceramic filter can be maintained at a specified temperature during collection. After the collection phase, comes the analysis phase. During this phase, the ceramic filter is heated from 250 ^{O}C to 750 ^{O}C. The temperature is ramped at a particular rate.

3.1.7.2.2 Oxides of Nitrogen, CO, CO_2 and Hydrocarbon Emissions.

A Fourier Transform Infrared analyzer was used to quantify the NOx, CO and CO_2 emissions. The one used was made by The Nicolet Instrument Corp. (model # 552), with a He-Ne laser. Moisture free exhaust gas was passed through the cell. The exhaust gas was stripped of moisture in a chiller. This was then directed to the FT-IR and an oxygen analyzer. The FT-IR measures the absorption spectrum of the exhaust sample gas. Prior to sampling, a background spectrum is taken with nitrogen as the purge gas. The FT-IR was calibrated using span NO, NO_2, CO and CO_2 gases. Various concentrations were made using mass flow controllers. The solvent gas used was nitrogen.

3.1.8 In Cylinder Pressure Measurement

A Kistler pressure transducer was used to measure the pressure in the cylinder through the engine cycle. The transducer used in this case was a noncooled type (6125 A), along with a suitable charge amplifier. A minimum of 40 consecutive traces and a maximum of about 140 traces were collected depending upon the speed of a particular mode of engine operation. These raw pressure traces were then processed using a software program, PTRAN by Optimum Power Technologies to get a pressure vs. crank angle trace for the recorded cycles. The same software was also used to get an average pressure trace of the collected cycles for each mode.

The heat release analysis was done using the generic equation as described in Heywood [24].

$$\frac{dQ_n}{dt} = \frac{g}{g-1} p \frac{dV}{dt} + \frac{1}{g-1} V \frac{dP}{dt} \tag{3.1}$$

Here;

Q_n is the net heat release

γ is the ratio of specific heats.

V is the cylinder volume

P is the cylinder pressure.

In actual calculations time was substituted by the crank angle.

The specific heat ratio was assumed to be 1.33 for all the cases for the 8 mode test. This analysis was done on the 'Average Pressure Trace' output of PTRAN. The resulting plots are compared in Chapter 4. Various combustion events like the start and end of combustion were estimated using the Heat release curves obtained as shown above.

3.2 High Pressure Viscometer Setup

To optimize the performance of a fuel injection system for a particular fuel or fuel blend, it is very important to have a good estimate of the physical properties of those fuels. It is equally important to know the change in properties with change in pressure and temperature. An experiment was set up to measure the viscosity of diesel, DME and their blends at various pressures. The high pressure viscometer apparatus used for this work was designed and built at The Pennsylvania State University in 1962-63. This equipment was modified to allow for charging of pressurized liquid samples, as is necessary when dealing with compressed liquids. Johnson [1] in his Master's thesis, gives a detailed description of the design and use of the apparatus. The equipment, very simple in design, nevertheless is extremely accurate in viscosity measurement up to a pressure of 10000 psig.

3.2.1 Description of High Pressure Viscometer

A schematic diagram of the apparatus setup is shown in *Figure 3-4*. The setup consists of a pressure intensifying system, a pressure measurement system, a constant temperature bath and the viscometer pressure vessel.

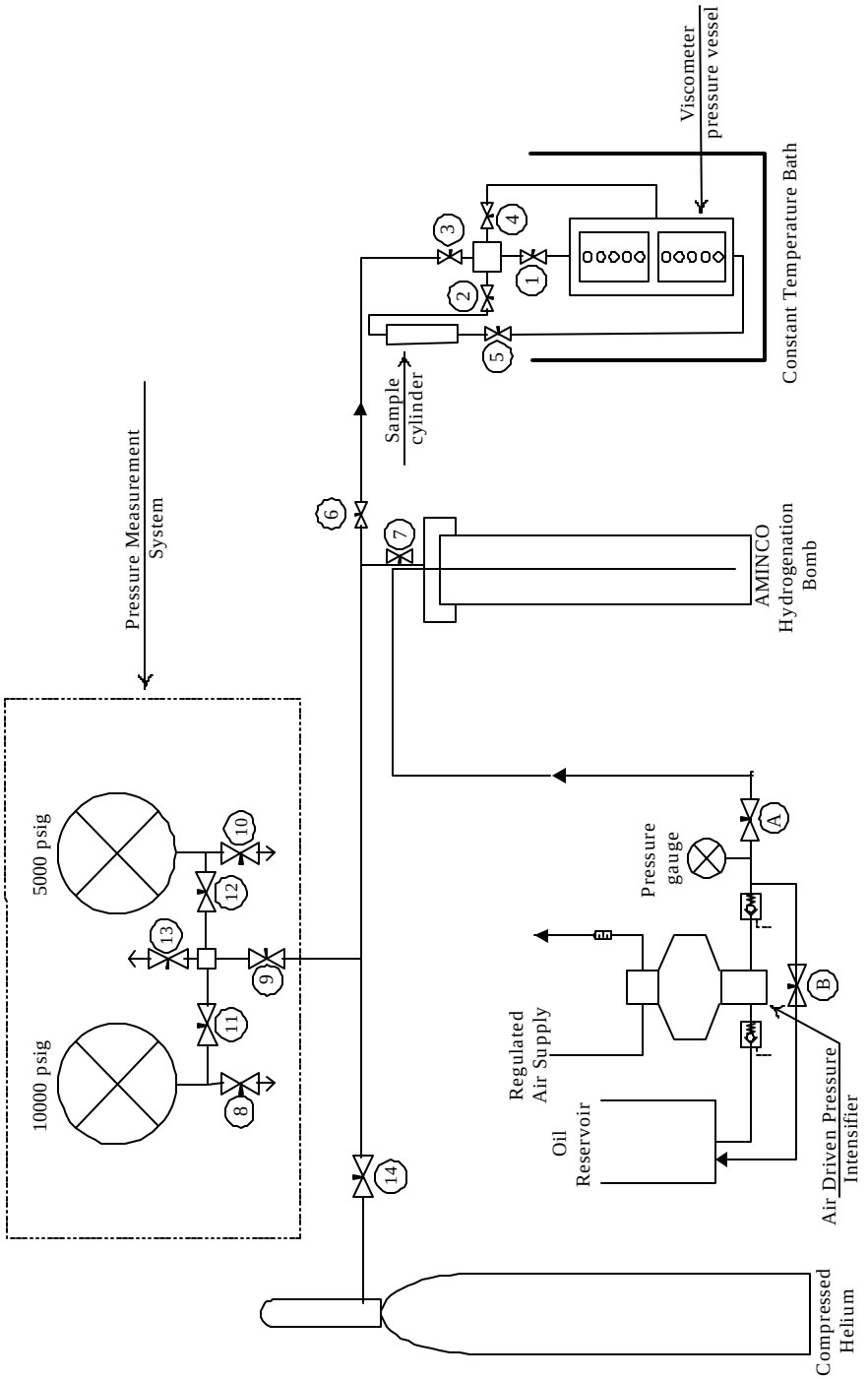

Figure 3-4: High Pressure Viscometer Setup

3.2.1.1 Pressure Supply and Measurement Equipment

Pressurized helium produces the high pressure required for this equipment. Initial studies were carried out with nitrogen as the pressurizing gas. It was found, however, that nitrogen is highly soluble in DME. Higher the solubility of a gas in DME, higher is the error in measurement of viscosity. For this reason it was decided to use helium, which is less soluble in DME as compared to nitrogen. Pressures up to 2000 psig can be attained by simply connecting a commercial helium gas cylinder to the system. For higher pressures, the air operated pressure intensifying pump is used. This system consists of an AMINCO dehydrogenation bomb with a volumetric capacity of 4.5 liter. This bomb is filled with helium from the gas bottle at the available pressure. This is further compressed by pumping oil into the bomb. A SAE30 oil was used in this case. For higher pressures, however, a SAE50 oil is recommended. The oil is pumped by an air driven pump (Teledyne Sprague Engineering Model # S-216-J-150). The 150 in the model number, indicates the factor by which the pressure of oil can be raised as compared to the pressure of the supplied driver air.

The pressurization procedure can be explained as follows with reference to *Figure 3.4*:

- Valve B, the return valve is closed and valve A is opened. The outlet oil pressure gauge will read the pressure of the helium in the bomb.

- Driver air is supplied to the pump at a pressure of about 25 psig. An air lubricator is installed upstream of the pump. If the air inlet valve to the pump is open, it will cause the pumping plunger to pump oil into the hydrogenation bomb. The addition of oil increases the pressure of helium already present in the bomb. There is a one way valve in the oil supply line, which prevents the oil from flowing back into the pump. The pressure of the helium in the bomb is read by an accurate pressure gauge.
- When the desired pressure is reached, the air inlet valve to the pump can be closed to stop the pump. The valve A is then closed. High pressure after the pump is relieved slowly by gradually opening the valve B.
- The bomb is now ready to supply pressurized helium to the viscometer apparatus. The pressure of helium is always kept a bit higher than the required pressure in the viscometer.
- The amount of oil in the bomb can be estimated by observing the change in the oil level in the oil reservoir.
- Care should be taken to prime the pump with oil. This can be achieved by gravity feeding the oil.

High pressure gauges are used to measure the pressure in the system. These gauges have a maximum readability of 5000 and 10000 psig and have a rated accuracy of 0.5% of full scale. For the present study, the gauge with a capacity of 5000 psig was used for its higher resolution.

3.2.1.2 Constant Temperature Bath

For the present study, the viscometer housing was kept at a constant temperature of 100 deg F. Water was used as the bath fluid. It was maintained at 100 deg F, using a temperature controller by Omega Engineering (Model CN9000A). This controller reads the temperature by means of a K-type thermocouple. There is a feedback loop that controls the electric immersion heater. Using this system, the temperature in the bath can be maintained to within 0.1 deg F. The bath is made out of a glass jar 12 inches in diameter. The water level in the bath is maintained at a certain height so that the viscometer pressure vessel is fully immersed in water. A submersible pump is used for water circulation, which helps maintain a constant temperature throughout the water bath. The bath temperature control is typically kept ON continuously to assure a stable operating temperature.

3.2.1.3 Viscometer Operation Procedure

The operating procedure for the viscometer is described with respect to *Figure 3-4.* Prior to beginning the viscosity measurement, the sample for viscosity measurement is prepared in the sample cylinder and maintained at a pressure of about 500 psig. The sample cylinder is then kept in the water bath overnight to ensure thermal equilibrium between the sample and the water bath. The AMINCO hydrogenation bomb is charged to the required pressure by operating the pressurizing equipment. The viscometer capillary is assembled in the pressure vessel and is brought up to the

operating pressures. The bath is brought up to the operating temperature of 100 deg F. The following steps are then taken to charge the viscometer capillary with the fluid and measure its viscosity:

1. The 5000 psig pressure gauge is used to measure the pressure in the viscometer housing. At this point valves 1, 3, 4, 6, 9 and 12 are open and valves 2, 5, 7, 8, 10, 11, 13 and 14 are shut off.
2. The sample cylinder is connected to the viscometer housing at valves 2 and 5. Valve 2 is opened to equalize the pressure between the sample cylinder and the viscometer housing. Valve 5 is used to introduce the desired amount of sample into the viscometer housing. The level of the sample is observed through the glass windows on the viscometer housing. As soon as the desired level is reached, the valve 5 is closed. The sample cylinder can then be disconnected from the viscometer housing.
3. As the test fluid is already at the operating temperature, the viscometer capillary can be immediately filled with the sample. To accomplish this, valves 3 and 4 are shut off. Helium is then vented very slowly to the atmosphere through valves 1 and 2. Valve 2 can be left fully open and the rate of capillary filling can be controlled by modulating valve 1. It is very important to fill the capillary very slowly. Rapid filling may cause boiling and separation of the sample. A rule of thumb is to allow the same time for filling as it takes for drainage. The liquid level in the capillary should be a little above the uppermost etched line above the degasification bulb as shown

in *Figure 3-5*. At this point valves 1 and 2 are closed. Valves 1 and 4 are then opened slightly to equalize the pressure between the top of the capillary and the reservoir. Valve 3 is then opened so as to read the correct pressure in the viscometer housing. Valve 1 is then closed immediately to maintain the level of the liquid in the capillary. The filling process can reduce the pressure to a great extent. It is important to begin with a pressure higher than desired. With sufficient practice, the desired level in the capillary can be reached at the desired pressure.

4. At this time the viscometer is left to equilibrate for a couple of hours. This is to ensure that the entire system has reached a constant desired temperature.
5. After about two hours, the viscometer is ready for viscosity measurement. Care should be taken that the liquid level hasn't changed significantly in the capillary. Starting drainage from different liquid levels may introduce errors as will be discussed later. Valve 1 is now opened to allow the liquid to start flowing down. The stop watch is started as soon as the lower liquid meniscus comes in line with the top etched line on the efflux bulb. The time is stopped when the lower meniscus reaches the lower etched line at the bottom of the efflux bulb. The time is measured with a resolution of 0.01 seconds. The measured efflux time along with the characteristic distance are the only two observations required of the viscosity test run. The characteristic distance is the distance between the liquid level at the bottom of the viscometer housing

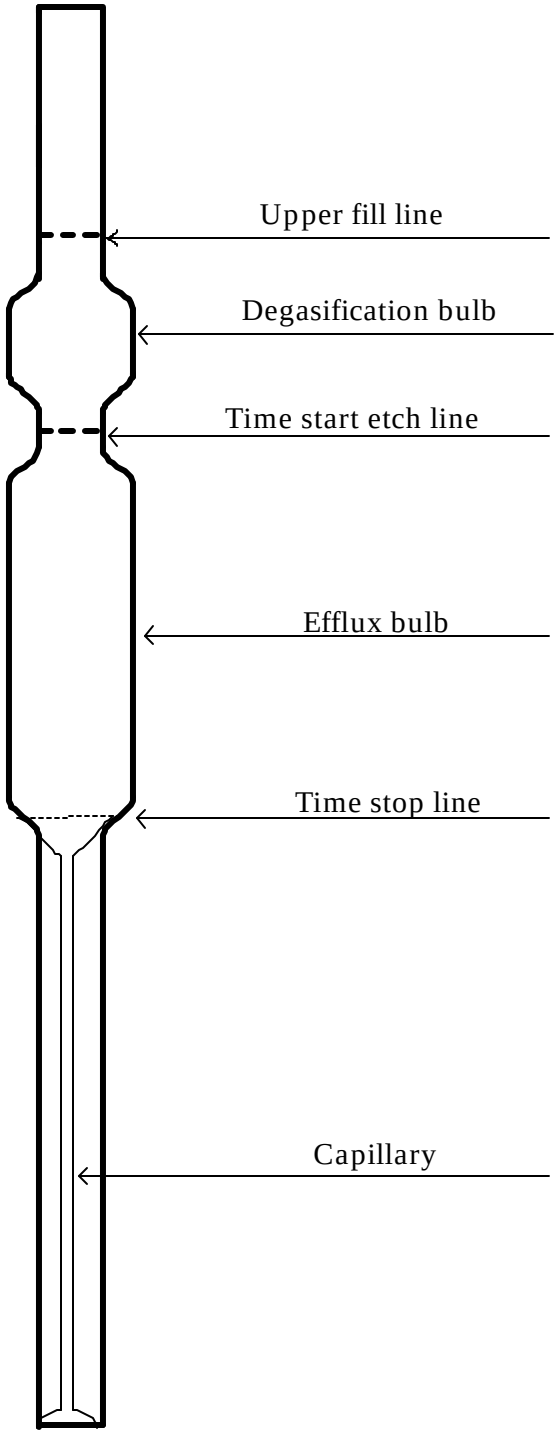

Figure 3-5: Viscometer Capillary

and the bottommost etched line on the capillary. This distance is measured by a cathetometer with a resolution of 0.005 cm.

3.2.1.4 Sample Preparation

The samples tested for viscosity were blends of Diesel and DME in various proportions. A schematic of the apparatus used for sample preparation is shown in *Figure 3-6*. It consists of a transparent pressue vessel used to hold the mixture under a pressure of about 90 psig. The pressurizing gas is Helium, which is chosen for its lower dissolution in DME. The following steps describe the preparation of a homogeneous sample and its transfer into the sample cylinder.

1. About 100g of DME are introduced into the sample cylinder. The sample cylinder is then pressurized to about 90 psig. The difference in mass of the sample cylinder with and without DME gives the exact amount of DME present in the cylinder.
2. The observation vessel is pressurized with Helium to about 90 psig. The sample cylinder filled with DME is attached in the circuit 1. The valves connecting the sample cylinder to the observation vessel are opened. Under the influence of gravity, DME flows down into the observation vessel. The circuit 1 helps in equalizing the pressures in the two connected vessels. Sufficient time is allowed for all the DME in the sample cylinder to drop down into the observation vessel. The sample cylinder is disconnected and

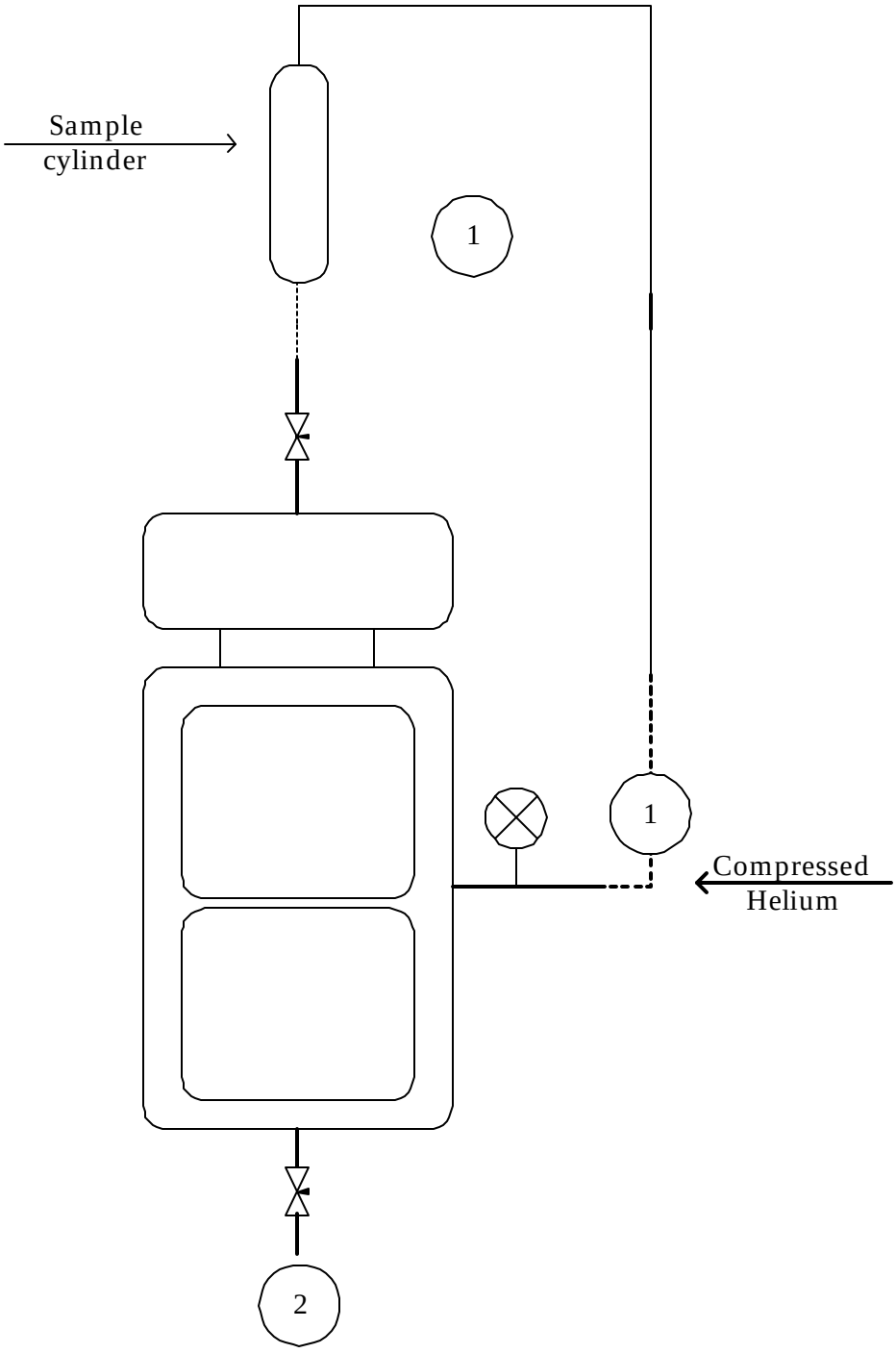

Figure 3-6 Diesel-DME Sample Preparation

weighed. The difference in mass is the mass of DME introduced into the observation vessel.

3. This known mass of DME dictates the mass of Diesel fuel to be put in to get the desired Diesel-DME blend ratio. The required amount of Diesel is then introduced into the observation vessel in a similar manner. The velocity of the Diesel fuel entering the observation vessel helps in forming a homogeneous mixture instantly.
4. This mixture is then introduced into the sample cylinder through circuit 2. The mixture blend ratio is calculated by taking the actual mass numbers as observed.

3.2.2 Viscometer Calibration and Data Analysis

The viscometer is a capillary type viscometer, in which a constant volume of liquid is allowed to flow under gravity into a reservoir of the same liquid. Reference lines are etched on the glass viscometer for measurement of head. The parameters measured are;

- time required for a predetermined volume of liquid to drain through the capillary with a resolution of 0.01 seconds.
- a characteristic distance, the distance between the bottommost etched line on the viscometer bulb to the liquid level in the reservoir in the viscometer housing.

The procedure followed for calibration of the viscometer is the same as that followed for viscosity measurement. The calibration is performed by allowing a liquid with a known viscosity to drain from the capillary. A series of runs are performed by varying the characteristic height. For every run, the characteristic height and drainage time are recorded. A viscometer constant is calculated as follows;

viscometer constant (s / cSt) = drainage time (s) / viscosity of calibration liquid (cSt).

For viscosity measurement, runs are performed within the range of characteristic height used during the calibration runs. The viscometer constant is obtained using the calibration curve and the characteristic height during viscosity measurement run. The constant together with the measured drainage time gives the viscosity of the liquid. Detailed discussion of the data analysis can be found in [1].

Chapter 4

RESULTS, DISCUSSIONS AND CONCLUSIONS

The ability to operate the Navistar T444 E engine on a fuel blend of Diesel-DME with a 2% O content was demonstrated. The pressurized fuel supply system that was designed to provide a liquid fuel blend to the fuel injectors / intensifier unit was also tested for its suitability and practicality. The viscosity of Diesel-DME blends with varying blend ratios was measured. Observations were made regarding the miscibility of diesel and DME for the blend ratios considered.

4.1 Miscibility Studies of Diesel – DME Blends

To ensure stable operation of a direct injection diesel engine, it is imperative that the fuel blend is always maintained in a homogeneous liquid state. The miscibility of the fuels is therefore an important aspect of any fuel blend.

The miscibility tests of Diesel-DME blends were carried out in a pressurized vessel with a transparent window for observation. Blend ratios were varied in steps of 25% by mass. Thus 0, 25, 50, 75 and 100 were the percentages of DME by mass in a blend comprising of DME and Diesel. Diesel has a density that is higher than that of DME. To separate the effect of gravitation on the mixing process, diesel was introduced as the lower layer in the observation vessel. DME, which was introduced

from the top as a liquid under pressure, formed the upper layer. The pressure was maintained at about 90 psig. This same pressure was later to be used in the pressurized fuel tanks for the engine. This non-homogeneous mixture was left undisturbed and the quality of the mixture was observed after various time intervals. This process ensured that the mixing would be only because of molecular diffusion and not because of any physical mixing via turbulence or density difference. It was observed that irrespective of the blend ratio, the blend became a homogeneous mixture in about 6 hours.

Under these testing conditions, minimal fluid mixing took place to assist the formation of a homogeneous mixture, relying primarily on molecular diffusion. Introduction of one fuel into the other at some velocity greatly helps the mixing process.

Separation of the two fuels is also an important issue. Once a homogeneous mixture is formed, the fuels do not separate until DME starts boiling. Boiling may occur due to a reduction in pressure or an increase in temperature. Boiling is very likely to occur in the fuel rail of a diesel engine due to elevated temperatures. During the test run with a 2% O_2 content Diesel-DME mixture, unsteady operation of the engine and a loss of power were observed. This could have been due to the boiling of the DME present in the blend. The resulting fuel blend entering the fuel injectors was a mixture of liquid and DME vapors. This is thought to be the cause of power loss and unsteady operation. The temperature of the fuel in the rail was measured at 53 ^{O}C, which is higher than the boiling point of DME at the rail pressure of 150 psig.

4.2 Viscosity of Diesel – DME Blends

The high pressure viscometer capillary was calibrated using a Cannon Certified Viscosity Standard N 1.0. *Figure 4.1* shows the calibration curve obtained for the capillary used. The procedure followed to obtain the calibration was similar to the procedure for data taking. The calibration curve is typically a straight line.

Mass was used as the controlled variable in determining the composition of the samples. *Table 4-1* shows the samples used for viscosity measurement.

Table 4–1*:* Samples for Viscosity Measurement

Sample number	Percent of DME by Mass
1	100
2	74
3	50
4	26
5	0

The remaining portion of the sample was made up by an Emissions Certification Diesel Fuel (ECD-LS) from Specified Fuels, a federal emissions certification fuel. *Figure 4.2* shows the effect of pressure on the viscosity of the various liquid samples. The kinematic viscosity is plotted on a logarithmic scale. Johnson [1] notes that a plot

of the logarithm of the kinematic viscosity versus the pressure results in a straight line. DME and diesel fuel-DME blends also follow a logarithmic relation with pressure.

The slope of this line can be used to extrapolate to higher pressures with a fair amount of accuracy. The line representing the ECD-LS fuel starts from ambient pressure. For the remaining samples with DME as a constituent, the starting point was 500 psig to ensure that the samples remain in a liquid state. The pressure range in which the viscosity measurements are made are typical in the low pressure circuit of a diesel engine. Previous studies, done with pure DME as the fuel, state that lower injection pressures can be used for DME as the condition in the cylinder just before the firing TDC allows a very rapid vaporization of DME.

Another use of the viscosity versus pressure relations for the various blends is to choose or design a fuel injection system for the optimized blend ratio. There are two ways in which the fuel system can be designed for an engine running on a Diesel-DME blend. The first one is to examine the capability of existing fuel systems .The deciding factor in this case will be the minimum viscosity that an existing fuel injection system can handle. The other way would be to optimize a blend ratio for a particular engine considering the exhaust emissions benefits and the energy density tradeoffs and to use the viscosity data of this particular blend to design a fuel injection system for that blend ratio.

Figure 4.3 shows the response of the kinematic viscosity to the ratio of DME in the blend. This graph shows the effect of pressure on the viscosity of a particular blend.

Sivebaek et al. [30] have measured the viscosity of pure and blended DME. The viscosity was measured at the vapor pressure at that temperature. The viscosity of pure DME as measured by Sivebaek et al. is 0.185 cSt at a temperature of 25 ^{O}C. In the present study, the viscosity of DME was not measured at the vapor pressure. This value can however, be estimated by extrapolating the pure DME viscosity line to lower pressures. The viscosity of DME in *Figure 4.2* shows a value of about 0.199 cSt, however, at a different temperature.

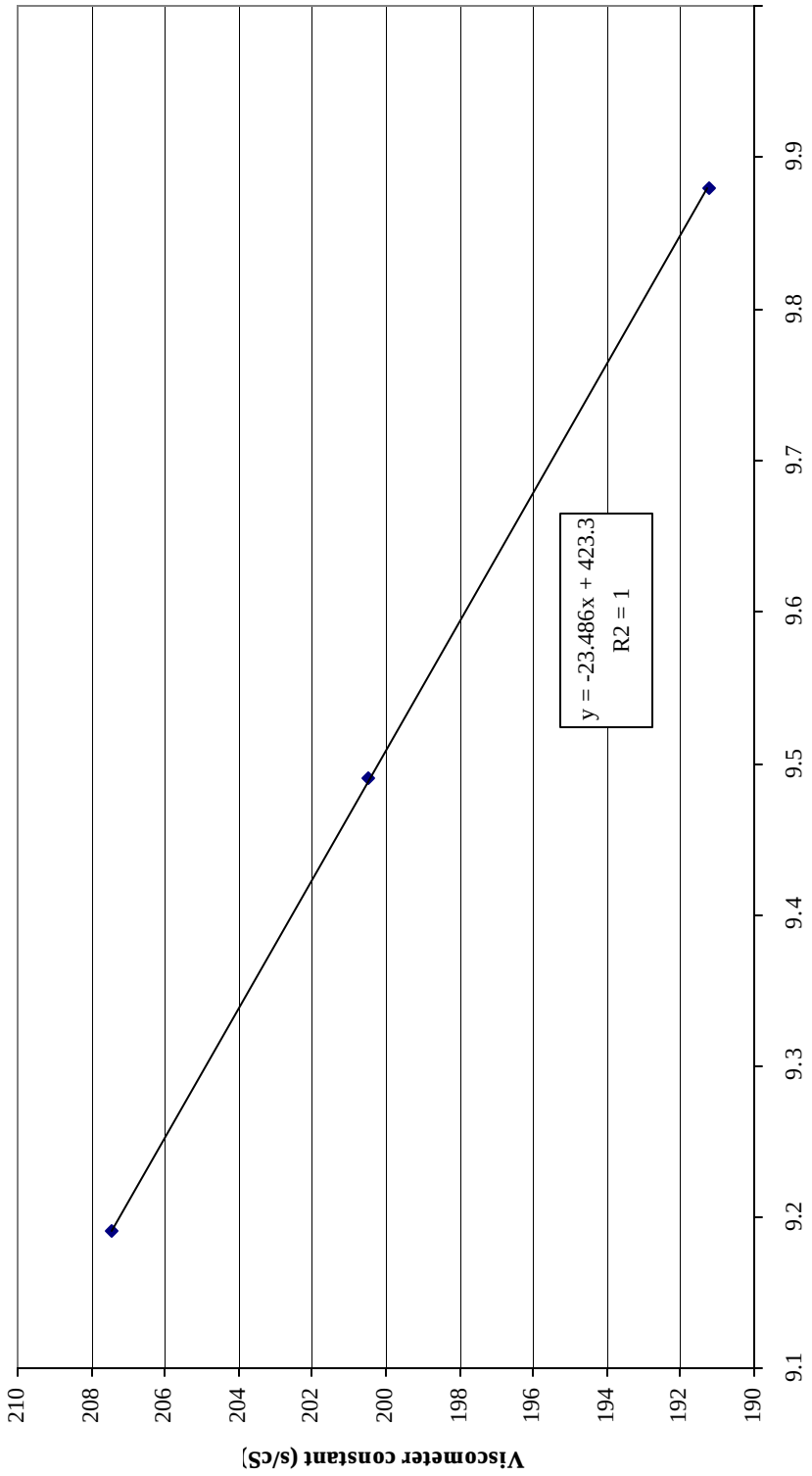

Figure 4.1: Viscometer Capillary Calibration Curve

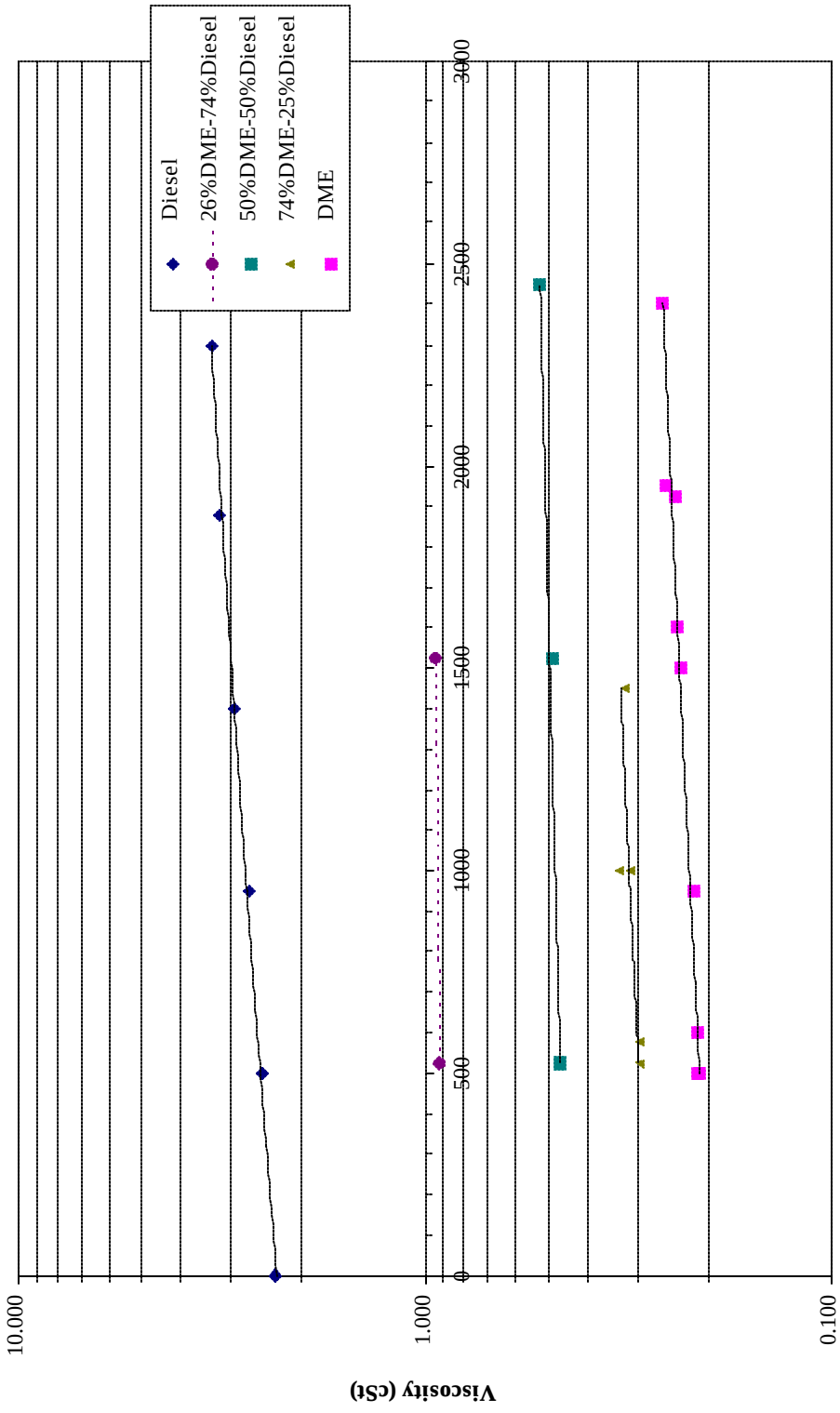

Figure 4.2:Pressure-Viscosity Relationship for Diesel-DME Samples @ 100 F

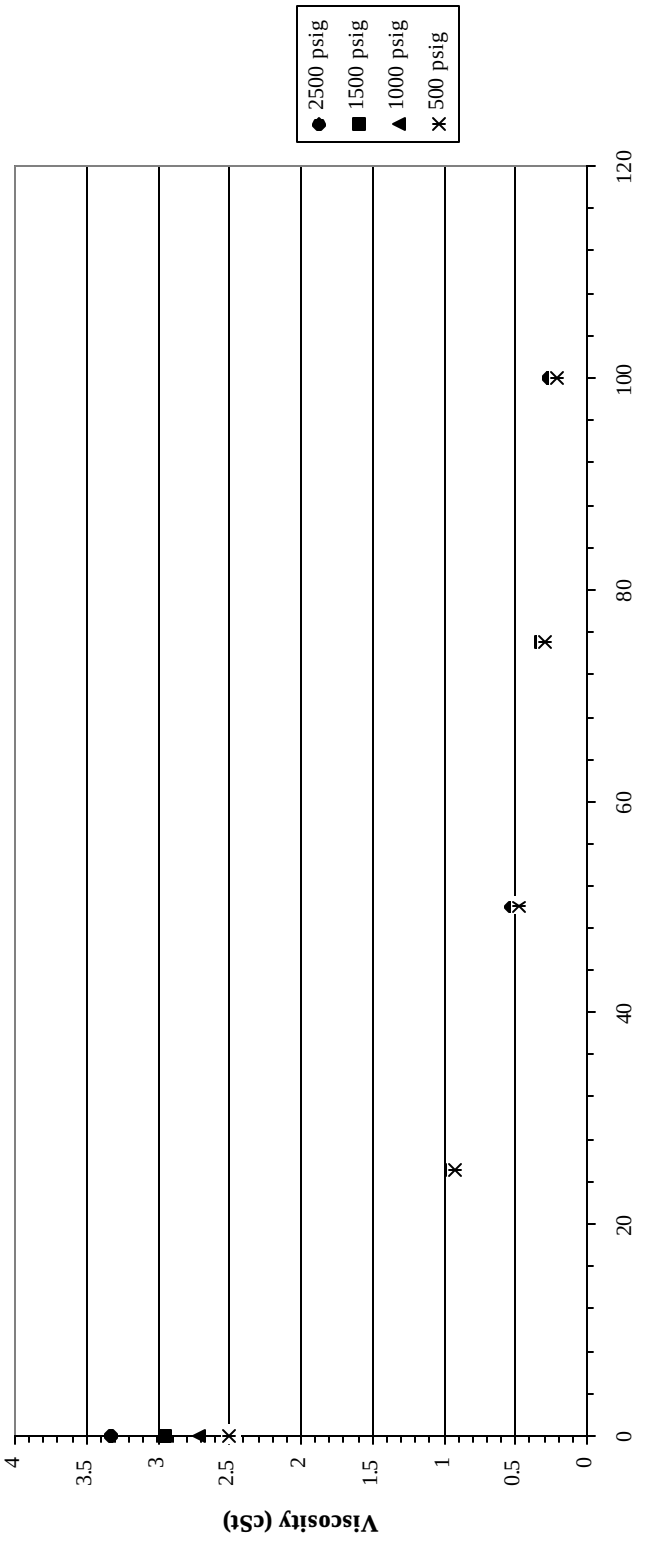

Figure 4.3: Relation of Blend ratio and Viscosity

4.3 Engine Operation With Diesel-DME Blend

The first Diesel-DME blend to be run in the engine was one with a blend ratio so as to contain 2% O by mass. This particular number was chosen for the blend to be equivalent to blends of diesel and other oxygenates in terms of the Oxygen content for comparison. The performance of the existing fuel system was studied and modifications were performed as described in the Chapter 3. Back to back AVL 8-mode tests were run with the ECD-LS fuel and the 2% O content Diesel-DME blend.

4.3.1 Modified Fuel System Performance

To maintain the DME in a liquid state, a fuel rail pressure of 150 psig was used. A necessary condition was to keep the temperature of the fuel in the rail below 50 ^{O}C. To help maintain the desired temperature in the fuel rail a chiller bath was used to cool the fuel as it exited the fuel rail. *Figure 4.4* shows the measured temperature of the fuel in the fuel rail of the engine for different configurations of the fuel system. As can be seen in the unmodified fuel system, the temperature of the fuel in the rail approaches the coolant temperature of around 80 ^{O}C. This is because the fuel system on the T444E engine is a dead head system where the fuel entering the rail must be injected into the engine over the next few engine cycles. The fuel return takes place just before the fuel enters the fuel rail.

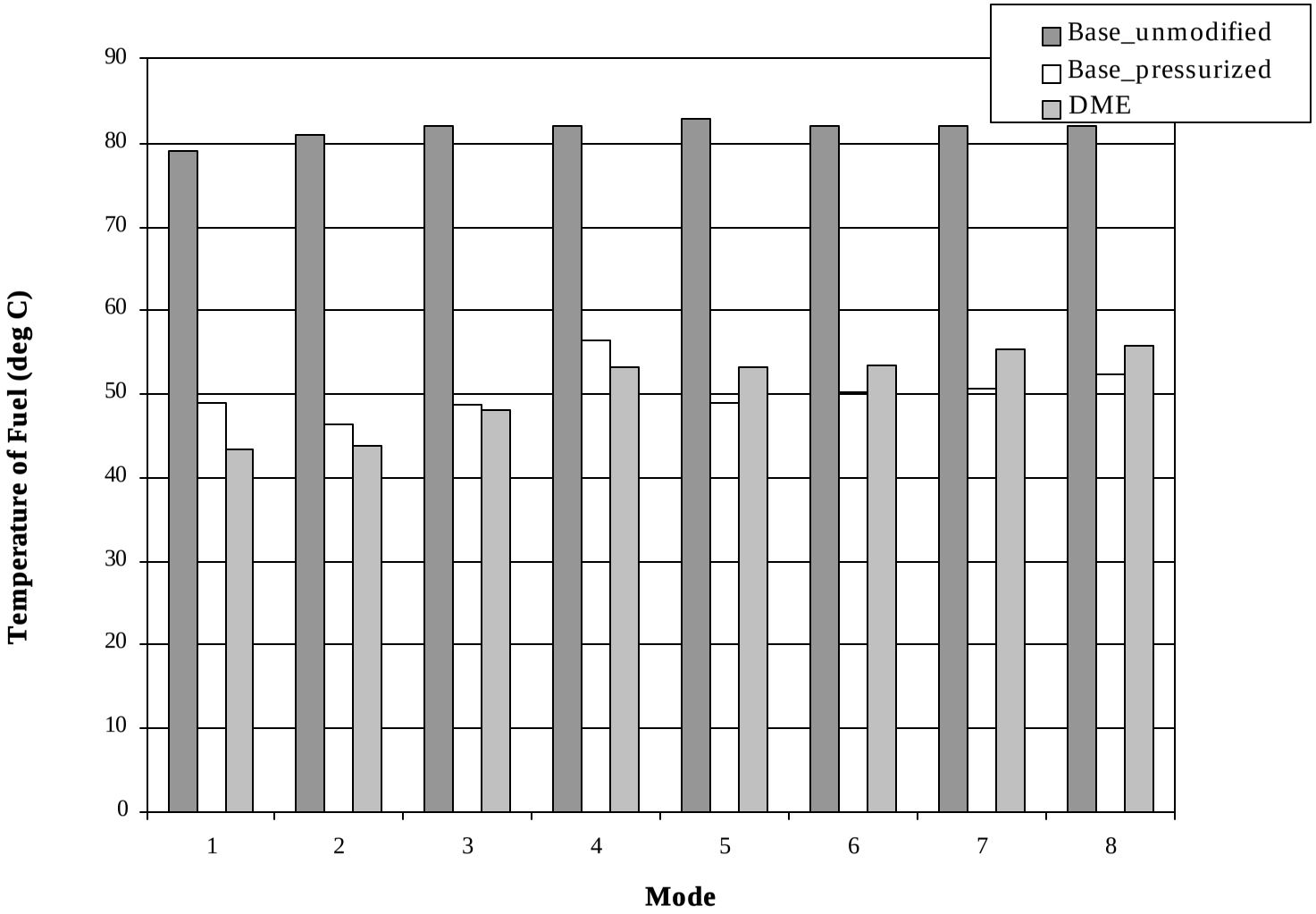

Figure 4.4: Temperature of Fuel in Rail

With this “dead head” setup, it is impossible to maintain the temperature of the fuel in the rail below the required 50 ^{O}C during steady state engine operation. In the modified fuel system, the fuel passing through the rail is returned allowing for cooling of the fuel in the return path. The drop in temperature seen in *Figure 4.4* was due to the cooling of the fuel as it returns from the rail. It can be seen however, that the fuel temperature for modes 4 and onwards was still higher than 50 ^{O}C. This resulted in an unsteady operation of the engine for mode 8. The engine was not able to maintain the required speed of 2124 rpm at a brake torque of 409 lb-ft. As seen in *Figure 4.5* the engine speed kept on falling. The unstable running condition seen at Mode 8 (the data represents approximately 2.5 minutes of running time), was caused by boiling of the DME in the transition passage from the fuel rail to the injector, where the fuel pressure is still equal to the rail pressure and the temperature higher than the fuel rail. In the stock fuel system, the fuel enters the injectors at a temperature in excess of 80 deg C. The T444E engine management system does not change injection timing to compensate for fuel temperature, which could lead to a poorer fuel spray in the cylinder if the fuel temperature is much less (in our case it was maintained below 50 deg C with the exception of Mode8).

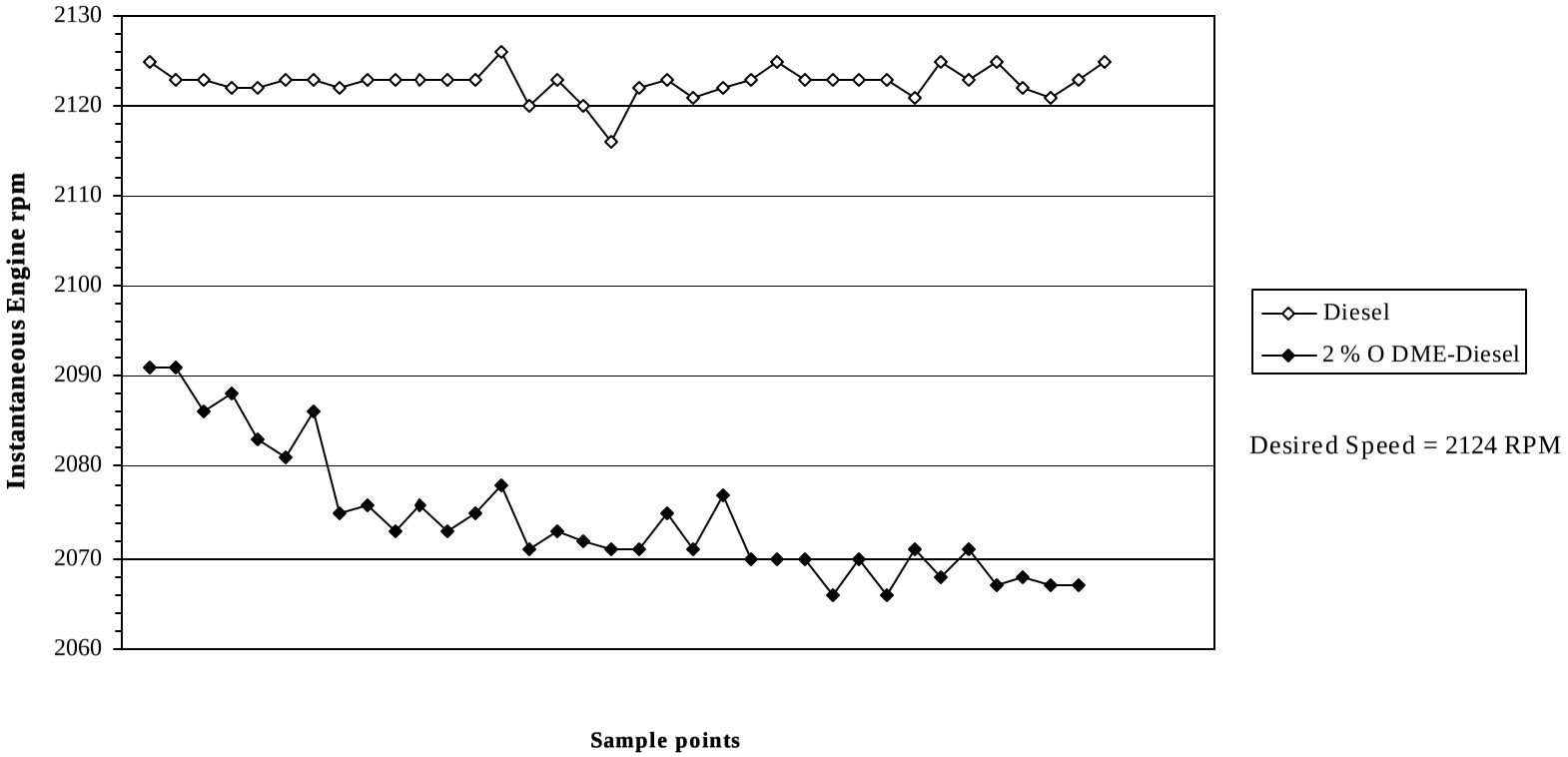

Figure 4.5: Engine Instantaneous Speed Comparison for Mode 8

4.3.2 Incylinder Pressure Trace Analysis

Cylinder pressure for cylinder number 1 was recorded for all the modes of the AVL test for both the fuels. Effect of the different fuels on combustion events such as start of burn and combustion duration was observed. A rate of heat release (ROHR) calculation was carried out. Figure 4-6 compares the “effective” ignition delay between the two fuels for various modes. The ignition delay numbers shown are a sum of the actual ignition delay and a "hydraulic+electric" delay in the fuel injectors. The hydraulic delay is caused by a finite amount of time that passes between the electronic command signal from the ECM to the injector and the occurrence of actual fuel injection. As the injector is a HEUI, the oil temperature and oil pressure influence this hydraulic delay. The electrical delay is the time delay between the initiation of a signal by the ECM, being converted to a higher voltage by the Injector Driver Unit (essentially a capacitive discharge ignition coil), then proceeding to open the oil supply solenoid to the injectors. In the absence of accurate knowledge of the hydraulic and electric delays, it is safe to assume that the delays will be constant at a particular engine operation mode regardless of the fuel used. Monitoring of the pressure and temperature of the oil supply to the injector was performed during the two runs with diesel and 2%O blend to show similar conditions. Based on this, the ignition delay numbers were reduced as a ratio between a particular mode and the maximum delay recorded.

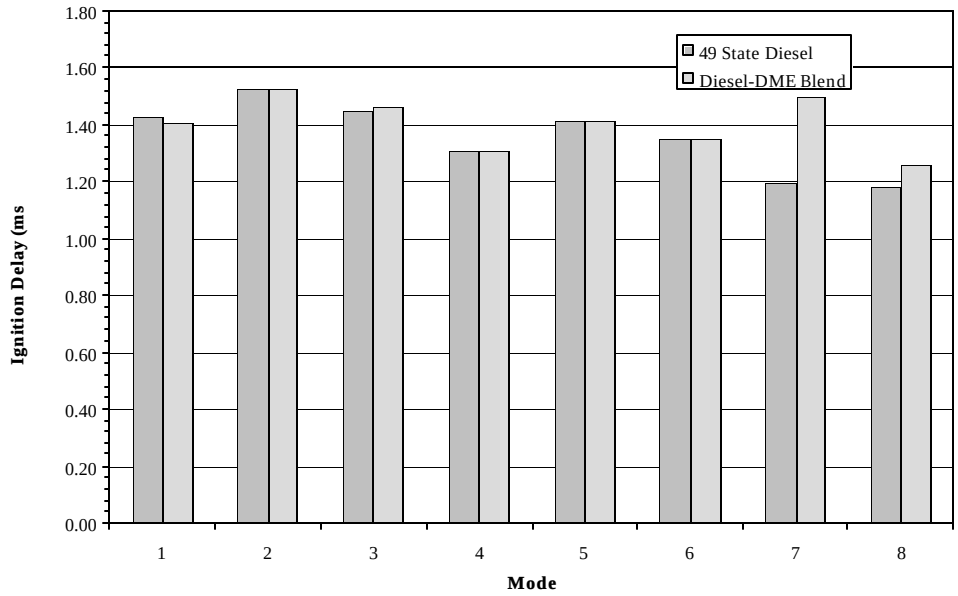

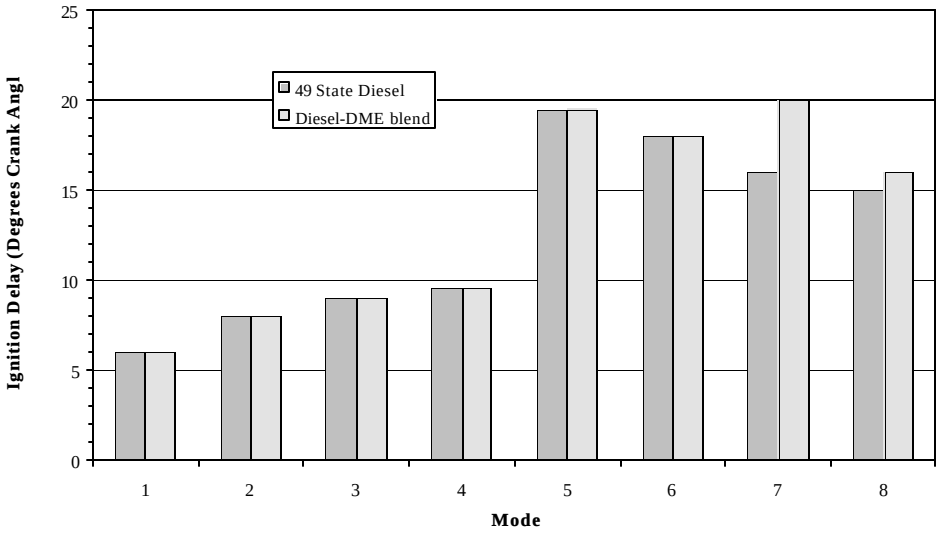

Figure 4-6: Ignition Delay Comparison

Figures 4-7 to 4-14 present a pressure trace comparison for all the modes of the AVL test between the two fuels. By looking at the heat release curves a comparison can be made between the diesel and blend pressure traces. The ROHR curves calculated here compare very well with the curves generated by commercial software such as PTRAN. Mode 2 seems to be the only mode where the "split-shot" injection is in evidence. The "split shot" is due to a spill port in the injector. The amount of pilot injection is the same for any operation mode of the engine. Mode 2 seems to be the only mode in which the pilot injection can really be differentiated from the rest of the injection. In general, slightly higher ROHR and peak cylinder pressures are observed for the operation with 2% O fuel blend. Mitsumasa Ikeda, et al [31], have studied the combustion of 8% DME blend (by mass) in diesel (2% O corresponds to 5.747% DME by mass). They have observed a "delayed heat release" for 8% DME blend as compared to Diesel fuel. The have also noted an increase in max ROHR with an increase in DME concentration. The present work with 5.747% DME and the above reference with 8% DME seem to indicate results opposite to expectations considering the higher Cetane number of DME. In both studies the injection timing was maintained the same for both fuels. This may be the cause of the anomaly. With a higher Cetane value, the diesel-DME blend will need an optimization of injection timing to strike a balance between too high ROHR and too high THC emissions. Thesis work by Matt Stoner [32] also suggests that there is not a significant difference in the ROHR (rather burn rate) of the different oxygenate blends with 2% O content. All oxygenates considered there, were within the boiling range of diesel

fuel. Boiling point of DME being drastically less than that of diesel fuel, an expectation was to see some effect of 2% O diesel-DME blend on the ROHR. However, this physical advantage of lower boiling point may not be realized at an Oxygen level of 2% (DME 5.747% by mass).

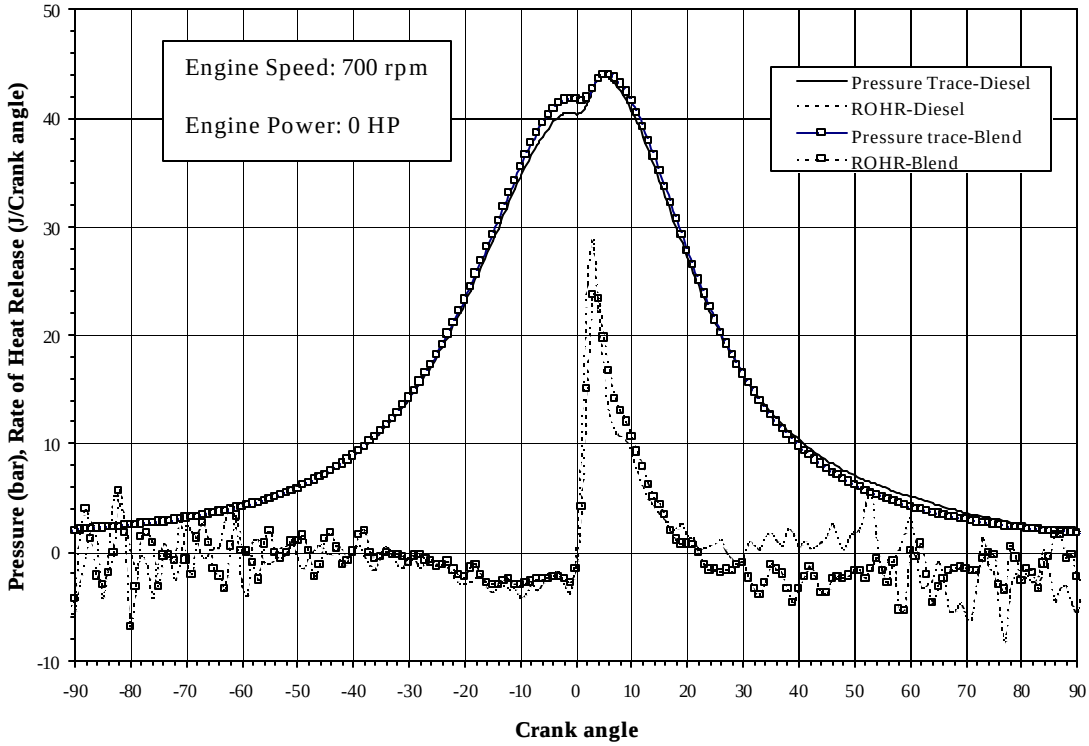

Combustion Event	Diesel	Diesel-DME Blend
Start of Injection (Degrees ATDC)	-6	-6
Start of Ignition (Degrees ATDC)	0	0
End of Burn (Degrees ATDC)	22	22
Max ROHR (J/crank angle degree)	28.78	23.74

Figure 4–7: Pressure Trace and ROHR-Mode 1

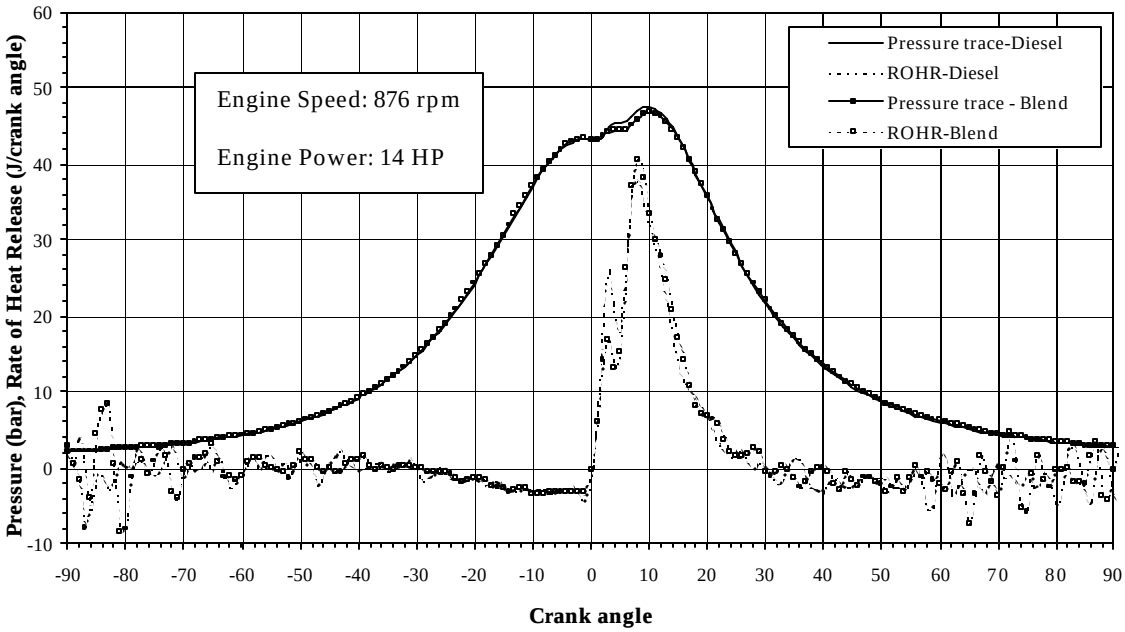

Combustion Event	Diesel	Diesel-DME Blend
Start of Injection (Degrees ATDC)	-8	-8
Start of Ignition (Degrees ATDC)	0	0
End of Burn (Degrees ATDC)	30	30
Max ROHR (J/crank angle degree)	37.70	40.61

Figure 4–8: Pressure Trace and ROHR-Mode 2

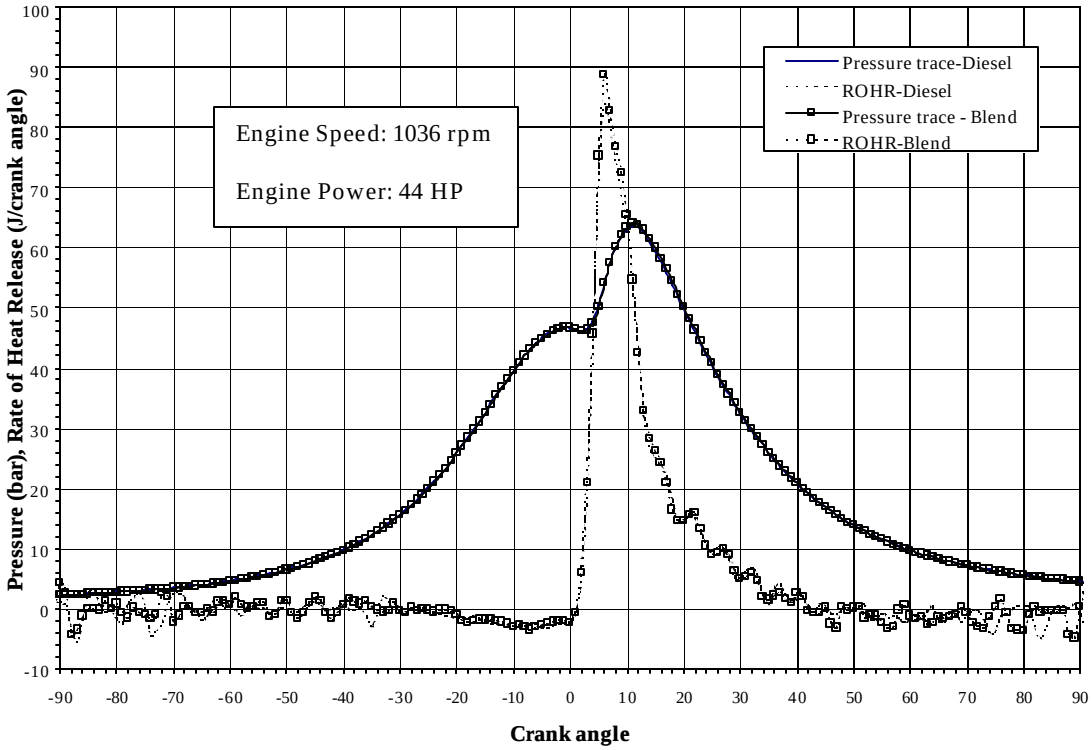

Combustion Event	Diesel	Diesel-DME Blend
Start of Injection (Degrees ATDC)	-8	-8
Start of Ignition (Degrees ATDC)	1	1
End of Burn (Degrees ATDC)	42	42
Max ROHR (J/crank angle degree)	83.87	88.69

Figure 4–9: Pressure Trace and ROHR-Mode 3

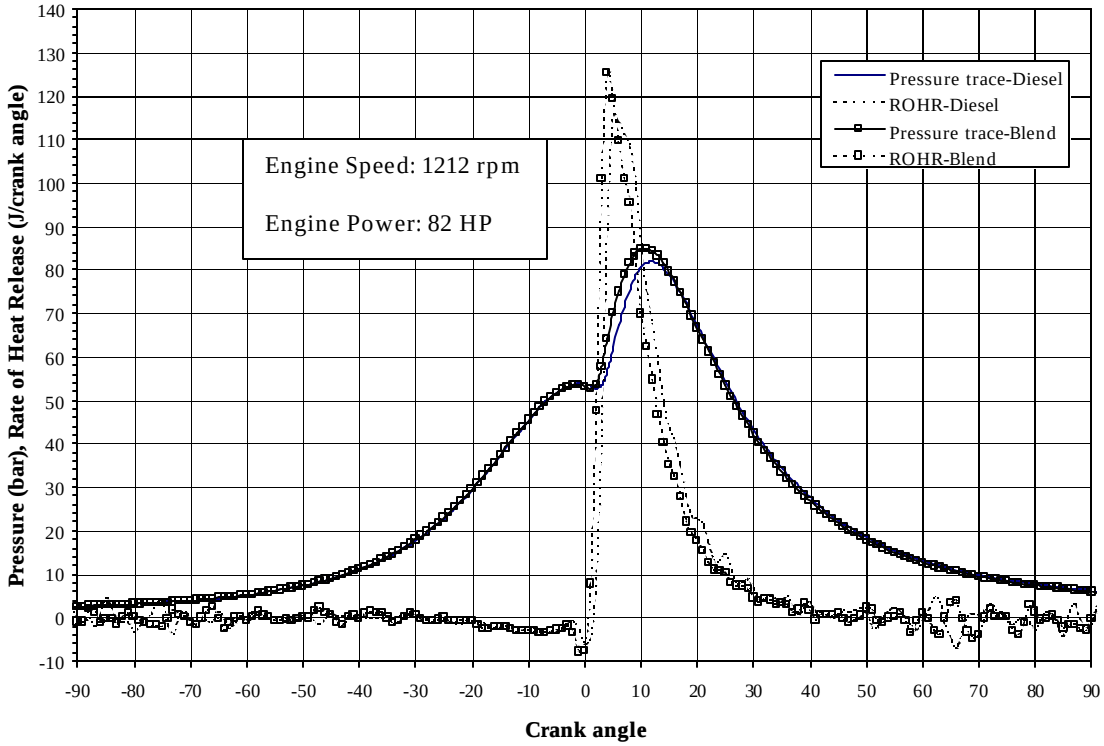

Combustion Event	Diesel	Diesel-DME Blend
Start of Injection (Degrees ATDC)	-8	-9
Start of Ignition (Degrees ATDC)	1.5	0.5
End of Burn (Degrees ATDC)	45	45
Max ROHR (J/crank angle degree)	115.55	125.19

Figure 4–10: Pressure Trace and ROHR-Mode 4

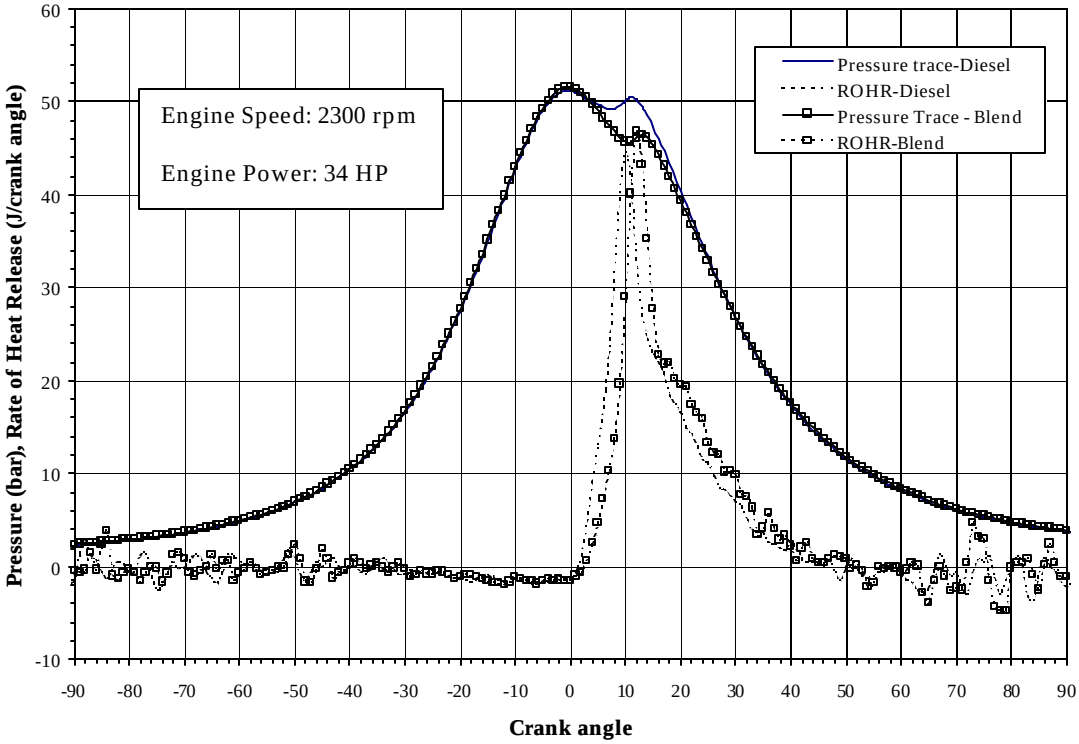

Combustion Event	Diesel	Diesel-DME Blend
Start of Injection (Degrees ATDC)	-18	-17
Start of Ignition (Degrees ATDC)	1.5	2.5
End of Burn (Degrees ATDC)	52	52
Max ROHR (J/crank angle degree)	44.53	46.74

Figure 4–11: Pressure Trace and ROHR-Mode 5

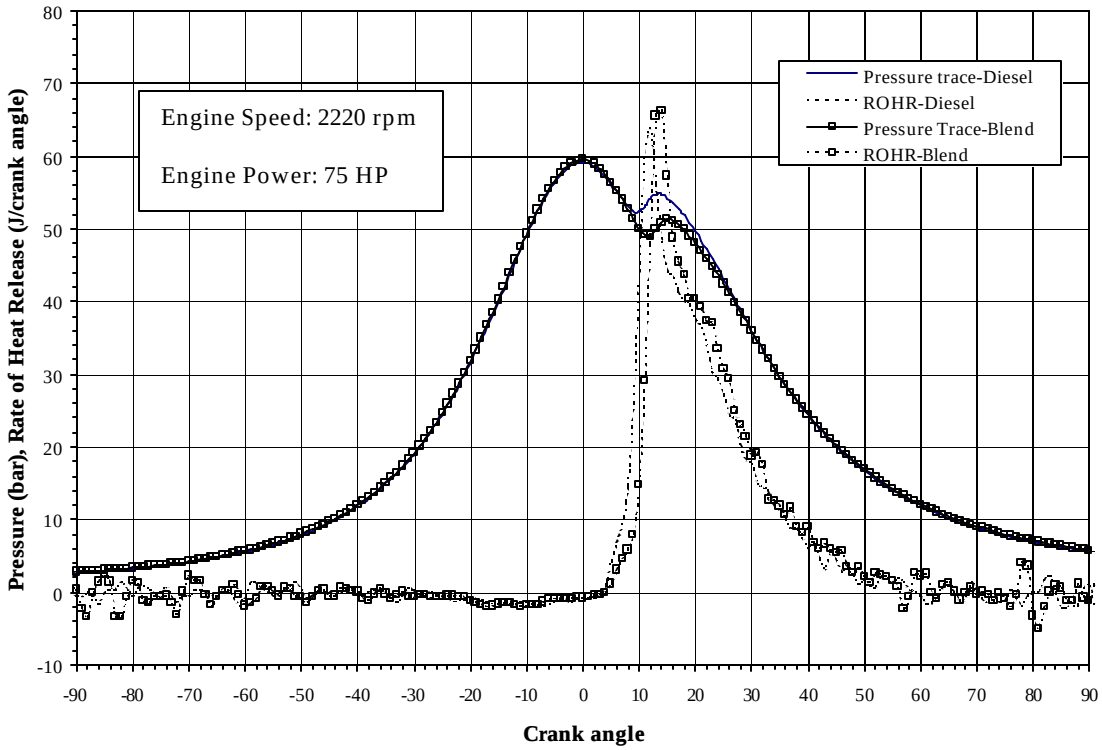

Combustion Event	Diesel	Diesel-DME Blend
Start of Injection (Degrees ATDC)	-14	-14
Start of Ignition (Degrees ATDC)	4	4
End of Burn (Degrees ATDC)	58	56
Max ROHR (J/crank angle degree)	63.83	66.27

Figure 4–12: Pressure Trace and ROHR-Mode 6

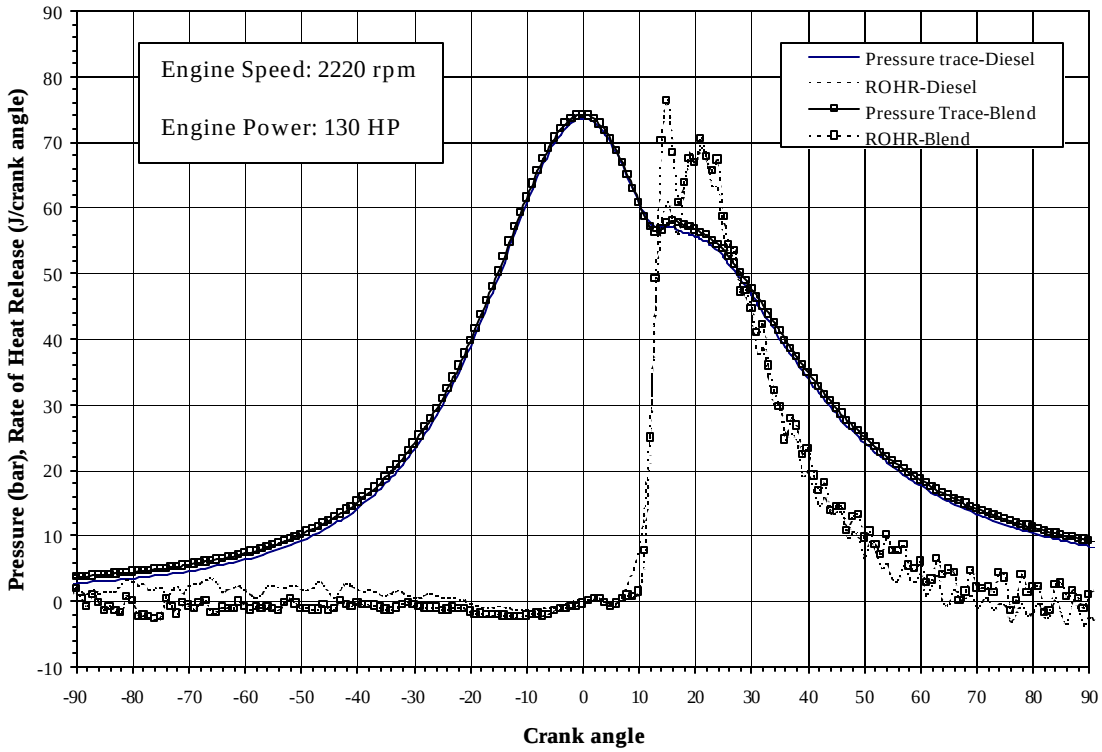

Combustion Event	Diesel	Diesel-DME Blend
Start of Injection (Degrees ATDC)	-10	-10
Start of Ignition (Degrees ATDC)	6	10
End of Burn (Degrees ATDC)	75	75
Max ROHR (J/crank angle degree)	69.07	76.36

Figure 4–13: Pressure Trace and ROHR-Mode 7

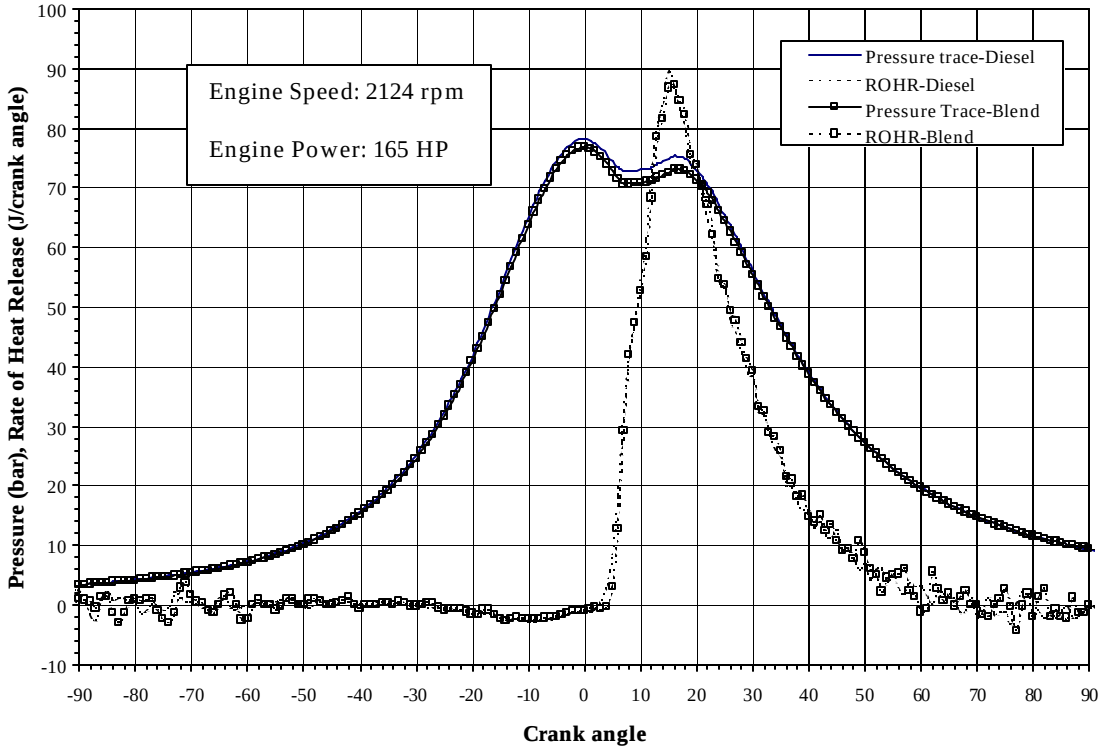

Combustion Event	Diesel	Diesel-DME Blend
Start of Injection (Degrees ATDC)	-13	-12
Start of Ignition (Degrees ATDC)	2	4
End of Burn (Degrees ATDC)	70	70
Max ROHR (J/crank angle degree)	89.54	87.20

Figure 4–14: Pressure Trace and ROHR-Mode 8

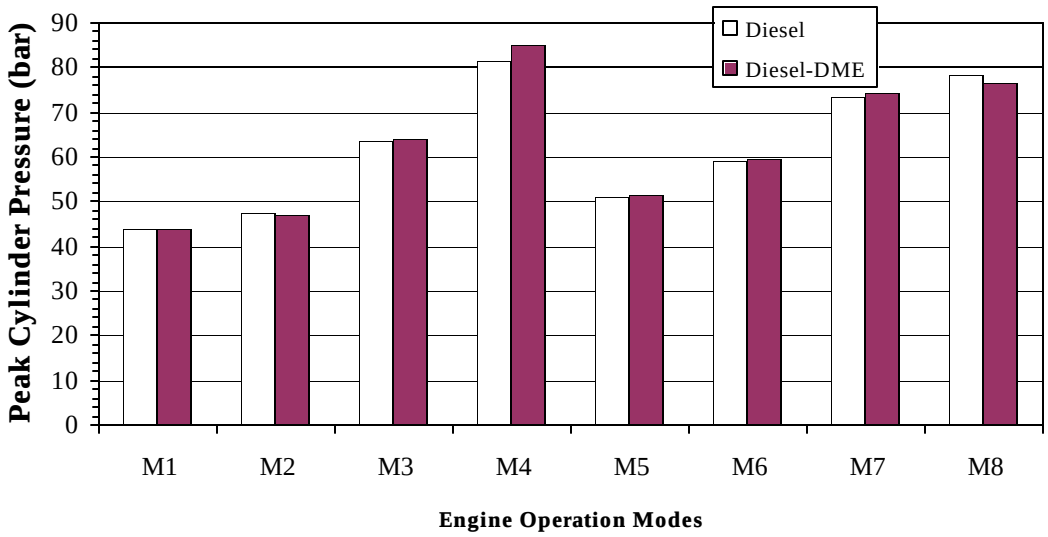

Figure 4–15: Peak Cylinder Pressure Comparison

4.4 Conclusions

The present study was the first attempt to use a blend of Diesel-DME in the Navistar T444E engine at The Pennsylvania State University. The pressurized fuel system was proven as a possible concept in the conversion of diesel engines to operate on diesel-DME blends with minimal modifications. This fuel system will be improved with successive iterations. Drawbacks of this system, which have come to light, are discussed below.

- It was necessary to keep the fuel temperature below 50 ^{O}C for DME to remain in the liquid state. It was seen on Mode 8 of the AVL test with the 2% O content fuel blend, that possible vaporization of the fuel caused reduced power output and unsteady operation of the engine. To prevent vaporization of DME, fuel cooling was implemented. In the original design by the manufacturer, the temperature of the fuel is close to 83 ^{O}C as it enters the HEUI fuel injector. By the time it is injected into the cylinder, the fuel temperature will have raised to a value much higher than that. This leads to a very good spray breakup, better atomization and mixing. In the modified fuel system for the blend, the fuel temperature is much lower than that designed by the manufacturer. This will perhaps lead to a poorer spray breakup and hence poorer mixing in the cylinder. This problem however, will only arise for very low concentrations of DME in the blend. With increasing amounts of

DME, its boiling point being much lower than diesel, the spray breakup and mixing will be much better even at lower fuel temperatures and injection pressures.

- The temperature of the fuel coming out of the fuel rail was monitored and kept below 50 ^{O}C. However, the fuel is heated all along its way from the entry into the HEUI injectors to the tip of the injectors exposed to the combustion chamber. This rise in temperature was not recorded. Vaporization of the fuel inside the injectors will also lead to unsteady engine operation as seen in mode 8 of the AVL 8-mode test. This rise in fuel temperature through the injectors should be either modeled or measured to estimate its impact on the injection process.

The pressure trace analysis and comparison of peak pressures does not indicate any significant difference between the burning of diesel and diesel-DME blend with 2% oxygen content. Figure 4-15 compares the peak pressures for engine operation on baseline diesel and diesel-DME blend. The peak pressures appear similar for operation with both fuels.

The viscosity studies show a logarithmic relation of viscosity and pressure as expected. These values can be important in design of the injector nozzle and the injector opening pressure to get an optimized spray pattern. The high miscibility of DME with diesel fuel in any proportion is an encouraging sign and will allow any mixture to be prepared.

Another important issue in use of DME as a fuel is its higher compressibility as compared to Diesel fuel. This will impact the injection process and should be measured for various blends of Diesel fuel and DME. The high pressure viscometer apparatus used for the viscosity work in this thesis can be converted to measure the bulk modulus.

Diesel–DME blends with higher DME concentrations are currently being studied. An optimum blend ratio will be identified with reference to exhaust emissions and fuel system compatibility.

BIBLIOGRAPHY

1. Johnson, R.H., M.S. Thesis, The Pennsylvania State University, University Park, PA., 1962
2. DuPont Fluorochemical Laboratories, *Dymel A*. Technical Information ATB-25
3. Sorenson, S.C., Mikkelsen. *Performance and Emissions of a 0.273 Liter DI Diesel Engine Fuelled with Neat Dimethyl Ether.* SAE Paper No. 950064
4. Hansen, Voss, Joensen, Siguroardottir. *Large Scale Manufacture of Dimethyl Ether – A New Alternative Diesel Fuel Frome Natural Gas.* SAE Paper No 950063.
5. Verbeek, R. and Van der Weide, J. *Global Assessment of Diemthyl Ether: Comparison With Other Fuels.* SAE Paper No 971607
6. Ofner, H., Gill, D.W., Krotscheck,C. *Dimethyl Ether As Fuel For CI Engines – A New Technology And Its Environmental Potential.* SAE Paper No 981158
7. Phillips, J.G., Reader, G.T., Potter, I.J. *The Use of Dimethyl Ether As A Transportation Fuel – A Canadian Perspective.* ASME 1998, ICE Vol. 31-3, 1998 Fall Technical Conference. Paper No 98-ICE-152
8. Kapus, P. and Ofner, H. *Development of Fuel Injection Equipment and Combustion System For DI Diesels Operated on Dimethyl Ether.* SAE Paper No 950062

9. McCandless, J. and Li, S. *Development of a Novel Fuel Injection System (NFIS) for Dimethyl Ether – and Other Alternative Fuels.* SAE Paper No 970220

10. McCandless, J., Teng, Ho, Schneyer, J. *Development of A Variable-Displacement, Rail-Pressure Supply Pump For Dimethyl Ether.* SAE Paper No 2000-01-0687

11. Ofner, H., Gill, D.W., Kammerdiener, T. *A Fuel Injection Concept For Dimethyl Ether.* Institution of Mechanical Engineers. Paper No C517/022/96

12. Sorenson, S.C. and Nielsen, K. *Lubricity Additives And Wear With DME In Diesel Injection Pumps.* ASME 1999, ICE Vol. 33-1, 1999 Fall Technical Conference. Paper No 99-ICE-217

13. Glensvig, M., Sorenson, S.C., Abata, D. *High Pressure Injection Of Dimethyl Ether.* ASME 1996, ICE Vol. 27-3, 1996 Fall Technical Conference.

14. Sovani, S.D., Sojka, P.E., Gore, J.P., Eckerle, W.A., Crofts, J.D. *Internal Flow Structure Of An Effervescent Diesel Injector.* ASME 1999, ICE Vol. 32-2, 1999 Spring Technical Conference. Paper No 99-ICE-181

15. Sovani, S.D., Sojka, P.E., Gore, J.P., Eckerle, W.A., Crofts, J.D. *Spray Performance of A Prototype Effervescent Diesel Injector.* ASME 1999, ICE Vol. 32-2, 1999 Spring Technical Conference. Paper No 99-ICE-184

16. Navistar International Transportation Corporation. *T444E Service ManuaI.* EGEs-120, January 1994.

17. Hower, M.J., Mueller, R.A., Oehlerking, D.A., Zielke, M.R. *The New Navistar T444E Direct Injection Turbocharged Diesel Engine.* SAE Paper No. 930269.

18. Stockner, A.R., Flinn, M.A., Camplin, F.A. *Development Of The HEUI Fuel System – Integration of Design, Test, Simulation And Manufacturing.* SAE Paper No. 930271.

19. Glassey, S.F., Stockner, A.R., Flinn, M.A. *HEUI – A New Direction For Diesel Engine Fuel Systems.* SAE Paper No. 930270.

20. Fleisch, T., McCarthy, C., Basu, A., Udovich, C., Charbonneau, P., Slodowske, W., Mikkelsen, S., McCandless, J. *A New Clean Diesel Technology: Demonstration of ULEV Emissions on a Navistar Diesel Engine Fueled with Dimethyl Ether.* SAE Paper No. 950061.

21. Sierra Instruments. *BG-1 Microdilution Test Stand.* Operations Manual.

22. Lapuerta, M., Armas, O., Ballesteros, R., Duran, A. *Influence of Mini Tunnel Operating Parameters and Ambient Conditions on Diesel Particulate Measurements and Analysis.* SAE Paper No. 1999-01-3531.

23. Okrent, D.A. *Description Of An Online Method For Measuring The Ratio Of Soot To Organics In Diesel Exhaust Particulates.* SAE Paper No. 960252.

24. Heywood, J.B. *Internal Combustion Engine Fundamentals.* McGraw-Hill Publication, April 1998.

25. Longbao, Z., Hewu, W., Deming, J., Zuohua, H. *Study Of Performance And Combustion Characteristics of a DME Fueled Light Duty DI Diesel Engine.* SAE Paper No. 1999-01-3669.

26. Kapus, P.E., Cartellieri, W.P. *ULEV Potential of a DI/TCI Diesel Passenger Car Engine Operated On Dimethyl Ether.* SAE Paper No. 952754

27. Edgar, B.L., Dibble, R.W., Naegeli, D.W. *Autoignition of Dimethyl Ether and Dimethoxy Methane Sprays at High Pressures.* SAE Paper No. 971677.

28. Kajitani, S., Chen, Z.L., Konno, M., Rhee, K.T. *Engine Performance And Exhaust Characteristics of DI Diesel Engine Operated With DME.* SAE Paper No. 972973.

29. Chiristensen, R., Sorenson, S.C., Jensen, M.G., Hansen, K.F. *Engine Operation on DME in a Naturally Aspirated, DI Diesel Engine.* SAE Paper No. 971665.

30. Sivebaek, I.M., Sorenson, S.C., Jakobsen, J. *Dimethyl Ether (DME)-Assessment Of Viscosity Using The New Volatile Fuel Viscometer.* SAE Paper No 2001-01-2013.